# An *in vivo* RNAi therapy screen identifies novel mediators of leukemia-microenvironment interaction

by

Eleanor Ruth Cameron

B.A. Molecular Biology
Pomona College, 2008

Submitted to the Department of Biology in partial fulfillment of the requirements for the degree of

Doctor of Philosophy in Biology
at the
Massachusetts Institute of Technology

February 2016



Signature of Author: Signature redacted

Department of Biology
December 14, 2015

Certified by: Signature redacted

Michael T. Hemann
Associate Professor of Biology
Thesis Supervisor

Accepted by: Signature redacted

Amy E. Keating
Professor of Biology
Co-chair, Biology Graduate Committee

# An *in vivo* RNAi therapy screen identifies novel mediators of leukemia-microenvironment interaction

by

Eleanor Ruth Cameron

Submitted to the Department of Biology on December 14, 2015 in partial fulfillment of the requirements for the degree of Doctor of Philosophy in Biology

## Abstract

Minimal residual disease refers to those cancer cells that persist following initial therapy. In precursor B-cell acute lymphoblastic leukemia (BCP-ALL), the presence of minimal residual disease is a strong prognostic indicator of relapse. The establishment of minimal residual disease fundamentally arises from leukemia cells that are resistant to drug-mediated killing due to alterations in a myriad of both cell-intrinsic and cell-extrinsic pathways. Understanding mechanisms by which leukemia cells can survive therapy is vital to our ability to target and eradicate minimal residual disease.

*BCR-ABL1*+ BCP-ALL is an aggressive subtype of BCP-ALL, and despite the use of tyrosine kinase inhibitors (TKIs) as additional therapeutics that directly inhibit *BCR-ABL1*, more than half of *BCR-ABL1*+ BCP-ALL patients will experience a relapse. We have adapted an *in vivo* RNAi screening approach to perform novel longitudinal studies both in mice and in cultured cells to identify genetic mediators of response to the TKI dasatinib in a transplantable syngeneic mouse model of *BCR-ABL1*+ BCP-ALL. The unique combination of a longitudinal screen design and independent component analysis of screening data allowed for identification of hairpins that have distinct behavior in different therapeutic contexts as well as in the *in vivo* versus *in vitro* settings.

From the set of hairpins found to have distinct behavior before versus after therapy, we identified *ABI3* as a potential biomarker of therapeutic response in *BCR-ABL1*+ BCP-ALL cells. Knockdown of *ABI3* promoted resistance to dasatinib *in vivo*, potentially due to alterations in the invasive capabilities of leukemic cells. We also found that loss of *PAFAH1B3* sensitizes cells to dasatinib specifically in the *in vivo* setting. Changes in Pafah1b3 levels alter the distribution of leukemic cells *in vivo,* and cells that express higher levels of Pafah1b3 are enriched in the bone marrow after dasatinib treatment. Therefore, sensitization after loss of *PAFAH1B3* may result from decreased ability of leukemia cells to migrate to or remain in the bone marrow, an established site of MRD in BCP-ALL. Pafah1b3 is a druggable enzyme and thus represents a potential target for combination therapy with TKIs for *BCR-ABL1*+ BCP-ALL.

Thesis Supervisor: Michael T. Hemann
Title: Associate Professor of Biology

**Table of Contents**

**Acknowledgements**

I would like to thank my advisor, Mike Hemann, for his guidance on matters both professional and personal as well as his continued support throughout my entire graduate career. He has provided me with excellent scientific ideas and advice on what to try next, as well as helped me realize when to let an unsuccessful line of questioning stop. Working with Mike, I learned how to be smart about what experiments I do while at the same time experimenting with new approaches. I've also gained valuable techniques for dealing with both my superiors and my peers, for which I am grateful. Mike manages to make the lab a more fun place to work while still encouraging us to actually do work, and his sense of humor provides us with a way to diffuse some of the stress of graduate study. I am thankful for this environment that he's created, his unending patience with our questions and complaints, and particularly that he gave me freedom to mostly control my own experiments but also guidance and technical help (for instance, performing tail vein injections) when I needed it.

I'd also like to thank my thesis committee members Matt Vander Heiden, David Sabatini, and in the later years, Doug Lauffenburger, for their continued advice and support. We've had some great discussions both in my committee meetings and more casually discussing science and potential careers around MIT or at scientific meetings, and I am grateful for both their support and their constructive criticism, which have improved my work and my development as a scientist. You've all gone above and beyond in your help with my research here and with deciding what to do next, and I really appreciate it.

All of the amazing, friendly, helpful people in the Swanson Biotechnology Center at MIT have aided in the completion of this work. In particular, I want to thank: Glenn Paradis, Michele Griffin, Michael Jennings, and Mervy Saturno-Condon of the Flow Cytometry core, who have taught me how to use machines, sorted samples, helped with analysis, and have always been willing to just chat or explain how things work; Scott Malstrom from the Animal Imaging and Preclinical Testing Core for help with *in vivo* imaging and data analysis; Richard Cook and Alla Leshinsky of the Biopolymers and Proteomics Core for running all of our screening data and helping us troubleshoot when we needed to update our protocols; Charlie Whittaker of the Bioinformatics and Computing Core for helping with my RNAi screening data; Kathy Cormier of the Histology Core for answering my many questions about histology and sample prep. This work was supported in part by the Koch Institute Support (core) Grant P30-CA14051 from the National Cancer Institute.

I'd also like to thank Arjun Bhutkar for all his hard work analyzing my RNAi screening data and for approaching me about trying ICA on the RNAi data in the first place. Without that idea, this screen would not have been what it is now; AJ not only worked with me on figuring out what analysis to perform, but then also did the ICA and helped me to interpret it. His help was invaluable in completing this thesis.

I'd like to thank the MIT School of Science for the fellowship that supported this work in the academic year of 2014-2015, as well as the Ludwig Foundation, ICBP at MIT, and the Go Mitch Go Foundation, all of which have also at times supported my research.

Thanks go out to my lab members Boyang Zhao, Faye Vassel, Yadira Soto-Feliciano, and Peter Bruno for critical reading of this manuscript. I'd also like to thank then entire Hemann Lab, past and present, for their help and support as well as for making sure that our lab is never boring. In particular, I'd like to thank those who helped with the work presented in this thesis: Emily Lawler and Jordan Bartlebaugh, both of whom worked on this project as summer undergraduates; Jordan, Yadira, Jennifer Shingleton, and Holly Criscione for splitting cells and checking on mice when I was out of town; and Corbin Meacham for helping me learn about RNAi screens and the transplantable leukemia model. I'd also like to thank Holly, our lab manager, for always making sure that things run smoothly, and Yadira, my baymate, for being my perfect OCD-level match and for our many conversations about leukemia, science, and life in general.

I'd like to thank my entire class and other friends at MIT, but particularly Daisy Riquelme, who has tirelessly been trying to co-immunoprecipitate proteins for this project and is great at getting me to relax and enjoy life a bit; Dahlia Perez, who TA'd with me and is a constant source of both happiness and support; and Leah Schmidt, for being a great friend who's always down to hang out and but is also happy to teach me lab techniques.

Thanks go out especially to my family: my dad Scott, my mom Penny, and my sister Katy all have advanced degrees, so they know the graduate school drill, and they have been incredibly supportive and don't panic when they don't hear from me for a while. They also have always been interested in what I'm doing even if they don't fully understand it, which is so special to me. Plus, they send me videos of my adorable nephew George, which always brightens my day.

Finally, I'd like to thank my husband, Steve. They don't warn you when you start graduate school that your significant other will take the brunt of the unpleasantness in the form of late nights, early mornings, having to go into lab every weekend day and holiday, and being hungry or tired or miserable from allergies. Steve has put up with all of it and supported me the whole way through, and there's no way I could have done this without him. He both appreciates the work that I'm doing and helps me remember that there's a world outside of the lab and outside of science, and that helps keep me happy and connected to life.

**Chapter I: Precursor B-cell acute lymphoblastic leukemia and the problem of minimal residual disease.**

---

Eleanor R. Cameron

David H. Koch Institute for Integrative Cancer Research, Massachusetts Institute of Technology. Cambridge, Massachusetts, 02139, United States.

This chapter is not published as of December 2015.

Precursor B-cell acute lymphoblastic leukemia (BCP-ALL) is a neoplasm of the B-lymphoid progenitors that affects both children and adults. There are over 6000 cases of acute lymphoblastic leukemia annually in the United States, the majority of which are BCP-ALL (1-3). While the five-year event free survival rate for ALL patients is around 80% for children and 40% for adults, relapse remains a persistent problem (3-8). Approximately 20% of children and 60 - 70% of adults with ALL experience a relapse, and the cure rate for relapsed ALL remains low, making relapsed ALL the most common cause of cancer-related death in children and adolescents (3, 5, 9-11).

The presence of minimal residual disease (MRD) after initial therapy has proven to be significantly associated with increased risk of relapse in both children and adults with BCP-ALL (12-21). MRD in BCP-ALL is defined as leukemia cells that persist in a patient's bone marrow or blood following treatment and that can be measured by flow cytometric or PCR-based assays (22, 23). Despite numerous genetic predictors of poor outcome in BCP-ALL, such as the presence of the Philadelphia chromosome, *MLL* gene rearrangement, or loss of specific genes e.g. *IKZF1* (Ikaros), multivariate analysis has shown that the presence of MRD is usually the strongest predictor of prognosis in BCP-ALL patients (14, 16-18, 20, 23-29). Even following allogeneic hematopoietic stem cell transplant, the only truly curative therapy available for BCP-ALL, the presence of MRD above a certain threshold predicts a poor outcome (30-33).

The cancer cells that make up MRD in BCP-ALL patients are thought to not only survive initial therapy but also expand out during and after treatment and fuel leukemic relapse. Cases in which relapse takes the form of a novel secondary leukemia are relatively rare in BCP-ALL (34-37). Analyses of changes in copy number abnormalities,

regions of loss of heterozygosity, and allele-specific gene dosage levels between matched BCP-ALL patient samples at diagnosis and relapse have shown that clonal evolution of leukemia cells after initial treatment results in a relapsed leukemia in which the major clone is either composed of a minor diagnosis clone or a genetically distinct clone that shares a common ancestral origin with the initially identified disease (19, 34-47). The clonal diversity present in BCP-ALL both at diagnosis and at relapse and the fact that BCP-ALL is thought to arise from a lymphoid progenitor cell rather than the hematopoietic stem cell makes it unlikely that there is a rare population of cancer stem cells that are the source of MRD and subsequent relapse; rather numerous leukemia initiating cells (LICs) seem to contribute to disease burden both before and after therapeutic intervention (19, 34-55). Here I will summarize the current treatment modalities for BCP-ALL and known methods of MRD development in this disease, discuss strategies being used to address MRD, and outline the work presented in this thesis, in which I investigate mechanisms of MRD following treatment with the TKI dasatinib in a transplantable mouse model of *BCR-ABL1*+ BCP-ALL.

**Minimal residual disease is the result of resistance to drug-induced cell death**

At its most basic level, MRD in BCP-ALL is the outgrowth of one or more drug resistant clones. Numerous studies have shown that *in vitro* resistance to anticancer agents in patient samples of leukemia at diagnosis correlates with both the presence of MRD and clinical outcome (12, 56-62). Resistance in BCP-ALL can be to a single type of agent, as exemplified by the numerous mutations in the Abl kinase domain that can

cause resistance to tyrosine kinase inhibitors, or can take the form of a more general multi-drug resistance (63-65). The latter phenomenon often arises via changes in intracellular drug concentration or alterations in cellular pathways vital to the functionality of an entire class of drugs, such as the apoptotic pathway for most chemotherapeutic agents (6, 46, 66-69). Resistance to single or multiple agents can also arise in an indirect but still cell-intrinsic manner by the activation of intracellular pathways that signal for survival in the presence of drug, such as the NFκB or PI3K pathways, or even potentially by maintenance of a less differentiated state that may confer a general resistance to drug-mediated cell death (5, 70, 71). Additionally, there can be cell-extrinsic drug resistance, a phenomenon by which leukemia cells survive therapy in certain anatomical sites due to altered drug exposure or pro-survival signaling from the local microenvironment, which can take the form of secreted factors or signaling via direct cell-to-cell contact (72-74).

Due to the relatively high percentage of LICs in BCP-ALL, it is likely that these different mechanisms of drug resistance can occur alone or in tandem in either a single or multiple leukemic clones. For simplicity's sake, I will discuss each potential mode of drug resistance separately, but it is important to remember that in the clinical setting effective elimination of MRD may require targeting of multiple resistance mechanisms at once. While the oligoclonal nature of BCP-ALL makes treatment challenging, it does provide a context in which we can examine how a single mitotically active cancer cell might survive and retain proliferative capacity in the presence of therapy. The mechanisms by which leukemia cells persist in BCP-ALL patients could potentially be extrapolated to other hematopoietic malignancies for which there do not appear to be

cancer stem cells as well as to non-dormant metastatic cells that can contribute to relapse in certain solid tumors. In addition, as numerous therapeutic modalities are used to treat BCP-ALL both clinically and in pre-clinical models, it provides a setting for the investigation of mechanisms of resistance to multiple different anti-tumor agents in the context of a single family of closely related cancers.

## The genetics and cytogenetics of BCP-ALL

### *Cytogenetic lesions*

Chromosomal abnormalities are common in BCP-ALL and are often used to classify the disease into subtypes with distinct prognoses and occasionally different treatment options (3, 4, 75, 76). Typical cytogenetic alterations include *ETV6-RUNX1* (*TEL-AML1*), *TCF3-PBX1* (*E2A-PBX1*), *BCR-ABL1* or the Philadelphia chromosome, rearrangements involving *MLL1* (e.g. *MLL1-AF4*), rearrangements involving *CRLF2* (particularly common in Down Syndrome-associated ALL), intrachromosomal amplification of chromosome 21 (iAMP21), hyperdiploidy with a gain of at least 5 chromosomes, and hypodiploidy with fewer than 44 chromosomes (75, 77, 78). These alterations can result in disruption of normal lymphoid development and hematopoiesis, activation of oncogenes or tyrosine kinase signaling, and promote growth factor independence (3, 4, 25, 77-80). Despite their relative prevalence, cytogenetic lesions are not always found in BCP-ALL patients and are often not sufficient to induce leukemia in model systems (75). In fact, cytogenetic abnormalities can be identified in

children years prior to the development of leukemia, indicating that gross chromosomal abnormalities alone are not sufficient for leukemic transformation (81).

*Submicroscopic genetic alterations*

Multiple studies over the last decade have identified a number of recurring submicroscopic genetic alterations that may contribute to the development of BCP-ALL (82-85). Interestingly, specific alterations are often associated with certain cytogenetic subtypes (82-85). The most commonly found genetic alterations involve genes that transcriptionally regulate lymphoid development (loss of *PAX5, IKZF1,* and *EBF1*), impart growth factor independence (activation of *JAK1/2*), or suppress tumor development (loss of *CDKN2A/B*) (5, 25, 77-80, 86).

These genetic profiling efforts have also led to the identification of a subset of BCP-ALL patients whose cells exhibit a gene expression profile similar to *BCR-ABL1*+ BCP-ALL but lack the Philadelphia chromosome (80, 87). These patients constitute the newly defined BCP-ALL subtype of *BCR-ABL1*- like ALL, which is characterized by *IKZF1* loss, overexpression of *CRLF2* and activation of various tyrosine kinases including *ABL1*, *JAK2*, and *PDGFRB* (88, 89). More recently, another novel subtype of BCP-ALL in which leukemia cells express and signal through a functional pre-B cell receptor via *BCL6* and downstream kinases including *SRC*, *SYK,* and *PI3K,* has been identified via examination of pre-BCR signaling in over 800 BCP-ALL cases (90). This pre-BCR+ BCP-ALL subset often expresses the *TCF3-PBX1* fusion gene, indicating overlap with an existing cytogenetic subset (90). Thus, while cytogenetic characteristics

define most BCP-ALL subtypes, submicroscopic genetic alterations also make significant contributions to BCP-ALL and may affect leukemic response to therapy (91).

## Frontline treatment of BCP-ALL

### *Chemotherapy*

BCP-ALL is typically treated with a chemotherapeutic regime consisting of three phases: remission-induction, consolidation, and maintenance (7, 76, 78). Patients may also receive central nervous system (CNS) prophylaxis during induction or consolidation, for which cranial radiation can be used but is being phased out in favor of intrathecal chemotherapy, typically in the form of methotrexate, hydrocortisone, and cytarabine (78). Induction therapy usually consists of a combination of the microtubule poison vincristine, a glucocorticoid (prednisone or dexamethasone), and an anthracycline (often doxorubicin or daunorubicin), with or without L-asparaginase (78). Some protocols, particularly in adult patients, also call for the alkylating agent cyclophosphamide (76). After remission induction, patients are given consolidation therapy in an attempt to eliminate any remaining leukemic cells; this typically consists of methotrexate with a nucleotide analog such as mercaptopurine, as well as re-administration and/or continuation of agents used for induction (78). The final phase, continuation therapy, mainly consists of continued methotrexate and mercaptopurine with or without intermittent vincristine and glucocorticoid administration (78). Because of the combination strategy used to treat BCP-ALL patients, it is important to keep in mind

that what causes resistance to a single agent *in vitro* may not actually contribute to minimal residual disease in patients.

*Targeted therapeutics*

In several BCP-ALL subtypes, yet another class of drugs can be added to or used in the place of the combination chemotherapeutic regime described above. Outcome in patients with *BCR-ABL1*+ BCP-ALL is poor with traditional chemotherapy, but has greatly improved since the introduction of the tyrosine kinase inhibitor imatinib, which directly inhibits the enzymatic activity of the Abl1 kinase (92-95). Tyrosine kinase inhibitors (TKIs) are a maintenance therapy and so are continuously taken and can be given alone or in combination with chemotherapy, which improves efficacy as compared to either TKI or chemotherapy alone (96-102). If patients relapse on imatinib, they are often then transitioned to a second-generation TKI such as dasatinib, which can inhibit some of the mutated forms of the Bcr-Abl protein that can arise after imatinib treatment, also targets Src tyrosine kinase signaling, and has better penetration into the CNS (103-107). Additionally, patients with resistance or intolerance to dasatinib or nilotinib, another second-generation TKI, can be treated with ponatinib, a third-generation TKI that can bind to and inhibit all clinically relevant single *BCR-ABL1* mutations, including the so-called gatekeeper T315I mutation (108-110).

Tyrosine kinase inhibitor therapy may also be a useful addition in patients with *BCR-ABL1*-like BCP-ALL, who often have inferior responses to traditional chemotherapy. Due to the activation of the *JAK2* and *ABL1* kinases in this disease subtype, clinical trials to study the efficacy of dasatinib as well as the Jak2 inhibitor

ruxolitinib in *BCR-ABL1-like* BCP-ALL subtype are currently underway (64, 88, 80). A small number of *BCR-ABL1-like* patients have already been treated with tyrosine kinase inhibitors in the clinic, and the majority of these patients showed good response to this mode of therapy; patient-derived *BCR-ABL1*-like cells also show *in vitro* sensitivity to TKIs directed against their activated kinases (8, 111). Similarly, in the same preclinical study that initially identified the novel pre-BCR+ subtype of BCP-ALL, researchers found that these leukemia cells were sensitive to inhibition of the *SYK*, *SRC*, and *BTK* enzymes in preclinical studies (90). However, these targeted therapeutics are not currently approved for general use in *BCR-ABL1*-like ALL or pre-BCR+ BCP-ALL.

*Hematopoietic stem cell transplant*

For patients with higher-risk or very aggressive BCP-ALL, including *BCR-ABL1*+ BCP-ALL, allogeneic hematopoietic stem cell transplant (allo-HSCT) can also be utilized as a form of cellular therapy (76, 78). Indications for the use of allo-HSCT are continuously evolving, but survival of patients receiving allo-HSCT is comparable regardless of the source of stem cells (78). However, multiple studies have shown that a higher level of MRD prior to transplant is strongly associated with relapse (31, 32, 33, 78). Because the successful eradication of MRD prior to allo-HSCT is typically achieved through the application of drug-based therapy, here we will discuss mechanisms of MRD establishment only after treatment using drug-based protocols as described above (78).

*The role of genetics in therapeutic response*

Response to therapy varies among the different BCP-ALL subtypes, from excellent in patients with hyperdiploidy and *ETV6-RUNX1* translocations to intermediate in patients with *TCF3-PBX1* translocations and poor in patients with hypodiploidy, *TCF3-HLF* translocation, *CRLF2* rearrangements, *MLL* rearrangements, iAMP21, *BCR-ABL1* translocations, and patients with *BCR-ABL1*-like expression patterns (112). Thanks to advances in microarray profiling and next generation sequencing, we now know that all of these subtypes are additionally characterized by recurrent submicroscopic genetic alterations that can also alter prognosis, such as the loss of *EBF1, IKZF1 or CDKN2A/B* (113). However, genomic profiling without mechanistic studies does not distinguish between mutations that actually fuel relapse and those that are carried along with functional changes, and so functional validation of the genetic changes found in relapsed BCP-ALL patients remains critical.

The genetic heterogeneity between and within subtypes of BCP-ALL in concert with its oligoclonal nature means that there are many different mechanisms by which leukemic cells may survive therapy and seed relapse. As with the recognition of activated tyrosine kinase signaling pathways and the development of TKIs for better treatment of *BCR-ABL1*+ leukemias, understanding how BCP-ALL cells can survive and proliferate after therapy will be crucial both to the development of future therapies and to better risk stratification utilizing currently available therapeutics (e.g. TKI treatment for *BCR-ABL1*-like BCP-ALL). It is likely that combination therapy will continue to be used in BCP-ALL patients in order to target the many pathways that can lead to the development of minimal residual disease and eventual leukemic relapse, and so

identification of novel drug targets that synergize with existing regimens is an active area of both clinical and preclinical research (78).

## Resistance through alteration of drug availability

Achieving sub-therapeutic drug levels is one mechanism by which leukemia cells may survive treatment and seed minimal residual disease, and this can occur on both the cellular and the organismal level. Lower drug concentrations in a particular anatomical site can lead to site-specific relapse; while most relapses occur in the bone marrow, relapse in the central nervous system, testes, and additional atypical sites such as the ocular cavity can also occur in ALL patients (114). The concentration of drug in a target cell or across certain permeability barriers, such as the blood-brain barrier, is regulated primarily by influx and efflux pumps which function to facilitate drug entry and exit from the cell or into privileged anatomical sites, and by enzymes within the cell that can change the activity of a drug by catabolizing it or sequestering it away from its target (66). Many such enzymes can act on the various drugs used to treat BCP-ALL *in vitro*, but whether or not these mechanisms actually help to fuel relapse in BCP-ALL patients is largely still under investigation.

### *Drug efflux pumps*

One of the classes of enzymes involved in regulating drug availability is the family of drug efflux pumps, which function to actively move their targets out of a cell and thus decrease intracellular drug accumulation and, in the case of cancer

therapeutics, associated toxicity (66). Several different drug efflux pumps can potentially export the assorted therapeutics used to treat BCP-ALL, including P-glycoprotein (*ABCB1/MDR1)*, the related multidrug resistance gene *ABCB5*, breast cancer resistance protein (*ABCG2)*, and the multidrug resistance proteins (*MRP1-MRP6)*. Numerous chemotherapeutics as well as multiple TKIs can be substrates for P-glycoprotein (P-gp), but while some studies indicate that higher P-gp or *ABCB5* expression is indicative of poorer response in ALL patients, others find no association between P-gp levels and clinical outcome (66, 115-127). In mouse models and cell lines P-gp inhibition can lead to increased sensitivity to TKIs, and total P-gp loss results in increased brain accumulation of both dasatinib and imatinib, but as of yet there are no clinical studies linking TKI resistance to the P-gp efflux pump (66, 128-135).

While most of the members of the MRP family of drug efflux pumps have increased expression in blasts from B- and T-ALL patients, only *MRP3* has been found to be significantly associated with poor outcome in patients (66, 120, 136-139). Interestingly, in a mouse model of *BCR-ABL1*+ BCP-ALL, loss of *MRP4* resulted in increased tumor burden and lower overall survival after dasatinib therapy, indicating that the MRP family members may have distinct effects on the activity of chemotherapeutic drugs versus TKIs (140).

Similarly, despite the fact that high levels of breast cancer resistance protein (BCRP) can cause *in vitro* resistance to anthracyclines, topoisomerase inhibitors, antifolates, and TKIs, several studies of ALL patients at diagnosis and relapse showed that BCRP level in leukemic blasts did not differ before versus after therapy, nor was BCRP associated with poor outcome or MRD development (66, 134, 141-145). As with

P-gp, high BCRP levels in mouse models seem to restrict brain accumulation of TKIs, but this has not been tested in BCP-ALL patients (134, 135, 143). In a small study of chronic myelogenous leukemia (CML) patients, who are also *BCR-ABL1+* and are treated with TKIs, BCRP expression had no effect on clinical response (146). Further studies are needed to clarify and confirm the role of drug efflux pumps in establishing MRD in BCP-ALL patients.

*Drug influx pumps*

For some drugs, transport into the cell is an active process mediated by a drug influx pump; in the case of the TKI imatinib, import is dependent on the organic cation transporter Oct1 (147-149). In contrast, dasatinib and ponatinib do not seem to require Oct1 for uptake into CML cell lines (148-150). Several studies of CML patients have shown that higher Oct1 levels are correlated to better initial response to imatinib therapy as well as longer relapse free survival and overall survival, and that this does seem to be due to improved imatinib uptake in the blasts patients with higher Oct1 (146, 151, 152). Studies looking specifically at the role of Oct1 in response to TKIs in *BCR-ABL1+* BCP-ALL have not yet been performed.

*Intracellular sequestration of drug*

The amount of available drug in a target cell can also be regulated by sequestration of drugs away from their intracellular targets. This is thought to be the function of lung resistance protein (LRP), also known as the major vault protein, which can cause *in vitro* resistance to several chemotherapeutics (66, 136, 137). While LRP

expression levels are increased in BCP-ALL cells as compared to other leukemic cells or normal lymphocytes, high LRP expression at diagnosis does not necessarily relate to poor prognosis, although LRP levels are sometimes significantly higher at second or later relapse (117, 120, 136, 153-155). Due to the conflicting results from various studies, it is unclear whether or not LRP plays a role in minimal residual disease in BCP-ALL. An interesting cytotoxic localization effect has also been noted in *BCR-ABL1*+ cells *in vitro*, in which trapping of Bcr-Abl in the nucleus causes cell death after imatinib treatment even in previously imatinib-resistant cells, but this effect has not been studied in patients (156, 157).

*Cellular metabolism of drug*

Metabolic enzymes also have the potential to alter the availability of active drug in leukemia cells. For example, methotrexate (MTX) can be converted to methotrexate polyglutamates (MTX-PGs) once inside a target cell, which allows for accumulation of higher intracellular levels of MTX (158). Multiple studies have shown that patients with impaired ability to accumulate MTX and MTX-PGs have poorer response to MTX alone, but as BCP-ALL patients are treated with a combination chemotherapeutic regime the effect of poor MTX accumulation on relapse rate is unclear (126, 158-166). Similarly, changes in the level of reduced folate carrier, which can transport MTX into cells, were found to have no effect on response to therapy, particularly after high dose MTX (167-169).

The role of metabolic enzymes in response to treatment with L-asparaginase and thioguanines has also been investigated. Sensitivity to L-asparaginase in ALL cells has

in the past been attributed to decreased levels of asparagine synthetase (AS), the enzyme that generates asparagine (170). However, AS expression or up-regulation in response to exposure to L-asparaginase is not always associated with poor response to L-asparaginase or PEG-asparaginase in ALL patients, and the dependency of asaparagine response on AS levels may differ among BCP-ALL subtypes (170-173). Similarly, BCP-ALL patients with lower enzymatic activity of thiopurine methyltransferase (TPMT), which detoxifies the nucleotide analogs 6-mercaptopurine and 6-thioguanine, were found in several studies to have significantly lower risk of relapse, although TPMT levels are not always predictive of relapse risk in the context of patients treated with a combination chemotherapeutic regimen (76, 174, 175).

*Organismal metabolism of drug*

Several studies have looked at the role of the glutathione S-transferases GSTM1 and GSTT1 in leukemia, as these enzymes are involved in the metabolism of wide variety of drugs and homozygous deletions of these enzymes are relatively common in some populations (65). Lower levels of these proteins have been found in various studies to either have no effect on patient outcome, result in poorer outcome, or, in the case of one study looking at a null GSTM1 genotype in high risk patients, improve patient outcome (65, 176-178). In general, while trends are sometimes identified in small groups of patients or groups that meet certain criteria, large-scale studies seem to indicate that *GSTT1* and *GSTM1* gene polymorphisms don't have a consistent effect on outcome in ALL patients.

The substrate for glutathione-S-transferases is the intracellular antioxidant glutathione (GSH). GSH levels are positively correlated to sensitivity to several antileukemic drugs in Bcl-2 overexpressing or otherwise multi-drug resistant ALL cells, and pharmacological depletion of GSH resensitizes cells to treatment *in vitro* (179, 180). In patients, elevated GSH levels are indicative of increased risk of relapse and decreased overall survival (181).

Activity of liver cytochrome P450 enzymes, which metabolize many anticancer drugs, may also have an effect on therapeutic outcome by increasing toxicity or rate of relapse (3, 182). Interestingly, certain drugs used for supportive care of leukemic patients can result in an increase or decrease of P450 levels (3). However, as with the glutathione-S-transferases, there is little consensus on the magnitude of the role that cytochrome P450 activity plays in BCP-ALL patient response (3, 182).

**Cell-intrinsic drug resistance via changes to drug target**

As many of the drugs used to treat BCP-ALL directly alter or inhibit specific enzymes or pathways within the leukemic cell, one of the simplest ways to achieve resistance to a single drug or class of drugs is to alter the structure or activity of the drug target. Alteration can be achieved via genetic mutation, gene amplification, or changes in regulation at the genetic, protein, or pathway level. This phenomenon of drug resistance by target alteration is one of the cell-intrinsic mechanisms by which BCP-ALL cells can become resistant to therapy, and is particularly well studied in the case of the tyrosine kinase inhibitors in *BCR-ABL1*+ BCP-ALL (64).

*Mutation or amplification of targeted gene*

Kinase-domain mutations in the Bcr-Abl protein can prevent TKIs from binding to the enzyme and lead to a reactivation of oncogenic signaling; such mutations have been described in *BCR-ABL1*+ cell lines, mouse models, and as a resistance mechanism in patients treated with front-line imatinib and second- or third- line dasatinib or nilotinib (64, 129, 183-186). Combination of TKI treatment with conventional chemotherapy reduces the rate of Bcr-Abl mutations in relapsed patients and in a mouse model of *BCR-ABL1*+ BCP-ALL, but they still occur (99, 101, 187). Patients with kinase domain mutations who are then treated with ponatinib, which can bind to and inhibit all of the clinically relevant single Bcr-Abl mutations, can develop compound mutations in a single *BCR-ABL1* allele that drive ponatinib resistance (109, 110). Relapse with mutation in *BCR-ABL1* has even been described in a case of *BCR-ABL1*-like BCP-ALL treated with dasatinib (188). Target alteration after TKI therapy in *BCR-ABL1*+ BCP-ALL is referred to as Bcr-Abl-dependent resistance to TKI therapy, and is also caused at lower rates by overexpression or amplification of the *BCR-ABL1* gene or the entire Philadelphia chromosome, particularly after treatment with the less potent TKIs imatinib and nilotinib (64, 128, 129).

Resistance via target alteration can also occur after treatment with various chemotherapeutics; higher levels of the MTX targets dihydrofolate reductase and thymidylate synthetase have been found in both preclinical models and small patient studies to be correlated with MTX response and time to relapse, although increased MTX doses can often overcome this effect (158, 169, 189, 190). Similarly, activating mutations in *NT5C2*, an purine metabolism enzyme that can dephosphorylate and

inactivate 6-mercaptopurine and 6-thioguanine, are found in relapsed BCP- and T-ALL patients and can confer resistance to thiopurines *in vitro* (47, 191, 192). Anthracyclines such as doxorubicin directly inhibit the DNA helicase topoisomerase II, and knockdown of the *TOP2A* gene was found to confer resistance to anthracyclines in a preclinical B-cell lymphoma model (193). However, while one clinical study found that *TOP2A* expression was increased at relapse in B- and T-ALL patients, another study found that in pediatric B-ALL low expression of *TOP2A* was associated with higher relapse risk, indicating that altered *TOP2A* levels may not be a reliable predictor of relapse after combination chemotherapy in BCP-ALL patients (194, 195).

A great deal of effort has been put into researching the potential role of target alteration in the development of resistance to glucocorticoids (GCs), as poor initial response as well as *in vitro* resistance to GCs are both poor prognostic indicators in BCP-ALL and T-ALL (196). GCs enter the cell by passive diffusion and then bind to the glucocorticoid receptor (GR) to affect transcriptional changes in GC-responsive genes (196). Changes in the level or activity of GR could potentially alter GC response, but there is no evidence that GR mutation, ability of the GR to translocate to the nucleus, or altered functionality of the GR have an effect on GC response in patients or preclinical mouse models (196-200). However, the GR gene *NR3C1* is sometimes lost or has altered copy number or splice variant usage in BCP-ALL patients at relapse, and in T-ALL cells GR expression level was found to determine extent of apoptotic response to GC therapy, indicating that alteration of the GR levels may play a role in leukemic relapse (6, 35, 36, 95, 196, 199, 201).

*Alteration of the targeted pathway*

Additional potential mediators of resistance via GC pathway alteration have emerged in the form of epigenetic regulators that act at the level of GR-mediated transcriptional changes. CREB binding protein (*CREBBP*) is a transcriptional co-activator that can acetylate both histone and non-histone targets, and can mediate response to GCs in non-leukemic cells (80, 202). Mutations in *CREBBP*, particularly in the histone acetyltransferase (HAT) domain, are both preserved and acquired at relapse in BCP-ALL patients (25, 47, 80, 203-206). Experiments in mouse embryonic fibroblasts indicated that HAT domain mutated-*CREBBP* can change the expression of GC-responsive genes, likely by altering histone acetylation, and T-ALL cell lines resistant to GC therapy are sensitive to histone deacetylase inhibitors (203).

Similarly, SWI/SNF chromatin-remodeling activity has been shown in human cells to be required for GC-mediated transcriptional changes, and in both B- and T-ALL patients under-expression of the core components of the SWI/SNF complex are associated with GC resistance *in vitro* (207, 208). More recently, loss of *TBL1XR1*, an F box protein that regulates the nuclear hormone repressor complex, has been identified as a mechanism of decreased GR recruitment to GC-responsive genes; *TBL1XR1* loss in leukemic cells can cause *in vitro* resistance to GCs that can be reversed by treatment with a histone deacetylase inhibitor (209). Loss of *TBL1XR1* is common in relapsed BCP-ALL patients or those who fail induction therapy, but is not predictive of clinical outcome (210). Knockdown of the long non-coding RNA *BALR2* leads to increased apoptosis, up-regulation of the GC responsive pathway, and sensitization to GCs; high *BALR2* expression is associated with decreased GC response and poor overall survival

(211). In contrast to *BALR2* and *TBL1XR1*, the SWI/SNF complex has not been directly implicated in GC response in BCP-ALL patients, but alterations at the epigenetic level do seem to affect the ability of GCs to mediate transcriptional changes in BCP-ALL cells.

**Cell-intrinsic multidrug resistance through altered cellular response to drug**

Genes involved in proliferation, cell cycle regulation, apoptosis, and DNA repair are frequently altered at relapse and in MRD-positive BCP-ALL patients (46, 69). Lower levels of apoptosis upon challenge with ionizing radiation or apoptotic cell culture conditions in diagnostic BCP-ALL patient samples is associated with higher risk of relapse, higher MRD after induction therapy, and significantly shorter event-free survival and overall survival (212, 213). Samples from relapsed or MRD-positive patients also show altered expression or changes in CpG methylation of genes associated with cellular proliferation and cell-cycle control and a trend towards increased glucose consumption, particularly after exposure to GCs (67, 194, 195, 214-217). Analysis of matched diagnosis and relapse samples from BCP-ALL patients also indicated changes in genes involved in DNA replication and repair at relapse, including multiple mismatch repair enzymes (37, 194, 205).

*Regulation of p53*

Mutations or deletions of *TP53*, a key regulator of apoptosis and a tumor suppressor, are gained at relapse in a small (~10 %) percentage of BCP-ALL patients

and are associated with poor clinical outcome (25, 47, 77, 218-220). In hypodiploid BCP-ALL, which has extremely poor prognosis, the rate of *TP53* mutations is much higher at about 90% (8, 22). BCP-ALL cells defective in p53 are resistant to ionizing radiation and the anthracycline etoposide *in vitro*, indicating that these cells have reduced capacity to undergo apoptosis following DNA damage, although in some p53 mutated cell lines p53-independent apoptosis can still occur (221, 222). Overexpression of *MDM2*, an ubiquitin ligase that targets p53 for degradation, is also found in BCP-ALL patients at diagnosis and at relapse and in acute leukemia is associated with high risk and poor clinical outcome (202, 223-226). Interestingly, in a small set of both BCP-ALL cell lines and primary patient samples, researchers identified either *TP53* mutation/deletion or *MDM2* over-expression but never both, indicating that these alterations are redundant and likely both function to decrease the ability of leukemia cells to undergo apoptosis (227).

A more common alteration to the apoptotic signaling pathway in BCP-ALL is deletion or hyper-methylation of the *CDKN2A/B* locus, which encodes the cell-cycle regulatory proteins p16Ink4a and p15Ink4b as well as the apoptotic regulatory protein p14Arf, which inhibits Mdm2 to stabilize p53 (5, 6, 25, 64, 80, 83, 202). Decreased levels of *CDKN2A/B* are found at diagnosis in BCP-ALL patients, but cells expressing low *CDKN2A/B* are enriched at relapse and in some studies have been found to be associated with poor clinical outcome and increased risk of relapse (36, 37, 43, 228-234). *CDKN2A/B* loss is extremely common in *BCR-ABL1*+ BCP-ALL patients, and in a mouse model of *BCR-ABL1*+ BCP-ALL specific loss of the Arf protein results in more aggressive disease and impaired response to imatinib (64, 74, 235). In patient-derived

xenograft mouse models, *CDKN2A/B* loss results in more aggressive disease from both *BCR-ABL1*+ and *ETV6-RUNX1*+ BCP-ALL patient samples (42, 49). The frequent loss of *CDKN2A/B* at both diagnosis and relapse and its effect in mouse models suggests that loss of this gene results in a more aggressive disease with inferior therapeutic response, particularly in the context of *BCR-ABL1*+ cases.

*Apoptotic regulation by Bcl-2 family members*

The Bcl-2 family of pro- and anti-apoptotic proteins has also been extensively studied in BCP-ALL; these proteins control the activation of mitochondrial membrane depolarization and thus caspase-mediated apoptosis (236). In gene expression analysis, *BCL2* was one of 15 apoptotic genes associated with relapse in BCP-ALL patients, but higher Bcl-2 levels in patients have been found in various studies to have positive, negative, or no effect on clinical outcome (115, 121, 237, 238). In preclinical studies in leukemic cell lines and mouse models, however, high Bcl-2 was associated with resistance to anthracyclines and glucocorticoids (197, 239, 240). Levels of the pro-apoptotic Bcl-2 family member Bim have been reported to mediate response to GCs *in vitro* in both a Bcl-2 dependent and independent manner, but Bim loss in patients does not affect clinical response (197, 241, 242).

In contrast, there is a more consistent increase in levels of the anti-apoptotic protein Mcl-1 in GC-resistant BCP-ALL cell lines and patient samples, although there is no data concerning clinical outcome of patients expressing high levels of *MCL1* (207, 243-245). Down-regulation of *MCL1* levels or inhibition of the Mcl-1 protein in cell lines and mouse models sensitized leukemic cells to GC treatment; *MCL1* levels have also

been implicated in leukemia engraftment and TKI response in a *BCR-ABL1*+ BCP-ALL mouse model and in resistance to a BH3 mimetic in a BCP-ALL xenograft model (214, 243, 246-249).

Additional Bcl-2 family members may also play a role in therapeutic response in BCP-ALL. Pro-apoptotic *BCL2L13* is a predictor of poor outcome in B- and T-ALL patients and is associated with L-asparaginase resistance (245). In a small study of *ETV6-RUNX1*+ BCP-ALL, several patients experienced loss of the pro-apoptotic Bcl-2 family member *BMF* at relapse, and knockdown of *BMF* in a *ETV6-RUNX1*+ BCP-ALL cell line increases resistance to GCs (35).

*Additional mediators of caspase-dependent apoptosis*

Other components of the intrinsic apoptotic cascade, including multiple caspases, have also been identified as part of a gene expression signature associated with clinical response (250). Pro-apoptotic caspases are activated downstream of Bcl-2 family proteins, and expression levels of caspases 1 and 2 in B-ALL cells have been found to affect *in vitro* response to GCs alone and in combination with several chemotherapeutics (245, 251). Similarly, inhibitor of apoptosis proteins which can bind to and activate caspases, such as survivin (*BIRC5),* have high expression in BCP-ALL patient samples; survivin is up-regulated at relapse and is an indicator of worse event-free survival and overall survival (46, 250, 252, 253). Knockdown of survivin in ALL cell lines and primary ALL samples decreases cellular viability and increases apoptosis and chemotherapeutic sensitivity, and in xenograft mouse models survivin knockdown reduced tumor growth of leukemic cells (253-256). Decreased levels of *XIAP*, another

inhibitor of apoptosis protein, were also found to sensitize ALL cells to chemotherapy *in vitro* (257).

*DNA repair enzymes*

Several of the drugs used to treat BCP-ALL induce apoptosis by causing DNA damage, and analysis of patient samples showed loss of the DNA repair enzymes *MSH2*, *MSH6,* and their regulatory genes at relapse (37, 205, 245, 258, 259). Loss of these genes in cell lines or primary patient samples was also associated with *in vitro* chemotherapeutic resistance (37, 205, 245, 258). Lower expression of *PARP*, an enzyme involved in both DNA repair and cell death, is found in leukemia patient samples that have *in vitro* resistance to chemotherapeutic agents, and inhibition of Parp in BCP-ALL patient samples can rescue defects in p53 activation and restore p53-dependent apoptosis in samples previously resistant to DNA-damage mediated apoptosis *in vitro* (221, 245).

*Cell cycle regulation*

Relapsed BCP-ALL samples often express altered levels of cell-cycle regulatory genes including cyclins B and E, their transcriptional activator Foxm1, and the cyclin dependent kinase inhibitor p57Kip2, as well as a general relaxation of cell-cycle checkpoints and a shift towards more mitotically active cells (67, 194, 216, 217, 260). Additionally, reduced levels or less activation of the retinoblastoma protein (*RB1*), a tumor suppressor and negative regulator of the cell-cycle, is associated with poor response to GCs and a higher probability of relapse (261, 262). Methylation of cell-cycle

genes is common in newly diagnosed and relapsed BCP-ALL samples, but has no association with clinical outcome with the exception of *BCR-ABL1*+ BCP-ALL; in patients of this subtype methylation of two or more cell-cycle regulatory genes is significantly associated with higher probability of relapse and lower overall survival (217). Accordingly, cells transformed with viral Abl show forced expression of *CDK6,* which promotes cell-cycle progression, cell division, and resistance to the TKI imatinib (263).

*Glucose consumption*

Alterations to carbohydrate metabolism can also affect drug response, particularly to GCs. GC resistant ALL cell lines often have increased glucose consumption, and shortly after GC exposure cells from BCP-ALL patients show a shift toward higher glucose uptake and higher rates of glycolysis and gluconeogenesis (215, 264). In *BCR-ABL1*+ BCP-ALL cells, higher glycolytic activity is associated with resistance to TKIs in a mouse model (265). Both TKI resistance and GC resistance can be overcome by inhibition of glycolysis, and Mcl-2 knockdown synergizes with glycolysis inhibitors in GC resistant cell lines, indicating that increased glycolysis in treated BCP-ALL cells may function to escape apoptosis (214, 264-266). However, while this metabolic shift has also been observed in patient samples, there are no studies correlating clinical outcome with changes in glycolysis or glucose consumption (214, 215).

## Cell-intrinsic resistance to therapy via pro-survival signaling

### *The NFκB pathway*

In response to the DNA damage induced by chemotherapeutic agents, the up-regulation of signaling through pro-survival pathways like the nuclear factor kappa-light-chain-enhancer of activated B cells (NFκB) pathway can contribute to drug resistance and the establishment of MRD (70, 221). Signaling through the NFκB pathway can suppress p53-dependent pro-apoptotic signaling in BCP-ALL cells, and BCP-ALL patients have higher expression or activation of NFκB and its upstream regulators, although NFκB signaling has not been associated with changes in patient outcome (215, 221, 267, 268). Inhibition of NFκB signaling in BCP-ALL cell lines, patient samples, and xenograft mouse models sensitizes leukemia cells to oxidative stress, which can be induced by chemotherapy (269, 270).

### *The PI3K/Akt/mTOR pathway*

Chemotherapeutic agents can also activate phosphoinositide-3-kinase (PI3K) and its downstream mediators protein kinase B (Akt) and mammalian target of rapamycin (mTOR) in leukemic cells (70). Activation of components or positive regulators of the PI3K/Akt/mTOR pathway or deactivation of its negative regulator, the phosphatase and tumor suppressor PTEN, are associated with resistance to TKIs and GCs *in vitro*, and in patients is associated with reduced event free survival and overall survival (243, 249, 271-274). PI3K/Akt/mTOR signaling is activated in response to oxidative stress after chemotherapy, and inhibition of this pathway in cell lines, patient

samples, and mouse models leads to cell death and sensitization to TKIs, GCs, and the anthracycline doxorubicin (64, 132, 243, 271, 272, 274-285).

*Syk and the pre B-cell receptor*

Both the NFκB and PI3K/Akt/mTOR signaling pathways are activated by spleen tyrosine kinase (Syk) in response to oxidative stress (70). Syk can also activate the pro-apoptotic/arrest PLCγ pathway, and differential regulation of these pathways can determine whether cells survive, arrest, or undergo apoptosis; Syk loss in B cells typically results in apoptosis or loss of cell-cycle checkpoints, and aberrant Syk signaling promotes growth or survival in several BCP-ALL subtypes (75, 90, 286, 287). Relapse in BCP-ALL is associated with higher levels of Syk and its family member the Zap70 kinase, and Syk inhibition induces apoptosis in patient-derived *BCR-ABL1* negative BCP-ALL cells and extends survival in xenograft mouse models (90, 270, 288, 289). Interestingly, it was recently shown in a patient-derived xenograft mouse model of *BCR-ABL1*+ BCP-ALL that an incremental increase in Syk activation can mimic hyperactivation of a self-reactive B-cell receptor and thus result in leukemic cell death via negative selection, indicating that the effect of Syk alteration may depend on genetic context (290).

*The Jak/Stat pathway*

Another commonly activated pro-survival signaling pathway in BCP-ALL cells is the Jak/Stat pathway; in normal B-cells the IL7 receptor can activate the Jak1 and Jak3 kinases to promote phosphorylation and activation of Stat3 and Stat5, which can in turn

effect transcriptional changes that promote survival and proliferation (291). *CRLF2*, which is rearranged in a subset of BCP-ALL patients, is also thought to activate the Jak kinases, as is signaling downstream of Bcr-Abl and the pre-BCR; Jak kinases themselves can also be rearranged or mutated to promote activation in BCP-ALL patients (64, 80, 90). While there are no clinical studies investigating whether alterations in Jak/Stat signaling are enriched at relapse in BCP-ALL patients, Jak kinase inhibitors have efficacy on Jak-activated cell lines, patient samples, mouse models, and even a small subset of patients with *BCR-ABL1*-like BCP-ALL, indicating that Jak/Stat signaling may be important for leukemia cell survival (111, 276, 278, 292). Interestingly, expression of CD45, a protein tyrosine phosphatase that inhibits signaling by Jak kinases, is associated with poor response to GCs, MRD positivity, and lower rate of EFS in BCP-ALL patients, indicating that Jak activation may not always be required for development of MRD (293). As Jak kinases are normally activated downstream of cytokine receptors, alterations to this signaling pathway may represent an example of leukemia cells hijacking normal survival signals from the microenvironment to become resistant to therapy.

*Wnt signaling*

Both the canonical Wnt/β-catenin and the noncanonical Wnt/$Ca^{2+}$/NFAT pro-survival signaling pathways have putative roles in BCP-ALL response to therapy. In a mouse model of *BCR-ABL1*+ BCP-ALL, Wnt/ $Ca^{2+}$/NFAT activation protects against imatinib-mediated cell death *in vitro*, and the NFAT inhibitor cyclosporine A synergizes with dasatinib *in vivo* (294, 295). Cyclosporine A can also induce apoptosis in multiple

drug-resistant BCP-ALL subtypes, but as cyclosporine A can also inhibit the multi-drug efflux pump P-gp it is unclear in this case whether Wnt/$Ca^{2+}$/NFAT signaling is responsible for this effect; the synergy with TKIs in *BCR-ABL1+* BCP-ALL was shown to be independent of drug efflux inhibition (294-296)

Similarly, regulators of the canonical Wnt/β-catenin pathway are expressed in most B-ALL cell lines and in patient samples (297-299). Expression of *LEF1*, a key mediator of Wnt signaling, and its targets are increased in BCP-ALL patients with shorter event free survival and a high relapse rate (281, 300). Overexpression of Wntless, a regulatory protein critical for the pro-survival effects of canonical Wnt signaling, is significantly correlated with relapse and poor survival in BCP-ALL patients (301). In general, decreased canonical Wnt signaling can induce apoptosis and sensitize to chemotherapy, GCs, and TKIs *in vitro* and in a xenograft mouse model, and stimulation of the Wnt pathway protects leukemic cells from apoptosis *in vitro* (297-303).

*MAPK cascades*

Mitogen-activated protein kinase (MAPK) pathways can also signal for either survival in the case of the classical MAPK pathway or cell death in the case of the p38 MAPK pathway (215, 304). Mutations in several components of the classical MAPK pathway that lead to increased pathway activation, including *NRAS, KRAS, FLT3, BRAF, and NF1*, are found in BCP-ALL patients and are associated with early relapse and CNS involvement (47, 304-308). Mutations in the Ras proteins in particular are enriched at relapse and are associated with chemo-resistance, GC resistance and reduced overall survival in BCP-ALL patients (306, 308, 309). Loss of *SPRED1*, a

negative regulator of the classical MAPK pathway, is associated with decreased event-free survival and overall survival in BCP-ALL patients (210). Similarly, inhibition of classical MAPK signaling is anti-leukemic against Ras-mutated BCP-ALL cells and results in sensitization to TKIs and GCs *in vitro* and in mouse models (308-310). In contrast, the p38 MAPK pathway has more diverse effects in preclinical studies, with its inhibition resulting in resistance to GCs *in vitro* but extending survival in a xenograft model of BCP-ALL (215, 311, 312).

*Other alterations in BCP-ALL cells*

In addition to these commonly affected mitogenic pathways, alterations in several other individual genes have been associated with cell-intrinsic drug resistance in BCP-ALL. For example, high expression of insulin-like growth factor binding protein 3 (*IGFBP3*) is characteristic of specific BCP-ALL subtypes and may predict relapse in *BCR-ABL1*+ BCP-ALL (313). Relapse specific mutations have also been identified in the *PRPS1* gene, a rate limited biosynthesis enzyme in the *de novo* purine synthesis pathway (314). BCP-ALL patients with these mutations have competitive inhibition of thiopurine activation and thus chemotherapeutic resistance and experience early relapse (314).

**MRD development is enhanced by ability to maintain a less differentiated state**

*B-cell development genes*

Mutations in B-cell development genes, including *EBF1*, *IKZF1*, *RAG1/2*, and *PAX5*, are found in around two-thirds of BCP-ALL cases (5, 64, 65, 315). Deletions or

mutations in *PAX5*, a transcription factor that controls B-cell lineage identity and commitment, are found in about a third of *BCR-ABL1* negative BCP-ALL patients and up to half of *BCR-ABL1*+ BCP-ALLs; loss of *PAX5* leads to a differentiation block early in B cell development and increases self-renewal, but is not associated with clinical outcome (5, 22, 25, 27, 37, 64, 77, 80, 83, 315). Similarly, mutations or deletions in early B cell factor 1 (*EBF1*), a B lineage transcription factor that co-regulates target genes with *PAX5*, are found in BCP-ALL patients and in some studies have been found to occasionally be gained at relapse, but are not associated with worse prognosis in patients (22, 27, 37, 64, 83). However, *EBF1* alterations can be associated with elevated MRD after induction therapy in pediatric BCP-ALL patients if high-risk patients (e.g. *BCR-ABL1*+, *MLL*-rearranged) are removed from the analysis set (315). *PAX5* and *EBF1* alterations may not affect clinical outcome because they don't exert an effect on hematopoietic stem cell (HSC) transcriptional programs; in contrast, the Ikaros transcription factor (*IKZF1*), the status of which does affect clinical outcome in BCP-ALL, normally functions to repress HSC-specific gene expression programs (29, 64).

*Transcriptional regulation by Ikaros*

Ikaros is a zinc-finger protein that plays a role in both T- and B-lineage specification, and while its loss results in ablation of the B-cell compartment, reduced levels of Ikaros result in a developmental block at the pro-B stage (29, 64). Deletions or mutations in the *IKZF1* gene are found in about 70 - 80% of *BCR-ABL1*+ BCP-ALL patients and about 15% of *BCR-ABL1* negative BCP-ALL patients, although they are enriched in the *BCR-ABL1*-like BCP-ALL subset (5, 25, 64, 77, 316). Recently, several

novel single-nucleotide mutations in the *IKZF1* gene, all of which are predicted to decrease gene function, were identified in more than 10% of a set of BCP-ALL patients previously identified as *IKZF1* wild-type, indicating that Ikaros alterations may be even more common than previously thought (317). The vast majority of patient studies indicate that *IKZF1* loss is more common at relapse, is associated with poor clinical outcome regardless of subtype, and promotes resistance to TKIs in *BCR-ABL1*+ BCP-ALL patients, particularly when studies compare *IKZF1* mutant patients to *IKZF1* wild-type patients that are matched in terms of other risk criteria (e.g. cytogenetic subtype or WBC count at diagnosis) (5, 22, 26, 27, 29, 37, 47, 64, 65, 77, 80, 89, 210, 315, 318-323). There is some disagreement concerning both the frequency of *IKZF1* alterations and their affect on clinical outcome, particularly in adult *BCR-ABL1* negative BCP-ALL patients, but the studies that have shown no effect of *IKZF1* loss on outcome have largely not controlled for other risk factors nor could they take into account the recently discovered single nucleotide mutations in *IKZF1*, and so they may be incorrectly identifying Ikaros-mutated patients as being Ikaros wild-type (29, 317, 324-326). Additionally, in mouse models and cell lines Ikaros loss results in differentiation block at an early B-cell stage, decreased TKI-mediated cell death, and more aggressive disease in mice if combined with Bcr-Abl, all of which are indicative of a more aggressive leukemia that may respond less well to treatment (64, 327, 328).

*The polycomb protein Bmi1*

Silencing of *CDKN2A/B*, which is often associated with poor prognosis in BCP-ALL, has also been implicated in hematopoietic self-renewal as part of a larger

transcriptional program put into place by the polycomb protein Bmi1 (64, 329). Loss of *CDKN2A/B* is particularly common in *BCR-ABL1*+ BCP-ALL, but not in the related *BCR-ABL1*+ disease chronic myelogenous leukemia with the exception of those CML patients who experience a transition to a lymphoid blast phase, indicating that *CDKN2A/B* loss may be specific to B-lineage leukemias (64, 86, 330). Interestingly, a recent study shows that *BMI1* expression can reprogram CML cells into BCP-ALL cells via induction of a HSC specific transcriptional changes and a blockage in B-lineage differentiation, indicating that Bmi1-mediated silencing of *CDKN2A/B* may be part of a transcriptional program that functions to halt differentiation of *BCR-ABL1*+ pre-B cells (329).

*Additional B-lineage genes*

A number of additional genes typically expressed in specific B-lineage cells are activated in BCP-ALL. Activation induced cytadine deaminase (*AICDA*), which causes somatic hypermutation and is normally only expressed in germinal center B cells, is found to be expressed *BCR-ABL1*+ BCP-ALL patient samples and can induce single-strand DNA breaks in genes involved in therapeutic response, such as *CDKN2A/B* (331). In *BCR-ABL1*+ leukemic cells, *AICDA* expression also has been shown to increase resistance to the TKI imatinib (332). The recombination-activating genes (*RAG1* and *RAG2*), which are typically expressed in developing lymphocytes and mediate antigen-receptor gene rearrangement, have also been postulated to be responsible for loss of tumor suppressor genes including *IKZF1* and *CDKN2A/B* in BCP-ALL patients (333).

*BCL6*, a transcriptional repressor normally required for germinal center formation and antibody affinity maturation in more differentiated B cells, can also be inappropriately activated in BCP-ALL cells (64, 334). In a mouse model of *BCR-ABL1*+ BCP-ALL, Bcl6 up-regulation promotes survival after TKI treatment, and inhibition of Bcl6 in both murine *BCR-ABL1*+ BCP-ALL and a patient-derived xenograft model synergized with TKI therapy (335). Bcl6 is also activated in pre-BCR+ BCP-ALL, and inhibition of Bcl6 in xenografts from pre-BCR+ patients leads to tumor reduction (90).

*General hematopoietic differentiation*

Other factors involved in differentiation in hematopoietic lineages have been identified in single studies to affect BCP-ALL response. High levels of the marker of early hematopoietic progenitor cells *BAALC* in BCP-ALL patients is associated with therapy resistance and poor prognosis, particularly in *BCR-ABL1* and *MLL-AF4* negative patients (336). While the function of *BAALC* is unknown, cells that express high *BAALC* have transcriptional up-regulation of stem cell markers and chemoresistance genes (336). *XBP1*, which is required for terminal differentiation of B cells and can mitigate ER stress by engaging the UPR, is highly expressed in BCP-ALL patients with poor outcome, and loss of *XBP1* or other UPR regulators in BCP-ALL cells and mouse models promotes leukemic cell death and longer survival in mice (337). In a study of pediatric BCP-ALL patients, a polymorphism that results in higher expression of the T-cell development-associated transcription factor *GATA3* is over-represented in *BCR-ABL1*-like BCP-ALL cases and is associated with increased risk of relapse (338). In general, genetic alterations that serve to change the differentiation state of BCP-ALL

cells are commonly identified in patients; maintenance of either a less differentiated or more mutable cell state in leukemic cells promotes the development of MRD.

## Drug resistance through interaction with the leukemic microenvironment

Multiple studies have found that resistance to therapeutics *in vivo* does not necessarily correlate with resistance *in vitro*, indicating that the *in vivo* microenvironment can mediate drug resistance and thus the development of MRD (74, 237, 339). Interaction of BCP-ALL cell lines or patient samples with bone-marrow derived stromal cells can promote leukemia cell survival, increase the percentage of actively dividing cells, and protect from cell death induced by chemotherapy (340-342). There is significant evidence that not only is the bone marrow a protective microenvironment for leukemia cell survival and growth, but also that leukemia cells can remodel the bone marrow niche to promote their own survival (340, 342-349).

### *Modulators of cell adhesion*

Integrins are a family of cell surface receptors composed of α and β subunits that are responsible for cell adhesion to the extracellular matrix, and with their counter receptors (VCAMs, ICAMs, fibronectin, collagen and laminin) integrins regulate the interaction of B-cell progenitors and thus BCP-ALL with the bone marrow niche (340, 342, 350, 351). High levels of $\alpha_4\beta_1$ integrin (VLA4) in BCP-ALL patients at first relapse is associated with poor response to therapy and poor clinical outcome, and in primary BCP-ALL samples and BCP-ALL cell lines VLA4 expression was required to maintain

leukemia cell adhesion to stroma (72, 73, 350, 352). VLA4-mediated adhesion of leukemic cells to the bone marrow stroma signals for cellular proliferation, differentiation, migration, adhesion, polarity, and survival, and can protect from TKI- and chemotherapy-mediated cell death in co-culture experiments and xenograft mouse models (72, 73, 350). The related integrin VLA5 ($\alpha_5\beta_1$) and its downstream signaling molecule focal adhesion kinase (*FAK*) can also promote adhesion of *BCR-ABL1*+ BCP-ALL cells to fibronectin, and in a xenograft mouse model inhibition of VLA5 or FAK delayed leukemic engraftment and sensitized cells to the TKI nilotinib (353). Additionally, BCP-ALL patients positive for CD11b (*ITGAM*), an α integrin subunit, have increased risk of MRD after induction therapy (354).

Additional cell adhesion molecules may also play a role in BCP-ALL engraftment in the bone marrow and therapeutic response. Selectins are expressed by bone marrow endothelial cells, and in a mouse model of chronic myelogenous leukemia E-selectin was shown to be crucial for bone marrow homing and engraftment, although this has not been shown for *BCR-ABL1*+ BCP-ALL (340, 355). About 30% of BCP-ALL patients express significant levels of Fat1 cadherin, and in two separate studies of matched diagnosis and relapse samples high *FAT1* expression was found to be predictive of shorter RFS and OS (356). *RPIB9*, which is though to be involved in B-cell adhesion to bone marrow stroma, is aberrantly over-expressed in BCP-ALL patients, but no connections have been made to clinical outcome (357). BCP-ALL patients with high expression of the *EMP1* gene, which signals via Src family kinases and is thought to participate in cell-cell junctions, have significantly worse clinical outcome and increased *in vitro* GC resistance; knockdown of *EMP1* in BCP-ALL cells results in abrogation of

leukemic migration towards and adhesion to stromal cells as well as increase leukemia cell apoptosis and sensitization to GCs (358).

*Cytokine/chemokine signaling*

Cytokines and chemokines, which can modulate growth, maturation, and response of normal B-lymphocytes, can also regulate BCP-ALL survival and localization (340, 343). The best-studied cytokine signaling axis in BCP-ALL is that of CXCL12, also known as stromal cell-derived factor 1 or SDF-1, and its receptor CXCR4 or the SDF-1 receptor (340, 359). CXCL12/CXCR4 signaling regulates the homing and retention of hematopoietic stem cells to the bone marrow; BCP-ALL cells typically express high levels of CXCR4 on their surface, and high CXCR4 surface expression or high levels of activated CXCR4 on BCP-ALL patient blasts is associated with worse clinical outcome (340, 359-361). Adding CXCL12 to BCP-ALL cultures results in increased leukemic proliferation, likely through CXCR4-mediated activation of Jak/Stat and Src family kinase signaling, and is protective against TKI-mediated killing of *BCR-ABL1*+ BCP-ALL cells (340, 362, 363). Blocking the CXCR4/CXCL12 axis using CXCR4 inhibitors or antagonists in both murine BCP-ALL models and xenograft models resulted in mobilization of leukemic cells into the blood, inhibition of CXCL12-mediated chemotaxis and homing to the bone marrow niche, and sensitization of leukemia cells to both TKIs and chemotherapy (340, 359, 364-367). Additionally, high levels of the oncofoetal antigen 5T4 in BCP-ALL patients are associated with poor clinical outcome, and 5T4 expression increased CXCL12/CXCR4 mediated chemotaxis of a BCP-ALL cell line in a mouse xenograft model (368).

Signaling via other cytokines outside of the CXCL12/CXCR4 axis can also promote leukemia survival (343, 348). Polymorphisms in BCP-ALL patients that result in higher levels of the anti-inflammatory cytokines IL-10 and TGFβ are associated with increased relapse rate and patient classification as high-risk (369). IL-7, which can activate downstream Jak/Stat signaling, was found to be protective against TKI-mediated killing of *BCR-ABL1*+ BCP-ALL cells in cell culture and in a murine model of leukemia (74, 235, 292, 370). Additionally, both IL-7 and thymic stromal lymphopoeitin (TSLP), which shares a receptor with IL-7, can stimulate proliferation of leukemia cells and protect against inhibitors of the mTOR signaling pathway in BCP-ALL cell lines and primary BCP-ALL samples (371). IL-3 can also have prosurvival effects; in *in vitro* experiments, a subset of *BCR-ABL1*+ cells resistant to imatinib was found to protect sensitive leukemic cells in co-culture via secretion of IL-3 (372). Similarly, signaling through both the CXCL13/CXCR5 and CCL19/CCR7 axes in BCP-ALL cells can protect leukemic cells from apoptosis mediated by the cytokine tumor necrosis factor alpha (TNFα) (348).

*Extrinsic cell death pathway*

TNFα is a member of the pro-death family of cytokines that can induce apoptotic cell death upon binding to their receptors, and ability to interact with or escape from pro-death cytokines can potentially also affect establishment of MRD in BCP-ALL (373). High expression of the TNF receptor CD40 in BCP-ALL patients has been shown to prevent late relapse and be predictive of good clinical outcome, although one study found that CD40 positive blasts also tended to up-regulate the Fas receptor CD95 (373,

374). Binding of Fas ligand (FasL) to the Fas receptor stimulates the extrinsic apoptotic pathway, but resistance to Fas-mediated cell death even when CD95 is expressed has been shown in BCP-ALL patient samples to be due to up-regulation of the caspase inhibitor c-FLIP (375). Similarly, an examination of multiple *BCR-ABL1*+ BCP-ALL cell lines and patient samples found that none of them were sensitive to Fas-mediated cell killing, and so the role of Fas-mediated apoptosis in MRD establishment in BCP-ALL patients is still unclear (376).

Another member of the tumor necrosis factor superfamily that may play a role in BCP-ALL is the pro-death cytokine TRAIL, or TNF-related apoptosis inducing ligand. TRAIL receptors were found to be over-expressed in samples from high hyperdiploid BCP-ALL patients, who generally have a favorable prognosis (245). TRAIL was also found to have anti-leukemic activity against both *BCR-ABL1*+ and *BCR-ABL1* negative BCP-ALL patient samples and BCP-ALL cell lines *in vitro* and in a xenograft mouse model, although some samples were resistant (376-382). Resistance to TRAIL-mediated apoptosis in BCP-ALL cells can be achieved via activation of the PI3K/Akt or NFκB pathways, presence of dysfunctional apoptotic machinery such as absence of caspase-8, or exogenous Wnt/β-catenin pathway activation (376, 380-382) Interestingly, in some TRAIL-resistant cells, TRAIL could actually stimulate proliferation of BCP-ALL cell lines in culture via up-regulation of the NFκB pathway, indicating that TRAIL has disparate effects on BCP-ALL cells with different genotypes (380).

*Growth factors*

Inappropriate growth factor signaling may also affect BCP-ALL cell survival. The epidermal growth factor receptor ErbB2 aka Her2 is expressed in about a third of BCP-ALL patients and more than half of *BCR-ABL1*+ BCP-ALL patients, and in adults ErbB2 positivity is associated with chemoresistance and increased rate of relapse (383, 384). In *BCR-ABL1*+ BCP-ALL cell lines, inhibition of ErbB2 increased TKI sensitivity, indicating that ErbB2 expression may promote resistance to targeted therapy as well as chemotherapy (383). Nerve growth factor, which is normally involved in hematopoiesis, proliferation, and B cell differentiation via binding to its high-affinity receptor, can also induce cell death via binding to its low affinity receptor p75NTR; relapsed or high-risk pediatric BCP-ALL patients expressed significantly lower levels of p75NTR than those patients who were stratified as low risk or did not relapse (385).

*Other secreted factors*

In addition to changes in cell adhesion and signaling via cytokines and growth factors, stromal cells have also been shown to provide substrates that directly promote BCP-ALL chemoresistance and survival. In particular, bone marrow-derived stromal cells have been shown to produce and secrete asparagine, which can be taken up by BCP-ALL cells and thus protect from L-asparaginase-mediated cell death (347, 386). This production and secretion of asparaginase by stromal cells is promoted by the expression of insulin like growth factor binding protein 7 (*IGFBP7*) in leukemic cells, and higher levels of *IGFBP7* expression in *BCR-ABL1* negative BCP-ALL patients is associated with significantly worse clinical outcome (386). Similarly, decreased ability of

stromal cells to produce and secrete cysteine, which is the limiting substrate to produce the antioxidant glutathione in BCP-ALL cells, impairs the ability of coc-cultured BCP-ALL cells to tolerate oxidative stress and results in leukemic cell death (387). Bone-marrow derived stromal cells have also been shown to produce prostaglandin $E_2$, which upon binding to its receptor on co-cultured primary BCP-ALL cells stimulates production of cAMP and activation of protein kinase A, thus preventing p53 accumulation and DNA-damage induced leukemic cell death (388). Additionally, in co-culture experiments of BCP-ALL cell lines with established bone marrow stromal lines, stromal cells generated galectin 3 (*LGALS3*) and secreted it or expressed it in their surface; galectin 3 was then internalized by BCP-ALL cells and stimulated transcription of endogenous *LGALS3*, which served to increase NFκB signaling and promote tolerance to chemotherapeutic agents (389). The clinical effects of stromal cell production of cysteine, prostaglandin $E_2$, and galectin 3 have not yet been investigated in BCP-ALL.

Up-regulation of basignin (*BSG*), a surface protein that induces production of matrix-metalloproteins and thus promotes tumor cell invasiveness, has been found in various small BCP-ALL patient studies to be predictive of poor clinical outcome, but other studies have found that it does not have a significant effect (390, 391). Activation of opiod receptors, which reduce intracellular cAMP levels and induce cell death, was shown in a xenograft model of BCP-ALL to inhibit tumor growth and sensitize to the anthracycline doxorubicin, although the effect of opiods has not been studied in BCP-ALL patients (392). Similarly, in mice xenografted with a BCP-ALL cell line or primary BCP-ALL samples, osteopontin secretion by osteoblasts in the bone marrow was shown

to promote tumor cell dormancy and thus protect from chemotherapy-mediated cell death, but this has not been studied in BCP-ALL patients (393).

*The role of hypoxia and angiogenesis*

There is accumulating evidence that leukemic cells can remodel the bone marrow microenvironment in order to make it more protective via leukemic cytokine secretion; small protective niches have been observed in the bone marrow of mice xenotransplanted with BCP-ALL cells after both chemotherapy and TKI treatment (345, 349). Additionally, the bone marrow of leukemia patients tends to be both angiogenic and hypoxic, and this is thought to be due to a remodeling effect of the BCP-ALL cells (340, 343, 348, 351, 394). The pro-angiogenic factors VEGF and HIF1α are both expressed in leukemic bone marrow, and expression of these factors is associated with worse prognosis in BCP-ALL patients (351, 394-397). In xenograft mouse models, hypoxia in the bone marrow promotes chemoresistance of BCP-ALL cell lines, and inhibition of hypoxia or HIF1α can sensitize BCP-ALL cells to therapy (395, 398).

*Leukemic interactions with non-stromal cells*

Additional interactions with the *in vivo* microenvironment have been implicated in BCP-ALL survival and response to therapy. Like all tumors, leukemia cells must avoid recognition by the immune system; BCP-ALL cells typically do not co-stimulate T cells to activate their cytotoxicity and so instead lead to T cell anergy, although modulation of toll-like receptors, particular *TLR2*, on the surface of BCP-ALL cells may be able to overcome this (399). Interestingly, mesenchymal stem cells from low or intermediate

risk B-ALL patients at diagnosis promote antitumor activity in NK cells, and can remodel mesenchymal stem cells from healthy patients to do the same, but is not yet clear what effect this has on patient outcome (400).

Finally, interaction with non-immune, non-bone marrow cells of the *in vivo* microenvironment can also have an effect on BCP-ALL survival and therapeutic response; co-culture of murine and human BCP-ALL cell lines with adipocytes protected from cell death mediated by chemotherapy, GCs, and TKIs independent of cell contact (401). This finding is particularly interesting in light of the fact that obesity is associated with increased rate of relapse in pediatric ALL patients, and obesity in a syngeneic mouse model increased relapse after chemotherapeutic treatment (401). In general, the *in vivo* tumor microenvironment can have diverse and sometimes opposing effects on the survival of BCP-ALL cells and the establishment of MRD in these patients.

## Strategies for treatment and investigation of MRD in BCP-ALL

### *Targeting known mechanisms of drug resistance*

A number of the signaling pathways that have been described as contributing to MRD in BCP-ALL can be targeted therapeutically; kinase inhibitors can be used to target not only the Abl kinase but also Src family kinases, Jak kinases, members of the classical MAPK signaling pathway like B-Raf or Flt3, the PI3K/Akt/mTOR pathway, and additional kinase signaling pathways that may be inappropriately activated in BCP-ALL, and in preclinical and clinical studies of preBCR+, *BCR-ABL1*+, and *BCR-ABL1*-like BCP-ALL these targeted therapeutics have been shown to be effective (90, 111, 402).

Modulation of epigenetic modifiers may overcome changes in histone acetylation or DNA methylation that can lead to MRD; for example, there is evidence that patients with GC resistance mediated by *CREBBP* mutations or other epigenetic changes may be sensitive to histone deactylase inhibitors (402-404). Proteasome inhibitors have also been an active area of study, as they tend to impair tumor growth and inactivate NFκB signaling, which can cause MRD in BCP-ALL through a variety of mechanisms (403). Current clinical trials for newly diagnosed and relapsed BCP-ALL include modifications to current protocols as well as a number of additional therapeutics, including novel chemotherapeutics not currently used to treat BCP-ALL, kinase inhibitors targeting Abl, Jak, mTor, Flt3 and other tyrosine kinases, PARP inhibitors, proteasome inhibitors, DNA methyl-transferase inhibitors, histone deacetylase inhibitors, and immunotherapies both of the antibody-based and cell-based variety (403).

*Immunotherapies*

Treatment with immunotherapies has recently proven to be effective in patients with relapsed BCP-ALL, which historically has extremely poor clinical prognosis (403, 405). These therapies can be either antibody-based or cell-based; antibody-based immunotherapies consist of both unconjugated and conjugated variants (405, 406). Unconjugated monoclonal antibodies recognize surface markers of BCP-ALL cells, such as CD20, CD22, or CD52, and engage the healthy immune system to recognize and kill leukemic cells via antibody-dependent cell cytotoxicity (405, 406). However, our lab recently showed in a humanized mouse model of two-hit B-cell lymphoma that resistance to these unconjugated antibodies can be achieved via down-regulation of

macrophage-mediated cell killing in specific microenvironments, indicating that resistance to the single agent can occur; these antibodies are typically given in combination with chemotherapy, which should overcome the single-agent resistance (405-407).

BCP-ALL patients can also be treated with conjugated antibodies, which consist of a monoclonal antibody (targets include CD22, CD19) conjugated to a toxic agent; these conjugated antibodies are effective as single agents (405, 406). Additionally, blinatumomab is a bispecific antibody that engages both CD19 on BCP-ALL cells and CD3 on T cells and leads to activation of cytotoxic T cells to induce leukemic cell death (405, 406). Addition of rituximab, an unconjugated CD20 antibody, to conventional chemotherapy has improved cure rates in adult BCP-ALL patients by about 15%, and both conjugated and bispecific T-cell engaging antibody therapy have improved outcome in relapsed BCP-ALL patients (406).

Recent studies have also made use of chimeric antigen receptors (CARs) to engineer autologous T cells from BCP-ALL patients to recognize CD19 on leukemic cells and thus generate immunity against the disease (408,409). This cell-based immunotherapy has been extremely effective in relapsed BCP-ALL patients, with response rates upwards of 70%; in contrast, only about 30% of relapsed BCP-ALL patients respond to salvage chemotherapy (408). However, there is associated toxicity with CAR-T cell therapy in the form of cytokine release syndrome, and at least one patient experienced relapse characterized by the expansion of CD19 negative leukemic blasts that could not be targeted by the CAR-T cells (408). This therapy has not yet been tested on newly diagnosed BCP-ALL patients, nor do any animal models currently

exist, which will be crucial for understanding those cases in which cell-based immunotherapy does not cause remission (408).

*Mouse models for the study of MRD in BCP-ALL*

Due to the numerous contributions that the microenvironment makes to the development of MRD in BCP-ALL, preclinical mouse models have been and will continue to be vital both for studying mechanisms of resistance to current therapies as well as testing novel therapeutics or new combinations of existing treatment modalities. Xenograft models, in which human cells are transplanted into mice, have improved to the point where leukemic cells transplanted into immunocompromised mice engraft into the bone marrow, rather than growing in intradermal or subcutaneous compartments (410). This approach allows for modeling of human disease in its native bone marrow niche, albeit in an immunocompromised host; however, these immunocompromised mice have a tendency toward spontaneous lymphomas and must be carefully monitored (410). Studies utilizing patient-derived xenografts (PDXs), in which samples from a BCP-ALL patient are each transplanted into several immunocompromised recipient mice, have allowed for isolation of populations of cells with varying genetic background, engraftment efficiencies, and therapeutic response (42, 43, 410, 411). While these PDXs can be used to study MRD development, it might be necessary to look at multiple different xenografts to fully encompasses the oligoclonality present in BCP-ALL patients (42, 43, 410, 411).

As an alternative to xenograft models, a number of models of murine BCP-ALL also exist, and can be generated either by retroviral transduction and transplantation of

murine precursor bone marrow cells or by creating a transgenic mouse (410). The transduction and transplantation models typically have a shorter time to leukemic presentation and allow for *ex vivo* manipulation of leukemia cells to perturb genes of interest, but they do not fully mimic human cancer origin, may require immunosuppression in the recipient mouse, and the associated viral integration into cells runs the risk of being mutagenic on unintended targets (412). There are also chemical carcinogen-induced mouse models of BCP-ALL, but it is difficult to control exactly what genes may be affected by carcinogenesis and so these models may diverge somewhat from the human disease (410).

Transgenic mouse models of *ETV6-RUNX1*, *E2A-PBX1*, *E2A-HLF*, *BCR-ABL1*, *MLL-AF4*, and *PAX5* +/- BCP-ALL all exist, as do transduction/transplantation models of *ETV6-RUNX1*, *E2A-HLF*, *BCR-ABL*, *MLL-AF4*, and *MLL-ENL* BCP-ALL (410). Many of these translocations are not sufficient to cause leukemia on their own, indicating that additional genetic alterations likely exist in these models, and these additional alterations may not faithfully replicate the human disease. Additionally, some therapeutic modalities, such as the immunotherapies, cannot be studied in murine leukemia models. Careful model selection is crucial to the design of preclinical studies for the treatment of BCP-ALL or investigation into causes of MRD in the disease.

### *In vivo* RNAi-based screening to investigate mechanisms of resistance to dasatinib in a transplantable model of *BCR-ABL1*+ BCP-ALL

Here I describe the use of a previously established transduction/transplantation $p19^{Arf-/-}$, *BCR-ABL1*+ BCP-ALL mouse model to study *in vivo* response to the TKI dasatinib. Leukemia cells in this model can be genetically manipulated *ex vivo,* and upon transplant into non-irradiated, immunocompetent, syngeneic recipient mice they seed to the bone marrow and spleen and then expand to give rise to a multiclonal BCP-ALL that responds to therapy in a manner similar to the human disease (74, 187, 235, 413). Previous work in our lab has shown that this model can be used to introduce genome-scale shRNA libraries *in vivo* to identify context-specific mediators of leukemia progression (413).

I have modified our previous approach in order to perform parallel longitudinal screens *in vivo* and *in vitro* with an unbiased shRNA library to identify genetic mediators of response to dasatinib. This longitudinal screen design is meant to minimize previously observed high levels of noise in *in vivo* screening datasets by allowing us to compare matched pre-treatment and post-treatment samples from the same mouse, rather than comparing samples from separate untreated and treated mice (413). In order to select candidate hits from this unique RNAi dataset, we have made use of independent component analysis, a form of blind-source separation that identifies latent variables in a dataset to isolate independent signals and separate those signals from background noise (414). The combination of longitudinal screening with independent component analysis allowed for identification of a set of high-value candidate hits that

validate in independent analyses as having significantly different behavior before therapy as compared to after.

We were also able to identify a number of hits that have behavior specific to the *in vivo* setting. Follow-up analysis on these hit identified *Pafah1b3*, a subunit of the platelet activating factor acetylhydrolase, as an *in vivo* specific mediator of response to dasatinib and potential therapeutic target for combination therapy, and *Abi3* as a potential essential gene in BCP-ALL, lower levels of which impede leukemia cell growth and promote resistance to dasatinib primarily *in vivo*. Together these studies illustrate the utility of unbiased *in vivo* RNAi screening for the investigation of mechanisms of MRD and identify a possible biomarker for therapeutic response in *BCR-ABL1*+ BCP-ALL as well as a potential drug target for combination therapy with tyrosine kinase inhibitors.

## References


1. American Cancer Society. *Cancer Facts & Figures 2014*. Atlanta: American Cancer Society; 2014.

2. American Cancer Society. *Cancer Facts & Figures 2015*. Atlanta: American Cancer Society; 2015.

3. Pui, C. H., Relling, M. V. & Downing, J. R. Acute lymphoblastic leukemia. *N Engl J Med.* **350,** 1535–1548 (2004).

4. Pui, C. H. & Evans, W. E. Treatment of acute lymphoblastic leukemia. *N Engl J Med.* **354,** 166–178 (2006).

5. Mullighan, C. G. New Strategies in Acute Lymphoblastic Leukemia: Translating Advances in Genomics into Clinical Practice. *Clin Cancer Res.* **17,** 396–400 (2011).

6. Bhojwani, D. D. & Pui, C.-H. Relapsed childhood acute lymphoblastic leukaemia. *Lancet Oncol.* **14,** e205–e217 (2013).

7. Litzow, M. R. Evolving paradigms in the therapy of Philadelphia-chromosome-negative acute lymphoblastic leukemia in adults. *Hematology Am Soc Hematol Educ Program.* 362–370 (2009).

8. Pui, C. H. Genomic and pharmacogenetic studies of childhood acute lymphoblastic leukemia. *Front Med.* **9,** 1–9 (2014).

9. Nguyen, K. *et al.* Factors influencing survival after relapse from acute lymphoblastic leukemia: a Children's Oncology Group study. *Leukemia.* **22,** 2142–2150 (2008).

10. Forman, S. J. & Rowe, J. M. The myth of the second remission of acute leukemia in the adult. *Blood.* **121,** 1077–1082 (2013).

11. Benjamini, O. *et al.* Phase II trial of hyper CVAD and dasatinib in patients with relapsed Philadelphia chromosome positive acute lymphoblastic leukemia or blast phase chronic myeloid leukemia. *Am J Hematol.* **89,** 282–287 (2014).

12. Styczynski, J. *et al.* Comparison of prognostic value of in vitro drug resistance and bone marrow residual disease on day 15 of therapy in childhood acute lymphoblastic leukemia. *Anticancer Res.* **32,** 5495–5499 (2012).

13. Volejnikova, J. *et al.* Minimal residual disease in peripheral blood at day 15 identifies a subgroup of childhood B-cell precursor acute lymphoblastic leukemia with superior prognosis. *Haematologica.* **96,** 1815–1821 (2011).

14. Borowitz, M. J. *et al.* Clinical significance of minimal residual disease in childhood acute lymphoblastic leukemia and its relationship to other prognostic factors: a Children's Oncology Group study. *Blood.* **111,** 5477–5485 (2008).

15. Brüggemann, M. Clinical significance of minimal residual disease quantification in adult patients with standard-risk acute lymphoblastic leukemia. *Blood.* **107,** 1116–1123 (2005).

16. Eckert, C. *et al.* Minimal residual disease after induction is the strongest predictor of prognosis in intermediate risk relapsed acute lymphoblastic leukaemia – Long-term results of trial ALL-REZ BFM P95/96. *Eur J Cancer.* **49,** 1346–1355 (2013).

17. Attarbaschi, A. *et al.* Minimal Residual Disease Values Discriminate Between Low and High Relapse Risk in Children With B-Cell Precursor Acute Lymphoblastic Leukemia and an Intrachromosomal Amplification of Chromosome 21: The Austrian and German Acute Lymphoblastic Leukemia Berlin-Frankfurt-Munster (ALL-BFM) Trials. *J Clin Oncol.* **26,** 3046–3050 (2008).

18. Beldjord, K. *et al.* Oncogenetics and minimal residual disease are independent outcome predictors in adult patients with acute lymphoblastic leukemia. *Blood.* **123,** 3739–3749 (2014).

19. de Haas, V. *et al.* Quantification of minimal residual disease in children with oligoclonal B-precursor acute lymphoblastic leukemia indicates that the clones that grow out during relapse already have the slowest rate of reduction during induction therapy. *Leukemia.* **15,** 134–140 (2001).

20. de Haas, V. *et al.* Minimal residual disease studies are beneficial in the follow-up of TEL/AML1 patients with B-precursor acute lymphoblastic leukaemia. *Br J Haematol.* **111,** 1080–1086 (2000).

21. Borowitz, M. J. *et al.* Prognostic significance of minimal residual disease in high risk B-ALL: a report from Children's Oncology Group study AALL0232. *Blood.* **126,** 964–971(2015).

22. Biondi, A. & Cazzaniga, G. Novel clinical trials for pediatric leukemias: lessons learned from genomic analyses. *Hematology Am Soc Hematol Educ Program.* **2013,** 612–619 (2013).

23. Ravandi, F. *et al.* Detection of MRD may predict the outcome of patients with Philadelphia chromosome-positive ALL treated with tyrosine kinase inhibitors plus chemotherapy. *Blood.* **122,** 1214–1221 (2013).

24. Pui, C.-H., Robison, L. L. & Look, A. T. Acute lymphoblastic leukaemia. *Lancet.* **371,** 1030–1043 (2008).

25. Mullighan, C. G. Molecular genetics of B-precursor acute lymphoblastic leukemia. *J Clin Invest.* **122,** 3407–3415 (2012).

26. Collins-Underwood, J. R. & Mullighan, C. G. Genomic profiling of high-risk acute lymphoblastic leukemia. *Leukemia.* **24,** 1676–1685 (2010).

27. Kuiper, R. P. *et al.* IKZF1 deletions predict relapse in uniformly treated pediatric precursor B-ALL. *Leukemia.* **24,** 1258–1264 (2010).

28. Krentz, S. *et al.* Prognostic value of genetic alterations in children with firstbone marrow relapse of childhood B-cell precursor acutelymphoblastic leukemia. *Leukemia.* **27,** 295–304 (2012).

29. Olsson, L. *et al.* The clinical impact of IKZF1 deletions in paediatric B-cell precursor acute lymphoblastic leukaemia is independent of minimal residual disease stratification in Nordic Society for Paediatric Haematology and Oncology treatment protocols used between 1992 and 2013. *Br J Haematol.* **170,** 847–858 (2015).

30. Burke, M. J. *et al.* Survival Differences between Adolescents/Young Adults and Children with B Precursor Acute Lymphoblastic Leukemia after Allogeneic Hematopoietic Cell Transplantation. *Biol Blood Marrow Transplant.* **19,** 138–142 (2013).

31. Bachanova, V. *et al.* Ph+ ALL patients in first complete remission have similar survival after reduced intensity and myeloablative allogeneic transplantation: Impact of tyrosine kinase inhibitor and minimal residual disease. *Leukemia.* **3**, 658 - 665 (2013).

32. Spinelli, O. *et al.* Clearance of minimal residual disease after allogeneic stem cell transplantation and the prediction of the clinical outcome of adult patients with high-risk acute lymphoblastic leukemia. *Haematologica.* **92,** 612–618 (2007).

33. Campana, D. & Leung, W. Clinical significance of minimal residual disease in patients with acute leukaemia undergoing haematopoietic stem cell transplantation. *Br J Haematol.* **162,** 147–161 (2013).

34. Germano, G. *et al.* Clonality profile in relapsed precursor-B-ALL children by GeneScan and sequencing analyses. Consequences on minimal residual disease monitoring. *Leukemia.* **17,** 1573–1582 (2003).

35. Kuster, L. *et al.* ETV6/RUNX1-positive relapses evolve from an ancestral clone and frequently acquire deletions of genes implicated in glucocorticoid signaling. *Blood.* **117,** 2658–2667 (2011).

36. Mullighan, C. G. *et al.* Genomic analysis of the clonal origins of relapsed acute lymphoblastic leukemia. *Science.* **322,** 1377–1380 (2008).

37. Yang, J. J. *et al.* Genome-wide copy number profiling reveals molecular evolution from diagnosis to relapse in childhood acute lymphoblastic leukemia. *Blood.* **112,** 4178–4183 (2008).

38. van Delft, F. W. *et al.* Clonal origins of relapse in ETV6-RUNX1 acute lymphoblastic leukemia. *Blood.* **117,** 6247–6254 (2011).

39. Kawamata, N. *et al.* Molecular allelokaryotyping of relapsed pediatric acute lymphoblastic leukemia. *Int J Oncol* **34,** 1603–1612(2009).

40. Choi, S. *et al.* Relapse in children with acute lymphoblastic leukemia involving selection of a preexisting drug-resistant subclone. *Blood.* **110,** 632–639 (2007).

41. Takeuchi, S. *et al.* Allelotype analysis in relapsed childhood acute lymphoblastic leukemia. *Oncogene.* **22,** 6970–6976 (2003).

42. Notta, F. *et al.* Evolution of human BCR–ABL1 lymphoblastic leukaemia-initiating cells. *Nature.* **469,** 362–367 (2011).

43. Patel, B. *et al.* Mouse xenograft modelling of human adult acute lymphoblastic leukemia provides mechanistic insights into adult LIC biology. *Blood.* **124,** 96–105 (2014).

44. Bokemeyer, A. *et al.* Copy number genome alterations are associated with treatment response and outcome in relapsed childhood ETV6/RUNX1-positive acute lymphoblastic leukemia. *Haematologica.* **99,** 706–714 (2014).

45. Bardini, M. *et al.* Clonal variegation and dynamic competition of leukemia-initiating cells in infant acute lymphoblastic leukemia with MLL rearrangement. *Leukemia.* **29,** 38–50 (2015).

46. Bhatla, T. *et al.* The Biology of Relapsed Acute Lymphoblastic Leukemia. *J Pediatr Hematol Oncol.* **36,** 413–418 (2014).

47. Ma, X. *et al.* Rise and fall of subclones from diagnosis to relapse in pediatric B-acute lymphoblastic leukaemia. *Nature Commun.* **6,** 1–12 (2015).

48. Davi, F., Gocke, C., Smith, S. & Sklar, J. Lymphocytic progenitor cell origin and clonal evolution of human B-lineage acute lymphoblastic leukemia. *Blood.* **88,** 609–621 (1996).

49. Anderson, K. *et al.* Genetic variegation of clonal architecture and propagating cells in leukaemia. *Nature.* **469,** 356–361 (2012).

50. Rai, L. *et al.* Antigen receptor gene rearrangements reflect on the heterogeneity of adult Acute Lymphoblastic Leukaemia (ALL) with implications of cell-origin of ALL subgroups: a UKALLXII study. *Br J Haematol.* **148,** 394–401 (2010).

51. Kong, Y. *et al.* CD34+CD38+CD19+ as well as CD34+CD38−CD19+ cells are leukemia-initiating cells with self-renewal capacity in human B-precursor ALL. *Leukemia.* **22,** 1207–1213 (2008).

52. Weston, V. J. *et al.* Molecular analysis of single colonies reveals a diverse origin of initial clonal proliferation in B-precursor acute lymphoblastic leukemia that can precede the t(12;21) translocation. *Cancer Res.* **61,** 8547–8553 (2001).

53. Cobaleda, C. & Sánchez-García, I. B-cell acute lymphoblastic leukaemia: towards understanding its cellular origin. *BioEssays.* **31,** 600–609 (2009).

54. Swaminathan, S. *et al.* Mechanisms of clonal evolution in childhood acute lymphoblastic leukemia. *Nat Immunol.* **16,** 766–774 (2015).

55. Gawad, C., Koh, W. & Quake, S. R. Dissecting the clonal origins of childhood acute lymphoblastic leukemia by single-cell genomics. *Proc Natl Acad Sci U S A.* **111,** 17947–17952 (2014).

56. Schmiegelow, K. *et al.* Post-induction residual leukemia in childhood acute lymphoblastic leukemia quantified by PCR correlates with in vitro prednisolone resistance. *Leukemia.* **15,** 1066–1071 (2001).

57. Appel, I. M. *et al.* Pharmacokinetic, pharmacodynamic and intracellular effects of PEG-asparaginase in newly diagnosed childhood acute lymphoblastic leukemia: results from a single agent window study. *Leukemia.* **22,** 1665–1679 (2008).

58. Hongo, T., Yajima, S., Sakurai, M., Horikoshi, Y. & Hanada, R. In vitro drug sensitivity testing can predict induction failure and early relapse of childhood acute lymphoblastic leukemia. *Blood.* **89,** 2959–2965 (1997).

59. Kaspers, G. J. *et al.* In vitro cellular drug resistance and prognosis in newly diagnosed childhood acute lymphoblastic leukemia. *Blood.* **90,** 2723–2729 (1997).

60. Kaspers, G. J. *et al.* Prednisolone resistance in childhood acute lymphoblastic leukemia: vitro-vivo correlations and cross-resistance to other drugs. *Blood.* **92,** 259–266 (1998).

61. Klumper, E. *et al.* In vitro cellular drug resistance in children with relapsed/refractory acute lymphoblastic leukemia. *Blood.* **86,** 3861–3868 (1995).

62. Lugthart, S. *et al.* Identification of genes associated with chemotherapy crossresistance and treatment response in childhood acute lymphoblastic leukemia. *Cancer Cell.* **7,** 375–386 (2005).

63. Lee, H. J., Thompson, J. E., Wang, E. S. & Wetzler, M. Philadelphia chromosome-positive acute lymphoblastic leukemia. *Cancer.* **117,** 1583–1594 (2010).

64. Bernt, K. M. & Hunger, S. P. Current concepts in pediatric Philadelphia chromosome-positive acute lymphoblastic leukemia. *Front Oncol.* **4,** 1–21 (2014).

65. Teachey, D. T. & Hunger, S. P. Predicting relapse risk in childhood acute lymphoblastic leukaemia. *Br J Haematol.* **162,** 606–620 (2013).

66. Swerts, K. *et al.* Prognostic significance of multidrug resistance-related proteins in childhood acute lymphoblastic leukaemia. *Eur J Cancer.* **42,** 295–309 (2006).

67. Cario, G. *et al.* Distinct gene expression profiles determine molecular treatment response in childhood acute lymphoblastic leukemia. *Blood.* **105,** 821–826 (2005).

68. Lønning, P. E. & Knappskog, S. Mapping genetic alterations causing chemoresistance in cancer: identifying the roads by tracking the drivers. *Oncogene.* **32,** 5315–5330 (2013).

69. Sitthi-amorn, J. *et al.* Transcriptome analysis of minimal residual disease in subtypes of pediatric B cell acute lymphoblastic leukemia. *Clin Med Insights Oncol.* **9,** 51–60 (2015).

70. Uckun, F. M. & Qazi, S. SYK as a new therapeutic target in B-cell precursor acute lymphoblastic leukemia. *J Cancer Ther.* **5,** 124–131 (2014).

71. Georgopoulos, K. Acute lymphoblastic leukemia--on the wings of IKAROS. *N Engl J Med.* **360,** 524–526 (2009).

72. Hsieh, Y. T. *et al.* Integrin alpha4 blockade sensitizes drug resistant pre-B acute lymphoblastic leukemia to chemotherapy. *Blood.* **121,** 1814–1818 (2013).

73. Hsieh, Y. T. *et al.* Effects of the small-molecule inhibitor of integrin a4, TBC3486, on pre-B-ALL cells. *Leukemia.* **28,** 2101–2104 (2014).

74. Williams, R. T., Besten, den, W. & Sherr, C. J. Cytokine-dependent imatinib resistance in mouse BCR-ABL+, Arf-null lymphoblastic leukemia. *Genes Dev.* **21,** 2283–2287 (2007).

75. Harrison, C. J. Cytogenetics of paediatric and adolescent acute lymphoblastic leukaemia. *Brit J Haematol.* **144,** 147–156 (2009).

76. Pui, C. H., Robison, L. L. & Look, A. T. Acute lymphoblastic leukaemia. *Lancet.* **371,** 1030–1043 (2008).

77. Mullighan, C. G. The molecular genetic makeup of acute lymphoblastic leukemia. *Hematology Am Soc Hematol Educ Program.* **2012,** 389–396 (2012).

78. Inaba, H., Greaves, M. & Mullighan, C. G. Acute lymphoblastic leukaemia. *Lancet.* **381,** 1943–1955 (2013).

79. Loh, M. L. & Mullighan, C. G. Advances in the genetics of high-risk childhood B-progenitor acute lymphoblastic leukemia and juvenile myelomonocytic leukemia: implications for therapy. *Clin Cancer Res.* **18,** 2754–2767 (2012).

80. Mullighan, C. G. Genomic profiling of B-progenitor acute lymphoblastic leukemia. *Best Pract Res Clin Haematol.* **24,** 489–503 (2011).

81. Wiemels, J. L. *et al.* Prenatal origin of acute lymphoblastic leukaemia in children. *Lancet.* **354,** 1499–1503 (1999).

82. Mullighan, C. G. *et al.* Genomic analysis of the clonal origins of relapsed acute lymphoblastic leukemia. *Science.* **322,** 1377–1380 (2008).

83. Kuiper, R. P. *et al.* High-resolution genomic profiling of childhood ALL reveals novel recurrent genetic lesions affecting pathways involved in lymphocyte differentiation and cell cycle progression. *Leukemia.* **21,** 1258–1266 (2007).

84. Kawamata, N. *et al.* Molecular allelokaryotyping of pediatric acute lymphoblastic leukemias by high-resolution single nucleotide polymorphism oligonucleotide genomic microarray. *Blood.* **111,** 776–784 (2008).

85. Strefford, J. C. *et al.* Genome complexity in acute lymphoblastic leukemia is revealed by array-based comparative genomic hybridization. *Oncogene.* **26,** 4306–4318 (2007).

86. Williams, R. T. & Sherr, C. J. The INK4-ARF (CDKN2A/B) locus in hematopoiesis and BCR-ABL-induced leukemias. *Cold Spring Harb Symp Quant Biol.* **73,** 461–467 (2008).

87. Den Boer, M. L. *et al.* A subtype of childhood acute lymphoblastic leukaemia withpoor treatment outcome: a genome-wide classification study. *Lancet Oncol.* **10,** 125–134 (2009).

88. Hoelzer, D. Personalized medicine in adult acute lymphoblastic leukemia. *Haematologica.* **100,** 855–858 (2015).

89. Boer, J. M. *et al.* Expression profiling of adult acute lymphoblastic leukemia identifies a BCR-ABL1-like subgroup characterized by high non-response and relapse rates. *Haematologica.* **100,** e261–4 (2015).

90. Geng, H. *et al.* Self-enforcing feedback activation between BCL6 and pre-B cell receptor signaling defines a distinct subtype of acute lymphoblastic leukemia. *Cancer Cell.* **27,** 409–425 (2015).

91. Bourquin, J.-P. The clinical path to integrated genomics in ALL. *Blood.* **124,** 1380–1381 (2014).

92. Druker, B. J. *et al.* Activity of a specific inhibitor of the BCR-ABL tyrosine kinase in the blast crisis of chronic myeloid leukemia and acute lymphoblastic leukemia with the Philadelphia chromosome. *N Engl J Med.* **344,** 1038–1042 (2001).

93. Sawyers, C. L. *et al.* Imatinib induces hematologic and cytogenetic responses in patients with chronic myelogenous leukemia in myeloid blast crisis: results of a phase II study. *Blood.* **99,** 3530–3539 (2002).

94. Schultz, K. R. *et al.* Improved early event-free survival with imatinib in Philadelphia chromosome-positive acute lymphoblastic leukemia: A Children's Oncology Group Study. *J Clin Oncol.* **27,** 5175–5181 (2009).

95. Gruber, F., Mustjoki, S. & Porkka, K. Impact of tyrosine kinase inhibitors on patient outcomes in Philadelphia chromosome-positive acute lymphoblastic leukaemia. *Br J Haematol.* **145,** 581–597 (2009).

96. Yanada, M. *et al.* High Complete Remission Rate and Promising Outcome by Combination of Imatinib and Chemotherapy for Newly Diagnosed BCR-ABL-Positive Acute Lymphoblastic Leukemia: A Phase II Study by the Japan Adult Leukemia Study Group. *J Clin Oncol.* **24,** 460–466 (2006).

97. de Labarthe, A. *et al.* Imatinib combined with induction or consolidation chemotherapy in patients with de novo Philadelphia chromosome-positive acute lymphoblastic leukemia: results of the GRAAPH-2003 study. *Blood.* **109,** 1408–1413 (2007).

98. Ravandi, F. *et al.* First report of phase 2 study of dasatinib with hyper-CVAD for the frontline treatment of patients with Philadelphia chromosome-positive (Ph+) acute lymphoblastic leukemia. *Blood.* **116,** 2070–2077 (2010).

99. Foa, R. *et al.* Dasatinib as first-line treatment for adult patients with Philadelphia chromosome-positive acute lymphoblastic leukemia. *Blood.* **118,** 6521–6528 (2011).

100. Fielding, A. K. *et al.* UKALLXII/ECOG2993: addition of imatinib to a standard treatment regimen enhances long-term outcomes in Philadelphia positive acute lymphoblastic leukemia. *Blood.* **123,** 843–850 (2014).

101. Daver, N. *et al.* Final report of a phase II study of imatinib mesylate with hyper-CVAD for the front-line treatment of adult patients with Philadelphia chromosome-positive acute lymphoblastic leukemia. *Haematologica.* **100,** 653–661 (2015).

102. Kim, D. Y. *et al.* Nilotinib combined with multiagent chemotherapy for newly diagnosed Philadelphia-positive acute lymphoblastic leukemia. *Blood.* **126,** 746–756 (2015).

103. O'Hare, T. *et al.* In vitro activity of Bcr-Abl inhibitors AMN107 and BMS-354825 against clinically relevant imatinib-resistant Abl kinase domain mutants. *Cancer Res.* **65,** 4500–4505 (2005).

104. Talpaz, M. *et al.* Dasatinib in imatinib-resistant Philadelphia chromosome-positive leukemias. *N Engl J Med.* **354,** 2531–2541 (2006).

105. Brave, M. *et al.* Sprycel for chronic myeloid leukemia and Philadelphia chromosome-positive acute lymphoblastic leukemia resistant to or intolerant of imatinib mesylate. *Clin Cancer Res.* **14,** 352–359 (2008).

106. Ottmann, O. *et al.* Dasatinib induces rapid hematologic and cytogenetic responses in adult patients with Philadelphia chromosome positive acute lymphoblastic leukemia with resistance or intolerance to imatinib: interim results of a phase 2 study. *Blood.* **110,** 2309–2315 (2007).

107. Porkka, K. *et al.* Dasatinib crosses the blood-brain barrier and is an efficient therapy for central nervous system Philadelphia chromosome-positive leukemia. *Blood.* **112,** 1005–1012 (2008).

108. O'Hare, T. *et al.* AP24534, a Pan-BCR-ABL inhibitor for chronic myeloid leukemia, potently inhibits the T315I mutant and overcomes mutation-based resistance. *Cancer Cell.* **16,** 401–412 (2009).

109. Cortes, J. E. *et al.* Ponatinib in refractory Philadelphia chromosome–positive leukemias. *N Engl J Med.* **367,** 2075–2088 (2012).

110. Cortes, J. E. *et al.* A phase 2 trial of ponatinib in Philadelphia chromosome–positive leukemias. *N Engl J Med.* **369,** 1783–1796 (2013).

111. Roberts, K. G. *et al.* Targetable kinase-activating lesions in Ph-like acute lymphoblastic leukemia. *N Engl J Med.* **371,** 1005–1015 (2014).

112. Ghazavi, F. *et al.* Molecular basis and clinical significance of genetic aberrations in B-cell precursor acute lymphoblastic leukemia. *Exp Hematol.* **43,** 640–653 (2015).

113. Ribera, J. *et al.* Prognostic significance of copy number alterations in adolescent and adult patients with precursor B acute lymphoblastic leukemia enrolled in PETHEMA protocols. *Cancer.* **121,** 3809–3817 (2015).

114. Jain, R. *et al.* Unusual sites of relapse in pre-B acute lymphoblastic leukemia. *J Pediatr Hematol Oncol.* **36,** e506–8 (2014).

115. Wuchter, C. *et al.* Clinical significance of P-glycoprotein expression and function for response to induction chemotherapy, relapse rate and overall survival in acute leukemia. *Haematologica.* **85,** 711–721 (2000).

116. Herweijer, H., Sonneveld, P., Baas, F. & Nooter, K. Expression of mdr1 and mdr3 multidrug-resistance genes in human acute and chronic leukemias and association with stimulation of drug accumulation by cyclosporine. *J Natl Cancer Inst.* **82,** 1133–1140 (1990).

117. Fedasenka, U. U., Shman, T. V., Savitski, V. P. & Belevcev, M. V. Expression of MDR1, LRP, BCRP and Bcl-2 genes at diagnosis of childhood all: comparison with MRD status after induction therapy. *Exp Oncol.* **30,** 248–252 (2008).

118. Brophy, N. A. *et al.* Mdr1 gene expression in childhood acute lymphoblastic leukemias and lymphomas: a critical evaluation by four techniques. *Leukemia.* **8,** 327–335 (1994).

119. Savignano, C. *et al.* The expression of the multidrug resistance related glycoprotein in adult acute lymphoblastic leukemia. *Haematologica.* **78,** 261–263 (1993).

120. Olson, D. P. *et al.* The prognostic significance of P-glycoprotein, multidrug resistance-related protein 1 and lung resistance protein in pediatric acute lymphoblastic leukemia: A retrospective study of 295 newly diagnosed patients by the Children's Oncology Group. *Leuk Lymphoma.* **46,** 681–691 (2005).

121. Del Principe, M. I. *et al.* P-glycoprotein and BCL-2 levels predict outcome in adult acute lymphoblastic leukaemia. *Br J Haematol.* **121,** 730–738 (2003).

122. Delville, J. P. *et al.* Comparative study of multidrug resistance evaluated by means of the quantitative immunohistochemical detection of P-glycoprotein and the functional release of rhodamine 123. *Am J Hematol.* **49,** 183–193 (1995).

123. Carulli, G. *et al.* P-glycoprotein and drug resistance in acute leukemias and in the blastic crisis of chronic myeloid leukemia. *Haematologica.* **75,** 516–521 (1990).

124. Asakura, K. *et al.* TEL/AML1 overcomes drug resistance through transcriptional repression of multidrug resistance-1 gene expression. *Mol Cancer Res.* **2,** 339–347 (2004).

125. Svirnovski, A. I. *et al.* ABCB1 and ABCG2 proteins, their functional activity and gene expression in concert with drug sensitivity of leukemia cells. *Hematology.* **14,** 204–212 (2009).

126. Yang, J. J. *et al.* Genome-wide association study identifies germline polymorphisms associated with relapse of childhood acute lymphoblastic leukemia. *Blood.* **120,** 4197–4204 (2012).

127. Gregers, J. *et al.* Polymorphisms in the ABCB1 gene and effect on outcome and toxicity in childhood acute lymphoblastic leukemia. *Pharmacogenomics J.* **15,** 372–379 (2015).

128. Mahon, F.-X. *et al.* Selection and characterization of BCR-ABL positive cell lines with differential sensitivity to the tyrosine kinase inhibitor STI571: diverse mechanisms of resistance. *Blood.* **96,** 1070–1079 (2000).

129. Mahon, F.-X. *et al.* Evidence that resistance to nilotinib may be due to BCR-ABL, Pgp, or Src kinase overexpression. *Cancer Res.* **68,** 9809–9816 (2008).

130. Widmer, N., Colombo, S., Buclin, T. & Decosterd, L. A. Functional consequence of MDR1 expression on imatinib intracellular concentrations. *Blood.* **102,** 1142 (2003).

131. Illmer, T. *et al.* P-glycoprotein-mediated drug efflux is a resistance mechanism of chronic myelogenous leukemia cells to treatment with imatinib mesylate. *Leukemia.* **18,** 401–408 (2004).

132. Xing, H. *et al.* The study of resistant mechanisms and reversal in an imatinib resistant Ph+ acute lymphoblastic leukemia cell line. *Leuk Res.* **36,** 509–513 (2012).

133. Dai, H. *et al.* Distribution of STI-571 to the brain Is limited by P-glycoprotein-mediated efflux. *J Pharmacol Exp Ther.* **304,** 1085–1092 (2002).

134. Chen, Y. *et al.* P-glycoprotein and breast cancer resistance protein influence brain distribution of dasatinib. *J Pharmacol Exp Ther.* **330,** 956–963 (2009).

135. Lagas, J. S. *et al.* Brain accumulation of dasatinib Is restricted by P-glycoprotein (ABCB1) and breast cancer resistance protein (ABCG2) and can be enhanced by elacridar treatment. *Clin Cancer Res.* **15,** 2344–2351 (2009).

136. den Boer, M. L. *et al.* Relationship between major vault protein/lung resistance protein, multidrug resistance-associated protein, P-glycoprotein expression, and drug resistance in childhood leukemia. *Blood.* **91,** 2092–2098 (1998).

137. den Boer, M. L. *et al.* Different expression of glutathione S-transferase alpha, mu and pi in childhood acute lymphoblastic and myeloid leukaemia. *Br J Haematol.* **104,** 321–327 (1999).

138. Plasschaert, S. L. A. *et al.* Expression of multidrug resistance-associated proteins predicts prognosis in childhood and adult acute lymphoblastic leukemia. *Clin Cancer Res.* **11,** 8661–8668 (2005).

139. Steinbach, D. *et al.* The multidrug resistance-associated protein 3 (MRP3) is associated with a poor outcome in childhood ALL and may account for the worse prognosis in male patients and T-cell immunophenotype. *Blood.* **102,** 4493–4498 (2003).

140. Furmanski, B. D. *et al.* Contribution of Abcc4-mediated gastric transport to the absorption and efficacy of dasatinib. *Clin Cancer Res.* **19,** 4359–4370 (2013).

141. Burger, H. *et al.* Imatinib mesylate (STI571) is a substrate for the breast cancer resistance protein (BCRP)/ABCG2 drug pump. *Blood.* **104,** 2940–2942 (2004).

142. Houghton, P. J. *et al.* Imatinib mesylate is a potent inhibitor of the ABCG2 (BCRP) transporter and reverses resistance to topotecan and SN-38 in vitro. *Cancer Res.* **64,** 2333–2337 (2004).

143. Breedveld, P. *et al.* The effect of Bcrp1 (Abcg2) on the in vivo pharmacokinetics and brain penetration of imatinib mesylate (Gleevec): implications for the use of breast cancer resistance protein and P-glycoprotein inhibitors to enable the brain penetration of imatinib in patients. *Cancer Res.* **65,** 2577–2582 (2005).

144. Nakanishi, T. *et al.* Complex interaction of BCRP/ABCG2 and imatinib in BCR-ABL-expressing cells: BCRP-mediated resistance to imatinib is attenuated by imatinib-induced reduction of BCRP expression. *Blood.* **108,** 678–684 (2006).

145. Brendel, C. *et al.* Imatinib mesylate and nilotinib (AMN107) exhibit high-affinity interaction with ABCG2 on primitive hematopoietic stem cells. *Leukemia.* **21,** 1267–1275 (2007).

146. Crossman, L. C. *et al.* hOCT 1 and resistance to imatinib. *Blood.* **106,** 1133–4 (2005).

147. Thomas, X. *et al.* Outcome of treatment in adults with acute lymphoblastic leukemia: analysis of the LALA-94 trial. *J Clin Oncol.* **22,** 4075–4086 (2004).

148. Giannoudis, A. *et al.* Effective dasatinib uptake may occur without human organic cation transporter 1 (hOCT1): implications for the treatment of imatinib-resistant chronic myeloid leukemia. *Blood.* **112,** 3348–3354 (2008).

149. Hiwase, D. K. *et al.* Dasatinib cellular uptake and efflux in chronic myeloid leukemia cells: therapeutic implications. *Clin Cancer Res.* **14,** 3881–3888 (2008).

150. Lu, L. *et al.* Ponatinib is not transported by ABCB1, ABCG2 or OCT-1 in CML cells. *Leukemia.* **29,** 1792–1794 (2015).

151. White, D. L. *et al.* Most CML patients who have a suboptimal response to imatinib have low OCT-1 activity: higher doses of imatinib may overcome the negative impact of low OCT-1 activity. *Blood.* **110,** 4064–4072 (2007).

152. Wang, L. *et al.* Expression of the uptake drug transporter hOCT1 is an important clinical determinant of the response to imatinib in chronic myeloid leukemia. *Clin Pharmacol Ther.* **83,** 258–264 (2007).

153. Volm, M. *et al.* Expression of lung resistance-related protein (LRP) in initial and relapsed childhood acute lymphoblastic leukemia. *Anticancer Drugs.* **8,** 662–665 (1997).

154. Ogretmen, B., Barredo, J. C. & Safa, A. R. Increased expression of lung resistance-related protein and multidrug resistance-associated protein messenger RNA in childhood acute lymphoblastic leukemia. *J Pediatr Hematol Oncol.* **22,** 45–49 (2000).

155. Ramakers-van Woerden, N. L. *et al.* In vitro drug-resistance profile in infant acute lymphoblastic leukemia in relation to age, MLL rearrangements and immunophenotype. *Leukemia.* **18,** 521–529 (2004).

156. Vigneri, P. & Wang, J. Y. Induction of apoptosis in chronic myelogenous leukemia cells through nuclear entrapment of BCR-ABL tyrosine kinase. *Nat Med.* **7,** 228–234 (2001).

157. Kancha, R. K. *et al.* Imatinib and leptomycin B are effective in overcoming imatinib-resistance due to Bcr-Abl amplification and clonal evolution but not due to Bcr-Abl kinase domain mutation. *Haematologica.* **93,** 1718–1722 (2008).

158. Rots, M. G. *et al.* Methotrexate resistance in relapsed childhood acute lymphoblastic leukaemia. *Br J Haematol.* **109,** 629–634 (2000).

159. Whitehead, V. M. *et al.* Accumulation of methotrexate and methotrexate polyglutamates in lymphoblasts at diagnosis of childhood acute lymphoblastic leukemia: a pilot prognostic factor analysis. *Blood.* **76,** 44–49 (1990).

160. Winick, N. *et al.* Intensive oral methotrexate protects against lymphoid marrow relapse in childhood B-precursor acute lymphoblastic leukemia. *J Clin Oncol.* **14,** 2803–2811 (1996).

161. Belkov, V. M. *et al.* Reduced folate carrier expression in acute lymphoblastic leukemia: a mechanism for ploidy but not lineage differences in methotrexate accumulation. *Blood.* **93,** 1643–1650 (1999).

162. Kager, L. *et al.* Folate pathway gene expression differs in subtypes of acute lymphoblastic leukemia and influences methotrexate pharmacodynamics. *J Clin Invest.* **115,** 110–117 (2005).

163. Panetta, J. C. *et al.* Modeling mechanisms of in vivo variability in methotrexate accumulation and folate pathway inhibition in acute lymphoblastic leukemia cells. *PLoS Comput Biol.* **6,** e1001019 (2010).

164. Göker, E. *et al.* Decreased polyglutamylation of methotrexate in acute lymphoblastic leukemia blasts in adults compared to children with this disease. *Leukemia.* **7,** 1000–1004 (1993).

165. Leclerc, G. J., Leclerc, G. M., Kinser, T. & Barredo, J. C. Analysis of folylpoly-gamma-glutamate synthetase gene expression in human B-precursor ALL and T-lineage ALL cells. *BMC Cancer.* **6,** 132 (2006).

166. Gómez-Gómez, Y. N. *et al.* Effect of folylpolyglutamate synthase A22G polymorphism on the risk and survival of patients with acute lymphoblastic leukemia. *Oncol Lett.* (2014). doi:10.3892/ol.2014.2175

167. Belkov, V. M. *et al.* Reduced folate carrier expression in acute lymphoblastic leukemia: a mechanism for ploidy but not lineage differences in methotrexate accumulation. *Blood.* **93,** 1643–1650 (1999).

168. Kaufman, Y. *et al.* Reduced folate carrier mutations are not the mechanism underlying methotrexate resistance in childhood acute lymphoblastic leukemia. *Cancer.* **100,** 773–782 (2004).

169. Kodidela, S., Suresh Chandra, P. & Dubashi, B. Pharmacogenetics of methotrexate in acute lymphoblastic leukaemia: why still at the bench level? *Eur J Clin Pharmacol.* **70,** 253–260 (2013).

170. Stams, W. A. G. Sensitivity to L-asparaginase is not associated with expression levels of asparagine synthetase in t(12;21)+ pediatric ALL. *Blood.* **101,** 2743–2747 (2002).

171. Appel, I. M. *et al.* Up-regulation of asparagine synthetase expression is not linked to the clinical response L-asparaginase in pediatric acute lymphoblastic leukemia. *Blood.* **107,** 4244–4249 (2006).

172. Stams, W. A. G. *et al.* Asparagine synthetase expression is linked with L-asparaginase resistance in TEL-AML1-negative but not TEL-AML1-positive pediatric acute lymphoblastic leukemia. *Blood.* **105,** 4223–4225 (2005).

173. Relling, M. V. & Ramsey, L. B. Pharmacogenomics of acute lymphoid leukemia: new insights into treatment toxicity and efficacy. *Hematology Am Soc Hematol Educ Program.* **2013,** 126–130 (2013).

174. Stanulla, M. *et al.* Thiopurine methyltransferase (TPMT) genotype and early treatment response to mercaptopurine in childhood acute lymphoblastic leukemia. *JAMA.* **293,** 1485–1489 (2005).

175. Schmiegelow, K. *et al.* Thiopurine methyltransferase activity is related to the risk of relapse of childhood acute lymphoblastic leukemia: results from the NOPHO ALL-92 study. *Leukemia.* **23,** 557–564 (2008).

176. Davies, S. M. *et al.* Glutathione S-transferase genotypes, genetic susceptibility, and outcome of therapy in childhood acute lymphoblastic leukemia. *Blood.* **100,** 67–71 (2002).

177. Takanashi, M. *et al.* Impact of glutathione S-transferase gene deletion on early relapse in childhood B-precursor acute lymphoblastic leukemia. *Haematologica.* **88,** 1238–1244 (2003).

178. Rocha, J. C. *et al.* Pharmacogenetics of outcome in children with acute lymphoblastic leukemia. *Blood.* **105,** 4752–4758 (2005).

179. Yoshida, A. *et al.* Inhibition of glutathione synthesis overcomes Bcl-2-mediated topoisomerase inhibitor resistance and induces nonapoptotic cell death via mitochondrial-independent pathway. *Cancer Res.* **66,** 5772–5780 (2006).

180. Seo, T., Urasaki, Y., Takemura, H. & Ueda, T. Arsenic trioxide circumvents multidrug resistance based on different mechanisms in human leukemia cell lines. *Anticancer Res.* **25,** 991–998 (2005).

181. Kearns, P. R., Pieters, R., Rottier, M. M., Pearson, A. D. & Hall, A. G. Raised blast glutathione levels are associated with an increased risk of relapse in childhood acute lymphocytic leukemia. *Blood.* **97,** 393–398 (2001).

182. Gézsi, A. *et al.* In interaction with gender a common CYP3A4 polymorphism may influence the survival rate of chemotherapy for childhood acute lymphoblastic leukemia. *Pharmacogenomics J.* **15,** 241–247 (2014).

183. Soverini, S. *et al.* Contribution of ABL kinase domain mutations to imatinib resistance in different subsets of Philadelphia-positive patients: by the GIMEMA working party on chronic myeloid leukemia. *Clin Cancer Res.* **12,** 7374–7379 (2006).

184. Soverini, S. *et al.* Resistance to dasatinib in Philadelphia-positive leukemia patients and the presence or the selection of mutations at residues 315 and 317 in the BCR-ABL kinase domain. *Haematologica.* **92,** 401–404 (2007).

185. Soverini, S. *et al.* Philadelphia-positive patients who already harbor imatinib-resistant Bcr-Abl kinase domain mutations have a higher likelihood of developing additional mutations associated with resistance to second- or third-line tyrosine kinase inhibitors. *Blood.* **114,** 2168–2171 (2009).

186. Soverini, S. *et al.* Drug resistance and BCR-ABL kinase domain mutations in Philadelphia chromosome-positive acute lymphoblastic leukemia from the imatinib to the second-generation tyrosine kinase inhibitor era: The main changes are in the type of mutations, but not in the frequency of mutation involvement. *Cancer.* **120,** 1002–1009 (2013).

187. Boulos, N. *et al.* Chemotherapeutic agents circumvent emergence of dasatinib-resistant BCR-ABL kinase mutations in a precise mouse model of Philadelphia chromosome-positive acute lymphoblastic leukemia. *Blood.* **117,** 3585–3595 (2011).

188. Yeung, D. T. *et al.* Relapse of *BCR-ABL1*-like ALL mediated by the ABL1 kinase domain mutation T315I following initial response to dasatinib treatment. *Leukemia.* **29,** 230–232 (2015).

189. Krajinovic, M., Costea, I. & Chiasson, S. Polymorphism of the thymidylate synthase gene and outcome of acute lymphoblastic leukaemia. *Lancet.* **359,** 1033–1034 (2002).

190. Lauten, M., Asgedom, G., Welte, K., Schrappe, M. & Stanulla, M. Thymidylate synthase gene polymorphism and its association with relapse in childhood B-cell precursor acute lymphoblastic leukemia. *Haematologica.* **88,** 353–354 (2003).

191. Meyer, J. A. *et al.* Relapse-specific mutations in NT5C2 in childhood acute lymphoblastic leukemia. *Nat Genet.* **45,** 290–294 (2013).

192. Tzoneva, G. *et al.* Activating mutations in the NT5C2 nucleotidase gene drive chemotherapy resistance in relapsed ALL. *Nat Med.* **19,** 368–371 (2013).

193. Burgess, D. J. *et al.* Topoisomerase levels determine chemotherapy response in vitro and in vivo. *Proc Natl Acad Sci U S A.* **105,** 9053–9058 (2008).

194. Bhojwani, D. *et al.* Biologic pathways associated with relapse in childhood acute lymphoblastic leukemia: a Children's Oncology Group study. *Blood.* **108,** 711–717 (2006).

195. Flotho, C. *et al.* A set of genes that regulate cell proliferation predicts treatment outcome in childhood acute lymphoblastic leukemia. *Blood.* **110,** 1271–1277 (2007).

196. Tissing, W. J. E., Meijerink, J. P. P., Boer, Den, M. L. & Pieters, R. Molecular determinants of glucocorticoid sensitivity and resistance in acute lymphoblastic leukemia. *Leukemia.* **17,** 17–25 (2003).

197. Bachmann, P. S., Gorman, R., Mackenzie, K. L., Lutze-Mann, L. & Lock, R. B. Dexamethasone resistance in B-cell precursor childhood acute lymphoblastic leukemia occurs downstream of ligand-induced nuclear translocation of the glucocorticoid receptor. *Blood.* **105,** 2519–2526 (2005).

198. Irving, J. A. *et al.* Loss of heterozygosity and somatic mutations of the glucocorticoid receptor gene are rarely found at relapse in pediatric acute lymphoblastic leukemia but may occur in a subpopulation early in the disease course. *Cancer Res.* **65,** 9712–9718 (2005).

199. Tissing, W. J. *et al.* Genetic variations in the glucocorticoid receptor gene are not related to glucocorticoid resistance in childhood acute lymphoblastic leukemia. *Clin Cancer Res.* **11,** 6050–6056 (2005).

200. Tissing, W. J. *et al.* Glucocorticoid-induced glucocorticoid-receptor expression and promoter usage is not linked to glucocorticoid resistance in childhood ALL. *Blood.* **108,** 1045–1049 (2006).

201. Haarman, E. G. *et al.* Glucocorticoid receptor alpha, beta and gamma expression vs in vitro glucocorticod resistance in childhood leukemia. *Leukemia.* **18,** 530–537 (2004).

202. Krug, U., Ganser, A. & Koeffler, H. P. Tumor suppressor genes in normal and malignant hematopoiesis. *Oncogene.* **21,** 3475–3495 (2002).

203. Mullighan, C. G. *et al.* CREBBP mutations in relapsed acute lymphoblastic leukaemia. *Nature.* **471,** 235–239 (2012).

204. Inthal, A. *et al.* CREBBP HAT domain mutations prevail in relapse cases of high hyperdiploid childhood acute lymphoblastic leukemia. *Leukemia.* **26,** 1797–1803 (2012).

205. Mar, B. G. *et al.* Mutations in epigenetic regulators including SETD2 are gained during relapse in paediatric acute lymphoblastic leukaemia. *Nat Commun.* **5,** 1–6 (2014).

206. Malinowska-Ozdowy, K. *et al.* Kras and CREBBP mutations: a relapse-linked malicious liaison in childhood high hyperdiploid acute lymphoblastic leukemia. *Leukemia.* **29,** 1656–1667 (2015).

207. Holleman, A. *et al.* Gene-expression patterns in drug-resistant acute lymphoblastic leukemia cells and response to treatment. *N Engl J Med.* **351,** 533–542 (2004).

208. Pottier, N. *et al.* The SWI/SNF chromatin-remodeling complex and glucocorticoid resistance in acute lymphoblastic leukemia. *J Natl Cancer Inst.* **100,** 1792–1803 (2008).

209. Jones, D. *et al.* Kinase domain point mutations in Philadelphia chromosome-positive acute lymphoblastic leukemia emerge after therapy with BCR-ABL kinase inhibitors. *Cancer.* **113,** 985–994 (2008).

210. Olsson, L. *et al.* Deletions of IKZF1 and SPRED1 are associated with poor prognosis in a population-based series of pediatric B-cell precursor acute lymphoblastic leukemia diagnosed between 1992 and 2011. *Leukemia.* **28,** 302–310 (2013).

211. Fernando, T. R. *et al.* LncRNA Expression Discriminates Karyotype and Predicts Survival in B-Lymphoblastic Leukemia. *Mol Cancer Res.* **13,** 839–851 (2015).

212. Meyer, L. H. *et al.* Cytochrome c-related caspase-3 activation determines treatment response and relapse in childhood precursor B-cell ALL. *Blood.* **107,** 4524–4531 (2006).

213. Marston, E. *et al.* Stratification of pediatric ALL by in vitro cellular responses to DNA double-strand breaks provides insight into the molecular mechanisms underlying clinical response. *Blood.* **113,** 117–126 (2009).

214. Aries, I. M. *et al.* The synergism of MCL1 and glycolysis on pediatric acute lymphoblastic leukemia cell survival and prednisolone resistance. *Haematologica.* **98,** 1905–1911 (2013).

215. Tissing, W. J. E. *et al.* Genomewide identification of prednisolone-responsive genes in acute lymphoblastic leukemia cells. *Blood.* **109,** 3929–3935 (2007).

216. Scuderi, R. *et al.* Cyclin E overexpression in relapsed adult acute lymphoblastic leukemias of B-cell lineage. *Blood.* **87,** 3360–3367 (1996).

217. Shen, L. *et al.* Aberrant DNA methylation of p57KIP2 identifies a cell-cycle regulatory pathway with prognostic impact in adult acute lymphocytic leukemia. *Blood.* **101,** 4131–4136 (2003).

218. Hof, J. *et al.* Mutations and deletions of the TP53 gene predict nonresponse to treatment and poor outcome in first relapse of childhood acute lymphoblastic leukemia. *J Clin Oncol.* **29,** 3185–3193 (2011).

219. Stengel, A. *et al.* TP53 mutations occur in 15.7% of ALL and are associated with MYC-rearrangement, low hypodiploidy and a poor prognosis. *Blood.* **124,** 251–258 (2014).

220. Chiaretti, S. *et al.* TP53 mutations are frequent in adult acute lymphoblastic leukemia cases negative for recurrent fusion genes and correlate with poor response to induction therapy. *Haematologica.* **98,** e59–61 (2013).

221. Weston, V. J. *et al.* Apoptotic resistance to ionizing radiation in pediatric B-precursor acute lymphoblastic leukemia frequently involves increased NF- B survival pathway signaling. *Blood.* **104,** 1465–1473 (2004).

222. Min, D.-J. *et al.* Diverse pathways mediate chemotherapy-induced cell death in acute lymphoblastic leukemia cell lines. *Apoptosis.* **11,** 1977–1986 (2006).

223. Gu, L., Findley, H. W. & Zhou, M. MDM2 induces NF-kappaB/p65 expression transcriptionally through Sp1-binding sites: a novel, p53-independent role of MDM2 in doxorubicin resistance in acute lymphoblastic leukemia. *Blood.* **99,** 3367–3375 (2002).

224. Zhou, M. *et al.* Incidence and prognostic significance of MDM2 oncoprotein overexpression in relapsed childhood acute lymphoblastic leukemia. *Leukemia.* **14,** 61–67 (2000).

225. Marks, D. I. *et al.* High incidence of potential p53 inactivation in poor outcome childhood acute lymphoblastic leukemia at diagnosis. *Blood.* **87,** 1155–1161 (1996).

226. Marks, D. I. *et al.* Altered expression of p53 and mdm-2 proteins at diagnosis is associated with early treatment failure in childhood acute lymphoblastic leukemia. *J Clin Oncol.* **15,** 1158–1162 (1997).

227. Zhou, M., Yeager, A. M., Smith, S. D. & Findley, H. W. Overexpression of the MDM2 gene by childhood acute lymphoblastic leukemia cells expressing the wild-type p53 gene. *Blood.* **85,** 1608–1614 (1995).

228. Maloney, K. W., McGavran, L., Odom, L. F. & Hunger, S. P. Acquisition of p16(INK4A) and p15(INK4B) gene abnormalities between initial diagnosis and relapse in children with acute lymphoblastic leukemia. *Blood.* **93,** 2380–2385 (1999).

229. Takeuchi, S. *et al.* Analysis of a family of cyclin-dependent kinase inhibitors: p15/MTS2/INK4B, p16/MTS1/INK4A, and p18 genes in acute lymphoblastic leukemia of childhood. *Blood.* **86,** 755–760 (1995).

230. Dalle, J. H. *et al.* p16(INK4a) immunocytochemical analysis is an independent prognostic factor in childhood acute lymphoblastic leukemia. *Blood.* **99,** 2620–2623 (2002).

231. Garcia-Manero, G. *et al.* DNA methylation patterns at relapse in adult acute lymphocytic leukemia. *Clin Cancer Res.* **8,** 1897–1903 (2002).

232. Carter, T. L., Reaman, G. H. & Kees, U. R. INK4A/ARF deletions are acquired at relapse in childhood acute lymphoblastic leukaemia: a paired study on 25 patients using real-time polymerase chain reaction. *Br J Haematol.* **113,** 323–328 (2001).

233. Carter, T. L. *et al.* Hemizygous p16INK4A deletion in pediatric acute lymphoblastic leukemia predicts independent risk of relapse. *Blood.* **97,** 572–574 (2001).

234. Ogawa, S. *et al.* Loss of the cyclin-dependent kinase 4-inhibitor (p16; MTS1) gene is frequent in and highly specific to lymphoid tumors in primary human hematopoietic malignancies. *Blood.* **86,** 1548–1556 (1995).

235. Williams, R. T., Roussel, M. F. & Sherr, C. J. Arf gene loss enhances oncogenicity and limits imatinib response in mouse models of Bcr-Abl-induced acute lymphoblastic leukemia. *Proc Natl Acad Sci U S A.* **103,** 6688–6693 (2006).

236. Hardwick, J. M. & Soane, L. Multiple Functions of BCL-2 Family Proteins. *Cold Spring Harb Perspect Biol.* **5,** a008722–a008722 (2013).

237. Salomons, G. S. *et al.* Bcl-2 family members in childhood acute lymphoblastic leukemia: relationships with features at presentation, in vitro and in vivo drug response and long-term clinical outcome. *Leukemia.* **13,** 1574–1580 (1999).

238. Haarman, E. G. *et al.* BCL-2 expression in childhood leukemia versus spontaneous apoptosis, drug induced apoptosis, and in vitro drug resistance. *Adv Exp Med Biol.* **457,** 325–333 (1999).

239. Inoue, H. *et al.* Dexamethasone-resistant human Pre-B leukemia 697 cell line evolving elevation of intracellular glutathione level: an additional resistance mechanism. *Jpn J Cancer Res.* **93,** 582–590 (2002).

240. Wall, N. R. *et al.* Modulation of cIAP-1 by novel antitubulin agents when combined with bryostatin 1 results in increased apoptosis in the human early pre-B acute lymphoblastic leukemia cell line Reh. *Biochem Biophys Res Commun.* **266,** 76–80 (1999).

241. Soh, S. X. *et al.* Multi-agent chemotherapy overcomes glucocorticoid resistance conferred by a BIM deletion polymorphism in pediatric acute lymphoblastic leukemia. *PLoS ONE.* **9,** e103435 (2014).

242. Abrams, M. T., Robertson, N. M., Yoon, K. & Wickstrom, E. Inhibition of glucocorticoid-induced apoptosis by targeting the major splice variants of BIM mRNA with small interfering RNA and short hairpin RNA. *J Biol Chem.* **279,** 55809–55817 (2004).

243. Wei, G. *et al.* Gene expression-based chemical genomics identifies rapamycin as a modulator of MCL1 and glucocorticoid resistance. *Cancer Cell.* **10,** 331–342 (2006).

244. Stam, R. W. *et al.* Association of high-level MCL-1 expression with in vitro and in vivo prednisone resistance in MLL-rearranged infant acute lymphoblastic leukemia. *Blood.* **115,** 1018–1025 (2010).

245. Holleman, A. *et al.* The expression of 70 apoptosis genes in relation to lineage, genetic subtype, cellular drug resistance, and outcome in childhood acute lymphoblastic leukemia. *Blood.* **107,** 769–776 (2006).

246. Suryani, S. *et al.* Cell and molecular determinants of in vivo efficacy of the BH3 mimetic ABT-263 against pediatric acute lymphoblastic leukemia xenografts. *Clin Cancer Res.* **20,** 4520–4531 (2014).

247. Koss, B. *et al.* Requirement for antiapoptotic MCL-1 in the survival of BCR-ABL B-lineage acute lymphoblastic leukemia. *Blood.* **122,** 1587–1598 (2013).

248. Spijkers-Hagelstein, J. A. P. *et al.* Glucocorticoid sensitisation in Mixed Lineage leukaemia-rearranged acute lymphoblastic leukaemia by the pan-BCL-2 family inhibitors gossypol and AT-101. *Eur J Cancer.* **50,** 1665–1674 (2014).

249. Zhou, M. *et al.* Targeting of the deubiquitinase USP9X attenuates B-cell acute lymphoblastic leukemia cell survival and overcomes glucocorticoid resistance. *Biochem Biophys Res Commun.* **459,** 333–339 (2015).

250. Chang, Y.-H., Yang, Y.-L., Chen, C.-M. & Chen, H.-Y. Apoptosis pathway signature for prediction of treatment response and clinical outcome in childhood high risk B-Precursor acute lymphoblastic leukemia. *Am J Cancer Res.* **5,** 1844–1853 (2015).

251. Paugh, S. W. *et al.* NALP3 inflammasome upregulation and CASP1 cleavage of the glucocorticoid receptor cause glucocorticoid resistance in leukemia cells. *Nat Genet.* **47,** 607–614 (2015).

252. Troeger, A. *et al.* Survivin and its prognostic significance in pediatric acute B-cell precursor lymphoblastic leukemia. *Haematologica.* **92,** 1043–1050 (2007).

253. Park, E. *et al.* Targeting survivin overcomes drug resistance in acute lymphoblastic leukemia. *Blood.* **118,** 2191–2199 (2011).

254. Okuya, M. *et al.* Up-regulation of survivin by the E2A-HLF chimera is indispensable for the survival of t(17;19)-positive leukemia cells. *J Biol Chem.* **285,** 1850–1860 (2010).

255. Morrison, D. J. *et al.* Endogenous knockdown of survivin improves chemotherapeutic response in ALL models. *Leukemia.* **26,** 271–279 (2012).

256. Croci, D. O. *et al.* Silencing survivin gene expression promotes apoptosis of human breast cancer cells through a caspase-independent pathway. *J Cell Biochem.* **105,** 381–390 (2008).

257. Jin, Y. *et al.* Tenovin-6-mediated inhibition of SIRT1/2 induces apoptosis in acute lymphoblastic leukemia (ALL) cells and eliminates ALL stem/progenitor cells. *BMC Cancer.* **15,** e205 (2015).

258. Diouf, B. *et al.* Somatic deletions of genes regulating MSH2 protein stability cause DNA mismatch repair deficiency and drug resistance in human leukemia cells. *Nat Med.* **17,** 1298–1303 (2011).

259. Deutsch, E. *et al.* BCR-ABL down-regulates the DNA repair protein DNA-PKcs. *Blood.* **97,** 2084–2090 (2001).

260. Kaaijk, P. *et al.* Cell proliferation is related to in vitro drug resistance in childhood acute leukaemia. *Br J Cancer.* **88,** 775–781 (2003).

261. Sauerbrey, A., Stammler, G., Zintl, F. & Volm, M. Expression and prognostic value of the retinoblastoma tumour suppressor gene (RB-1) in childhood acute lymphoblastic leukaemia. *Br J Haematol.* **94,** 99–104 (1996).

262. Addeo, R. *et al.* Glucocorticoids induce G1 arrest of lymphoblastic cells through retinoblastoma protein Rb1 dephosphorylation in childhood acute lymphoblastic leukemia in vivo. *Cancer Biol Ther.* **3,** 470–476 (2004).

263. Kuo, T. C., Chavarria-Smith, J. E., Huang, D. & Schlissel, M. S. Forced expression of cyclin-dependent kinase 6 confers resistance of pro-B acute lymphocytic leukemia to Gleevec treatment. *Mol Cell Biol.* **31,** 2566–2576 (2011).

264. Hulleman, E. *et al.* Inhibition of glycolysis modulates prednisolone resistance in acute lymphoblastic leukemia cells. *Blood.* **113,** 2014–2021 (2009).

265. Liu, T. *et al.* Glucose transporter 1-mediated glucose uptake is limiting for B-cell acute lymphoblastic leukemia anabolic metabolism and resistance to apoptosis. *Cell Death Dis.* **5,** e1470–13 (2014).

266. Eberhart, K. *et al.* Low doses of 2-deoxy-glucose sensitizes acute lymphoblastic leukemia cells to glucocorticoid induced apoptosis. *Leukemia.* **23,** 2167–2170 (2009).

267. Kordes, U., Krappmann, D., Heissmeyer, V., Ludwig, W. D. & Scheidereit, C. Transcription factor NF-kappaB is constitutively activated in acute lymphoblastic leukemia cells. *Leukemia.* **14,** 399–402 (2000).

268. Xu, Y. *et al.* Overexpression of MALT1-A20-NF-κBin adult B-cell acute lymphoblastic leukemia. *Cancer Cell Int.* **15,** 73 (2015).

269. Uckun, F. M., Ozer, Z., Qazi, S., Tuel-Ahlgren, L. & Mao, C. Polo-like-kinase 1 (PLK1) as a molecular target to overcome SYK-mediated resistance of B-lineage acute lymphoblastic leukaemia cells to oxidative stress. *Br J Haematol.* **148,** 714–725 (2010).

270. Uckun, F. M., Ek, R. O., Jan, S.-T., Chen, C.-L. & Qazi, S. Targeting SYK kinase-dependent anti-apoptotic resistance pathway in B-lineage acute lymphoblastic leukaemia (ALL) cells with a potent SYK inhibitory pentapeptide mimic. *Br J Haematol.* **149,** 508–517 (2010).

271. Quentmeier, H., Eberth, S., Romani, J., Zaborski, M. & Drexler, H. G. BCR-ABL1-independent PI3Kinase activation causing imatinib-resistance. *J Hematol Oncol.* **4,** 6 (2011).

272. Nishioka, C., Ikezoe, T., Yang, J. & Yokoyama, A. Long-term exposure of leukemia cells to multi-targeted tyrosine kinase inhibitor induces activations of AKT, ERK and STAT5 signaling via epigenetic silencing of the PTEN gene. *Leukemia.* **24,** 1631–1640 (2010).

273. Morishita, N. *et al.* Activation of Akt is associated with poor prognosis and chemotherapeutic resistance in pediatric B-precursor acute lymphoblastic leukemia. *Pediatr Blood Cancer.* **59,** 83–89 (2011).

274. Montiel-Duarte, C. *et al.* Resistance to Imatinib Mesylate-induced apoptosis in acute lymphoblastic leukemia is associated with PTEN down-regulation due to promoter hypermethylation. *Leuk Res.* **32,** 709–716 (2008).

275. Badura, S. *et al.* Differential effects of selective inhibitors targeting the PI3K/AKT/mTOR pathway in acute lymphoblastic leukemia. *PLoS ONE.* **8,** e80070 (2013).

276. Maude, S. L. *et al.* Targeting JAK1/2 and mTOR in murine xenograft models of Ph-like acute lymphoblastic leukemia. *Blood.* **120,** 3510–3518 (2012).

277. Neri, L. M. *et al.* Targeting the PI3K/Akt/mTOR signaling pathway in B-precursor acute lymphoblastic leukemia and its therapeutic potential. *Leukemia.* **28,** 739–748 (2014).

278. Tasian, S. K. *et al.* Aberrant STAT5 and PI3K/mTOR pathway signaling occurs in human CRLF2-rearranged B-precursor acute lymphoblastic leukemia. *Blood.* **120,** 833–842 (2012).

279. Avellino, R. *et al.* Rapamycin stimulates apoptosis of childhood acute lymphoblastic leukemia cells. *Blood.* **106,** 1400–1406 (2005).

280. Chu, S. *et al.* BCR/ABL kinase inhibition by imatinib mesylate enhances MAP kinase activity in chronic myelogenous leukemia CD34+ cells. *Blood.* **103,** 3167–3174 (2004).

281. Guo, Y. *et al.* Curcumin potentiates the anti-leukemia effects of imatinib by downregulation of the AKT/mTOR pathway and BCR/ABL gene expression in Ph+ acute lymphoblastic leukemia. *Int J Biochem Cell Biol.* **65,** 1–11 (2015).

282. Hasan, M. N. *et al.* Targeting of hyperactivated mTOR signaling in high-risk acute lymphoblastic leukemia in a pre-clinical model. *Oncotarget.* **6,** 1382–1395 (2015).

283. Simioni, C. *et al.* Activity of the novel mTOR inhibitor Torin-2 in B-precursor acute lymphoblastic leukemia and its therapeutic potential to prevent Akt reactivation. *Oncotarget.* **5,** 10034–10047 (2014).

284. Wang, W.-Z. *et al.* Targeting miR-21 sensitizes Ph+ ALL Sup-b15 cells to imatinib-induced apoptosis through upregulation of PTEN. *Biochem Biophys Res Commun.* **454,** 423–428 (2014).

285. Wong, J., Welschinger, R., Hewson, J., Bradstock, K. F. & Bendall, L. J. Efficacy of dual PI-3K and mTOR inhibitors in vitro and in vivo in acute lymphoblastic leukemia. *Oncotarget.* **5,** 10460–10472 (2014).

286. Takano, T., Sada, K. & Yamamura, H. Role of protein-tyrosine kinase syk in oxidative stress signaling in B cells. *Antioxid Redox Signal.* **4,** 533–541 (2002).

287. Ding, J. *et al.* Syk Is Required for the Activation of Akt Survival Pathway in B Cells Exposed to Oxidative Stress. *J Biol Chem.* **275,** 30873–30877 (2000).

288. Chiaretti, S. *et al.* ZAP-70 expression in acute lymphoblastic leukemia: association with the E2A/PBX1 rearrangement and the pre-B stage of differentiation and prognostic implications. *Blood.* **107,** 197–204 (2006).

289. Perova, T. *et al.* Therapeutic potential of spleen tyrosine kinase inhibition for treating high-risk precursor B cell acute lymphoblastic leukemia. *Sci Transl Med.* **6,** 236ra62 (2014).

290. Chen, Z. *et al.* Signalling thresholds and negative B-cell selection in acute lymphoblastic leukaemia. *Nature.* **521,** 357–361 (2015).

291. Degryse, S. & Cools, J. JAK kinase inhibitors for the treatment of acute lymphoblastic leukemia. *J Hematol Oncol.* **8,** 91 (2015).

292. Appelmann, I. *et al.* Janus kinase inhibition by ruxolitinib extends dasatinib- and dexamethasone-induced remissions in a mouse model of Ph+ ALL. *Blood.* **125,** 1444–1451 (2015).

293. Cario, G. *et al.* High CD45 surface expression determines relapse risk in children with precursor B-cell and T-cell acute lymphoblastic leukemia treated according to the ALL-BFM 2000 protocol. *Haematologica.* **99,** 103–110 (2014).

294. Gregory, M. A. *et al.* Wnt/Ca2+/NFAT Signaling Maintains Survival of Ph+ Leukemia Cells upon Inhibition of Bcr-Abl. *Cancer Cell.* **18,** 74–87 (2010).

295. Gardner, L. A. *et al.* Inhibition of calcineurin combined with dasatinib has direct and indirect anti-leukemia effects against BCR-ABL1(+) leukemia. *Am J Hematol.* **89,** 896–903 (2014).

296. Ito, C. *et al.* Cyclosporin A induces apoptosis in childhood acute lymphoblastic leukemia cells. *Blood.* **91,** 1001–1007 (1998).

297. Khan, N. I., Bradstock, K. F. & Bendall, L. J. Activation of Wnt/β-catenin pathway mediates growth and survival in B-cell progenitor acute lymphoblastic leukaemia. *Br J Haematol.* **138,** 338–348 (2007).

298. Mazieres, J. *et al.* Inhibition of Wnt16 in human acute lymphoblastoid leukemia cells containing the t(1;19) translocation induces apoptosis. *Oncogene.* **24,** 5396–5400 (2005).

299. Dandekar, S. *et al.* Wnt inhibition leads to improved chemosensitivity in paediatric acute lymphoblastic leukaemia. *Brit J Haematol.* **167,** 87–99 (2014).

300. Kuhnl, A. *et al.* Overexpression of LEF1 predicts unfavorable outcome in adult patients with B-precursor acute lymphoblastic leukemia. *Blood.* **118,** 6362–6367 (2011).

301. Chiou, S. S. *et al.* Wntless (GPR177) expression correlates with poor prognosis in B-cell precursor acute lymphoblastic leukemia via Wnt signaling. *Carcinogenesis.* **35,** 2357–2364 (2014).

302. Gang, E. J. *et al.* Small-molecule inhibition of CBP/catenin interactions eliminates drug-resistant clones in acute lymphoblastic leukemia. *Oncogene.* **33,** 2169–2178 (2013).

303. Thiago, L. S. *et al.* The Wnt signaling pathway regulates Nalm-16 b-cell precursor acute lymphoblastic leukemic cell line survival and etoposide resistance. *Biomed Pharmacother.* **64,** 63–72 (2010).

304. Knight, T. and Irving, J. A. E. Ras/Raf/MEK/ERK pathway activation in childhood acute lymphoblastic leukemia and its therapeutic targeting. *Front Oncol.* **4,** 160–172 (2014).

305. Liang, D.-C. *et al.* K-ras mutations and N-ras mutations in childhood acute leukemias with or without mixed-lineage leukemia gene rearrangements. *Cancer.* **106,** 950–956 (2006).

306. Driessen, E. M. C. *et al.* Frequencies and prognostic impact of RAS mutations in MLL-rearranged acute lymphoblastic leukemia in infants. *Haematologica.* **98,** 937–944 (2013).

307. Case, M. *et al.* Mutation of genes affecting the RAS pathway is common in childhood acute lymphoblastic leukemia. *Cancer Res.* **68,** 6803–6809 (2008).

308. Irving, J. *et al.* Ras pathway mutations are prevalent in relapsed childhood acute lymphoblastic leukemia and confer sensitivity to MEK inhibition. *Blood.* **124,** 3420–3430 (2014).

309. Ariës, I. M. *et al.* Towards personalized therapy in pediatric acute lymphoblastic leukemia: RAS mutations and prednisolone resistance. *Haematologica.* **100,** e132–6 (2015).

310. Ma, L. *et al.* A therapeutically targetable mechanism of BCR-ABL-independent imatinib resistance in chronic myeloid leukemia. *Sci Transl Med.* **6,** 252ra121 (2014).

311. Miller, A. L. *et al.* Epigenetic alteration by DNA-demethylating treatment restores apoptotic response to glucocorticoids in dexamethasone-resistant human malignant lymphoid cells. *Cancer Cell Int.* **14,** 1–17 (2014).

312. Alsadeq, A. *et al.* Effects of p38α/β inhibition on acute lymphoblastic leukemia proliferation and survival in vivo. *Leukemia.* ePub (2015).

313. Stoskus, M. *et al.* Identification of characteristic IGF2BP expression patterns in distinct B-ALL entities. *Blood Cells Mol Dis.* **46,** 321–326 (2011).

314. Li, B. *et al.* Negative feedback–defective PRPS1 mutants drive thiopurine resistance in relapsed childhood ALL. *Nat Med.* **21,** 563–571 (2015).

315. Mullighan, C. G. *et al.* Deletion of IKZF1and Prognosis in Acute Lymphoblastic Leukemia. *N Engl J Med.* **360,** 470–480 (2009).

316. Harvey, R. C. *et al.* Rearrangement of CRLF2 is associated with mutation of JAK kinases, alteration of IKZF1, Hispanic/Latino ethnicity, and a poor outcome in pediatric B-progenitor acute lymphoblastic leukemia. *Blood.* **115,** 5312–5321 (2010).

317. Lana, T. *et al.* Refinement of IKZF1 status in pediatric Philadelphia-positive acute lymphoblastic leukemia. *Leukemia.* **10,** 2107–2110 (2015).

318. Martinelli, G. *et al.* IKZF1 (Ikaros) deletions in BCR-ABL1-positive acute lymphoblastic leukemia are associated with short disease-free survival and high rate of cumulative incidence of relapse: A GIMEMA AL WP Report. *J Clin Oncol.* **27,** 5202–5207 (2009).

319. van der Veer, A. *et al.* Independent prognostic value of BCR-ABL1-like signature and IKZF1 deletion, but not high CRLF2 expression, in children with B-cell precursor ALL. *Blood.* **122,** 2622–2629 (2013).

320. Burmeister, T. *et al.* Germline variants in IKZF1, ARID5B, and CEBPE as risk factors for adult-onset acute lymphoblastic leukemia: an analysis from the GMALL study group. *Haematologica.* **99,** e23–5 (2014).

321. Clappier, E. *et al.* IKZF1 deletion is an independent prognostic marker in childhood B-cell precursor acute lymphoblastic leukemia, and distinguishes patients benefiting from pulses during maintenance therapy: results of the EORTC Children's Leukemia Group study 58951. *Leukemia.* **29,** 2154–2161 (2015).

322. Olsson, L. & Johansson, B. Ikaros and leukaemia. *Br J Haematol.* **169,** 479–491 (2015).

323. van der Veer, A. *et al.* IKZF1 status as a prognostic feature in BCR-ABL1-positive childhood ALL. *Blood.* **123,** 1691–1698 (2014).

324. Qazi, S. & Uckun, F. M. Incidence and biological significance of IKZF1/Ikaros gene deletions in pediatric Philadelphia chromosome negative and Philadelphia chromosome positive B-cell precursor acute lymphoblastic leukemia. *Haematologica.* **98,** e151–e152 (2013).

325. Palmi, C. *et al.* Impact of IKZF1 deletions on IKZF1 expression and outcome in Philadelphia chromosome negative childhood BCP-ALL. Reply to 'Incidence and biological significance of IKZF1/Ikaros gene deletions in pediatric Philadelphia chromosome negative and Philadelphia chromosome positive B-cell precursor acute lymphoblastic leukemia'. *Haematologica.* **98,** e164–e165 (2013).

326. Uckun, F. M. *et al.* Constitutive function of the Ikaros transcription factor in primary leukemia cells from pediatric newly diagnosed high-risk and relapsed B-precursor ALL patients. *PLoS ONE.* **8,** e80732 (2013).

327. Virely, C. *et al.* Haploinsufficiency of the IKZF1 (IKAROS) tumor suppressor gene cooperates with BCR-ABL in a transgenic model of acute lymphoblastic leukemia. *Leukemia.* **24,** 1200–1204 (2010).

328. Iacobucci, I. *et al.* Expression of spliced oncogenic Ikaros isoforms in Philadelphia-positive acute lymphoblastic leukemia patients treated with tyrosine kinase inhibitors: implications for a new mechanism of resistance. *Blood.* **112,** 3847–3855 (2008).

329. Sengupta, A., Ficker, A. M., Dunn, S. K., Madhu, M. & Cancelas, J. A. Bmi1 reprograms CML B-lymphoid progenitors to become B-ALL-initiating cells. *Blood.* **119,** 494–502 (2012).

330. Mullighan, C. G., Williams, R. T., Downing, J. R. & Sherr, C. J. Failure of CDKN2A/B (INK4A/B-ARF)-mediated tumor suppression and resistance to targeted therapy in acute lymphoblastic leukemia induced by BCR-ABL. *Genes Dev.* **22,** 1411–1415 (2008).

331. Feldhahn, N. *et al.* Activation-induced cytidine deaminase acts as a mutator in BCR-ABL1-transformed acute lymphoblastic leukemia cells. *J Exp Med.* **204,** 1157–1166 (2007).

332. Klemm, L. *et al.* The B cell mutator AID promotes B lymphoid blast crisis and drug resistance in chronic myeloid leukemia. *Cancer Cell.* **16,** 232–245 (2009).

333. Mullighan, C. G. *et al.* BCR–ABL1 lymphoblastic leukaemia is characterized by the deletion of Ikaros. *Nature.* **453,** 110–114 (2008).

334. Müschen, M. Rationale for targeting the pre-B-cell receptor signaling pathway in acute lymphoblastic leukemia. *Blood.* **125,** 3688–3693 (2015).

335. Duy, C. *et al.* BCL6 enables Ph+ acute lymphoblastic leukemia cells to survive BCR-ABL1 kinase inhibition. *Nature.* **473,** 384–388 (2012).

336. Kuhnl, A. *et al.* High BAALC expression predicts chemoresistance in adult B-precursor acute lymphoblastic leukemia. *Blood.* **115,** 3737–3744 (2010).

337. Masouleh, K. B. *et al.* Mechanistic rationale for targeting the unfolded protein response in pre-B acute lymphoblastic leukemia. *Proc Natl Acad Sci U S A.* **111,** e2219–e2228 (2014).

338. Perez-Andreu, V. *et al.* Inherited GATA3 variants are associated with Ph-like childhood acute lymphoblastic leukemia and risk of relapse. *Nat Genet.* **45,** 1494–1498 (2013).

339. Kaur, P. *et al.* Nilotinib treatment in mouse models of P190 Bcr/Abl lymphoblastic leukemia. *Mol Cancer.* **6,** 67 (2007).

340. Sison, E. A. R. & Brown, P. The bone marrow microenvironment and leukemia: biology and therapeutic targeting. *Expert Rev Hematol.* **4,** 271–283 (2011).

341. Zhang, Y. *et al.* Bone marrow mesenchymal stromal cells affect the cell cycle arrest effect of genotoxic agents on acute lymphocytic leukemia cells via p21 down-regulation. *Ann Hematol.* **93,** 1499–1508 (2014).

342. Mudry, R. E., Fortney, J. E., York, T., Hall, B. M. & Gibson, L. F. Stromal cells regulate survival of B-lineage leukemic cells during chemotherapy. *Blood.* **96,** 1926–1932 (2000).

343. Ayala, F., Dewar, R., Kieran, M. & Kalluri, R. Contribution of bone microenvironment to leukemogenesis and leukemia progression. *Leukemia.* **23,** 2233–2241 (2009).

344. Manabe, A., Coustan-Smith, E., Behm, F. G., Raimondi, S. C. & Campana, D. Bone marrow-derived stromal cells prevent apoptotic cell death in B-lineage acute lymphoblastic leukemia. *Blood.* **79,** 2370–2377 (1992).

345. Duan, C.-W. *et al.* Leukemia propagating cells rebuild an evolving niche in response to therapy. *Cancer Cell.* **25,** 778–793 (2014).

346. Manabe, A. *et al.* Adhesion-dependent survival of normal and leukemic human B lymphoblasts on bone marrow stromal cells. *Blood.* **83,** 758–766 (1994).

347. Iwamoto, S., Mihara, K., Downing, J. R., Pui, C.-H. & Campana, D. Mesenchymal cells regulate the response of acute lymphoblastic leukemia cells to asparaginase. *J Clin Invest.* **117,** 1049–1057 (2007).

348. Tripodo, C. *et al.* The bone marrow stroma in hematological neoplasms—a guilty bystander. *Nat Rev Clin Oncol.* **8,** 456–466 (2011).

349. Mallampati, S. *et al.* Tyrosine kinase inhibitors induce mesenchymal stem cell-mediated resistance in BCR-ABL+ acute lymphoblastic leukemia. *Blood.* **125,** 2968–2973 (2015).

350. Shishido, S. *et al.* Role of integrin alpha4 in drug resistance of leukemia. *Front Oncol.* **4,** 99 (2014).

351. Konopleva, M., Tabe, Y., Zeng, Z. & Andreeff, M. Therapeutic targeting of microenvironmental interactions in leukemia: Mechanisms and approaches. *Drug Resist Updat.* **12,** 103–113 (2009).

352. Shalapour, S. *et al.* High VLA-4 expression is associated with adverse outcome and distinct gene expression changes in childhood B-cell precursor acute lymphoblastic leukemia at first relapse. *Haematologica.* **96,** 1627–1635 (2011).

353. Hu, Z. & Slayton, W. B. Integrin VLA-5 and FAK are good targets to improve treatment response in the Philadelphia chromosome positive acute lymphoblastic leukemia. *Front Oncol.* **4,** 112. (2014).

354. Rhein, P. *et al.* CD11b is a therapy resistance- and minimal residual disease-specific marker in precursor B-cell acute lymphoblastic leukemia. *Blood.* **115,** 3763–3771 (2010).

355. Krause, D. S., Lazarides, K., Lewis, J. B., Andrian, von, U. H. & Van Etten, R. A. Selectins and their ligands are required for homing and engraftment of BCR-ABL1+ leukemic stem cells in the bone marrow niche. *Blood.* **123,** 1361–1371 (2014).

356. de Bock, C. E. *et al.* The Fat1 cadherin is overexpressed and an independent prognostic factor for survival in paired diagnosis--relapse samples of precursor B-cell acute lymphoblastic leukemia. *Leukemia.* **26,** 918–926 (2011).

357. Taylor, K. H. *et al.* Large-scale CpG methylation analysis identifies novel candidate genes and reveals methylation hotspots in acute lymphoblastic leukemia. *Cancer Res.* **67,** 2617–2625 (2007).

358. Aries, I. M. *et al.* EMP1, a novel poor prognostic factor in pediatric leukemia regulates prednisolone resistance, cell proliferation, migration and adhesion. *Leukemia.* **28**, 1828-1837 (2014).

359. de Lourdes Perim, A., Amarante, M. K., Guembarovski, R. L., de Oliveira, C. E. C. & Watanabe, M. A. E. CXCL12/CXCR4 axis in the pathogenesis of acute lymphoblastic leukemia (ALL): a possible therapeutic target. *Cell Mol Life Sci.* **72,** 1715–1723 (2015).

360. van den Berk, L. C. J. *et al.* Disturbed CXCR4/CXCL12 axis in paediatric precursor B-cell acute lymphoblastic leukaemia. *Br J Haematol.* **166,** 240–249 (2014).

361. Konoplev, S. *et al.* Phosphorylated CXCR4 is associated with poor survival in adults with B-acute lymphoblastic leukemia. *Cancer.* **117,** 4689–4695 (2011).

362. Mishra, S. *et al.* Resistance to imatinib of Bcr/Abl p190 lymphoblastic leukemia cells. *Cancer Res.* **66,** 5387–5393 (2006).

363. Fei, F. *et al.* Development of resistance to dasatinib in Bcr/Abl-positive acute lymphoblastic leukemia. *Leukemia.* **24,** 813–820 (2010).

364. Yu, M. *et al.* AMD3100 sensitizes acute lymphoblastic leukemia cells to chemotherapy in vivo. *Blood Cancer J.* **1,** e14 (2011).

365. Welschinger, R. *et al.* Plerixafor (AMD3100) induces prolonged mobilization of acute lymphoblastic leukemia cells and increases the proportion of cycling cells in the blood in mice. *Exp Hematol.* **41,** 293–302.e1 (2013).

366. Sison, E. A. R. *et al.* Plerixafor as a chemosensitizing agent in pediatric acute lymphoblastic leukemia: efficacy and potential mechanisms of resistance to CXCR4 inhibition. *Oncotarget* **5,** 8947–8958 (2014).

367. Parameswaran, R. *et al.* Effector-mediated eradication of precursor B acute lymphoblastic leukemia with a novel Fc-engineered monoclonal antibody targeting the BAFF-R. *Mol Cancer Ther.* **13,** 1567–1577 (2014).

368. Castro, F. V. *et al.* 5T4 oncofetal antigen is expressed in high risk of relapse childhood pre-B acute lymphoblastic leukemia and is associated with a more invasive and chemotactic phenotype. *Leukemia.* **26,** 1487–1498 (2012).

369. Winkler, B. *et al.* TGFβ and IL10 have an impact on risk group and prognosis in childhood ALL. *Pediatr Blood Cancer.* **62,** 72–79 (2014).

370. Singh, H. *et al.* A screening-based approach to circumvent tumor microenvironment-driven intrinsic resistance to BCR-ABL+ inhibitors in Ph+ acute lymphoblastic leukemia. *J Biomol Screen.* **19,** 158–167 (2013).

371. Brown, V. I. *et al.* Thymic stromal-derived lymphopoietin induces proliferation of pre-B leukemia and antagonizes mTOR inhibitors, suggesting a role for interleukin-7Rα signaling. *Cancer Res.* **67,** 9963–9970 (2007).

372. Liu, J. *et al.* BCR-ABL mutants spread resistance to non-mutated cells through a paracrine mechanism. *Leukemia.* **22,** 791–799 (2008).

373. Troeger, A. *et al.* High expression of CD40 on B-cell precursor acute lymphoblastic leukemia blasts is an independent risk factor associated with improved survival and enhanced capacity to up-regulate the death receptor CD95. *Blood.* **112,** 1028–1034 (2008).

374. Troeger, A. *et al.* Reduced expression and defective modulation of TNF Receptor/Ligand Family Molecules on proB-ALL blasts. *Klin Padiatr.* **220,** 353–357 (2008).

375. Troeger, A. *et al.* Up-regulation of c-FLIPS+R upon CD40 stimulation is associated with inhibition of CD95-induced apoptosis in primary precursor B-ALL. *Blood.* **110,** 384–387 (2007).

376. Uno, K. TNF-related apoptosis-inducing ligand (TRAIL) frequently induces apoptosis in Philadelphia chromosome-positive leukemia cells. *Blood.* **101,** 3658–3667 (2002).

377. Ehrhardt, H., Wachter, F., Grunert, M. & Jeremias, I. Cell cycle-arrested tumor cells exhibit increased sensitivity towards TRAIL-induced apoptosis. *Cell Death Dis.* **4,** e661–10 (2013).

378. Clodi, K. *et al.* Expression of tumour necrosis factor (TNF)-related apoptosis-inducing ligand (TRAIL) receptors and sensitivity to TRAIL-induced apoptosis in primary B-cell acute lymphoblastic leukaemia cells. *Br J Haematol.* **111,** 580–586 (2000).

379. Castro Alves, C. *et al.* Leukemia-initiating cells of patient-derived acute lymphoblastic leukemia xenografts are sensitive toward TRAIL. *Blood.* **119,** 4224–4227 (2012).

380. Ehrhardt, H. *et al.* TRAIL induced survival and proliferation in cancer cells resistant towards TRAIL-induced apoptosis mediated by NF-κB. *Oncogene.* **22,** 3842–3852 (2003).

381. Doubravská, L. *et al.* Wnt-expressing rat embryonic fibroblasts suppress Apo2L/TRAIL-induced apoptosis of human leukemia cells. *Apoptosis.* **13,** 573–587 (2008).

382. Dida, F. *et al.* Resistance to TRAIL-induced apoptosis caused by constitutional phosphorylation of Akt and PTEN in acute lymphoblastic leukemia cells. *Exp Hematol.* **36,** 1343–1353 (2008).

383. Irwin, M. E. *et al.* Small molecule ErbB inhibitors decrease proliferative signaling and promote apoptosis in Philadelphia chromosome–positive acute lymphoblastic leukemia. *PLoS ONE.* **8,** e70608 (2013).

384. Chevallier, P. *et al.* Overexpression of Her2/neu is observed in one third of adult acute lymphoblastic leukemia patients and is associated with chemoresistance in these patients. *Haematologica.* **89,** 1399–1401 (2004).

385. Troeger, A. *et al.* High nerve growth factor receptor (p75NTR) expression is a favourable prognostic factor in paediatric B cell precursor-acute lymphoblastic leukaemia. *Br J Haematol.* **139,** 450–457 (2007).

386. Laranjeira, A. B. A. *et al.* IGFBP7 participates in the reciprocal interaction between acute lymphoblastic leukemia and BM stromal cells and in leukemia resistance to asparaginase. *Leukemia.* **26,** 1001–1011 (2011).

387. Boutter, J. *et al.* Image-based RNA interference screening reveals an individual dependence of acute lymphoblastic leukemia on stromal cysteine support. *Oncotarget.* **5,** 11501–11512 (2014).

388. Naderi, E. *et al.* Bone marrow stroma-derived PGE2 protects BCP-ALL cells from DNA damage-induced p53 accumulation and cell death. *Mol Cancer.* **14,** 14 (2015).

389. Fei, F. *et al.* B-cell precursor acute lymphoblastic leukemia and stromal cells communicate through Galectin-3. *Oncotarget.* **6,** 11378–11394 (2015).

390. de Vries, J. F. *et al.* The potential use of basigin (CD147) as a prognostic marker in B-cell precursor acute lymphoblastic leukaemia. *Br J Haematol.* **150,** 624–626 (2010).

391. Beesley, A. H. *et al.* The gene expression signature of relapse in paediatric acute lymphoblastic leukaemia: implications for mechanisms of therapy failure. *Br J Haematol.* **131,** 447–456 (2005).

392. Friesen, C. *et al.* Cell death sensitization of leukemia cells by opioid receptor activation. *Oncotarget.* **4,** 677–690 (2013).

393. Boyerinas, B. *et al.* Adhesion to osteopontin in the bone marrow niche regulates lymphoblastic leukemia cell dormancy. *Blood.* **121,** 4821–4831 (2013).

394. Tavor, S. & Petit, I. Can inhibition of the SDF-1/CXCR4 axis eradicate acute leukemia? *Semin Cancer Biol.* **20,** 178–185 (2010).

395. Frolova, O. *et al.* Regulation of HIF-1α signaling and chemoresistance in acute lymphocytic leukemia under hypoxic conditions of the bone marrow microenvironment. *Cancer Biol Ther.* **13,** 858–870 (2012).

396. Wellmann, S. *et al.* Activation of the HIF pathway in childhood ALL, prognostic implications of VEGF. *Leukemia.* **18,** 926–933 (2004).

397. Stachel, D., Albert, M., Meilbeck, R., Paulides, M. & Schmid, I. Expression of angiogenic factors in childhood B-cell precursor acute lymphoblastic leukemia. *Oncol Rep.* **17,** 147–152 (2007).

398. Benito, J. *et al.* Pronounced hypoxia in models of murine and human leukemia: high efficacy of hypoxia-activated prodrug PR-104. *PLoS ONE.* **6,** e23108 (2011).

399. Corthals, S. L. *et al.* Differential immune effects mediated by Toll-like receptors stimulation in precursor B-cell acute lymphoblastic leukaemia. *Br J Haematol.* **132**, 452-458 (2005).

400. Entrena, A. *et al.* Mesenchymal stem cells derived from low risk acute lymphoblastic leukemia patients promote NK cell antitumor activity. *Cancer Lett.* **363,** 156–165 (2015).

401. Behan, J. W. *et al.* Adipocytes impair leukemia treatment in mice. *Cancer Res.* **69,** 7867–7874 (2009).

402. Harrison, C. J. Targeting signaling pathways in acute lymphoblastic leukemia: new insights. *Hematology Am Soc Hematol Educ Program.* **2013,** 118–125 (2013).

403. Annesley, C. E. & Brown, P. Novel agents for the treatment of childhood acute leukemia. *Ther Adv Hematol.* **6,** 61–79 (2015).

404. Jones, C. L. *et al.* Loss of TBL1XR1 Disrupts Glucocorticoid Receptor Recruitment to Chromatin and Results in Glucocorticoid Resistance in a B-Lymphoblastic Leukemia Model. *J Biol Chem.* **289,** 20502–20515 (2014).

405. Kebriaei, P. & Poon, M. L. Future of therapy in acute lymphoblastic leukemia (ALL)—potential role of immune-based therapies. *Curr Hematol Malig Rep.* **10,** 76–85 (2015).

406. Jabbour, E., O'Brien, S., Konopleva, M. & Kantarjian, H. New insights into the pathophysiology and therapy of adult acute lymphoblastic leukemia. *Cancer.* **121,** 2517–2528 (2015).

407. Pallasch, C. P. *et al.* Sensitizing Protective Tumor Microenvironments to Antibody-Mediated Therapy. *Cell.* **156,** 590–602 (2014).

408. Bouhassira, D. C., Thompson, J. J. & Davila, M. L. Using gene therapy to manipulate the immune system in the fight against B-cell leukemias. *Expert Opin Biol Ther.* **15,** 403–416 (2015).

409. Hutchinson, L. CAR-modified T cells targeting CD19—curing the incurable. *Nat Rev Clin Oncol.* **11,** 683–683 (2014).

410. Jacoby, E. *et al.* Murine models of acute leukemia: important tools in current pediatric leukemia research. *Front Oncol.* **4,** 95 (2014).

411. Nowak, D. *et al.* Variegated clonality and rapid emergence of new molecular lesions in xenografts of acute lymphoblastic leukemia are associated with drug resistance. *Exp Hematol.* **43,** 32–43 (2015).

412. Hauer, J., Borkhardt, A., Sánchez-García, I. & Cobaleda, C. Genetically engineered mouse models of human B-cell precursor leukemias. *Cell Cycle.* **13,** 2836–2846 (2014).

413. Meacham, C. E. *et al.* A genome-scale in vivo loss-of-function screen identifies Phf6 as a lineage-specific regulator of leukemia cell growth. *Genes Dev.* **29,** 483–488 (2015).

414. Hyvärinen, A. & Oja, E. Independent component analysis: algorithms and applications. *Neural Netw.* **13,** 411–430 (2000).

**Chapter II: *In vivo* RNAi screening in *BCR-ABL1+* BCP-ALL differentiates genetic requirements for leukemia cell growth versus therapeutic response in a setting-specific manner.**

---

Eleanor R. Cameron, Arjun Bhutkar, Michael T. Hemann

David H. Koch Institute for Integrative Cancer Research, Massachusetts Institute of Technology. Cambridge, Massachusetts, 02139, United States.

This chapter is not published as of December 2015.

## Introduction

Expression of the oncogenic tyrosine kinase *BCR-ABL1* typically arises from the t(9;22) balanced chromosomal translocation known as the Philadelphia chromosome (1, 2). This cytogenetic abnormality is associated with two separate hematological malignancies: chronic myelogenous leukemia (CML) and Philadelphia chromosome-positive acute lymphoblastic leukemia, a subtype of precursor B-cell acute lymphoblastic leukemia (1,2). In Philadelphia chromosome-positive acute lymphoblastic leukemia (*BCR-ABL1*+ BCP-ALL), Bcr-Abl kinase expression cooperates with additional genetic changes including activation of *SRC* family kinases and/or loss of tumor suppressors like *ARF* and *IKZF1* (3-5). Tyrosine kinase inhibitors (TKIs) that directly inhibit Bcr-Abl and related mitogenic kinases are effective and well-tolerated treatments for Philadelphia-positive leukemias, but relapse after therapy is a persistent clinical problem (3, 6-12). Recent drug development efforts have largely focused on targeting mutated forms of the Bcr-Abl kinase, which are often responsible for resistance to TKI therapy, but Bcr-Abl independent relapse also occurs in approximately a third of *BCR-ABL1*+ BCP-ALL patients after treatment with all currently approved TKIs (12-21).

One of the described mechanisms of Bcr-Abl independent resistance to TKIs is the activation of parallel pathways, such as the observed activation of Src family kinases in CML after treatment with imatinib (14, 15, 19). Dasatinib, a second-generation TKI approved for imatinib-resistant or intolerant *BCR-ABL1*+ BCP-ALL patients, inhibits both Abl and Src family kinases as well as many of the mutated forms of Bcr-Abl (8, 9, 22-25). However, *BCR-ABL1*+ BCP-ALL patients experience a short response to dasatinib followed by relapse; even when dasatinib is combined with

conventional chemotherapeutics, more than half of patients relapse within two years (8, 9, 26, 27). Bcr-Abl independent resistance to dasatinib therapy, as with drug resistance in other BCP-ALL subtypes, can be fueled by activation of parallel intracellular signaling pathways, inhibition of apoptotic pathways, and leukemia cell interactions with the microenvironment (3, 4, 19, 28-34). Due to the multiclonal nature of BCP-ALL, it is possible that more than one resistance mechanism could arise in a single patient, making combination therapy the most likely path to success in treatment of this disease (35-38). Identification of specific drug targets for combination therapy with TKIs is crucial in understanding and treating relapses that lack Bcr-Abl mutations and, by improving drug efficacy, may allow for the eradication of all *BCR*-ABL1+ BCP-ALL cells before Bcr-Abl mutant clones can be strongly selected for (34).

In recent years, loss-of-function screens using RNAi to interrogate cellular phenotypes have been incredibly useful in dissecting the genes involved in both cellular growth and drug response (39). Transplantable malignancies, patient-derived xenograft models, direct delivery of shRNAs or siRNAs to tissues of interest, and transduction of mouse embryos have allowed for *in vivo* RNAi screening in the context of a functional microenvironment (40-46). We and others have shown that pool-based shRNA screening *in vivo* can identify mediators of tumor growth and progression as well as ability to disseminate to distinct anatomical sites (42-45, 47-49). In the context of therapy, RNAi based screens have been used *in vitro* and *in vivo* to identify genes or pathways that mediate therapeutic response in tumor cells (32, 47, 50-52). Unbiased shRNA screening in particular can allow for the identification of completely novel genetic

regulators of a phenotype, such as those genes or pathways that might function as targets for combination therapy (42, 52).

Here we have utilized a transplantable mouse model of *BCR-ABL1*+ BCP-ALL to perform a pooled, unbiased shRNA screen for genetic mediators of response to dasatinib in the context of the native microenvironment (28, 29). Using this model, we can transplant murine $p19^{Arf-/-}$ pre-B cells expressing p185 *BCR-ABL1* into immunocompetent recipient mice to produce an aggressive polyclonal B-cell leukemia that responds to therapy in a manner similar to the human disease (28, 29, 53). shRNA screening in this model allows for isolation of genes that differentially affect leukemic growth *in vivo* versus *in vitro*, and here we use a longitudinal method of screening to show that this model can also be used to identify shRNAs that promote resistance or sensitivity to dasatinib therapy specifically in the *in vivo* setting (42). Additionally, we found that independent component analysis is an effective method for identifying high-value candidate hits from RNAi screens performed in settings where strong clonal signals or high levels of noise mask the signal associated with the phenotype of interest.

**Results**

To identify genes that confer resistance or sensitivity to dasatinib *in vivo* in an unbiased manner, we took advantage of the fact that the transplantable $p19^{Arf-/-}$ mouse model of *BCR-ABL1*+ BCP-ALL allows for the *in vivo* introduction of large sets of shRNAs (42). We performed pooled shRNA screens for mediators of dasatinib response in mice and in culture by transducing leukemia cells with an unbiased pool of 20,000 shRNAs and either transplanting infected cells into multiple

recipient mice or plating them in culture for a parallel *in vitro* screen. After disease development, we took both pre- and post-treatment blood samples, as well as samples from cultured *in vitro* screens, and then amplified out and sequenced the library hairpins present in all samples. By comparing matched pre- and post-treatment samples from the blood of an individual mouse or a single cell culture dish, we were able to perform a longitudinal study measuring changes in hairpin representation before and after therapy both *in vivo* and *in vitro*. (Figure 1A). We found that we were able to represent an average of 15,000 unique hairpins both before and after therapy *in vivo*, and between 17,500 and 18,500 unique hairpins *in vitro* both before and after therapy (Figure 1B).

Due to the serial sampling method used in our screen, we were able to measure the enrichment or depletion of shRNAs both before and after dasatinib treatment in mice and in cell culture, and thus could compare changes in shRNA representation between the two separate time periods as well as between *in vivo* and *in vitro* screens. We observed a strong clonal effect of cells *in vivo*, as both pre- and post-treatment samples from each mouse clustered together based hierarchical clustering of the normalized representation of all hairpins in the library (Figure 1C). Unsurprisingly, the input sample, which is a sample of leukemia cells at the time of transplantation into mice, clusters independently from all of the *in vivo* samples. In contrast, if we perform the same clustering analysis on the data from our parallel *in vitro* screen, we see that input and pre-treatment samples clustered independently of post-treatment samples (Figure 1D).

When we looked at hairpin behavior over time, as measured by fold changes in shRNA representation, we found that clonal effects no longer dominated the *in vivo* data. Principal component analysis of the log fold changes before and after therapy *in*

*vivo* and *in vitro* revealed that hairpin behavior over time causes screening samples to cluster based on both setting and therapeutic context (Figure 1E). As expected, the *in vitro* samples before or after treatment clustered very closely together, whereas there was much larger variation between *in vivo* samples both before and after therapy. Similarly, we also found via hierarchical clustering of fold changes in hairpin representation that *in vivo* samples after dasatinib treatment segregate from the matched sample before treatment based on enrichment or depletion of library shRNAs during each time period, despite having taken these samples from the same mice (Supplementary Figure S1). Hierarchical clustering of fold changes in hairpin representation also segregated *in vivo* and *in vitro* samples both before and after therapy (Supplementary Figure S1).

If we repeated principal component analysis but included the fold change in hairpin representation over the entire course of the screen (post-treatment/input), we found that for the *in vivo* screen these values cluster with the fold changes before treatment (Supplementary Figure S1). In contrast, the post-treatment/input fold changes for the *in vitro* screen clustered independently, but were closer to the after treatment *in vitro* cluster than the before treatment *in vitro* cluster. This may indicate that while the presence or absence of therapy is the strongest variable defining hairpin behavior *in vitro*, hairpin behavior *in vivo* is primarily defined by clonal signals that identify the distinct set of hairpins transplanted into each mouse (e.g. differences in transplant or engraftment of leukemic cells).

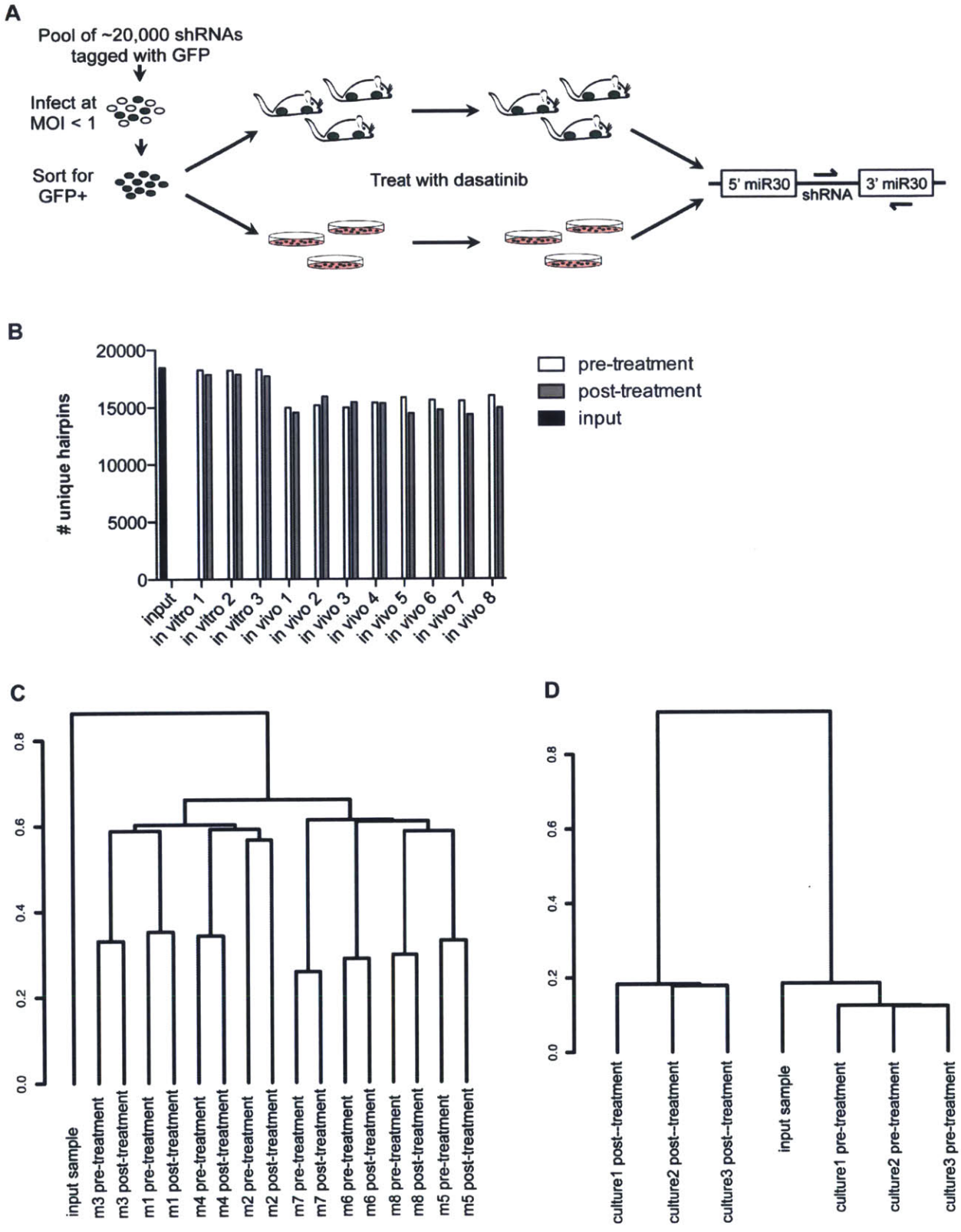


**Figure 1.** continued on next page

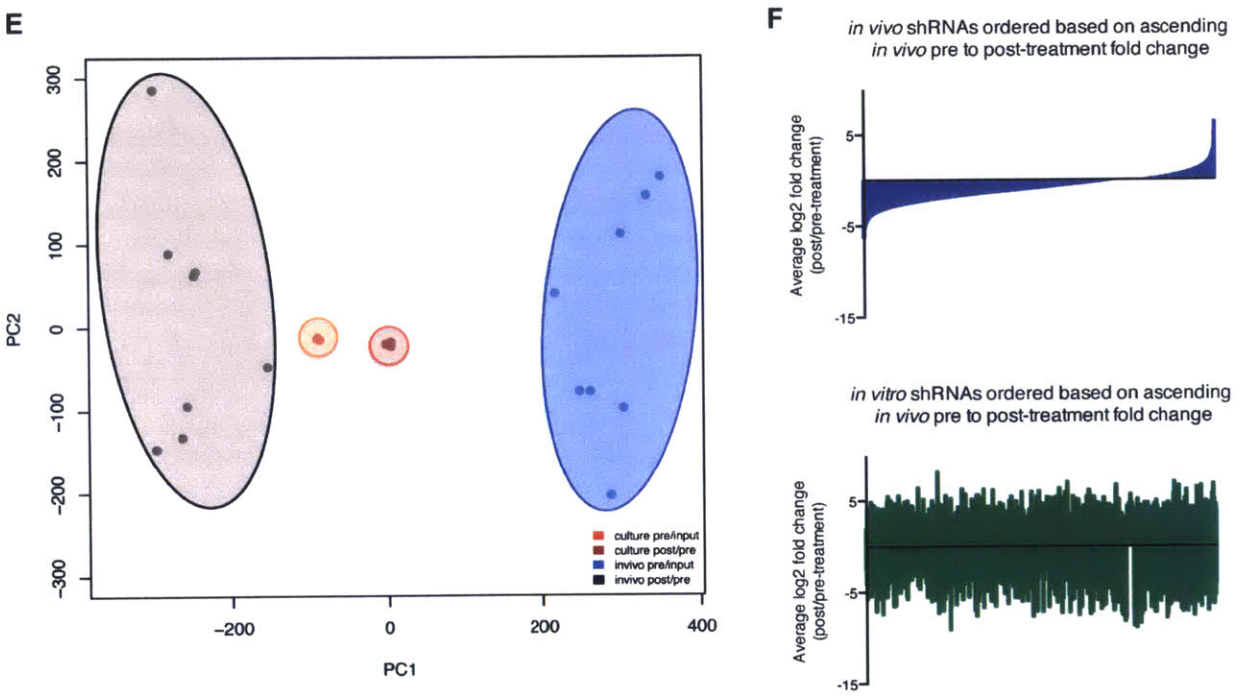


**Figure 1. RNAi screening for genetic mediators of response to dasatinib *in vivo* using a transplantable *BCR-ABL1*+ BCP-ALL model.**
(A) Schematic representation of the longitudinal screening strategy. Leukemia cells were transduced with a pooled shRNA library and then either injected into recipient mice for *in vivo* screening or cultured for *in vitro* screening, and at overt leukemia presentation mice and cultured cells were treated with dasatinib. High throughput sequencing was used to assess hairpin representation at transplant (input), before treatment (pre-treatment), and at morbidity (post-treatment) in the blood of individual mice or in cell culture dishes. (B) Bar graph showing the number of unique hairpins detected in each *in vivo* and *in vitro* sample both before and after treatment, as well as at transplant/plating (input). (C) & (D) Dendrograms generated by hierarchical clustering of normalized hairpin representation at transplant and before and after treatment *in vivo* (C) and *in vitro* (D) shows that pre- and post-treatment samples from the same mice cluster together *in vivo*, but *in vitro* all the pre-treatment and post-treatment samples cluster separately. (E) Principal component analysis of $\log_2$ fold changes before and (pre/input) after treatment (post/pre) *in vivo* and *in vitro* shows that all four groups cluster independently of one another, but there is much less variation *in vitro* than *in vivo*. (F) Waterfall plots representing the $\log_2$ fold changes after dasatinib therapy of all shRNAs in the library *in vivo* (blue) and *in vitro* (green), with shRNAs arranged in rank ascending order based on their $\log_2$ fold change *in vivo*. Hairpin behavior after dasatinib therapy *in vivo* does not predict behavior *in vitro*.

We also found that the behavior of shRNAs after dasatinib treatment *in vivo* does not predict their behavior after treatment *in vitro*, as illustrated by comparison of rank-order lists of shRNA depletion or enrichment before versus after therapy (Figure 1F). This phenomenon of limited mutual information between *in vivo* and *in vitro* screens can also been seen before therapy is administered (Supplemental Figure S2). Similarly, the fold change of hairpins before therapy *in vivo* or *in vitro* does not predict their fold change after therapy in the same setting (Supplemental Figure S2). While this lack of correlation between groups could simply be due to extremely poor correlation among biological replicates, we found that in all cases biological replicates are more correlated to each other than they are to non-replicates (Supplemental Figure S3).

This dataset produced an extremely large number of hairpins that have distinct behavior after therapy as compared to before. Additionally, the high variability between biological replicates and the clonal effects that we have observed *in vivo* add a significant amount of noise to the dataset. The goal of this screen was to identify those hairpins that affect therapeutic response, which should be a non-clonal signal that is shared across multiple mice. Hierarchical clustering of shRNA fold changes suggests that this signal exists, but it may be overwhelmed by the noise and clonal signals in the raw *in vivo* RNAi data. In order to identify those high-confidence hits whose behavior is determined by the non-clonal signature associated with response to therapy in the *in vivo* setting, we turned to independent component analysis (ICA).

Independent component analysis is a form of blind-source separation that can be used to reduce clonality and identify latent variables in a dataset (54). ICA generates (n-1) independent components, each of which has an associated signature of hairpins

whose representation across samples significantly matches that component; this data is best represented in a Hinton plot (Figure 2A). In our *in vivo* screening data, independent component 10 (IC10) identified a signature of shRNAs that have significantly different representation before therapy as compared to after therapy in the *in vivo* screen ($p = 0.0078$, Mann-Whitney U-test). This signature encompassed both those hairpins that have higher representation after dasatinib as compared to before and thus may enrich after therapy as well as those hairpins that have lower representation after treatment and thus may deplete after therapy (Figure 2B, 2C). The component 10 Z-score for each hairpin quantifies the extent of its contribution to that component, and a Z-score greater than 2 or less than -2 for component 10 identifies those hairpins that have either significantly lower or significantly higher representation after therapy as compared to before, respectively (Figure 2B, 2C). The gene identifiers associated with hairpins that had a Z-score with an absolute value greater than 2 for IC10 are listed in Supplemental Tables I and II; importantly, IC10 also identified hairpins that target undescribed regions of the mouse genome, although they are not listed here.

We separated the 15 components identified by ICA into two categories: those that describe clonal effects, defined here as variations in hairpin representation common to a single mouse or several mice both before and after treatment, and those that describe non-clonal effects, including IC10 (Supplementary Figure S4). While there are many more independent components that describe clonal behavior in the dataset, the only components that describe significant changes in hairpin representation (by the Mann Whitney U-test) are IC10 and IC12, both of which are non-clonal. IC12 represents

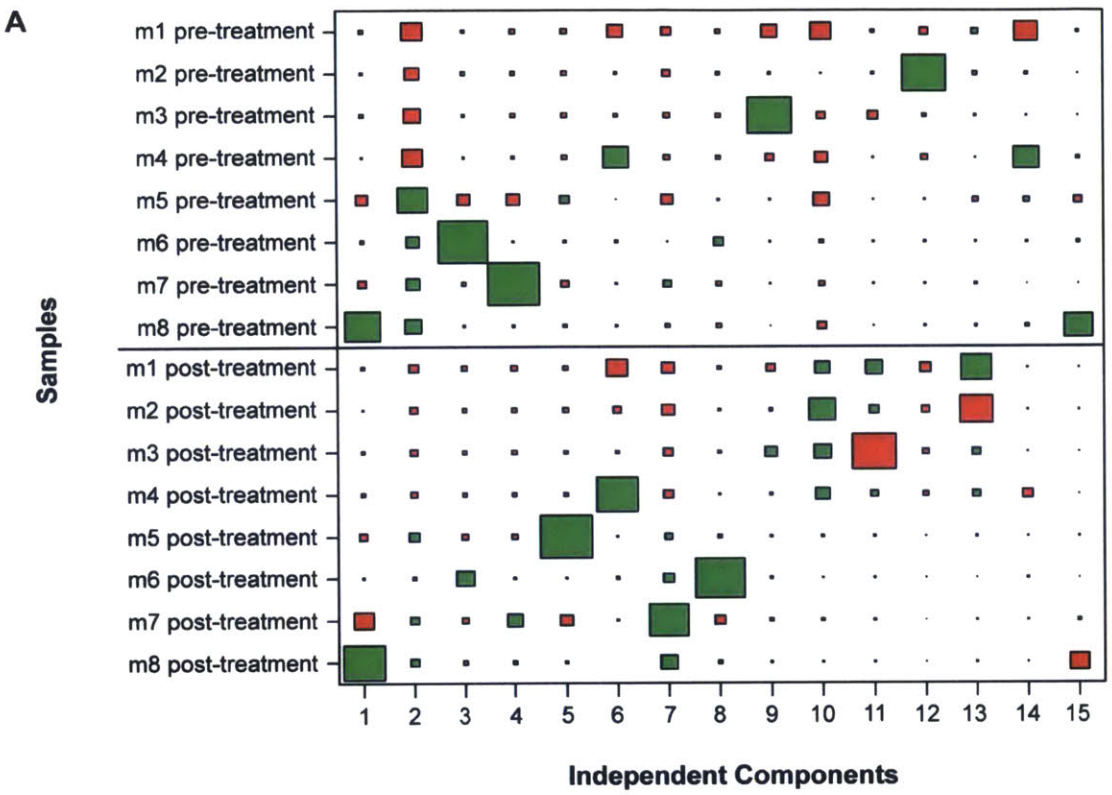
A
m1 pre-treatment
m2 pre-treatment
m3 pre-treatment
m4 pre-treatment
m5 pre-treatment
m6 pre-treatment
m7 pre-treatment
m8 pre-treatment
m1 post-treatment
m2 post-treatment
m3 post-treatment
m4 post-treatment
m5 post-treatment
m6 post-treatment
m7 post-treatment
m8 post-treatment
Samples
1 2 3 4 5 6 7 8 9 10 11 12 13 14 15
Independent Components

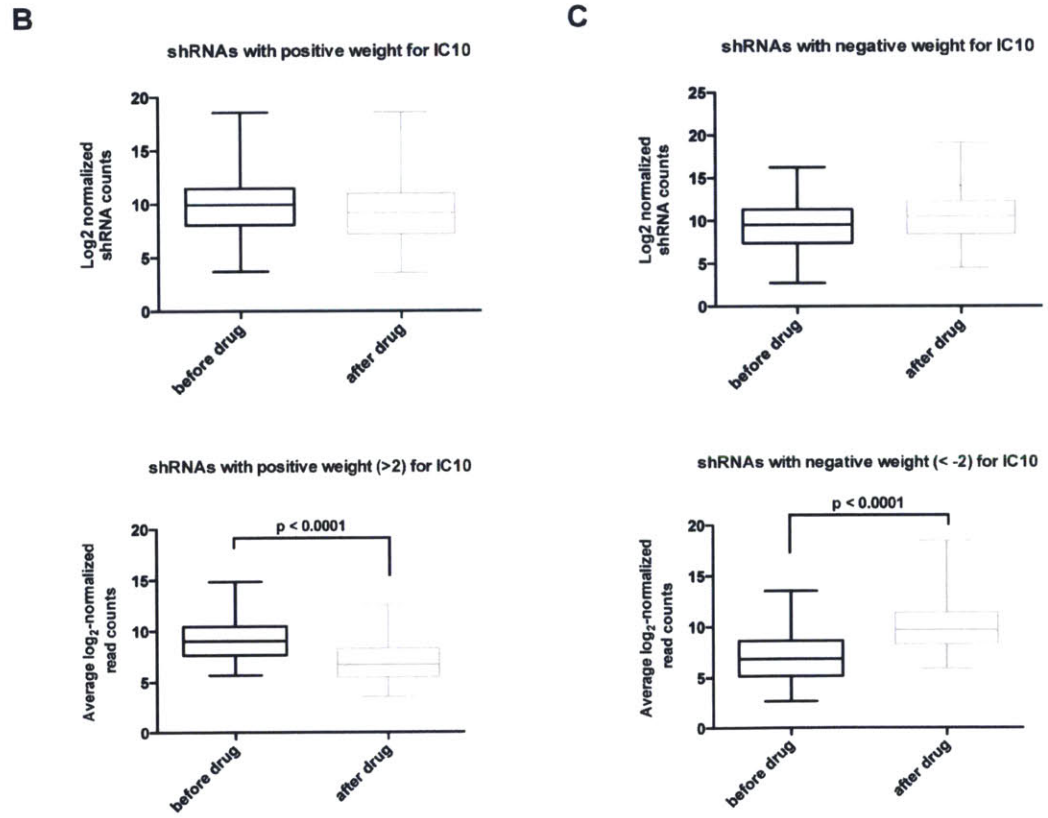
B
shRNAs with positive weight for IC10
Log2 normalized shRNA counts
before drug
after drug
C
shRNAs with negative weight for IC10
Log2 normalized shRNA counts
before drug
after drug
shRNAs with positive weight (>2) for IC10
Average log2-normalized read counts
p < 0.0001
before drug
after drug
shRNAs with negative weight (< -2) for IC10
Average log2-normalized read counts
p < 0.0001
before drug
after drug

**Figure 2. Independent component analysis of RNAi screening data identifies a signature of hairpins that enrich or deplete after therapy.**
(A) Hinton plot of the independent components shows the signature generated by each component across all *in vivo* samples before and after dasatinib treatment. Colors represent the directionality of hairpin representation (red enriched, green depleted), and the size of each rectangle quantifies the strength of the signature for that sample. Each component identifies a two-sided signature, such that there are enriched and depleted hairpins within each sample for each signature; only one side of the component is depicted here. Independent component 10 identifies a signature of hairpins that are all relatively enriched before treatment and depleted after, and vice-versa. (B) Box and whisper plots showing the normalized shRNA representation before and after dasatinib treatment for all shRNAs with a positive weight or Z-score for IC10 (top) and just those with a Z-score > 2 (bottom). (C) Box and whisper plots showing the normalized shRNA representation before and after dasatinib treatment for all shRNAs with a negative Z-score for IC10 (top) and just those with a Z-score< -2 (bottom). P-values were calculated using Student's t-test.

a set of hairpins that are depleted in the pre-treatment sample from a single mouse as compared to the rest of the dataset; this is likely due to stochastic hairpin loss because of poor sampling or reduced hairpin amplification in this particular pre-treatment sample. The fact that IC10, which describes the effect of therapy, is the only non-stochastic significant component in the *in vivo* data argues that after separation of independent variables the strongest and most consistent signal across multiple mice in this dataset was that conferred by dasatinib treatment.

From the set of shRNAs with a Z-score > 2 or < -2 for IC10, we selected a small validation set of 29 hairpins, 13 of which are predicted by ICA to have higher representation after therapy as compared to before, and 16 of which are predicted to have lower representation after therapy as compared to before. We first checked whether or not these 29 hairpins enriched or depleted after therapy *in vivo* by performing longitudinal GFP competition assays with each hairpin (Supplementary Figure S5). Only one of the 16 hairpins predicted to deplete after therapy *in vivo* failed

to do so in independent assays (Figure 3A). In contrast, 7 of the 13 hairpins predicted to enrich after therapy actually depleted after therapy in independent assays (Figure 3B). Overall, about 72% of the hairpins that we tested had the general behavior predicted by IC10, but the prediction of enrichment versus depletion is more often correct for those hairpins predicted to deplete (at a rate of 94% for depletors versus 46% for enrichers). These relatively high rates of correct predictions could be due to the small number of hairpins tested; rates might be lower in a larger validation set. From this data, ICA seems to be better at predicting hairpins that deplete after therapy than those that enrich. This could be due to the fact that the fold changes *in vivo* skew towards depletion after therapy, meaning that the pool of potential enrichers is much smaller than the pool of potential depletors (Figure 1F). IC10 produced balanced lists of hairpins predicted to deplete and enrich; 400 hairpins had a Z-score < -2, and 391 had Z scores > 2. Because the pool of enriched hairpins is much smaller, it makes sense that if we try to select balanced lists of candidate shRNAs that deplete or enrich, we will end up with many more false positives in the set predicted to enrich than the set predicted to deplete.

We are interested in hairpins that not only enrich or deplete after therapy, but that have significantly different behavior before therapy as compared to after. As with our earlier screen-wide hierarchical clustering, we did this by comparing the fold change after therapy with the fold change before therapy in order to see if they are significantly different. One can imagine a case in which a hairpin might deplete both before and after therapy and be correctly selected as a depleting hairpin by ICA, but does not actually have different behavior before therapy as compared to after it. To remove hairpins that

have similar behavior before and after therapy from the validation set, we further filtered our list of candidate shRNAs by requiring that they have at least 1.5-fold difference between the average fold changes before versus after therapy of all the mice in the screen. GFP competition assays of the 16 hairpins that fit this criterion showed that 8 hairpins had significantly different behavior after therapy as compared to before as predicted by IC10; 5 of the 8 hairpins significantly deplete after therapy, and 3 significantly enrich after therapy (Figure 3C, 3D). In parallel *in vitro* GFP competition assays, we found that 3 of 5 hairpins that deplete after therapy *in vivo* do not do so *in vitro*; similarly, 1 of the 3 hairpins that enrich after therapy *in vivo* actually depletes after therapy *in vitro* (Supplementary Figure S5).

We also performed Gene Set Enrichment Analysis (GSEA) of the genes targeted by the hairpins in IC10, which did not reveal any gene sets that were significant at the commonly used cutoff of false discovery rate (FDR) < 0.25. However, we did observe some gene sets that are enriched or depleted after dasatinib therapy at a nominal p-value < 0.01 (Supplementary Tables III and IV). There are fewer significant gene sets (at nominal p-value < 0.01) that are enriched after dasatinib therapy then are depleted after dasatinib therapy; this may reflect the fact that the majority of hairpins in the library deplete after therapy (Figure 1F). Unsurprisingly, genes involved in drug metabolism were enriched after dasatinib treatment, and those involved in development of B-lymphocytes as well as protein tyrosine kinase activity were depleted after dasatinib treatment. We also saw enrichment or depletion of a number of immunologic gene signatures, likely reflecting the changes in cytokine signaling that can occur in *BCR-ABL1*+ BCP-ALL after TKI treatment *in vivo* (31, 34, 55, 56).

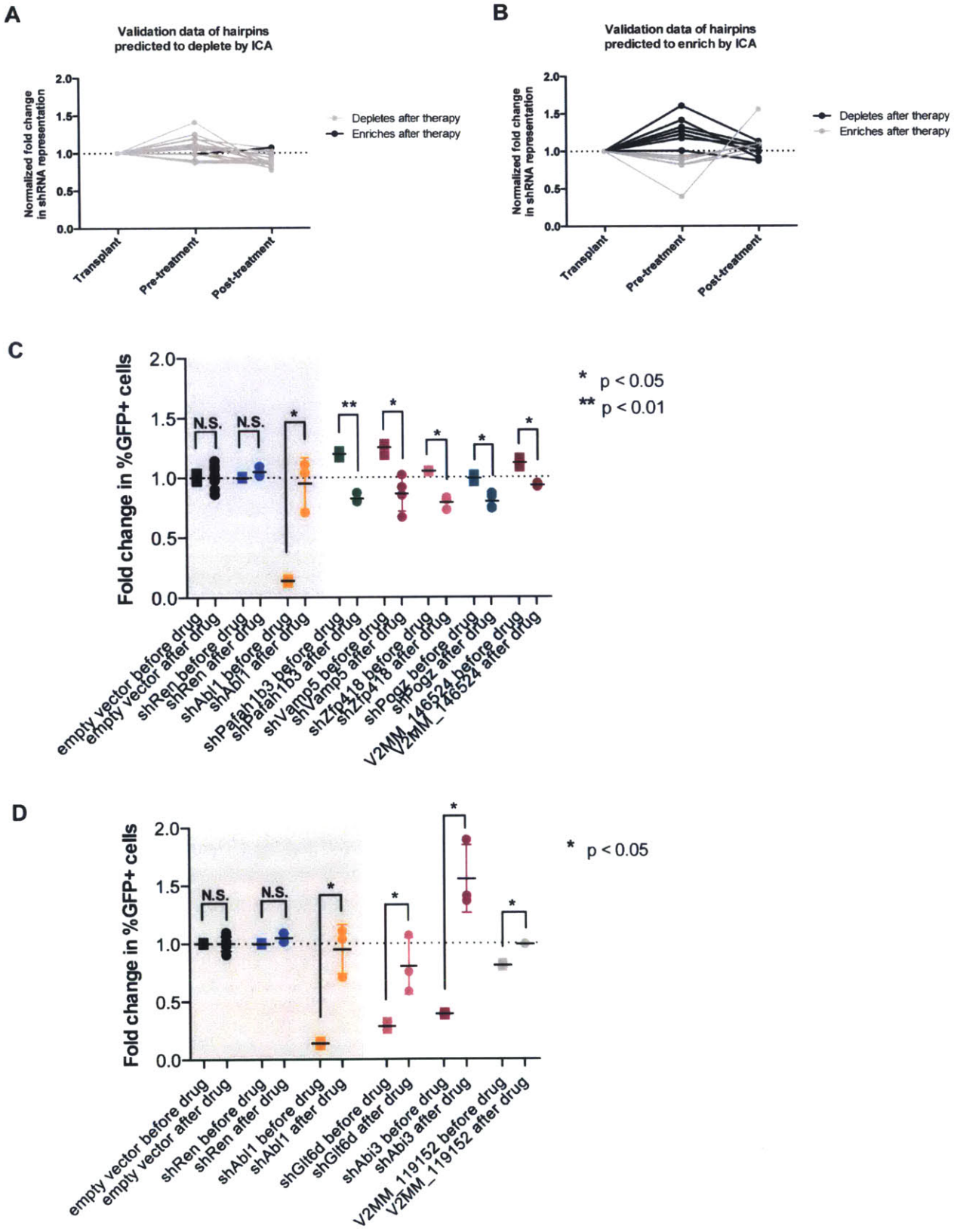
A
Validation data of hairpins predicted to deplete by ICA
Normalized fold change in shRNA representation
2.0
1.5
1.0
0.5
0.0
Transplant
Pre-treatment
Post-treatment
Depletes after therapy
Enriches after therapy
B
Validation data of hairpins predicted to enrich by ICA
Normalized fold change in shRNA representation
2.0
1.5
1.0
0.5
0.0
Transplant
Pre-treatment
Post-treatment
Depletes after therapy
Enriches after therapy
C
Fold change in %GFP+ cells
2.0
1.5
1.0
0.5
0.0
N.S.
N.S.
*
**
*
*
*
*
empty vector before drug
empty vector after drug
shRen before drug
shRen after drug
shAbl1 before drug
shAbl1 after drug
shPafah1b3 before drug
shPafah1b3 after drug
shVamp5 before drug
shVamp5 after drug
shZfp418 before drug
shZfp418 after drug
shPogz before drug
shPogz after drug
V2MM_146524 before drug
V2MM_146524 after drug
* p < 0.05
** p < 0.01
D
Fold change in %GFP+ cells
2.0
1.5
1.0
0.5
0.0
N.S.
N.S.
*
*
*
*
empty vector before drug
empty vector after drug
shRen before drug
shRen after drug
shAbl1 before drug
shAbl1 after drug
shGlt6d before drug
shGlt6d after drug
shAbi3 before drug
shAbi3 after drug
V2MM_119152 before drug
V2MM_119152 after drug
* p < 0.05

**Figure 3. Hairpins identified to enrich or deplete after therapy validate in individual assays.**
(A) A graph showing normalized hairpin representation from individual GFP competition assays over the course of the assay of 16 shRNAs predicted by IC10 to deplete after therapy. One hairpin (black) enriches rather than depletes after therapy. (B) A graph showing normalized hairpin representation from individual GFP competition assays over the course of the assay of 13 shRNAs predicted by IC10 to enrich after therapy. Seven hairpins (black) deplete rather than enrich after therapy. (C) and (D) Scatterplots showing normalized fold change of shRNA-expressing cells before and after dasatinib treatment *in vivo* in GFP competition assays or hairpins predicted to deplete after therapy (C) or enrich after therapy (D) by IC10. Controls are in the grey box: an empty hairpin vector and a hairpin targeting Renilla luciferase, which these cells do not express, are negative controls, and a hairpin targeting Abl1, which is the driving oncogene in these cells and the target of therapy, is included as a positive control of an shRNA that has significantly different fold change before versus after therapy. Fold changes are normalized to an empty vector or a hairpin targeting Renilla luciferase. Error bars represent standard deviation; p-values were calculated using Student's t-test.

## Discussion

Despite the initial apparent success of tyrosine kinase inhibitors for treatment of Philadelphia positive leukemias, relapse both with and without mutations in Bcr-Abl remains a persistent clinical problem, particularly in *BCR-ABL1*+ BCP-ALL (3, 6-21). Non-mutational resistance to TKI therapy in *BCR-ABL1*+ BCP-ALL has been shown in clinical and preclinical studies to occur via activation of alternative signaling such as the Jak/Stat pathway or the Wnt/$Ca^{2+}$/NFAT pathway, deactivation of apoptotic pathways by loss of the *CDKN2A/B* locus or up-regulation of Bcl6, and interaction with the tumor microenvironment via either adhesion to stromal cells or response to secreted factors (3, 4, 31-33, 57, 58). Due to the myriad mechanisms by which *BCR-ABL1*+ BCP-ALL can become resistant to TKIs, it seems likely that combination therapy will be required to fully eradicate leukemia. An unbiased screening approach allows for identification of unique pathways that may mediate TKI response and therefore might be targets for

potential combination therapy. Such work is ideally performed *in vivo* in order to account for the role of the microenvironment in leukemic response to TKI treatment.

In order to identify novel genes that promote resistance or sensitivity to dasatinib in the context of a functional tumor microenvironment, we performed a large-scale RNAi screen *in vivo* in an established preclinical mouse model of *BCR-ABL1*+ BCP-ALL. We have previously shown that shRNA screening in this model can identify regulators of leukemic growth that function specifically in the *in vivo* setting. In fact, there is little overlap between the set of hairpins that regulate *BCR-ABL1*+ BCP-ALL growth *in vivo* and those that regulate it *in vitro* (42). Additionally, this model responds to dasatinib therapy in a manner similar to human disease in that transplanted mice initially respond to drug but relapse after prolonged treatment (8, 9, 53). As in the human disease, relapse after dasatinib therapy is often but not always characterized by the presence of mutations in Bcr-Abl that prevent drug binding, but in this preclinical model Bcr-Abl mutations are not detectable in naïve leukemia cells (12-21, 53).

The lack of pre-existing Bcr-Abl mutations allows us to study response to dasatinib in a Bcr-Abl-independent context, provided that dasatinib treatment duration remains short (53). Previous studies in this model have shown that leukemia cells can interact with the microenvironment to escape TKI-mediated cell killing, meaning that even in the transplant context host-dependent mechanisms of dasatinib resistance are an important escape route for leukemic cells (29, 34, 59). Additionally, several mechanisms of cell-intrinsic, Bcr-Abl independent resistance to TKI therapy have been identified in this transplantable *BCR-ABL1*+ BCP-ALL model, indicating that an

unbiased screen in this model should be capable of identifying both cell autonomous and microenvironment-dependent mediators of dasatinib response (32, 33, 58, 60).

Large-scale pooled *in vivo* RNAi screens are often noisier than their *in vitro* counterparts, as evidenced by high variation between biological replicates or recovery of a relatively low number of candidate hits (40, 42, 48). A therapy screen has added complexity and requires the ability to separate the effects of drug response from those of normal cellular growth during data analysis. Because our previous screening work in this model showed high levels of variation between replicate screening mice, we decided to address the issue of noise by performing a longitudinal screen in which we measure changes in hairpin representation before versus after drug within the same mouse, rather than comparing treated and untreated mice (42). We were able to take advantage of the hematopoietic burden in this malignancy and use a serial blood sampling method to measure changes in shRNA representation over time. Whereas differences between samples from treated and untreated mice might be due to clonal variation, transplant/engraftment effects, and differences in lifespan between mice as well as the presence of drug, the only differences between matched pre- and post-treatment samples in our screen should be the addition of dasatinib and the continuation of leukemic growth after treatment.

The clonal effect of *in vivo* but not *in vitro* screening samples is illustrated by hierarchical clustering, in which the pre- and post-treatment samples taken from the same mouse cluster together but all the pre-treatment and post-treatment culture samples cluster independently of one another. In contrast, we found that if we cluster log fold changes either before treatment or after treatment, they clustered independently

of one another based on hairpin depletion or enrichment both *in vivo* and *in vitro*. Similarly, there was limited mutual information both before and after therapy between *in vivo* and *in vitro* screens, which is consistent what we have observed in previous RNAi screens in this model (42). Our clustering analysis also illustrated that while the largest determinant of hairpin behavior in our *in vitro* RNAi screen was the presence or absence of therapy, clonal effects between mice tend to dominate in unfiltered RNAi data from the *in vivo* setting. This suggests that in *in vivo* screens, removal of or ability to control for the clonal signals that dominate hairpin behavior is likely to be essential for identification of candidate hits for follow-up validation.

In our *in vivo* longitudinal screen, this meant separating the effects of therapy from clonal growth effects within the mice, as well as identifying those hairpins that had differential behavior after therapy across multiple mice. Independent component analysis successfully isolated the different sources of variation in our dataset, most of which were clonal effects in specific sets of mice, and isolated a signature of hairpins that have significantly different representation after therapy as compared to before. Importantly, this was only one of two signatures that were significant in the dataset, with the other significant signature likely being due stochastic hairpin loss. This falls in line with our observation that *in vivo* samples taken before therapy have distinct shRNA depletion or enrichment patterns relative to those taken after therapy.

In our small validation set, we found that 28% of the hairpins tested validated as having significantly different behavior after dasatinib as compared to before. Of the hairpins that had both a Z-score with an absolute value > 2 and at least a 1.5 fold difference between average *in vivo* fold changes before and after therapy, 50%

validated as significantly enriching or depleting after therapy as compared to before in the direction predicted by IC10. Interestingly, the ICA alone was capable of predicting general hairpin behavior as defined by depletion or enrichment after therapy about 72% of the time, indicating that ICA may be capable of identifying behavioral trends in large-scale RNAi datasets, even if the changes conferred by individual hairpins are small.

These data suggest that ICA is capable of isolating not just those hairpins that have significant changes in behavior, but also those that trend in a certain direction. Given that knockdown by shRNAs is imperfect, a non-significant change after RNAi-mediated knockdown may turn into a significant behavioral change after full gene knockout, and so isolating even these smaller changes in hairpin behavior may be useful now that Crispr/Cas9 technology has made rapid genetic knockout generation possible. In libraries with multiple hairpins per gene, selection of candidate hits often relies on requiring that a minimum number of shRNAs meet some criterion, without prior knowledge of the extent of target knockdown by each shRNA. A method that identifies even those hairpins that have small biological effects may reduce the rate of false negatives. Additionally, ICA might be useful for analysis of Crispr/Cas9 screens in diploid cells, as some cells in a Crispr screen may only lose one allele of their target gene and thus may experience a smaller biological effect. Retaining these small but consistent effects in the context of a large-scale screen might be important to successful analysis of both RNAi and Crispr screening data.

Here we have shown that we can utilize a longitudinal screen design to perform unbiased, pool-based *in vivo* RNAi screens for mediators of therapeutic response in a mouse model of *BCR-ABL1*+ BCP-ALL. Our screen design produces datasets in which

library hairpin enrichment or depletion is sufficient to differentiate between both the *in vivo* versus *in vitro* settings as well as between the period of general leukemia growth versus therapeutic response. Independent component analysis of this dataset allowed for isolation of high-value candidate hits with a validation rate of approximately 28% in the small set of hairpins tested. Our novel longitudinal screen design, in combination with independent component analysis of data, allowed for isolation of shRNAs that specifically affect therapeutic response versus leukemic growth, as well as those that are only relevant in the *in vivo* context. To our knowledge, this is the first use application of independent component analysis on RNAi screening data, and it represents an ideal methodology for candidate hit selection in cases in which multiple different variables regulate changes in shRNA representation.

**Acknowledgements and Author Contributions**

We'd like to thank Corbin Meacham for help with the screening protocols, Alla Leshinsky for running high-throughput sequencing samples, Charlie Whittaker for bioinformatics processing of data, Arjun Bhutkar for designing and performing ICA and associated normalization and clustering of data, Michael Hemann for tail vein injections of mice, and members of the Hemann lab for advice and technical assistance. Eleanor Cameron and MH designed the experiments, and EC wrote the chapter except for the computational methods, which were written by AB and edited by EC. The chapter was edited by MH and critically reviewed by Yadira Soto-Feliciano. EC performed the screen and subsequent validation experiments; AB performed ICA and GSEA and created Hinton plots, dendrograms, and performed PCA.

## References


1. Daley, G. Q. *et al.* Induction of chronic myelogenous leukemia in mice by the P210bcr/abl gene of the Philadelphia chromosome. *Science.* **247**, 824-830 (1990).

2. Westbrook C. A. *et al.* Clinical significance of the BCR-ABL fusion gene in adult acute lymphoblastic leukemia: a Cancer and Leukemia Group B Study (8762). *Blood.* **80**, 2983-2990 (1992).

3. Bernt, K. M. & Hunger, S. P. Current concepts in pediatric Philadelphia chromosome-positive acute lymphoblastic leukemia. *Front Oncol.* **4,** 1–21 (2014).

4. Mullighan, C. G., Williams, R. T., Downing, J. R. & Sherr, C. J. Failure of CDKN2A/B (INK4A/B-ARF)-mediated tumor suppression and resistance to targeted therapy in acute lymphoblastic leukemia induced by BCR-ABL. *Genes Dev.* **22,** 1411–1415 (2008).

5. Mullighan, C. G. *et al.* Genomic analysis of the clonal origins of relapsed acute lymphoblastic leukemia. *Science.* **322,** 1377–1380 (2008).

6. Druker, B. J. *et al.* Activity of a specific inhibitor of the BCR-ABL tyrosine kinase in the blast crisis of chronic myeloid leukemia and acute lymphoblastic leukemia with the Philadelphia chromosome. *N Engl J Med.* **344,** 1038–1042 (2001).

7. Druker, B. J. *et al.* Efficacy and safety of a specific inhibitor of the BCR-ABL tyrosine kinase in chronic myeloid leukemia. *N Engl J Med.* **344,** 1031–1037 (2001).

8. Talpaz, M. *et al.* Dasatinib in imatinib-resistant Philadelphia chromosome-positive leukemias. *N Engl J Med.* **354,** 2531–2541 (2006).

9. Ottmann, O. *et al.* Dasatinib induces rapid hematologic and cytogenetic responses in adult patients with Philadelphia chromosome positive acute lymphoblastic leukemia with resistance or intolerance to imatinib: interim results of a phase 2 study. *Blood.* **110,** 2309–2315 (2007).

10. Saglio, G. *et al.* Dasatinib in imatinib-resistant or imatinib-intolerant chronic myeloid leukemia in blast phase after 2 years of follow-up in a phase 3 study. *Cancer.* **116,** 3852–3861 (2010).

11. Cortes, J. E. *et al.* Ponatinib in refractory Philadelphia chromosome–positive leukemias. *N Engl J Med.* **367,** 2075–2088 (2012).

12. Cortes, J. E. *et al.* A phase 2 trial of ponatinib in Philadelphia chromosome–positive leukemias. *N Engl J Med.* **369,** 1783–1796 (2013).

13. Shah, N. P. *et al.* Multiple BCR-ABL kinase domain mutations confer polyclonal resistance to the tyrosine kinase inhibitor imatinib (STI571) in chronic phase and blast crisis chronic myeloid leukemia. *Cancer Cell.* **2,** 117–125 (2002).

14. Donato, N. J. BCR-ABL independence and LYN kinase overexpression in chronic myelogenous leukemia cells selected for resistance to STI571. *Blood.* **101,** 690–698 (2003).

15. Donato, N. J. Imatinib mesylate resistance through BCR-ABL independence in chronic myelogenous leukemia. *Cancer Res.* **64,** 672–677 (2004).

16. Soverini, S. *et al.* Resistance to dasatinib in Philadelphia-positive leukemia patients and the presence or the selection of mutations at residues 315 and 317 in the BCR-ABL kinase domain. *Haematologica.* **92,** 401–404 (2007).

17. Garg, R. J. *et al.* The use of nilotinib or dasatinib after failure to 2 prior tyrosine kinase inhibitors: long-term follow-up. *Blood.* **114,** 4361–4368 (2009).

18. Fei, F., Stoddart, S., Groffen, J. & Heisterkamp, N. Activity of the Aurora kinase inhibitor VX-680 against Bcr/Abl-positive acute lymphoblastic leukemias. *Mol Cancer Ther.* **9,** 1318–1327 (2010).

19. Quentmeier, H., Eberth, S., Romani, J., Zaborski, M. & Drexler, H. G. BCR-ABL1-independent PI3Kinase activation causing imatinib-resistance. *J Hematol Oncol.* **4,** 6 (2011).

20. O'Hare, T., Deininger, M. W. N., Eide, C. A., Clackson, T. & Druker, B. J. Targeting the BCR-ABL signaling pathway in therapy-resistant Philadelphia chromosome-positive leukemia. *Clin Cancer Res.* **17,** 212–221 (2011).

21. Soverini, S. *et al.* Drug resistance and BCR-ABL kinase domain mutations in Philadelphia chromosome-positive acute lymphoblastic leukemia from the imatinib to the second-generation tyrosine kinase inhibitor era: The main changes are in the type of mutations, but not in the frequency of mutation involvement. *Cancer.* **120,** 1002–1009 (2013).

22. Shah, N. P. *et al.* Overriding imatinib resistance with a novel ABL kinase inhibitor. *Science.* **305,** 399–401 (2004).

23. Brave, M. *et al.* Sprycel for chronic myeloid leukemia and Philadelphia chromosome-positive acute lymphoblastic leukemia resistant to or intolerant of imatinib mesylate. *Clin Cancer Res.* **14,** 352–359 (2008).

24. Guilhot, F. *et al.* Dasatinib induces significant hematologic and cytogenetic responses in patients with imatinib-resistant or -intolerant chronic myeloid leukemia in accelerated phase. *Blood.* **109,** 4143–4150 (2007).

25. Hochhaus, A. *et al.* Dasatinib induces durable cytogenetic responses in patients with chronic myelogenous leukemia in chronic phase with resistance or intolerance to imatinib. *Leukemia.* **22,** 1200–1206 (2008).

26. Ravandi, F. *et al.* First report of phase 2 study of dasatinib with hyper-CVAD for the frontline treatment of patients with Philadelphia chromosome-positive (Ph+) acute lymphoblastic leukemia. *Blood.* **116,** 2070–2077 (2010).

27. Foa, R. *et al.* Dasatinib as first-line treatment for adult patients with Philadelphia chromosome-positive acute lymphoblastic leukemia. *Blood.* **118,** 6521–6528 (2011).

28. Williams, R. T., Roussel, M. F. & Sherr, C. J. Arf gene loss enhances oncogenicity and limits imatinib response in mouse models of Bcr-Abl-induced acute lymphoblastic leukemia. *Proc Natl Acad Sci U S A.* **103,** 6688–6693 (2006).

29. Williams, R. T., Besten, den, W. & Sherr, C. J. Cytokine-dependent imatinib resistance in mouse BCR-ABL+, Arf-null lymphoblastic leukemia. *Genes Dev.* **21,** 2283–2287 (2007).

30. Bewry, N. N. *et al.* Stat3 contributes to resistance toward BCR-ABL inhibitors in a bone marrow microenvironment model of drug resistance. *Mol Cancer Ther.* **7,** 3169–3175 (2008).

31. Fei, F. *et al.* Development of resistance to dasatinib in Bcr/Abl-positive acute lymphoblastic leukemia. *Leukemia.* **24,** 813–820 (2010).

32. Gregory, M. A. *et al.* Wnt/Ca2+/NFAT signaling maintains survival of Ph+ leukemia cells upon inhibition of Bcr-Abl. *Cancer Cell.* **18,** 74–87 (2010).

33. Duy, C. *et al.* BCL6 enables Ph+ acute lymphoblastic leukemia cells to survive BCR-ABL1 kinase inhibition. *Nature.* **473,** 384–388 (2012).

34. Appelmann, I. *et al.* Janus kinase inhibition by ruxolitinib extends dasatinib- and dexamethasone-induced remissions in a mouse model of Ph+ ALL. *Blood.* **125,** 1444–1451 (2015).

35. Mullighan, C. G. *et al.* Genomic analysis of the clonal origins of relapsed acute lymphoblastic leukemia. *Science.* **322,** 1377–1380 (2008).

36. Notta, F. *et al.* Evolution of human BCR–ABL1 lymphoblastic leukaemia-initiating cells. *Nature.* **469,** 362–367 (2011).

37. Soverini, S. *et al.* Philadelphia-positive acute lymphoblastic leukemia patients already harbor BCR-ABL kinase domain mutations at low levels at the time of diagnosis. *Haematologica.* **96,** 552–557 (2011).

38. Patel, B. *et al.* Mouse xenograft modelling of human adult acute lymphoblastic leukemia provides mechanistic insights into adult LIC biology. *Blood.* **124,** 96 - 105 (2014).

39. Mohr, S. E., Smith, J. A., Shamu, C. E., Neumüller, R. A. & Perrimon, N. RNAi screening comes of age: improved techniques and complementary approaches. *Nat Rev Mol Cell Biol.* **15,** 591–600 (2014).

40. Beronja, S. *et al.* RNAi screens in mice identify physiological regulators of oncogenic growth. *Nature.* **501,** 185–190 (2013).

41. Schramek, D. *et al.* Direct in vivo RNAi screen unveils myosin IIa as a tumor suppressor of squamous cell carcinomas. *Science.* **343,** 309–313 (2014).

42. Meacham, C. E. *et al.* A genome-scale in vivo loss-of-function screen identifies Phf6 as a lineage-specific regulator of leukemia cell growth. *Genes Dev.* **29,** 483–488 (2015).

43. Meacham, C. E., Ho, E. E., Dubrovsky, E., Gertler, F. B. & Hemann, M. T. In vivo RNAi screening identifies regulators of actin dynamics as key determinants of lymphoma progression. *Nat Genet.* **41,** 1133–1137 (2009).

44. Sa, J. K. *et al.* In vivo RNAi screen identifies NLK as a negative regulator of mesenchymal activity in Glioblastoma. *Oncotarget.* **6,** 20145–20159 (2015).

45. Gargiulo, G. *et al.* In vivo RNAi screen for BMI1 targets identifies TGF-b/BMP-ER stress pathways as key regulators of neural- and malignant glioma-stem cell homeostasis. *Cancer Cell.* **23,** 660–676 (2013).

46. Wuestefeld, T. *et al.* A direct in vivo RNAi screen identifies MKK4 as a key regulator of liver regeneration. *Cell.* **153,** 389–401 (2013).

47. Pallasch, C. P. *et al.* Sensitizing protective tumor microenvironments to antibody-mediated therapy. *Cell.* **156,** 590–602 (2014).

48. Lin, L. *et al.* A large-scale RNAi-based mouse tumorigenesis screen identifies new lung cancer tumor suppressors that repress FGFR signaling. *Cancer Discov.* **4,** 1168–1181 (2014).

49. Miller, P. G. *et al.* In vivo RNAi screening identifies a leukemia-specific dependence on Integrin Beta 3 signaling. *Cancer Cell.* **24,** 45–58 (2013).

50. Singel, S. M. *et al.* A targeted RNAi screen of the breast cancer genome identifies KIF14 and TLN1 as genes that modulate docetaxel chemosensitivity in triple-negative breast cancer. *Clin Cancer Res.* **19,** 2061–2070 (2013).

51. Toyoshima, M., Howie, H. L. & Imakura, M. Functional genomics identifies therapeutic targets for MYC-driven cancer. *Proc Natl Acad Sci U S A.* **109,** 9545-9550 (2012).

52. Sudo, M. *et al.* Short-hairpin RNA library: identification of therapeutic partners for gefitinib-resistant non-small cell lung cancer. *Oncotarget.* **6,** 814–824 (2015).

53. Boulos, N. *et al.* Chemotherapeutic agents circumvent emergence of dasatinib-resistant BCR-ABL kinase mutations in a precise mouse model of Philadelphia chromosome-positive acute lymphoblastic leukemia. *Blood.* **117,** 3585–3595 (2011).

54. Hyvärinen, A. & Oja, E. Independent component analysis: algorithms and applications. *Neural Netw.* **13,** 411–430 (2000).

55. Sison, E. A. R. & Brown, P. The bone marrow microenvironment and leukemia: biology and therapeutic targeting. *Expert Rev Hematol.* **4,** 271–283 (2011).

56. Mishra, S. *et al.* Resistance to imatinib of Bcr/Abl P190 lymphoblastic leukemia cells. *Cancer Res.* **66,** 5387–5393 (2006).

57. Hazlehurst, L. A., Argilagos, R. F. & Dalton, W. S. β1 integrin mediated adhesion increases Bim protein degradation and contributes to drug resistance in leukaemia cells. *Br J Haematol.* **136,** 269–275 (2007).

58. Koss, B. *et al.* Requirement for antiapoptotic MCL-1 in the survival of BCR-ABL B-lineage acute lymphoblastic leukemia. *Blood.* **122,** 1587–1598 (2013).

59. Singh, H. *et al.* A screening-based approach to circumvent tumor microenvironment-driven intrinsic resistance to BCR-ABL+ inhibitors in Ph+ acute lymphoblastic leukemia. *J Biomol Screen.* **19,** 158–167 (2013).

60. Hu, Y. *et al.* Targeting multiple kinase pathways in leukemic progenitors and stem cells is essential for improved treatment of Ph+ leukemia in mice. *Proc Natl Acad Sci U S A.* **103,** 16870–16875 (2006).

61. Dickins, R. A. *et al.* Probing tumor phenotypes using stable and regulated synthetic microRNA precursors. *Nat Genet.* **37**, 1289-1295 (2005).

62. Li H. and Durbin R. Fast and accurate short read alignment with Burrows-Wheeler Transform. *Bioinformatics.* **25**,1754-60 (2009).

63. Bullard J. H. *et al.* Evaluation of statistical methods for normalization and differential expression in mRNA-Seq experiments. *BMC Bioinformatics.* **11**, 94 (2010).

64. Subramanian A. *et al.* Gene set enrichment analysis: a knowledge-based approach for interpreting genome-wide expression profiles. *Proc Natl Acad Sci U S A.* **102**, 15545–15550 (2005).

65. Bhutkar, A., Blat, I., Boutz, P.L., Cameron, E.R., Chen, P.Y., Chen, S., Ferretti, R., Gurtan, A.M., Ianari, A., Muzumdar, M.D., et al. High-resolution signature discovery in NGS expression datasets using Blind Source Separation (*In Preparation*).

66. Rutledge, D.N., and Jouan-Rimbaud Bouveresse, D. Independent Components Analysis with the JADE algorithm. *TrAC Trends in Analytical Chemistry* **50,** 22–32 (2013).

67. Biton, A., Zinovyev, A., Barillot, E., and Radvanyi, F. MineICA: Independent component analysis of transcriptomic data. (2013).

68. Nordhausen, K., Cardoso, J.F., Miettinen, J., Oja, H., and Ollila, E. JADE: JADE and other BSS methods as well as some BSS performance criteria (R package version). (2012).

## Materials and Methods

*Cell culture*

Murine p19$^{Arf-/-}$ *BCR-ABL1*+ BCP-ALL cells (28) were cultured in RPMI media supplemented with 10% FBS, 4 mM L-glutamine, and 55 μM β-mercaptoethanol.

*Vectors*

All shRNAs were expressed in the mir30 context; the vector and shRNA cloning and design are described in the referenced mir30 shRNA study (61).

*RNAi screening and validation assays*

Detailed screening and validation information is available in Supplementary Methods. PCR primer sequences are provided in Supplemental Table V.

*Preclinical therapeutics*

Dasatinib (LC Laboratories) was dissolved in DMSO and diluted into cell culture media for *in vitro* studies. For *in vivo* use, dasatinib was dissolved in 80 mM citric acid at pH 2.3 and administered via oral gavage at 0.01 mL/g. Dasatinib was given at 10 mg/kg for 3 days for the *in vivo* screen; in subsequent GFP competition assays, dasatinib was given at 20 mg/kg for 3 days.

**Computational Methods**

*Read mapping and quantification*

Sequencing was performed on an Illumina HiSeq 2000 instrument to obtain single-end 51-nt reads. Reads were mapped to library sequences using the BWA aligner (62). Hairpin representation counts were based on reads that mapped to library sequences with at most one mismatch.

Read counts were upper-quartile normalized to a count of 4000 (63). Hairpins with normalized upper quartile values less than 100 for across all *in vivo* samples were eliminated from downstream analyses in order to reduce low-level quantification noise in the dataset. Hierarchical clustering was performed with Pearson correlation based distance and average linkage. Independent Component Analysis (ICA) was performed as described below to identify biologically relevant signatures that characterize hairpin enrichment/depletion profiles in these samples. All analyses were conducted in the R

Statistical Programming language (http://www.r-project.org/), including ICA signature analysis, hierarchical clustering, and PCA based sample clustering. Gene set enrichment analysis (GSEA) was carried out using the pre-ranked mode with default settings (64).

*Independent Component Analysis (ICA)*

For signature analysis, an unsupervised blind source separation strategy using Independent Component Analysis (ICA) was applied to elucidate statistically independent hairpin representation signatures (54, 65, 66). ICA is a general-purpose signal processing and multivariate data analysis technique in the category of unsupervised matrix factorization methods. Based on input data consisting of a hairpins-samples matrix, ICA uses higher order moments to characterize the dataset as a linear combination of statistically independent latent variables. All computations were done in the R Statistical Programming Language. The R implementation of the core JADE algorithm (Joint Approximate Diagonalization of Eigenmatrices) (66, 67, 68) was used along with custom R utilities.

## Supplementary Figures

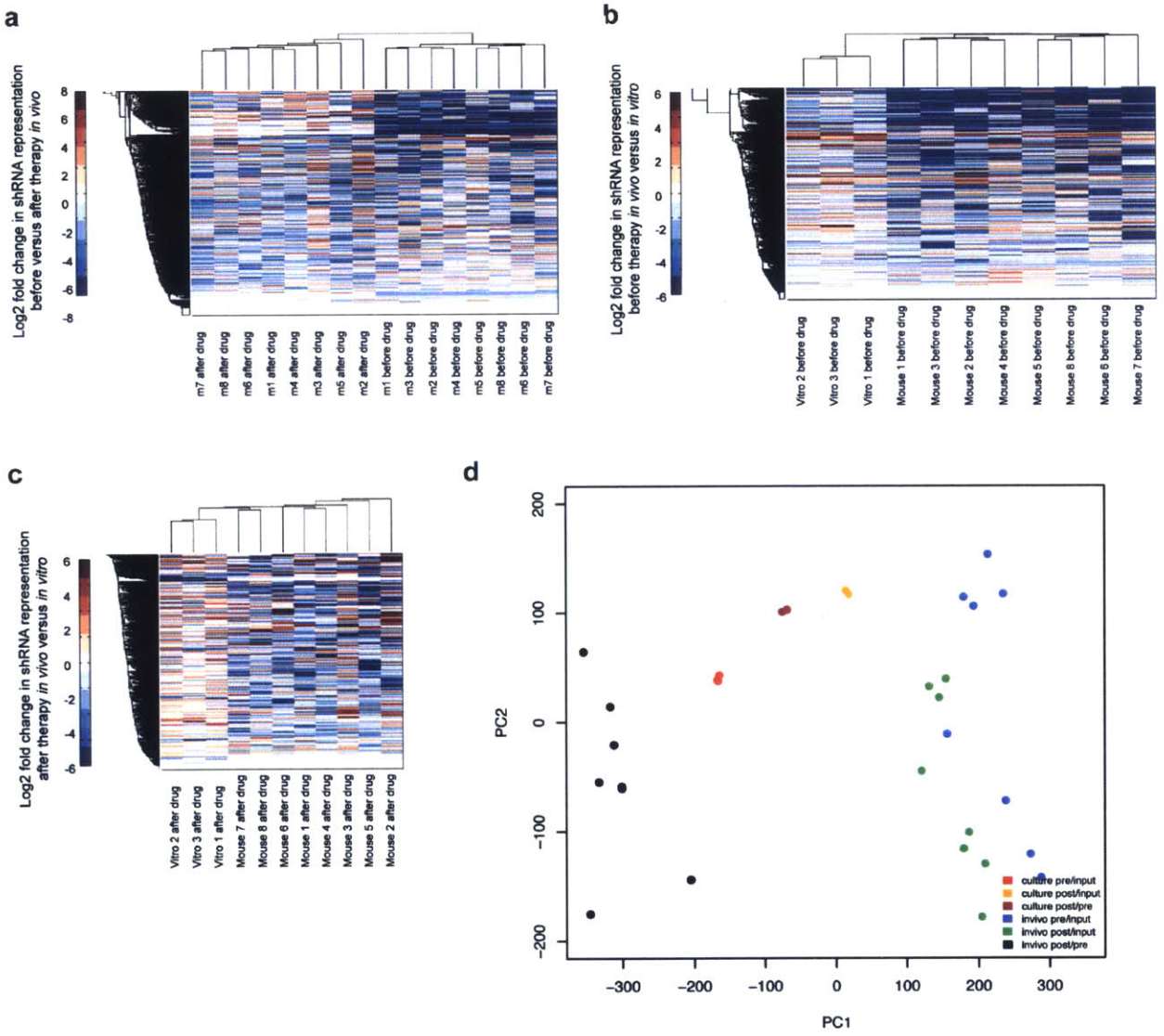


**Supplementary Figure S1. Hierarchical clustering separates pre- and post-treament samples as well as samples from *in vivo* vs *in vitro* screens.**
(a) Hierarchical clustering of $\log_2$ fold change in shRNA representation before vs after therapy shows that hairpins have distinct behavior before dasatinib vs after *in vivo.* (b) and (c) Hierarchical clustering of $\log_2$ fold change in shRNA representation *in vivo* vs *in vitro* during period (b) before treatment shows that hairpins have distinct behavior *in vivo* during general leukemia progression, and (c) during and after treatment shows that hairpins have distinct behavior *in vivo* during therapeutic response. (d) Principal component analysis of $\log_2$ fold changes before (pre/input) and after treatment (post/pre) as well as over the entire screening period (post/input) *in vivo* and *in vitro* shows that while the post/input fold change *in vitro* forms a distinct cluster, the post/input fold change *in vivo* clusters with the before treatment samples, indicating that hairpin behavior *in vivo* is primarily defined by clonal effects between different mice.

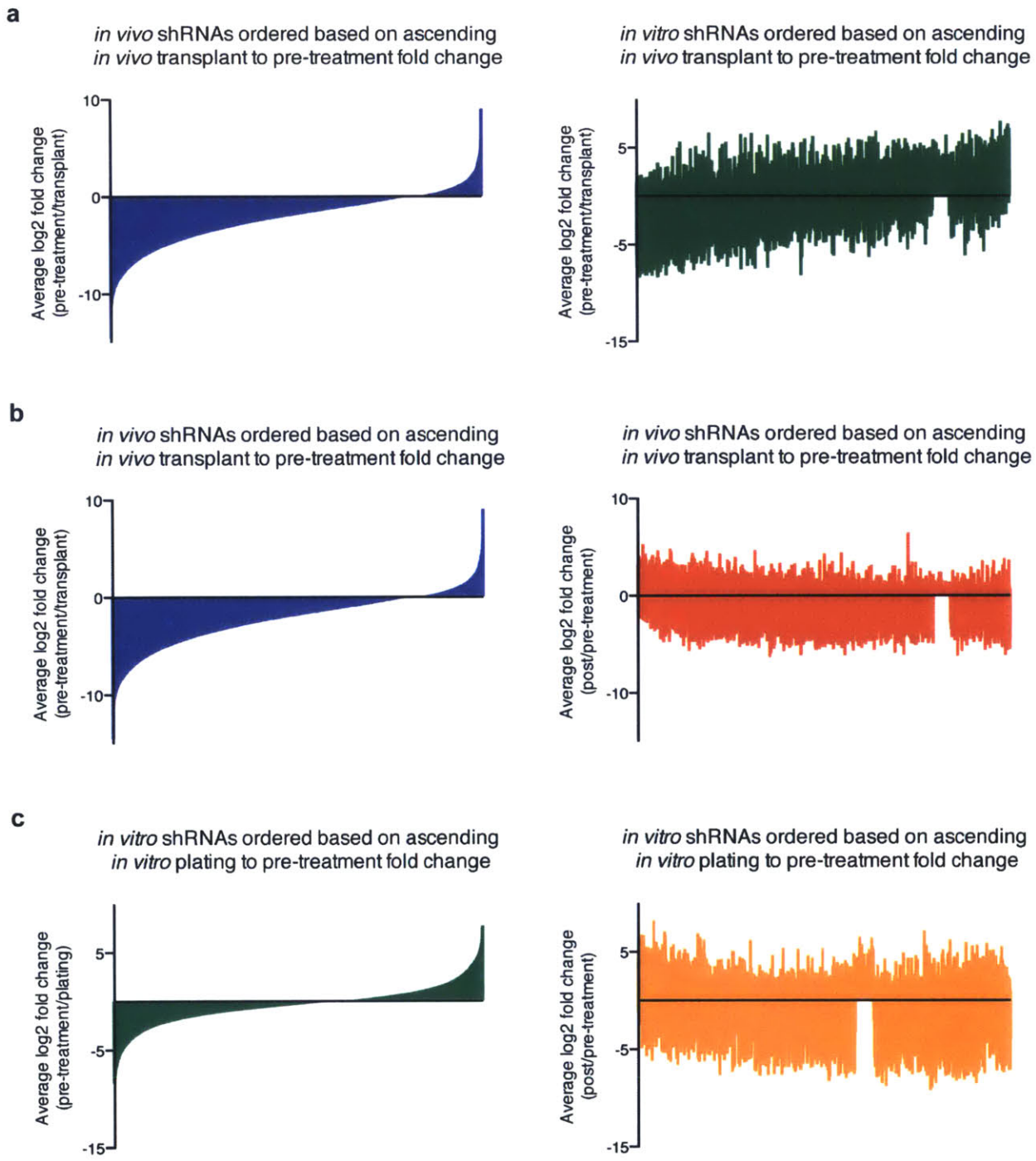


**Supplementary Figure S2. There is limited mutual information before versus after therapy as well as *in vivo* as compared to *in vitro*.**
(a) Waterfall plots representing the $\log_2$ fold changes before dasatinib therapy of all shRNAs in the library *in vivo* (blue) and *in vitro* (green), with shRNAs arranged in rank ascending order based on their $\log_2$ fold change *in vivo*. Hairpin behavior *in vivo* does not predict behavior *in vitro* before therapy. (b) Waterfall plots representing the $\log_2$ fold changes *in vivo* of all shRNAs in the library before therapy (blue) and after therapy

(red), with shRNAs arranged in rank ascending order based on their $log_2$ fold change *in vivo* before therapy. Hairpin behavior before therapy does not predict behavior after therapy *in vivo*. (c) Waterfall plots representing the $log_2$ fold changes *in vitro* of all shRNAs in the library before therapy (green) and after therapy (orange), with shRNAs arranged in rank ascending order based on their $log_2$ fold change *in vitro* before therapy. Hairpin behavior before therapy does not predict behavior after therapy *in vitro*

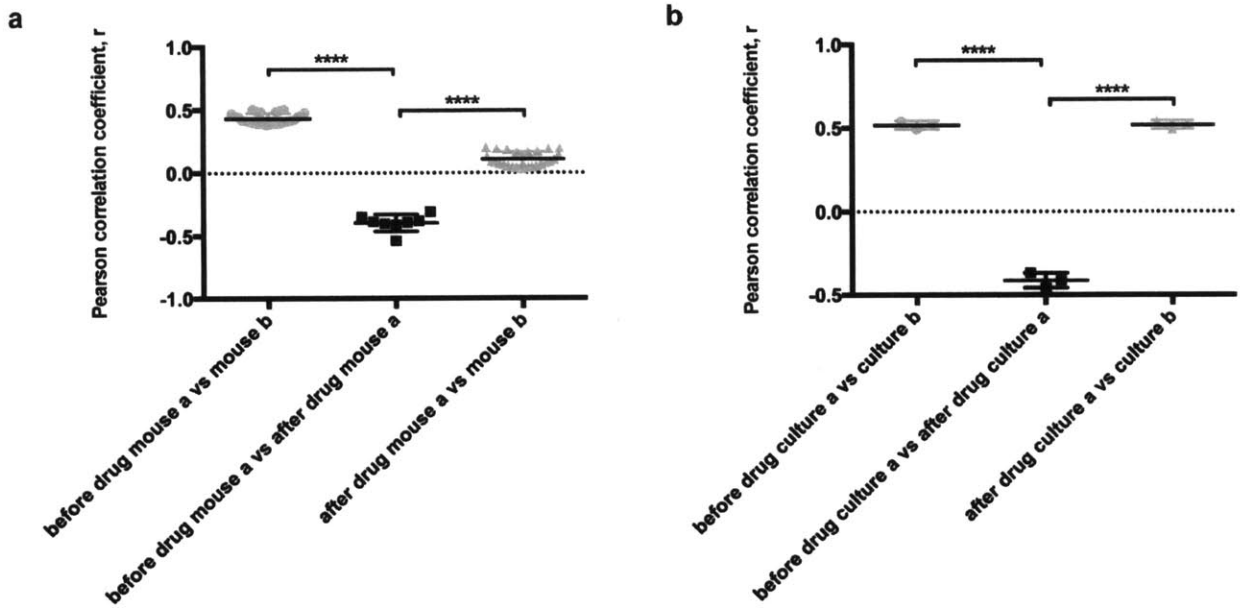


**Supplementary Figure S3. Correlation between biological replicates in longitudinal RNAi screen is significantly higher than between non-replicates.** (a) Scatterplot showing Pearson correlation coefficients of $log_2$ fold changes *in vivo* of all shRNAs in library between biological replicates (grey) as compared to non-replicates (black). (b) Scatterplot showing Pearson correlation coefficients of $log_2$ fold changes *in vitro* of all shRNAs in library between biological replicates (grey) as compared to non-replicates (black). Biological replicates are significantly more correlated to each other than they are to non-replicate samples (different setting or therapeutic context). Error bars represent standard deviation; p-values were calculated using Student's t-test.

a

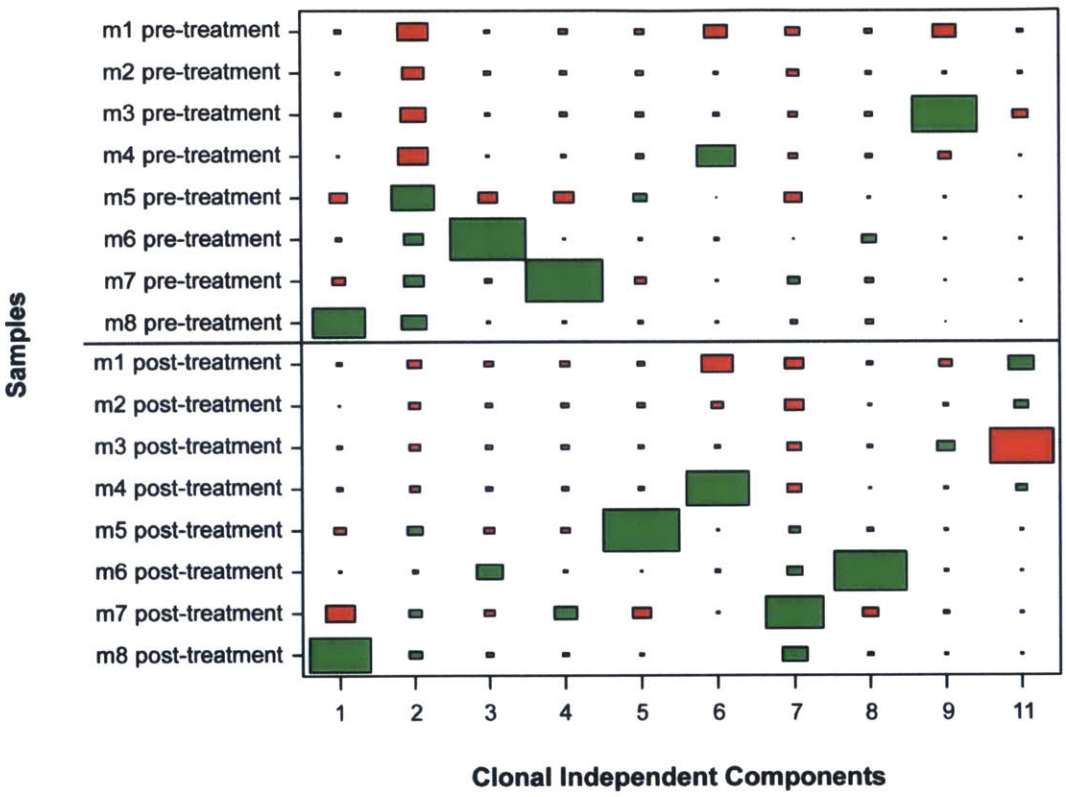
m1 pre-treatment
m2 pre-treatment
m3 pre-treatment
m4 pre-treatment
m5 pre-treatment
m6 pre-treatment
m7 pre-treatment
m8 pre-treatment
m1 post-treatment
m2 post-treatment
m3 post-treatment
m4 post-treatment
m5 post-treatment
m6 post-treatment
m7 post-treatment
m8 post-treatment
Samples
1
2
3
4
5
6
7
8
9
11
Clonal Independent Components

b

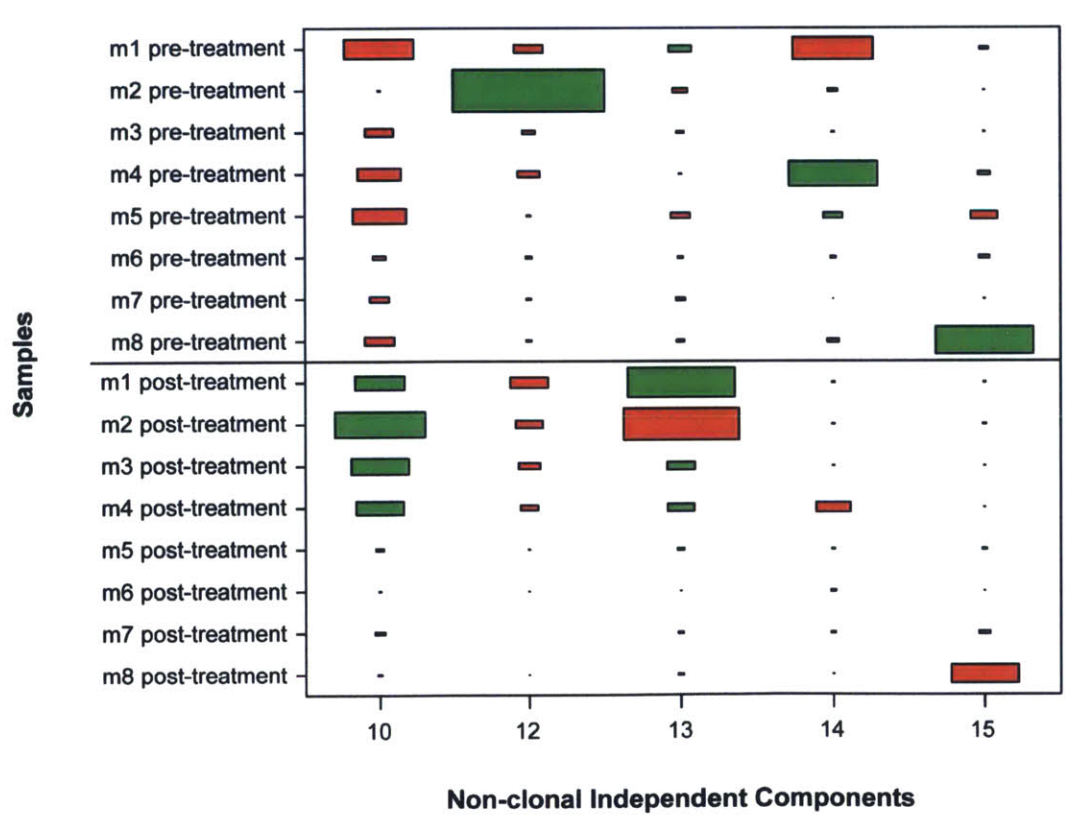
m1 pre-treatment
m2 pre-treatment
m3 pre-treatment
m4 pre-treatment
m5 pre-treatment
m6 pre-treatment
m7 pre-treatment
m8 pre-treatment
m1 post-treatment
m2 post-treatment
m3 post-treatment
m4 post-treatment
m5 post-treatment
m6 post-treatment
m7 post-treatment
m8 post-treatment
Samples
10
12
13
14
15
Non-clonal Independent Components

**Supplementary Figure S4. Independent component analysis of longitudinal *in vivo* RNAi screening data isolates clonal and non-clonal signatures.**
(A) and (B) Hinton plot of independent components show the signature generated by each clonal (A) or non-clonal (B) component across all *in vivo* samples before and after dasatinib treatment. Colors represent the directionality of hairpin representation (red enriched, green depleted), and the size of each rectangle quantifies the strength of the signature for that sample. Each component identifies a two-sided signature, such that there are enriched and depleted hairpins within each sample for each signature; components are numbered according to their original identification in the ICA.

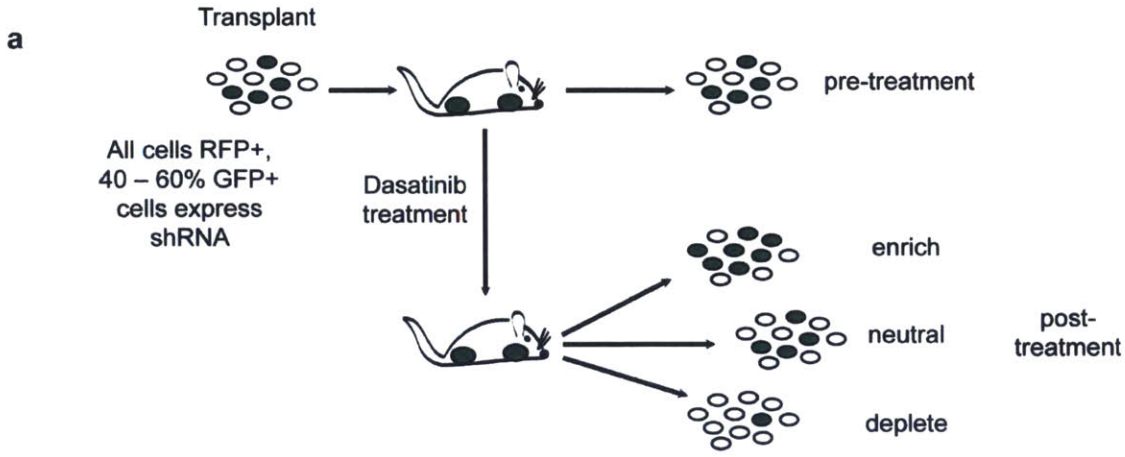
a
Transplant
All cells RFP+,
40 – 60% GFP+
cells express
shRNA
Dasatinib
treatment
pre-treatment
enrich
neutral
deplete
post-
treatment

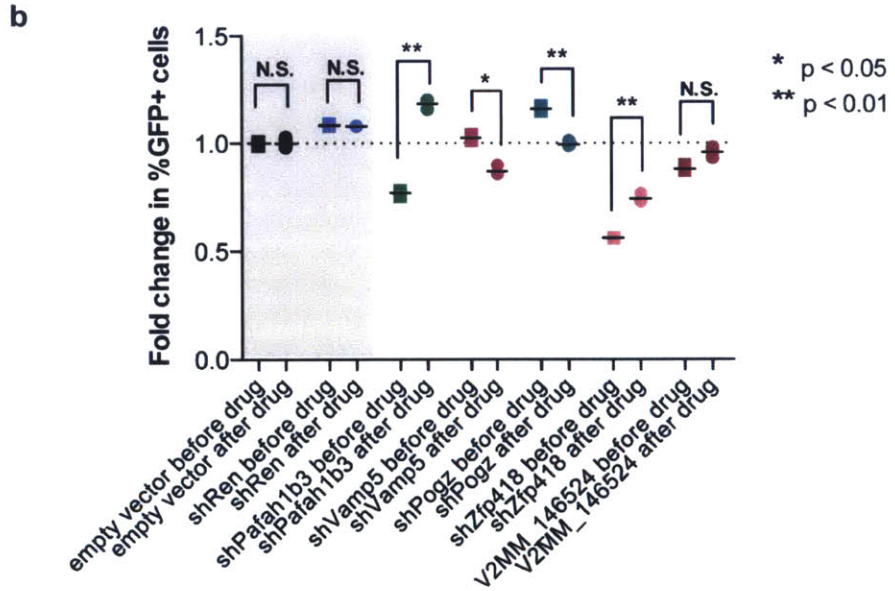
b
Fold change in %GFP+ cells
1.5
1.0
0.5
0.0
N.S.
N.S.
**
*
**
**
N.S.
* p < 0.05
** p < 0.01
empty vector before drug
empty vector after drug
shRen before drug
shRen after drug
shPafah1b3 before drug
shPafah1b3 after drug
shVamp5 before drug
shVamp5 after drug
shPogz before drug
shPogz after drug
shZfp418 before drug
shZfp418 after drug
V2MM_146524 before drug
V2MM_146524 after drug

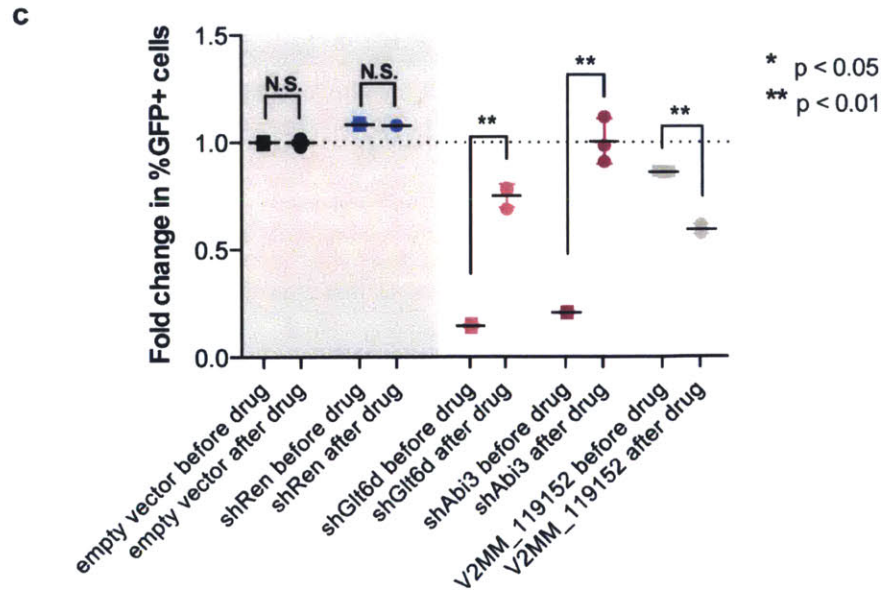
c
Fold change in %GFP+ cells
1.5
1.0
0.5
0.0
N.S.
N.S.
**
**
**
* p < 0.05
** p < 0.01
empty vector before drug
empty vector after drug
shRen before drug
shRen after drug
shGlt6d before drug
shGlt6d after drug
shAbi3 before drug
shAbi3 after drug
V2MM_119152 before drug
V2MM_119152 after drug

**Supplementary Figure S5. Validation of shRNAs predicted to enrich or deplete by GFP competition assay.**
(A) Schematic for validation of individual hairpins identified as potential enrichers or depletors by ICA. Leukemia cells are partially transduced with a construct containing GFP and the shRNA of interest, and then are transplanted into recipient mice or plated *in vitro* as in the screen. At transplant, pre- and post-treatment, the percentage of shRNA-expressing cells is assessed by flow cytometric analysis, and fold change of % shRNA-expressing cells over time can be calculated. An empty vector or shRNA against Renilla luciferase, which these cells do not express, are used as controls. (B) and (C) Scatterplots showing normalized fold change of shRNA-expressing cells before and after dasatinib treatment *in vitro* in GFP competition assays or hairpins predicted to deplete after therapy (B) or enrich after therapy (C) by IC10. Controls are in the grey box: an empty hairpin vector and a hairpin targeting Renilla luciferase are negative controls, and a hairpin targeting Abl1, which is the driving oncogene in these cells and the target of therapy, is included as a positive control of an shRNA that has significantly different fold change before versus after therapy. Fold changes are normalized to an empty vector or a hairpin targeting Renilla luciferase. Error bars represent standard deviation; p-values were calculated using Student's t-test.

## Supplementary Tables

**Supplementary Table I. Genes targeted by hairpins that have a Z-score < -2 for IC10.** The RefSeq accession number, unique gene identifier (if available), and Z-score for component 10 are shown. Hairpins targeting these genes are predicted by ICA to enrich after dasatinib therapy *in vivo*.

| Accession # | Gene ID | Z-score (IC10) |
|---|---|---|
| AC147806.5 | | -4.95 |
| AC124202.3 | | -4.52 |
| NM_177865 | OTTMUSG00000008540 | -4.42 |
| NM_009644 | Ahrr | -4.20 |
| NM_194357 | Rya3 | -4.03 |
| AK137052.1 | | -4.02 |
| CT009738.8 | | -3.96 |
| AK087644.1 | | -3.95 |
| NM_026844 | 2310061C15Rik | -3.81 |
| AC090869.7 | | -3.80 |
| NM_001013024 | Usp13 | -3.78 |
| NM_009619 | Adam3 | -3.65 |
| NM_172415 | Arhgef10l | -3.65 |
| NM_145575 | Cald1 | -3.62 |
| NM_181414 | Pik3c3 | -3.58 |
| NM_026674 | Aph1c | -3.55 |
| NM_029186 | Tmem180 | -3.55 |
| NM_146642 | Olfr1140 | -3.53 |
| AC163615.5 | | -3.50 |
| NM_146691 | Olfr1467 | -3.43 |
| NM_028198 | Xpo5 | -3.40 |
| NM_175021.3 | Samd4b | -3.37 |
| NM_173789 | Helt | -3.37 |
| NM_001081391 | Csmd3 | -3.37 |
| NM_145450 | BC022687 | -3.34 |
| AC158549.8 | | -3.34 |
| NM_001009949 | Mcart1 | -3.33 |
| NM_181275 | Tas2r139 | -3.31 |
| NM_010290 | Gja9 | -3.31 |
| AL626770.9 | | -3.30 |
| AC125217.3 | | -3.24 |
| AL603907.12 | | -3.21 |
| NM_172445 | Wdr37 | -3.20 |
| NM_026918 | 1810010M01Rik | -3.19 |
| AC099884.12 | | -3.18 |

| | | |
|---|---|---|
| NM_172470 | Wdr35 | -3.16 |
| NM_145476 | Tbc1d22a | -3.15 |
| AC134908.5 | | -3.15 |
| AC107756.9 | | -3.14 |
| NM_175130 | Trpm4 | -3.13 |
| NM_175218 | 4930544M13Rik | -3.12 |
| NM_145126 | Chi3l4 | -3.11 |
| NM_146163 | - | -3.09 |
| NM_001163425.1 | Myeov2 | -3.09 |
| AC159888.2 | | -3.07 |
| NM_030715 | Polh | -3.06 |
| NM_177293 | Mtap7d3 | -3.03 |
| AC132317.2 | | -3.03 |
| NM_178224 | Cbs | -3.02 |
| NM_177075 | C030019I05Rik | -3.02 |
| NM_024236 | Qdpr | -3.02 |
| AK016124.1 | | -3.02 |
| NM_175170 | Pogk | -3.02 |
| NM_030715 | Polh | -3.00 |
| NM_133910 | Tbc1d14 | -3.00 |
| NM_145538 | AI840826 | -2.98 |
| AC109140.6 | | -2.96 |
| NM_146110 | Aamp | -2.96 |
| NM_172585 | Larp5 | -2.96 |
| NM_001029867 | Ugt2b36 | -2.95 |
| NM_178734 | Zfp473 | -2.95 |
| AK034494.1 | | -2.95 |
| NM_144925 | Tnrc6a | -2.94 |
| NM_145548 | Cyp2j13 | -2.94 |
| NM_025338 | Aurkaip1 | -2.92 |
| NM_198059 | Nrap | -2.91 |
| NM_198170 | BC059842 | -2.91 |
| NM_177081 | Ptpn7 | -2.88 |
| NM_172477 | Dennd2a | -2.88 |
| AC102693.9 | | -2.88 |
| NM_026592 | B230118H07Rik | -2.87 |
| NM_133789 | Strn4 | -2.87 |
| NM_027995 | Paqr7 | -2.87 |
| AC161754.4 | | -2.85 |
| AL844181.9 | | -2.83 |
| NM_172684 | Rsbn1 | -2.83 |

| | | |
|---|---|---|
| AC122895.5 | | -2.83 |
| NM_026812 | Hddc3 | -2.82 |
| NM_199153 | Tas2r102 | -2.82 |
| NM_146256 | Hpdl | -2.82 |
| NM_020576 | Psors1c2 | -2.80 |
| AC153486.6 | | -2.79 |
| NM_183281 | 2310005G13Rik | -2.79 |
| NM_175443 | Etnk2 | -2.78 |
| NM_001014997 | Gm156 | -2.78 |
| NM_024473 | BC005537 | -2.77 |
| NM_001042501 | 5830415L20Rik | -2.77 |
| NM_133792 | Lypla3 | -2.77 |
| NG_002057.2 | | -2.76 |
| NM_028643 | Efha1 | -2.75 |
| NM_017382 | Rab11a | -2.75 |
| AC122117.10 | | -2.74 |
| NM_172521 | Nut | -2.74 |
| NM_016813 | Nxf1 | -2.73 |
| NM_175682 | 9930021D14Rik | -2.73 |
| AC121874.2 | | -2.73 |
| NM_027807 | Cul5 | -2.73 |
| NM_026255 | Slc25a26 | -2.72 |
| NM_001029937 | Sec14l3 | -2.72 |
| BC080301.1 | | -2.71 |
| AC135861.5 | | -2.71 |
| AC026767.30 | | -2.70 |
| NM_001082476 | Ndor1 | -2.69 |
| NM_145473 | Csdc2 | -2.68 |
| BN000872.1 | | -2.68 |
| NM_010196 | Fga | -2.67 |
| NM_027144 | Arhgef12 | -2.66 |
| NM_021397 | Zbtb32 | -2.66 |
| AC121579.3 | | -2.66 |
| NM_028274 | Exosc6 | -2.65 |
| NM_198637 | 1700016K19Rik | -2.65 |
| NM_178220 | Arrb1 | -2.64 |
| NM_027175 | Ndufaf1 | -2.64 |
| AC098709.3 | | -2.63 |
| NM_029297 | Dynlrb2 | -2.62 |
| NM_177393 | Vgcnl1 | -2.61 |
| NM_153398 | Zbtb24 | -2.61 |

| | | |
|---|---|---|
| NM_172303 | Phf17 | -2.61 |
| AC102150.10 | | -2.61 |
| NM_029253.1 | Atf7ip2 | -2.61 |
| NM_147090 | - | -2.61 |
| NM_146288 | Olfr122 | -2.61 |
| NM_144837 | - | -2.60 |
| NM_133996 | Apon | -2.60 |
| NM_174868 | C030011O14Rik | -2.59 |
| NM_148938 | Slc1a3 | -2.59 |
| AC121826.3 | | -2.58 |
| NM_001002239 | Rpl17 | -2.58 |
| NG_007240.1 | | -2.58 |
| NM_025659 | Abi3 | -2.58 |
| NM_172453 | Pif1 | -2.57 |
| NM_001141922.1 | Bean1 | -2.57 |
| AK019736.1 | | -2.57 |
| NM_028430.1 | Ppil6 | -2.57 |
| NM_175096 | D5Ertd593e | -2.56 |
| NM_201405 | Btnl1 | -2.56 |
| NM_028064 | Slc39a4 | -2.55 |
| NM_153144 | Ggnbp2 | -2.55 |
| NM_025910 | Mina | -2.55 |
| NM_025280 | Kin | -2.55 |
| NM_001033435 | Gm885 | -2.55 |
| NM_001038015 | Gnpda2 | -2.55 |
| NM_028534 | Smap1 | -2.55 |
| AC123807.4 | | -2.55 |
| NM_145433 | Mrm1 | -2.54 |
| AC125045.4 | | -2.54 |
| NM_007978 | F8a | -2.54 |
| NM_001164580.1 | BC030336 | -2.53 |
| NM_001004142.2 | Nlrp1a | -2.51 |
| NG_012988.1 | | -2.51 |
| NG_001704.2 | | -2.51 |
| NM_134134 | A630042L21Rik | -2.49 |
| NM_172609 | Tomm22 | -2.49 |
| NM_175343 | Chdh | -2.49 |
| AC158586.8 | | -2.48 |
| AC009725.12 | | -2.45 |
| NM_146414 | Olfr1431 | -2.45 |
| NM_008866 | Lypla1 | -2.45 |

| | | |
|---|---|---|
| NM_019770 | Tmed2 | -2.44 |
| BX649260.4 | | -2.44 |
| NM_147053 | Olfr582 | -2.44 |
| AC154374.1 | | -2.44 |
| NM_145513 | Tiprl | -2.44 |
| NM_177244 | Fastkd1 | -2.43 |
| NM_178017 | Hmgb2l1 | -2.43 |
| NM_025343 | Rmnd1 | -2.43 |
| XR_105165.1 | B130055M24Rik | -2.43 |
| NM_080440 | Slc8a3 | -2.43 |
| NM_172601 | Rab2b | -2.42 |
| AC152398.7 | | -2.42 |
| AC154395.4 | | -2.41 |
| NM_130865 | Atx | -2.41 |
| AC112261.4 | | -2.40 |
| NM_145416 | BC021438 | -2.40 |
| NM_175315.1 | Ceacam15 | -2.40 |
| NM_173766 | A630023P12Rik | -2.40 |
| NM_173427 | Klhdc7a | -2.40 |
| NM_027395.2 | Basp1 | -2.40 |
| NM_133350 | Mapre3 | -2.40 |
| NM_010211 | Fhl1 | -2.40 |
| NM_146494 | Olfr722 | -2.40 |
| NM_145938 | Rpp40 | -2.40 |
| NM_001025572 | Ankrd12 | -2.39 |
| AC068911.38 | | -2.39 |
| NM_016658 | Galt | -2.39 |
| NM_001081389 | Nlrp6 | -2.39 |
| NM_134077 | Rbm26 | -2.38 |
| NM_175297 | - | -2.38 |
| NG_018374.1 | | -2.38 |
| AL627349.8 | | -2.38 |
| NM_177355 | Plcxd3 | -2.37 |
| NM_001033149 | Ttc9 | -2.37 |
| NM_147029 | Olfr1120 | -2.35 |
| AC158388.2 | | -2.34 |
| XM_001477076.2 | LOC675594 | -2.34 |
| AL844208.5 | | -2.34 |
| NM_144818 | Ncaph | -2.33 |
| NR_033538.1 | | -2.33 |
| NM_172722 | C330023M02Rik | -2.33 |

| | | |
|---|---|---|
| BX004985.6 | | -2.33 |
| NM_024282 | 5830417C01Rik | -2.32 |
| AC109183.17 | | -2.32 |
| NM_007935 | Epc1 | -2.32 |
| AC098886.4 | | -2.31 |
| NM_177607 | 4933430I17Rik | -2.31 |
| AC125373.4 | | -2.31 |
| NM_177893 | - | -2.31 |
| NM_007756 | Cplx1 | -2.31 |
| AK036683.1 | | -2.30 |
| NM_020252 | Nrxn1 | -2.30 |
| AC124520.4 | | -2.30 |
| AC108915.12 | | -2.29 |
| NM_027353 | Cd2bp2 | -2.29 |
| AK043809.1 | | -2.29 |
| NM_146079 | Guca1b | -2.29 |
| NM_001013376 | Rpp38 | -2.28 |
| NM_027904.3 | Cpn2 | -2.28 |
| NM_181819.2 | Wfikkn2 | -2.27 |
| NM_001018031 | Gm414 | -2.27 |
| NM_175448 | A330019N05Rik | -2.27 |
| NM_019763 | Spen | -2.27 |
| NM_177608 | 3110001I20Rik | -2.27 |
| NM_026385 | Pllp | -2.27 |
| NM_001081157 | Lmod3 | -2.27 |
| NM_177697 | E030013G06Rik | -2.27 |
| NM_146218 | Rfwd3 | -2.26 |
| CT030197.14 | | -2.26 |
| NM_009521 | Wnt3 | -2.26 |
| NG_017822.1 | | -2.25 |
| AC131084.13 | | -2.25 |
| NM_013475 | Apoh | -2.25 |
| NM_146646 | Olfr152 | -2.25 |
| NM_001081653.1 | Cntnap5c | -2.24 |
| AC114003.4 | | -2.24 |
| AC099625.11 | | -2.24 |
| BC042508.1 | | -2.24 |
| NM_145401 | Prkag2 | -2.24 |
| NM_025504 | 2310004L02Rik | -2.23 |
| NM_138590 | - | -2.23 |
| NM_023699 | Nfatc4 | -2.23 |

| | | |
|---|---|---|
| NM_016716 | Cul3 | -2.23 |
| NM_177913 | A430089I19Rik | -2.23 |
| NM_177904 | 6030452D12Rik | -2.23 |
| NM_001163136.1 | Macc1 | -2.23 |
| NM_026547.1 | 1520402A15Rik | -2.23 |
| NM_172937 | Shprh | -2.23 |
| NM_028820 | 1700017B05Rik | -2.23 |
| NM_177380 | Cyp3a44 | -2.22 |
| AC126276.3 | | -2.22 |
| NG_018731.1 | | -2.22 |
| NM_146768 | Olfr1099 | -2.22 |
| NM_001001335 | Plekha8 | -2.22 |
| AC138214.8 | | -2.22 |
| NM_178771 | Klhl26 | -2.22 |
| NM_001033454 | AI427809 | -2.21 |
| NM_175325 | Bbs4 | -2.21 |
| NM_001011775 | Olfr1419 | -2.20 |
| NM_012052 | Rps3 | -2.20 |
| BX842660.2 | | -2.20 |
| NM_027493 | Actr8 | -2.20 |
| BC006792.1 | | -2.20 |
| AC104139.6 | | -2.20 |
| AL928998.9 | | -2.20 |
| AL589737.11 | | -2.20 |
| AK138212.1 | | -2.20 |
| BK000964.1 | | -2.20 |
| AC154463.2 | | -2.20 |
| NM_177829 | Spink10 | -2.20 |
| AL732417.19 | | -2.19 |
| NM_146223 | Cplx3 | -2.19 |
| NM_183016 | Cdc42bpb | -2.19 |
| NM_146567 | Olfr843 | -2.19 |
| AL672244.15 | | -2.19 |
| NG_005612.1 | | -2.18 |
| NM_012015 | H2afy | -2.18 |
| NM_001013025 | Tgfbrap1 | -2.18 |
| NM_138658 | Gnas | -2.18 |
| AC107711.13 | | -2.17 |
| BC108341.1 | | -2.17 |
| NM_172786 | Il20ra | -2.17 |
| AL670292.9 | | -2.17 |

| | | |
|---|---|---|
| NM_019583 | Il17rb | -2.17 |
| NM_023526 | Nkiras1 | -2.16 |
| NM_026521 | Zfp706 | -2.16 |
| NM_146485 | Olfr183 | -2.16 |
| NM_177032 | - | -2.15 |
| NM_008474 | Krt84 | -2.15 |
| NM_178901 | AI467606 | -2.15 |
| NM_177059 | Fstl4 | -2.15 |
| AC005992.15 | | -2.15 |
| NM_027375 | Gcc2 | -2.15 |
| NG_017806.1 | | -2.15 |
| NM_207527 | 4930504O13Rik | -2.15 |
| NM_026465 | 2010316F05Rik | -2.15 |
| NM_008367 | Il2ra | -2.14 |
| NM_001033348 | A230067G21Rik | -2.14 |
| NM_001029937 | Sec14l3 | -2.13 |
| AC117797.9 | | -2.13 |
| NM_009401 | Tnfrsf8 | -2.13 |
| AC110235.13 | | -2.13 |
| AK018099.1 | | -2.13 |
| NM_133981 | Alg9 | -2.13 |
| NM_130879 | Usp48 | -2.13 |
| NM_029868 | Gpbp1l1 | -2.13 |
| NG_019354.1 | | -2.13 |
| AL731682.20 | | -2.12 |
| NM_177025 | Cobll1 | -2.12 |
| XM_003085666.1 | 4933406P04Rik | -2.12 |
| NM_025362 | Wbscr18 | -2.12 |
| NM_030553 | Olfr160 | -2.12 |
| NM_022986 | Irak1bp1 | -2.12 |
| AK021136.1 | | -2.12 |
| AC121271.8 | | -2.12 |
| AL808127.4 | | -2.11 |
| AC114988.21 | | -2.11 |
| NM_153528 | Gramd1c | -2.11 |
| NM_133697 | 1110003E01Rik | -2.11 |
| NM_009738 | Bche | -2.11 |
| NM_026574 | Inoc1 | -2.11 |
| AC109196.12 | | -2.11 |
| NM_183098 | 1700084P21Rik | -2.10 |
| NM_138594 | D6Wsu163e | -2.09 |

| | | |
|---|---|---|
| AK017899.1 | | -2.09 |
| NM_177389 | Mia3 | -2.09 |
| AC145211.3 | | -2.09 |
| NM_001081265 | Heatr2 | -2.09 |
| NM_027013.2 | Scnm1 | -2.09 |
| AC124568.3 | | -2.09 |
| NM_013485 | C9 | -2.08 |
| NM_001013376 | Rpp38 | -2.08 |
| NM_001081977 | Rnf144 | -2.08 |
| NM_023799 | Mgea5 | -2.07 |
| AC159632.2 | | -2.07 |
| NM_001003950 | Rab3ip | -2.07 |
| NG_020062.1 | | -2.07 |
| NM_172528 | Lrrc1 | -2.07 |
| AC155274.2 | | -2.07 |
| AC087417.27 | | -2.07 |
| NM_194342 | Unc84b | -2.06 |
| NG_007909.3 | | -2.06 |
| AC119870.17 | | -2.06 |
| NR_029414.1 | | -2.06 |
| NM_013516 | Ms4a2 | -2.06 |
| AC191865.3 | | -2.06 |
| NM_026648 | Lrrc50 | -2.06 |
| NM_010859 | Myl3 | -2.06 |
| NM_028110 | Dennd2d | -2.06 |
| NM_030024 | Prr15 | -2.06 |
| NM_173441 | Iws1 | -2.05 |
| NM_022655 | Ireb2 | -2.05 |
| CT025157.6 | | -2.05 |
| NM_027230 | Prkcbp1 | -2.05 |
| NM_001162933.1 | Rpl10l | -2.05 |
| AC133203.3 | | -2.05 |
| NM_053228 | V1rb7 | -2.04 |
| NM_001005358 | BC018101 | -2.04 |
| AK007040.1 | | -2.04 |
| NM_175358 | Zdhhc15 | -2.04 |
| AC132414.4 | | -2.04 |
| NM_178901 | AI467606 | -2.04 |
| NM_009689 | Birc5 | -2.03 |
| AC119810.8 | | -2.03 |
| NM_175003 | AU040829 | -2.03 |

| | | |
|---|---|---|
| NM_016852 | Wbp2 | -2.03 |
| NM_007420 | Adrb2 | -2.02 |
| NM_172530 | She | -2.02 |
| NM_019988 | Gbl | -2.02 |
| NM_001029867 | Ugt2b36 | -2.01 |
| AK139810.1 | | -2.01 |
| NM_177234 | B230340J04Rik | -2.01 |
| NM_016716 | Cul3 | -2.01 |
| AC153803.1 | | -2.01 |
| AC113068.9 | | -2.01 |
| NM_172616 | C330027C09Rik | -2.01 |
| AK156200.1 | | -2.01 |
| NM_146423 | Olfr887 | -2.01 |
| NM_024290 | Tnfrsf23 | -2.00 |
| NM_153555 | Wdr42a | -2.00 |
| AC154224.1 | | -2.00 |

**Supplementary Table II. Genes targeted by hairpins that have a Z-score > 2 for IC10.** The RefSeq accession number, unique gene identifier (if available), and Z-score for component 10 are shown. Hairpins targeting these genes are predicted by ICA to deplete after dasatinib therapy *in vivo*.

| Accession # | Gene ID | Z-score (IC10) |
|---|---|---|
| NM_001195255.1 | Gm581 | 4.45 |
| NM_175251 | Arid2 | 3.93 |
| AL805899.20 | | 3.93 |
| NM_134142 | Tmem109 | 3.88 |
| AC087799.43 | | 3.52 |
| NM_175246 | Snip1 | 3.51 |
| AK089806.1 | | 3.50 |
| NM_144815 | Cecr5 | 3.48 |
| AC130821.3 | | 3.46 |
| NM_011452 | Serpinb9b | 3.40 |
| AC127173.17 | | 3.40 |
| NM_001039485.3 | Fam38b | 3.33 |
| NM_016717 | Scly | 3.25 |
| AK041457.1 | | 3.24 |
| BX664729.3 | | 3.23 |
| AK076377.1 | | 3.23 |
| NM_175263 | 5730593N15Rik | 3.22 |
| NM_001001335 | Plekha8 | 3.22 |
| NG_020660.1 | | 3.20 |

| | | |
|---|---|---|
| NM_001003913 | Mars | 3.17 |
| NM_007892 | E2f5 | 3.16 |
| NM_001002897.3 | Atg9b | 3.16 |
| NM_009535 | Yes1 | 3.14 |
| NM_138630 | Arhgap4 | 3.14 |
| AK037912.1 | | 3.14 |
| NM_010228 | Flt1 | 3.10 |
| AC102232.12 | | 3.10 |
| NM_008169 | Grin1 | 3.07 |
| AC138739.8 | | 3.07 |
| AC130474.12 | | 3.06 |
| NM_009428 | Trpc5 | 3.06 |
| NM_177848 | OTTMUSG00000015529 | 3.06 |
| AC154367.1 | | 3.05 |
| NM_020503 | Tas2r119 | 3.04 |
| NM_010747 | Lyn | 3.03 |
| NM_030166 | Galntl2 | 3.02 |
| NM_001085511.1 | 4932429P05Rik | 3.01 |
| XM_127665.6 | 9230112D13Rik | 2.99 |
| NM_172614 | Tmem44 | 2.96 |
| NM_024456 | Rab5c | 2.96 |
| NM_001081202 | L1td1 | 2.96 |
| NM_177060 | 9930039A11Rik | 2.95 |
| NM_001029936 | Specc1 | 2.95 |
| AC132408.2 | | 2.92 |
| XR_104808.1 | Fam188b2 | 2.92 |
| NM_001033235 | Trim40 | 2.92 |
| AC156798.2 | | 2.92 |
| NM_016872 | Vamp5 | 2.91 |
| NM_011890 | Sgcb | 2.89 |
| NM_016959 | Rps3a | 2.88 |
| NM_001044697 | Zfp2 | 2.88 |
| NM_173388 | Slc43a2 | 2.87 |
| NM_145590 | BC017158 | 2.87 |
| NG_002028.2 | | 2.86 |
| AL591854.18 | | 2.85 |
| NM_001099328.1 | Zfp831 | 2.83 |
| NG_012580.1 | | 2.81 |
| AC154558.2 | | 2.81 |
| NM_019685 | Ruvbl1 | 2.81 |
| NM_023814 | Tbx18 | 2.80 |

| | | |
|---|---|---|
| NM_001033314 | C530028I08Rik | 2.79 |
| NM_177009 | Smyd4 | 2.77 |
| NM_175441 | D830007F02Rik | 2.77 |
| NM_146577 | Olfr1043 | 2.76 |
| NM_026128 | 4930403L05Rik | 2.74 |
| NM_029773 | 4921517N04Rik | 2.74 |
| NM_198619 | MGC67181 | 2.73 |
| NM_201369.3 | N4bp2l2 | 2.72 |
| NM_001101461.2 | 9130204L05Rik | 2.72 |
| NG_018204.1 | | 2.71 |
| NM_177661 | C130079G13Rik | 2.70 |
| AC087116.13 | | 2.70 |
| NM_030701 | Gpr109a | 2.69 |
| NM_025310 | Ftsj3 | 2.68 |
| NM_153591 | Nars2 | 2.68 |
| XR_106273.1 | 4933407E24Rik | 2.68 |
| NM_026522 | Chid1 | 2.68 |
| NM_146494 | Olfr722 | 2.67 |
| NM_020565 | Sult3a1 | 2.67 |
| XM_003084620.1 | Ccdc149 | 2.66 |
| NM_182995 | 6330503K22Rik | 2.66 |
| AL732456.6 | | 2.64 |
| AL929524.16 | | 2.64 |
| NM_183392 | Nup54 | 2.64 |
| AC155825.2 | | 2.63 |
| NM_011774 | Slc30a4 | 2.63 |
| NM_172793 | Btnl9 | 2.63 |
| NM_145139 | Eif3s6ip | 2.62 |
| AC165969.5 | | 2.62 |
| NM_146179 | Zfp418 | 2.61 |
| NM_001081217 | Zfp174 | 2.61 |
| AC124553.4 | | 2.61 |
| NM_145985 | Arcn1 | 2.60 |
| NM_198967 | Tmtc1 | 2.59 |
| NM_177095 | - | 2.59 |
| NM_025821 | Carhsp1 | 2.59 |
| XM_003084831.1 | 9130014G24Rik | 2.59 |
| BX649226.1 | | 2.59 |
| NM_175303 | Sall4 | 2.58 |
| AK052410.1 | | 2.58 |
| NM_001081287 | Mpp7 | 2.58 |

| | | |
|---|---|---|
| AC154224.1 | | 2.57 |
| AC055817.12 | | 2.57 |
| AC156271.5 | | 2.57 |
| AK019125.1 | | 2.57 |
| AC156607.5 | | 2.56 |
| NM_001101478.1 | D3Ertd254e | 2.55 |
| NM_177847 | A730036I17Rik | 2.55 |
| NM_178734 | Zfp473 | 2.54 |
| NM_198001 | 1110008P14Rik | 2.54 |
| NM_010785 | Mdm1 | 2.53 |
| NM_027180 | Centd2 | 2.53 |
| XM_003084471.1 | LOC100502613 | 2.53 |
| AL929142.6 | | 2.52 |
| AK032662.1 | | 2.52 |
| AC122486.4 | | 2.51 |
| AC153377.5 | | 2.51 |
| XM_003085977.1 | Gm8973 | 2.51 |
| NM_130453 | Gpha2 | 2.50 |
| NM_146328 | Olfr110 | 2.50 |
| NM_007460 | Ap3d1 | 2.49 |
| AK078603.1 | | 2.49 |
| NM_146382 | Olfr461 | 2.49 |
| NM_008508 | Lor | 2.49 |
| NM_010275 | Gdnf | 2.48 |
| NM_172272 | Pars2 | 2.47 |
| NM_028030 | Rbpms2 | 2.46 |
| AL645797.11 | | 2.46 |
| NM_153546 | Mboat1 | 2.46 |
| NM_027338 | Vps36 | 2.46 |
| NM_027191 | Nup37 | 2.46 |
| NM_175134 | Ankrd46 | 2.45 |
| NM_031875 | Otof | 2.45 |
| CT030722.6 | | 2.45 |
| NM_152821 | Purg | 2.45 |
| NM_026467 | Rps27l | 2.44 |
| NM_144517 | Tbc1d19 | 2.43 |
| AL627123.13 | | 2.42 |
| NG_018471.1 | | 2.41 |
| NM_145744 | Dusp15 | 2.41 |
| NM_027872 | Slc46a3 | 2.40 |
| NM_172937 | Shprh | 2.40 |

| | | |
|---|---|---|
| NM_001081204 | B3galtl | 2.40 |
| NM_146186 | - | 2.40 |
| NM_144790 | Ankrd33 | 2.40 |
| NG_012017.1 | | 2.40 |
| NM_152813 | Plcd3 | 2.39 |
| NM_146350 | Olfr1123 | 2.39 |
| NM_175259 | Tmem58 | 2.38 |
| AK028613.1 | | 2.38 |
| NM_024180 | Ormdl2 | 2.38 |
| AC139572.4 | | 2.38 |
| NM_177150 | Cenpt | 2.37 |
| NM_198034 | Sidt1 | 2.36 |
| AC105905.10 | | 2.36 |
| NM_016889 | Insm1 | 2.36 |
| NM_146451 | Olfr164 | 2.36 |
| NM_133724 | Cno | 2.35 |
| NM_020252 | Nrxn1 | 2.35 |
| AA682037 | Rps6kc1 | 2.35 |
| NM_175693 | - | 2.34 |
| NM_020521 | V1rb5 | 2.34 |
| AC102430.9 | | 2.34 |
| NM_019988 | Gbl | 2.34 |
| AC130821.3 | | 2.34 |
| AC107758.19 | | 2.34 |
| NM_172770 | Ttc12 | 2.33 |
| AC154640.2 | | 2.33 |
| NM_010147 | Epn1 | 2.32 |
| NM_028030 | Rbpms2 | 2.32 |
| NM_175347 | Srl | 2.32 |
| NM_021389 | Sh3kbp1 | 2.32 |
| AK006663.1 | | 2.32 |
| NM_001081306 | Ptprz1 | 2.31 |
| NM_001013755 | 5730409E04Rik | 2.31 |
| AC119177.11 | | 2.31 |
| AC139241.4 | | 2.30 |
| NM_016982 | Vpreb1 | 2.30 |
| AK034470.1 | | 2.30 |
| NM_009462 | Usp10 | 2.30 |
| NM_011807 | Dlg2 | 2.30 |
| NM_010136 | Eomes | 2.30 |
| AC124533.4 | | 2.30 |

| | | |
|---|---|---|
| NM_054077 | Prelp | 2.30 |
| NM_027698 | Exod1 | 2.29 |
| NM_011920 | Abcg2 | 2.29 |
| NM_008592 | Foxc1 | 2.29 |
| NM_134192 | V1re3 | 2.29 |
| AC121832.3 | | 2.29 |
| NM_001081247 | Polr3a | 2.29 |
| NM_001126316.1 | Gm438 | 2.29 |
| NM_177697 | E030013G06Rik | 2.28 |
| NM_010154.1 | Erbb4 | 2.28 |
| NM_027121 | Vkorc1l1 | 2.28 |
| AL929413.13 | | 2.28 |
| NM_146261 | BC031748 | 2.28 |
| AK040340.1 | | 2.28 |
| NM_145550 | Yipf1 | 2.28 |
| NM_177624 | A430083B19Rik | 2.27 |
| NM_001081391 | Csmd3 | 2.27 |
| NM_177471 | Ccdc69 | 2.27 |
| AL589876.11 | | 2.27 |
| NM_172740 | - | 2.27 |
| NM_026886 | 1500001A10Rik | 2.27 |
| NM_134469 | Fdps | 2.26 |
| AC133090.4 | | 2.26 |
| AB116374.1 | | 2.26 |
| NM_144920 | Plekha5 | 2.26 |
| XM_137324.3 | Gm4801 | 2.25 |
| NM_015733 | Casp9 | 2.25 |
| AC122818.4 | | 2.24 |
| AC108777.7 | | 2.24 |
| NM_146306 | Olfr518 | 2.23 |
| NM_016796 | Vamp4 | 2.23 |
| AC114998.13 | | 2.23 |
| NM_008776 | Pafah1b3 | 2.23 |
| NM_178402 | - | 2.23 |
| NM_026438 | Ppa1 | 2.23 |
| AC109281.5 | | 2.23 |
| AC152951.2 | | 2.23 |
| NM_198671 | Gse1 | 2.22 |
| NM_018739 | rp9 | 2.22 |
| NM_001081080 | Phf3 | 2.22 |
| NG_020564.1 | | 2.22 |

| | | |
|---|---|---|
| NG_018172.1 | | 2.21 |
| AC154451.2 | | 2.21 |
| NM_001003919 | Ddx11 | 2.21 |
| AC124765.2 | | 2.21 |
| NM_053008 | Olig3 | 2.21 |
| NG_019793.1 | | 2.20 |
| NM_182930 | Plekha6 | 2.19 |
| NM_177622 | A230042K10Rik | 2.19 |
| NM_153564 | Gbp2 | 2.19 |
| NM_133905 | Papd4 | 2.19 |
| AC124742.4 | | 2.18 |
| NM_080638 | Mvp | 2.18 |
| NM_009254 | Serpinb6a | 2.18 |
| NM_019951 | Sec11a | 2.18 |
| NM_177471 | Ccdc69 | 2.17 |
| NM_177264 | 9230112E08Rik | 2.17 |
| AC132612.3 | | 2.17 |
| AC107811.28 | | 2.17 |
| NM_029491 | D030074E01Rik | 2.17 |
| NM_007925 | Eln | 2.17 |
| NM_177290 | Itgb8 | 2.17 |
| AC114547.12 | | 2.17 |
| AC159476.5 | | 2.17 |
| NG_018964.1 | | 2.16 |
| NM_010705 | Lgals3 | 2.16 |
| NG_019793.1 | | 2.16 |
| AC154872.10 | | 2.16 |
| AC101221.12 | | 2.16 |
| NM_172721 | Fbxw8 | 2.16 |
| NM_028134 | Lysmd1 | 2.16 |
| NM_009968 | Cryz | 2.16 |
| NM_030718 | Abo | 2.16 |
| NM_029884 | Hgsnat | 2.15 |
| NM_026785 | Ube2c | 2.15 |
| NM_009917 | Ccr5 | 2.15 |
| AK020104.1 | | 2.15 |
| NM_025814 | Serbp1 | 2.15 |
| NG_018021.1 | | 2.15 |
| NM_027547 | Prdm5 | 2.15 |
| AK086549.1 | | 2.15 |
| NM_177098 | 4930412M03Rik | 2.14 |

| | | |
|---|---|---|
| NM_012022 | Ppnr | 2.14 |
| NM_172607 | Naprt1 | 2.14 |
| NM_130856 | Krtap16-8 | 2.14 |
| AC139349.4 | | 2.14 |
| NM_133954 | AA960436 | 2.14 |
| NM_023813 | Camk2d | 2.14 |
| NM_175254 | 9330180L21Rik | 2.14 |
| NM_175317 | Eftud1 | 2.13 |
| NM_146409 | Olfr1080 | 2.12 |
| NM_001080931 | Thrap1 | 2.12 |
| AK006847.1 | | 2.12 |
| NM_211138 | Pcyt1b | 2.12 |
| NM_145491 | Rhoq | 2.11 |
| AC115805.12 | | 2.11 |
| NM_177192 | D030011O10Rik | 2.11 |
| NM_009686 | Apbb2 | 2.11 |
| NM_011857 | Odz3 | 2.11 |
| NM_031493 | Xlr5c | 2.11 |
| NM_175540 | Eda2r | 2.11 |
| NM_032400 | Sucnr1 | 2.11 |
| NM_026083 | Zc3h13 | 2.11 |
| NM_001081111 | Tmf1 | 2.11 |
| AC153597.13 | | 2.11 |
| NM_008698 | Nipsnap1 | 2.11 |
| NM_172264 | Chdh | 2.10 |
| NM_173865 | Slc41a1 | 2.10 |
| AC161246.2 | | 2.10 |
| NM_001085500.2 | Cisd3 | 2.10 |
| NM_001099277.1 | Zfp541 | 2.10 |
| NM_177326 | Pak2 | 2.10 |
| NM_153803 | BC038479 | 2.10 |
| NM_001159942.1 | Plekhg1 | 2.09 |
| NM_021446 | 0610007P14Rik | 2.09 |
| AK017517.1 | | 2.09 |
| NG_007741.3 | | 2.09 |
| NM_010082 | Adam28 | 2.09 |
| NM_053170 | Trim33 | 2.08 |
| NM_026866 | Disp1 | 2.08 |
| NM_021326 | Rbak | 2.08 |
| AC114924.5 | | 2.08 |
| NM_024444 | Cyp4f18 | 2.08 |

| | | |
|---|---|---|
| NM_001001319 | Pramel4 | 2.08 |
| NM_146152 | Ipo13 | 2.08 |
| NM_134123 | - | 2.08 |
| AC126943.5 | | 2.08 |
| NM_138753 | Hexim1 | 2.07 |
| NM_178243 | 5830403L16Rik | 2.07 |
| NM_011200 | Ptp4a1 | 2.07 |
| NM_016799 | Srrm1 | 2.07 |
| AC098875.3 | | 2.07 |
| NM_001081059 | Ccdc90a | 2.06 |
| AC116386.9 | | 2.06 |
| AC119842.9 | | 2.06 |
| NM_182928 | Adm2 | 2.06 |
| NG_006498.2 | | 2.06 |
| AC060761.10 | | 2.06 |
| NM_001081191 | Eml5 | 2.06 |
| NM_173771 | 4933406M09Rik | 2.05 |
| NM_134077 | Rbm26 | 2.05 |
| AK020394.1 | | 2.05 |
| AC118642.11 | | 2.05 |
| NM_029707 | 1700023I07Rik | 2.05 |
| AC125223.3 | | 2.05 |
| NM_019419 | Arl6ip1 | 2.05 |
| NM_172740 | - | 2.05 |
| AC132305.3 | | 2.05 |
| NM_009459 | Ube2h | 2.05 |
| NM_021455 | Mlxipl | 2.04 |
| AC122251.4 | | 2.04 |
| NM_146126 | Sord | 2.04 |
| NM_145402 | Tmem51 | 2.04 |
| AC164290.4 | | 2.04 |
| NM_130450 | Elovl6 | 2.04 |
| AL773540.18 | | 2.04 |
| NM_024237 | 1600015H20Rik | 2.04 |
| NM_019776 | Snd1 | 2.03 |
| NM_021319 | Pglyrp2 | 2.03 |
| NM_001111317.1 | BC048609 | 2.03 |
| NM_175381 | 2700081O15Rik | 2.03 |
| NM_001003915 | Slc5a12 | 2.03 |
| NM_152811 | Ugt2b1 | 2.03 |
| NM_172683 | Pogz | 2.03 |

| | | |
|---|---|---|
| AC129180.3 | | 2.03 |
| NM_172935 | Amdhd2 | 2.03 |
| AK089280.1 | | 2.03 |
| AC135861.5 | | 2.02 |
| NM_026776 | Vps25 | 2.02 |
| NM_146359 | Olfr564 | 2.02 |
| NM_145460 | Oxnad1 | 2.02 |
| NM_133917 | Mlxip | 2.02 |
| NM_009734 | Azi1 | 2.02 |
| NG_020439.1 | | 2.02 |
| NM_001040434.1 | Rgag1 | 2.02 |
| AC157521.2 | | 2.02 |
| NM_146311 | Olfr510 | 2.01 |
| NM_145921 | Olah | 2.01 |
| NM_146543 | Olfr1360 | 2.01 |
| NM_024478 | Grpel1 | 2.01 |
| AK006834.1 | | 2.01 |
| NM_177292 | C530024P05Rik | 2.01 |
| NM_001029979 | Safb2 | 2.01 |
| AK030544.1 | | 2.01 |
| AC153512.2 | | 2.01 |
| NM_053156 | Allc | 2.01 |
| AC025586.4 | | 2.00 |
| NM_133791 | Wwc2 | 2.00 |
| NM_028111 | 2010109K11Rik | 2.00 |
| NM_001033535 | Tnfaip8l3 | 2.00 |
| AC117635.6 | | 2.00 |

**Supplementary Table III. Gene sets identified by GSEA as being enriched in the set of genes targeted by IC10 hairpins that have higher representation after therapy as compared to before.**

| Gene Set ID | Description | Collection | Nominal p-value |
|---|---|---|---|
| KEGG_DRUG_METABOLISM_OTHER_ENZYMES | Drug metabolism - other enzymes | Curated gene sets | 0.00000 |
| LIU_PROSTATE_CANCER_UP | Genes up-regulated in prostate cancer samples. | Curated gene sets | 0.00247 |
| LEE_EARLY_T_LYMPHOCYTE_DN | Genes down-regulated at early stages of progenitor T lymphocyte maturation compared to the late stages. | Curated gene sets | 0.00476 |

| | | | |
|---|---|---|---|
| KOYAMA_SEMA3B_TARGETS_DN | Genes down-regulated in NCI-H1299 cells (large cell neuroendocrine carcinoma) stably expressing SEMA3B | Curated gene sets | 0.00639 |
| MILI_PSEUDOPODIA_CHEMOTAXIS_DN | Transcripts depleted in pseudopodia of NIH/3T3 cells (fibroblast) in response to the chemotactic migration stimulus by lysophosphatidic acid (LPA) | Curated gene sets | 0.00704 |
| SMIRNOV_RESPONSE_TO_IR_2HR_DN | Genes down-regulated in B lymphocytes at 2 h after exprosure to 10 Gy dose of ionizing radiation | Curated gene sets | 0.00779 |
| RCGCANGCGY_V$NRF1_Q6 | Genes with promoter regions [-2kb,2kb] around transcription start site containing the motif RCGCANGCGY which matches annotation for NRF1: nuclear respiratory factor 1 | Motif gene sets | 0.00000 |
| GCM_SMARCD1 | Neighborhood of SMARCD1 SWI/SNF related, matrix associated, actin dependent regulator of chromatin, subfamily d, member 1 in the GCM expression compendium | Computational gene sets | 0.00000 |
| MODULE_308 | Genes in the cancer module 308 | Computational gene sets | 0.00462 |
| GSE11057_EFF_MEM_VS_CENT_MEM_CD4_TCELL_DN | Genes down-regulated in comparison of effector memory T cells versus central memory T cells from peripheral blood mononuclear cells (PBMC) | Immunologic signatures | 0.00539 |
| GSE8515_CTRL_VS_IL1_4H_STIM_MAC_DN | Genes down-regulated in comparison of untreated macrophages versus those treated with IL1 | Immunologic signatures | 0.00800 |

**Supplementary Table IV. Gene sets identified by GSEA as being enriched in the set of genes targeted by IC10 hairpins that have lower representation after therapy as compared to before.**

| Gene Set ID | Description | Collection | Nominal p-value |
|---|---|---|---|

| | | | |
|---|---|---|---|
| YANG_BREAST_CANCER_ESR1_LASER_DN | Genes down-regulated in laser microdissected (LCM) samples of early primary breast tumors expressing ESR1 vs the ESR1 negative ones | Curated gene sets | 0.00000 |
| DACOSTA_UV_RESPONSE_VIA_ERCC3_XPCS_DN | Genes exclusively down-regulated in fibroblasts expressing the XP/CS mutant form of ERCC3 after high dose UVC irradiation | Curated gene sets | 0.00000 |
| AMUNDSON_RESPONSE_TO_ARSENITE | Genes discriminating responses to sodium arsenite from other stresses | Curated gene sets | 0.00000 |
| TONKS_TARGETS_OF_RUNX1_RUNX1T1_FUSION_ERYTHROCYTE_UP | Genes up-regulated in erythroid lineage cells by RUNX1-RUNX1T1 fusion | Curated gene sets | 0.00000 |
| KEGG_UBIQUITIN_MEDIATED_PROTEOLYSIS | Ubiquitin mediated proteolysis | Curated gene sets | 0.00155 |
| Ji_RESPONSE_TO_FSH_DN | Down-regulated in ovarian epithelial cells (MCV152) 72 hours following FSH treatment, compared to untreated | Curated gene sets | 0.00169 |
| KANG_GIST_WITH_PDGFRA_UP | Genes up-regulated in gastrointestinal stromal tumors (GIST) with PDGFRA [GeneID=5156]mutations | Curated gene sets | 0.00174 |
| CUI_TCF21_TARGETS_2_DN | All significantly down-regulated genes in kidney glomeruli isolated from TCF21 knockout mice | Curated gene sets | 0.00256 |
| THUM_SYSTOLIC_HEART_FAILURE_DN | Genes down-regulated in samples with systolic heart failure compared to normal hearts | Curated gene sets | 0.00313 |
| MORI_PRE_BI_LYMPHOCYTE_DN | Down-regulated genes in the B lymphocyte developmental signature, based on expression profiling of lymphomas from the Emu-myc transgenic mice: the Pre-BI | Curated gene sets | 0.00334 |

| | | | |
|---|---|---|---|
| | stage. | | |
| DURAND_STROMA_MAX_DN | | Curated gene sets | 0.00471 |
| GRAHAM_NORMAL_QUIESCENT_VS_NORMAL_DIVIDING_UP | Genes up-regulated in quiescent vs dividing CD34+ cells isolated from peripheral blood of normal donors. | Curated gene sets | 0.00532 |
| RIZKI_TUMOR_INVASIVENESS_3D_UP | Genes up-regulated in three-dimentional (3D) cultures of preinvasive (S3-C) vs invasive (T4-2) breast cancer cells | Curated gene sets | 0.00614 |
| GUTIERREZ_CHRONIC_LYMPHOCYTIC_LEUKEMIA_DN | Genes exclusively down-regulated in B lymphocytes from CLL (chronic lymphocytic leukemia) patients but with a similiar expression pattern in the normal cells and in the cells from WM (Waldenstroem's macroblobulinemia) patients | Curated gene sets | 0.00690 |
| BREDEMEYER_RAG_SIGNALING_NOT_VIA_ATM_UP | Genes up-regulated in pre B lymphocyte after induction of physiological DNA double-strand breaks (DSB) by RAG2; the changes are independent of ATM signaling | Curated gene sets | 0.00791 |
| MARTENS_BOUND_BY_PML_RARA_FUSION | Genes with promoters occupied by PML-RARA fusion protein in acute promyelocytic leukemia(APL) cells NB4 and two APL primary blasts, based on Chip-seq data | Curated gene sets | 0.00853 |
| GOTZMANN_EPITHELIAL_TO_MESENCHYMAL_TRANSITION_DN | Genes down-regulated in MMH-RT cells (hepatocytes displaying an invasive, metastatic phenotype) during epithelial to mesenchymal transition (EMT) | Curated gene sets | 0.00955 |
| V$EN1_01 | Genes with promoter regions [-2kb,2kb] around transcription start site containing the motif GTANTNN which matches annotation for EN1: engrailed homolog 1 | Motif gene sets | 0.00000 |

| | | | |
|---|---|---|---|
| V$FOXJ2_01 | Genes with promoter regions [-2kb,2kb] around transcription start site containing the motif NNNWAAAYAAAYANNNNN which matches annotation for FOXJ2: forkhead box J2 | Motif gene sets | 0.00160 |
| V$FOX_Q2 | Genes with promoter regions [-2kb,2kb] around transcription start site containing the motif KATTGTTTRTTTW which matches annotation for FOXF2: forkhead box F2 | Motif gene sets | 0.00310 |
| V$AMEF2_Q6 | Genes with promoter regions [-2kb,2kb] around transcription start site containing motif CKGDYTAAAAATAACYMM. Motif does not match any known transcription factor | Motif gene sets | 0.00327 |
| V$BRN2_01 | Genes with promoter regions [-2kb,2kb] around transcription start site containing the motif NNCATNSRWAATNMRN which matches annotation for POU3F2: POU domain, class 3, transcription factor 2 | Motif gene sets | 0.00635 |
| TTANTCA_UNKNOWN | Genes with promoter regions [-2kb,2kb] around transcription start site containing motif TTANTCA. Motif does not match any known transcription factor | Motif gene sets | 0.00650 |
| MORF_ESPL1 | Neighborhood of ESPL1 extra spindle poles like 1 (S. cerevisiae) in the MORF expression compendium | Computational gene sets | 0.00000 |
| MORF_BUB1 | Neighborhood of BUB1 BUB1 budding uninhibited by benzimidazoles 1 homolog (yeast) in the MORF expression compendium | Computational gene sets | 0.00166 |
| MORF_RRM1 | Neighborhood of RRM1 ribonucleotide reductase M1 polypeptide in the MORF expression compendium | Computational gene sets | 0.00485 |
| CELL_CYCLE_PROCESS | Genes annotated by the GO term GO:0022402. A cellular | GO gene sets | 0.00000 |

| | | | |
|---|---|---|---|
| | process that is involved in the progression of biochemical and morphological phases and events that occur in a cell during successive cell replication or nuclear replication events | | |
| M_PHASE | Genes annotated by the GO term GO:0000279. Progression through M phase, the part of the cell cycle comprising nuclear division. | GO gene sets | 0.00156 |
| CELL_CYCLE_PHASE | Genes annotated by the GO term GO:0022403. A cell cycle process comprising the steps by which a cell progresses through one of the biochemical and morphological phases and events that occur during successive cell replication or nuclear replication events | GO gene sets | 0.00299 |
| MITOTIC_CELL_CYCLE | Genes annotated by the GO term GO:0000278. Progression through the phases of the mitotic cell cycle, the most common eukaryotic cell cycle, which canonically comprises four successive phases called G1, S, G2, and M and includes replication of the genome and the subsequent segregation of chromosomes into daughter cells. In some variant cell cycles nuclear replication or nuclear division may not be followed by cell division, or G1 and G2 phases may be absent | GO gene sets | 0.00325 |
| PROTEIN_TYROSINE_KINASE_ACTIVITY | Genes annotated by the GO term GO:0004713. Catalysis of the reaction: ATP + a protein tyrosine = ADP + protein tyrosine phosphate | GO gene sets | 0.00864 |
| CELL_CYCLE_GO_0007049 | Genes annotated by the GO term GO:0007049. The progression of biochemical | GO gene sets | 0.00875 |

| | | | |
|---|---|---|---|
| | and morphological phases and events that occur in a cell during successive cell replication or nuclear replication events. Canonically, the cell cycle comprises the replication and segregation of genetic material followed by the division of the cell, but in endocycles or syncytial cells nuclear replication or nuclear division may not be followed by cell division | | |
| SYSTEM_DEVELOPMENT | Genes annotated by the GO term GO:0048731. The process whose specific outcome is the progression of an organismal system over time, from its formation to the mature structure. A system is a regularly interacting or interdependent group of organs or tissues that work together to carry out a given biological process | GO gene sets | 0.00952 |
| KRAS.KIDNEY_UP.V1_UP | Genes up-regulated in epithelial kidney cancer cell lines over-expressing an oncogenic form of KRAS gene | Oncogenic signatures | 0.00324 |
| GSE2706_R848_VS_LPS_8H_STIM_DC_DN | Genes down-regulated in comparison of dendritic cells (DC) stimulated with R848 at 8 h versus DCs stimulated with LPS (TLR4 agonist) for 8 h | Immunologic signatures | 0.00000 |
| GSE11864_CSF1_VS_CSF1_PAM3CYS_IN_MAC_DN | Genes down-regulated in comparison of macrophages cultured with M-CSF versus macrophages cultured with M-CSF and Pam3Cyc. | Immunologic signatures | 0.00000 |
| GSE24634_IL4_VS_CTRL_TREATED_NAIVE_CD4_TCELL_DAY3_DN | Genes down-regulated in comparison of CD25- T cells treated with IL4 at day 3 versus untreated CD25- T cells at day 3 | Immunologic signatures | 0.00161 |
| GSE1432_CTRL_ | Genes down-regulated in | Immunologic | 0.00162 |

| | | | |
|---|---|---|---|
| VS_IFNG_24H_MICROGLIA_DN | comparison of control microglia cells versus those 24 h after stimulation with IFNG | signatures | |
| GSE17721_POLYIC_VS_CPG_4H_BMDM_DN | Genes down-regulated in comparison of dendritic cells (DC) stimulated with poly(I:C) (TLR3 agonist) at 4 h versus DC cells stimulated with CpG DNA (TLR9 agonist) at 4 h | Immunologic signatures | 0.00303 |
| GSE17721_CTRL_VS_CPG_4H_BMDM_UP | Genes up-regulated in comparison of control dendritic cells (DC) at 4 h versus those stimulated with CpG DNA (TLR9 agonist) at 4 h | Immunologic signatures | 0.00462 |
| GSE3982_NEUTROPHIL_VS_TH1_DN | Genes down-regulated in comparison of neutrophils versus Th1 cells | Immunologic signatures | 0.00479 |
| GSE3337_CTRL_VS_16H_IFNG_IN_CD8POS_DC_DN | Genes down-regulated in comparison of untreated CD8+ dendritic cells (DC) at 16 h versus those treated with IFNG at 16 h | Immunologic signatures | 0.00485 |
| GSE17721_PAM3CSK4_VS_GADIQUIMOD_4H_BMDM_UP | Genes up-regulated in comparison of dendritic cells (DC) stimulated with Pam3Csk4 (TLR1/2 agonist) at 4 h versus DC cells stimulated with Gardiquimod (TLR7 agonist) at 4 h. | Immunologic signatures | 0.00603 |
| GSE13411_NAIVE_BCELL_VS_PLASMA_CELL_UP | Genes up-regulated in comparison of naive B cells versus plasma cells | Immunologic signatures | 0.00611 |
| GSE1432_1H_VS_24H_IFNG_MICROGLIA_DN | Genes down-regulated in comparison of microglia cells 1 h after stimulation with IFNG versus microglia cells 24 h after the stimulation | Immunologic signatures | 0.00759 |
| GSE17721_CPG_VS_GARDIQUIMOD_4H_BMDM_UP | Genes up-regulated in comparison of dendritic cells (DC) stimulated with CpG DNA (TLR9 agonist) at 4 h versus DC cells stimulated with Gardiquimod (TLR7 agonist) at 4 h | Immunologic signatures | 0.00790 |
| GSE360_DC_VS_MAC_M_TUBERC | Genes down-regulated in comparison of dendritic cells | Immunologic signatures | 0.00926 |

| | | | |
|---|---|---|---|
| ULOSIS_DN | (DC) exposed to M. tuberculosis versus macrophages exposed to L. major | | |

**Supplementary Table V. Primer sequences used for hairpin amplification and barcoding in *in vivo* and *in vitro* screens.** To ensure that two mutations would be required to change the barcode of one sample to another functional barcode, the unmutated primers are not used.

| 5' unmutated primer |
|---|
| NNNNNTAGTGAAGCCACAGATGTA |
| 5' primers with one basepair mutation to mark individual samples |
| NNNNNTAGTGACGCCACAGATGTA |
| NNNNNTAGTGAAGCCACCGATGTA |
| NNNNNTAGTGAGGCCACAGATGTA |
| NNNNNTAGTGAAGCCACGGATGTA |
| NNNNNTAGTGAAGCCGCAGATGTA |
| NNNNNTAGTGAAGCCACAGCTGTA |
| NNNNNTAGTGAAGCCACAGGTGTA |
| NNNNNTAGGGAAGCCACAGATGTA |
| 3' unmutated primer |
| NNNNTTGAATTCCGAGGCAGTAGG |
| 3' primers with one basepair mutation to mark individual samples |
| NNNNTTGCATTCCGAGGCAGTAGG |
| NNNNTTGGATTCCGAGGCAGTAGG |
| NNNNTTGACTTCCGAGGCAGTAGG |
| NNNNTTGAGTTCCGAGGCAGTAGG |
| NNNNTTGAATTCCGAGGCGGTAGG |
| NNNNTTGAATTCCGCGGCAGTAGG |
| NNNNTTGAACTCCGAGGCAGTAGG |
| NNNNTTGAAGTCCGAGGCAGTAGG |

**Supplementary Methods**

*RNAi screening and validation assays*

To preserve library complexity, a minimum of 50-fold coverage of shRNA libraries was maintained at each step of the screens with the exception of the pre-treatment sample. Pre-treatment blood samples were limited in size and therefore were at approximately 20- to 40-fold coverage. 100 million leukemia cells were infected with a pool of approximately 20,000 shRNAs tagged with GFP at a final infection percentage of 5 – 10%. The average number of shRNAs per gene is 2. The average number of sequencing reads mapped to the 20K pool was 19 million.

Spin infections were performed in the presence of 4 ug/mL polybrene. 48 hours after infection, leukemia cells were sorted for GFP positive cells, obtaining enough cells for approximately 250x library coverage. After expanding in culture for three days, 1 x $10^6$ leukemia cells were plated in triplicate for *in vitro* screen. Four days after sorting, 1 x $10^6$ leukemia cells were injected into eight non-irradiated, syngeneic (C57BL6/J) recipient mice by tail vein injection. At the time of injection, three aliquots of 2 x $10^6$ leukemia cells were collected to serve as the input sample. At five days after initial plating of screening samples in culture, approximately 2 x $10^6$ cells from each culture was taken as a pre-treatment sample and cultures were then treated with 0.6 nM dasatinib (~LD30) for 3 days. After treatment, approximately 2 x $10^6$ cells were taken from each culture as post-treatment samples. For the *in vivo* screen, a pre-treatment blood sample was taken via retro-orbital bleed at the presentation of overt symptoms of leukemia eleven days post-injection, and mice were then treated with 10 mg/kg dasatinib for three days. Mice were allowed to relapse and at morbidity (fourteen –

sixteen days post-injection) leukemia cells were collected from peripheral blood for post-treatment samples.

Genomic DNA was isolated by proteinase K digestion and isopropanol precipitation from all samples. The antisense strand of shRNAs was amplified from genomic DNA utilizing primers that include 1-basepair mutations to barcode individual samples on both the 5' and 3' ends as previously described (42). Hairpins were amplified in multiple 50 uL reactions, and in the case of smaller pre-treatment sample the entire genomic DNA sample was amplified. After PCR amplification, samples were pooled and prepped for sequencing with Illumina's genomic adaptor kit and PCR products were sequenced with an Illumina HiSeq 2000 machine. PCR primer sequences are provided in Supplementary Table V.

Hairpins were validated using GFP competition assays by infecting a pure population of tdTomato positive leukemia cells at 40 – 50% with single constructs expressing GFP and the shRNA of interest. 1 x $10^6$ cells were injected into non-irradiated six – ten week old C57BL6/J female mice 48 hours after infection, and the GFP percentage at injection was measured using flow cytometry. Pre- and post-treatment samples were collected as in the screen; mice were treated with 20 mg/kg dasatinib via oral gavage for three days. GFP percentage was assessed at pre- and post-treatment by flow cytometric analysis. All flow data was collected on LSR analyzers and analyzed using FACSDiva software (BD Biosciences).

**Supplementary computational methods**

*Signature discovery*

Given the clonal relationships and diversity of samples in the dataset, a high resolution signature discovery approach was employed to characterize global hairpin representation profiles. Independent Component Analysis (ICA), an unsupervised blind source separation technique, was used on this discrete count-based dataset to elucidate statistically independent and biologically relevant signatures (Bhutkar et al. in preparation). ICA is a signal processing and multivariate data analysis technique in the category of unsupervised matrix factorization methods.

Conceptually, ICA decomposes the overall dataset into independent signals (hairpin representation patterns) that represent distinct signatures. High-ranking positively and negatively correlated hairpins in each signature represent hairpin-sets that drive the corresponding enrichment (or depletion) pattern. Signatures were visualized using the sample-to-signature correspondence schematic afforded by Hinton plots where colors represent directionality of hairpin representation (red enriched, green depleted) and the size of each rectangle quantifies the strength of a signature (column) in a given sample (row). Each signature is two-sided, allowing for identification of enriched and depleted hairpins for each signature within each sample.

Formally, utilizing input data consisting of a hairpins-samples count matrix, ICA uses higher order moments to characterize the dataset as a linear combination of statistically independent latent variables. These latent variables represent independent components based on maximizing non-gaussianity, and can be interpreted as independent source signals that have been mixed together to form the dataset under

consideration. Each component includes a weight assignment to each hairpin that quantifies its contribution to that component. Additionally, ICA derives a mixing matrix that describes the contribution of each sample towards the signal embodied in each component. This mixing matrix can be used to select signatures among components with distinct hairpin representation profiles across the set of samples.

This page intentionally left blank.

**Chapter III: Loss of *Pafah1b3* sensitizes a transplantable mouse model of *BCR-ABL1*+ BCP-ALL cells to dasatinib specifically *in vivo*.**

---

Eleanor R. Cameron, Emily Lawler, Michael T. Hemann

David H. Koch Institute for Integrative Cancer Research, Massachusetts Institute of Technology. Cambridge, Massachusetts, 02139, United States.

This chapter is not published as of December 2015.

## Introduction

From an RNAi screen for *in vivo* mediators of response to dasatinib in *BCR-ABL1*+ precursor B-cell acute lymphoblastic leukemia (BCP-ALL), we identified a hairpin targeting *Pafah1b3* as depleting after dasatinib therapy specifically in the *in vivo* setting. *PAFAH1B3* encodes the $\alpha_1$ subunit of platelet activating factor acetyl hydrolase Ib, a member of the Group VIII family of phospholipase $A_2$ enzymes (1). Pafah1b is made up of two catalytic α subunits and one regulatory β subunit; the *PAFAH1B2* gene encodes the $\alpha_2$ subunit, and the functional enzyme can consist of homo- or heterodimers of α subunits (1, 2). Pafah1b is one of a family of Pafah enzymes; there is also another intracellular acetyl hydrolase, Pafah2 (*PAFAH2*), as well as a secreted version known as plasma Pafah (*PLA2G7*) (1). All of the Pafah enzymes hydrolyze an *sn*-2 acetyl residue off of the phospholipid signaling molecule platelet activating factor (PAF), thereby inactivating it (1, 2). Pafah enzymes can also recognize and hydrolyze other related phospholipids, although the intracellular Pafah enzymes are relatively specific for PAF (1). There is also evidence that Pafah1b can have PAF-independent effects in cells, and that the $\alpha_1$ and $\alpha_2$ catalytic subunits are not completely interchangeable; they each have distinct effects independent of PAF, and may have different binding efficiencies for PAF and other phospholipid substrates (3-7).

PAF is synthesized within cells of the hematopoietic system as well as endothelial cells, fibroblasts, keratinocytes, liver and intestinal cells; PAF facilitates intercellular signaling via its binding to the PAF receptor (PAFR), a G-protein coupled receptor that is expressed on many hematopoietic cells (8-10). PAF binding to PAFR results in increased synthesis of inositol triphosphate, $Ca^{2+}$ mobilization within the cell,

activation of p38 MAPK, trans-activation of the EGF receptor, and in some cells activation of the Ras signaling pathway (8-10). In leukocytes, PAF induces activation, cell motility, and polarization, and promotes leukocyte accumulation at sites of inflammation (9, 11). There is additional evidence that PAF can also act as an intracellular messenger either in the cell where it is synthesized or after receptor binding and internalization; intracellular Pafah enzymes seem to function to regulate intracellular levels of PAF, as Pafah inhibition can induce PAF accumulation to levels equivalent to extracellular PAF stimulation (2, 3, 8, 10, 12).

PAFR is expressed in normal B-lymphocytes and B-cell lines, but membrane levels typically depend on the activation state of the cell (8). Normal B lymphocytes can also produce PAF when stimulated, and PAF is metabolized in B-cells by Pafah enzymes (8). Human leukemia cells have been shown to release PAF *in vitro*, but leukemic patients typically have lower levels of PAF in their bone marrow and blood plasma than healthy individuals do (8, 13, 14). In some leukemic cell lines, PAFR antagonists have antileukemic activity *in vitro* (15, 16). Both PAFR mRNA and cell surface PAFR have been found in/on the blasts of acute lymphoblastic leukemia patients, indicating that the PAF pathways is active in ALL patients, although the role it plays in leukemia is unclear (8, 17, 18).

Here we investigate the role of Pafah1b3 in a transplantable mouse model of *BCR-ABL1*+ BCP-ALL. Independent component analysis of our longitudinal RNAi screening data provided us with a number of shRNAs that either depleted or enriched significantly after dasatinib treatment *in vivo*. About half of these hairpins did not validate *in vitro*, meaning that they either did not have the same behavior *in vitro* as they

did *in vivo*, or the changes *in vitro* simply were not significant. In the former category is a hairpin directed against *Pafah1b3*, which depletes strongly after dasatinib therapy *in vivo* but has the opposite behavior *in vitro*. Additionally, the hairpin targeting *Pafah1b3* enriched before therapy *in vivo*, indicating a complete shift in behavior after the addition of drug to the system. Such a hairpin may posses an *in vivo*-specific, therapy-specific effect, and so we decided to perform follow up analysis to confirm whether or not *Pafah1b3* loss does in fact sensitize *BCR-ABL1*+ BCP-ALL cells to dasatinib.

We confirmed that additional shRNAs that knock down *Pafah1b3* sensitize *BCR-ABL1*+ BCP-ALL cells to therapy specifically in the *in vivo* setting, and that this effect can be rescued by re-expression of a non-targetable Pafah1b3 cDNA. Furthermore, we were able to generate *BCR-ABL1*+ BCP-ALL cells that completely lack the Pafah1b3 protein, and found that mice transplanted with these cells had significantly increased survival specifically after dasatinib treatment; our evidence suggests that this might be due to altered distribution of *BCR-ABL1*+ BCP-ALL cells between specific anatomical sites within recipient mice.

**Results**

Our screen identified a hairpin that targets *Pafah1b3* as depleting after therapy *in vivo*, and in multiple independent validation experiments we found that the original shRNA against *Pafah1b3* depletes significantly after dasatinib *in vivo* but not *in vitro* (Figure 1A). We generated additional shRNAs that knock down Pafah1b3 at the protein level and found that all three hairpins deplete in dasatinib-treated mice as compared to untreated mice; this assay is more stringent than comparing before versus after

dasatinib treatment as there is greater noise and thus a greater signal required to achieve significance (Figures 1B, 1C). In order to confirm that Pafah1b3 loss, rather than an off-target effect of the hairpins, is mediating the observed sensitization to dasatinib therapy, we transduced leukemia cells with wild-type Pafah1b3 cDNA and confirmed that those shRNAs that target the 3'untranslated region of the *Pafah1b3* gene cannot knock down the Pafah1b3 cDNA (Supplementary Figure S1). GFP competition experiments in the presence or absence of the Pafah1b3 cDNA revealed that cDNA expression could rescue the sensitizing effect of Pafah1b3 knockdown (Supplementary Figure S1).

In order to confirm that the PAF pathway can function in this model of *BCR-ABL1*+ BCP-ALL cells, we analyzed the expression of the PAFR on the surface of leukemia cells. A small percentage of leukemia cells expressed surface PAFR *in vitro*, but this percentage increased slightly when leukemia cells were co-cultured with bone marrow- or spleen-derived stromal cells (Supplementary Figure S2). Interestingly, we found that the addition of dasatinib to co-cultures resulted in a significant decrease in the percentage of leukemia cells expressing PAFR on their surface; this decrease in PAFR-expressing cells did not occur after dasatinib treatment of leukemia cells cultured alone (Supplementary Figure S2).

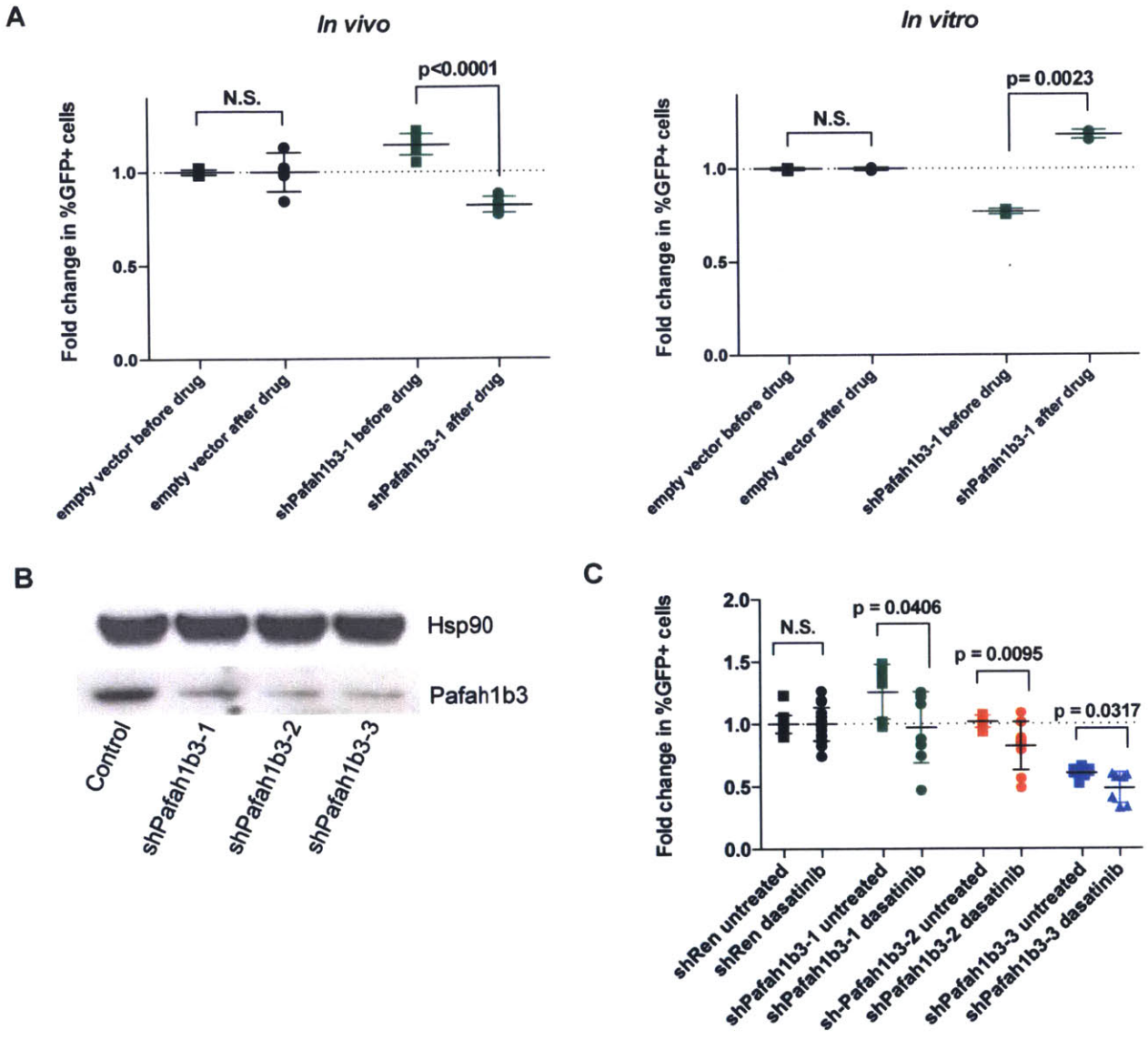


**Figure 1. Pafah1b3 loss confers sensitivity to dasatinib specifically *in vivo*.** (A) Scatterplots showing that the initial hairpin against *Pafah1b3* from the 20K library screen depletes significantly after dasatinib treatment *in vivo* but not *in vitro*. Fold changes are normalized to a control empty vector or control hairpin targeting Renilla luciferase, which these cells do not express. Values are an average of at least seven mice from multiple independent experiments. (B) Western blot showing Pafah1b3 knockdown by shRNAs. shPafah1b3-1 is the initial shRNA identified in 20K screen; shPafah1b3-2 and shPafah1b3-3 are additional shRNAs targeting the 3'UTR of the *Pafah1b3* gene. Hsp90 is used as a loading control. (C) Scatterplots showing fold change in percent shPafah1b3-expressing cells from transplant to morbidity in both untreated and dasatinib-treated mice. Fold changes are normalized to a control empty vector or a hairpin targeting Renilla luciferase. Values are an average of at least seven mice from multiple independent experiments. Error bars indicate standard deviation; p-values were calculated using Student's t-test.

In longitudinal *in vitro* GFP competition assays, neither of the additional hairpins that we cloned to knockdown *Pafah1b3* deplete after dasatinib treatment as compared to before (Supplementary Figure S3). In contrast, in comparisons of dasatinib treated cultures versus untreated cultures, shPafah1b3-2 expressing cells are depleted in treated cultures versus untreated ones (Supplementary Figure S3). However, in a separate experiment we found that the depletion of shPafah1b3-2 expressing cells in dasatinib treated cultures cannot be rescued by the expression of a non-targetable Pafah1b3 cDNA and therefore is unlikely to be due to Pafah1b3 knockdown (Supplementary Figure S3).

To study the effect of complete *Pafah1b3* loss, rather than knockdown, we made use of the Crispr/Cas9 system to generate single cell clones (SCCs) of leukemia cells that either still express wild-type levels of Pafah1b3 or are Pafah1b3 knockouts. Sanger sequencing at the *Pafah1b3* locus confirmed that the knockout clones contained deletions in both alleles, while sequences from wild-type clones express un-mutated Pafah1b3 (Supplementary Figure S4). By transducing these clones with Pafah1b3 cDNA, we generated pairs of clonal populations with either wild-type Pafah1b3 versus over-expression of Pafah1b3 or knockout of Pafah1b3 versus over-expression of Pafah1b3 (Figure 2A and Supplementary Figure S4). To avoid mistaking effects of clonality for the effect of Pafah1b3 loss, in experiments with these single cell clones we always compared a clone to itself. Specifically, we compared Pafah1b3 knockout cells (Pafah1b3 KO - cDNA) to Pafah1b3 over-expressing cells generated from the same clone (Pafah1b3 KO + cDNA). Because the Pafah1b3 cDNA results in over-expression of Pafah1b3 at the protein level, we also used a wild-type single cell clone as a control

by comparing cells with wild-type Pafah1b3 levels (Pafah1b3 WT - cDNA) to Pafah1b3 over-expressing cells generated from the same clone (Pafah1b3 WT + cDNA).

Over-expression of Pafah1b3 on either a Pafah1b3 wild-type or Pafah1b3 knockout background had no effect on the survival of mice transplanted with these clones and then treated with vehicle (Figures 2B, 2C). However, after brief dasatinib treatment, mice that received transplants of unrescued Pafah1b3 knockout cells had significantly longer lifespans than those mice that received transplants of Pafah1b3 over-expressing cells from the same clone (Figure 2C). There was no difference in the survival after dasatinib treatment of mice transplanted with Pafah1b3 wild-type cells versus Pafah1b3 overexpressing cells from the same clone, indicating that over-expression of Pafah1b3 alone does not confer a shorter lifespan after dasatinib treatment (Figure 2B). As Pafah1b3 over-expression was able to rescue the phenotype of increased survival after dasatinib in Pafah1b3 knockout cells, it seems evident that total loss of Pafah1b3 expression significantly sensitizes leukemia cells to dasatinib therapy.

The brief dasatinib treatment used in this survival experiment does cause a significant increase in the lifespan of all the mice, regardless of the genotype of transplanted cells (Supplementary Figure S5). In mice transplanted with leukemic cells that express wild-type or over-expressing Pafah1b3 the increases in lifespan due to dasatinib treatment are similar regardless of the clone or presence or absence of a Pafah1b3 cDNA, but in mice receiving transplants of unrescued Pafah1b3 knockout (KO - cDNA) cells the increase in lifespan after dasatinib treatment is significantly increased (Supplementary Figure S5). Interestingly, vehicle-treated mice receiving transplants of

the Pafah1b3 knockout clone have significantly longer lifespans than mice receiving transplants of the Pafah1b3 wild-type clone, but as Pafah1b3 over-expression in either clone has no effect on lifespan of vehicle-treated recipient mice this effect can be attributed to variations in the *in vivo* growth rate between the two clones rather than changes in Pafah1b3 levels (Supplementary Figure S5).

As the transplanted leukemia cells express luciferase, we were able to utilize *in vivo* bioluminescent imaging to measure leukemic burden in survival experiment mice both before and after dasatinib treatment (19). While all transplanted mice have disseminated leukemia before therapy, a few mice that received transplants of unrescued Pafah1b3 knockout cells (KO - cDNA) lacked measurable disease after dasatinib (Figure 2D). In fact, the whole body luminescent signal after dasatinib treatment of mice transplanted with unrescued Pafah1b3 knockout cells (KO - cDNA) was, on average, significantly lower than that of mice transplanted with Pafah1b3 overexpressing cells (KO + cDNA) from the same clone (Figure 2E). There is no significant difference in disease burden either before or after treatment in mice receiving either Pafah1b3 wild-type cells (WT - cDNA) or Pafah1b3 overexpressing cells (WT + cDNA) from the same clone (Figure 2E). Similarly, Pafah1b3 overexpression on either the wild-type or the knockout background has no significant effect on disease burden in vehicle-treated mice both before and after vehicle treatment (Supplementary Figure S6).

A

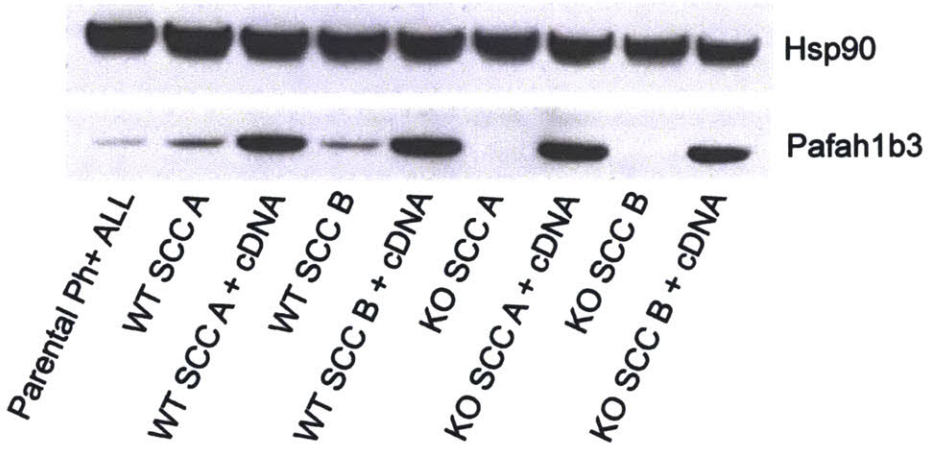


B

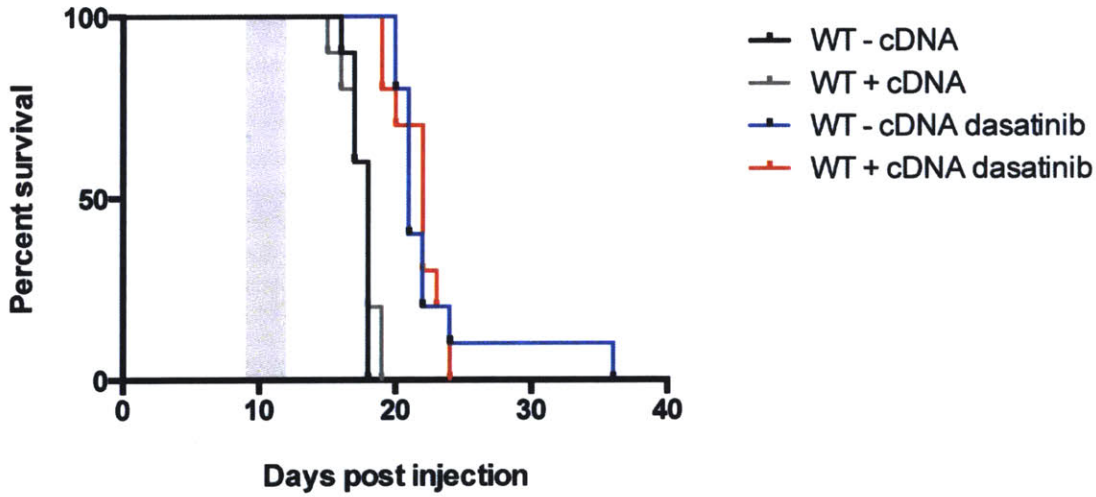


C

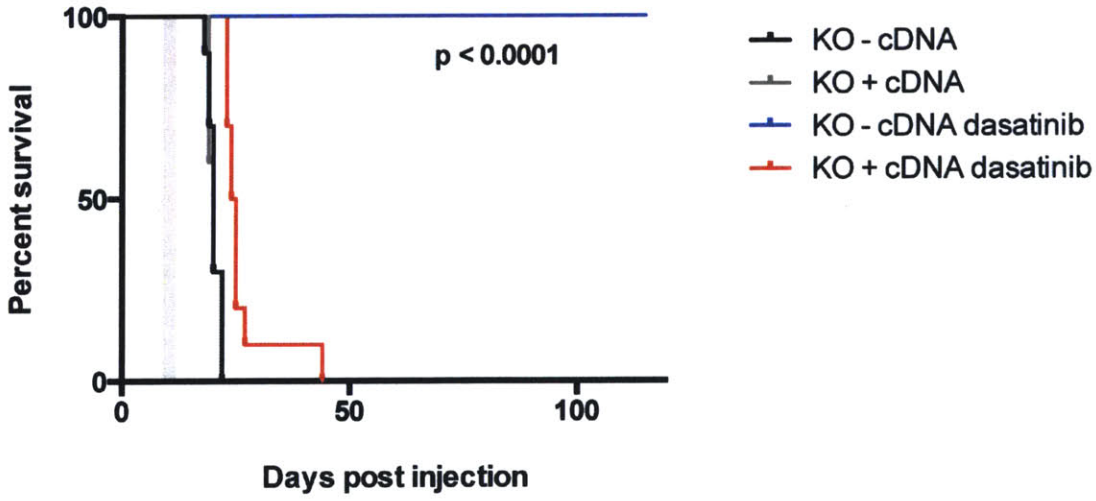


continued on next page

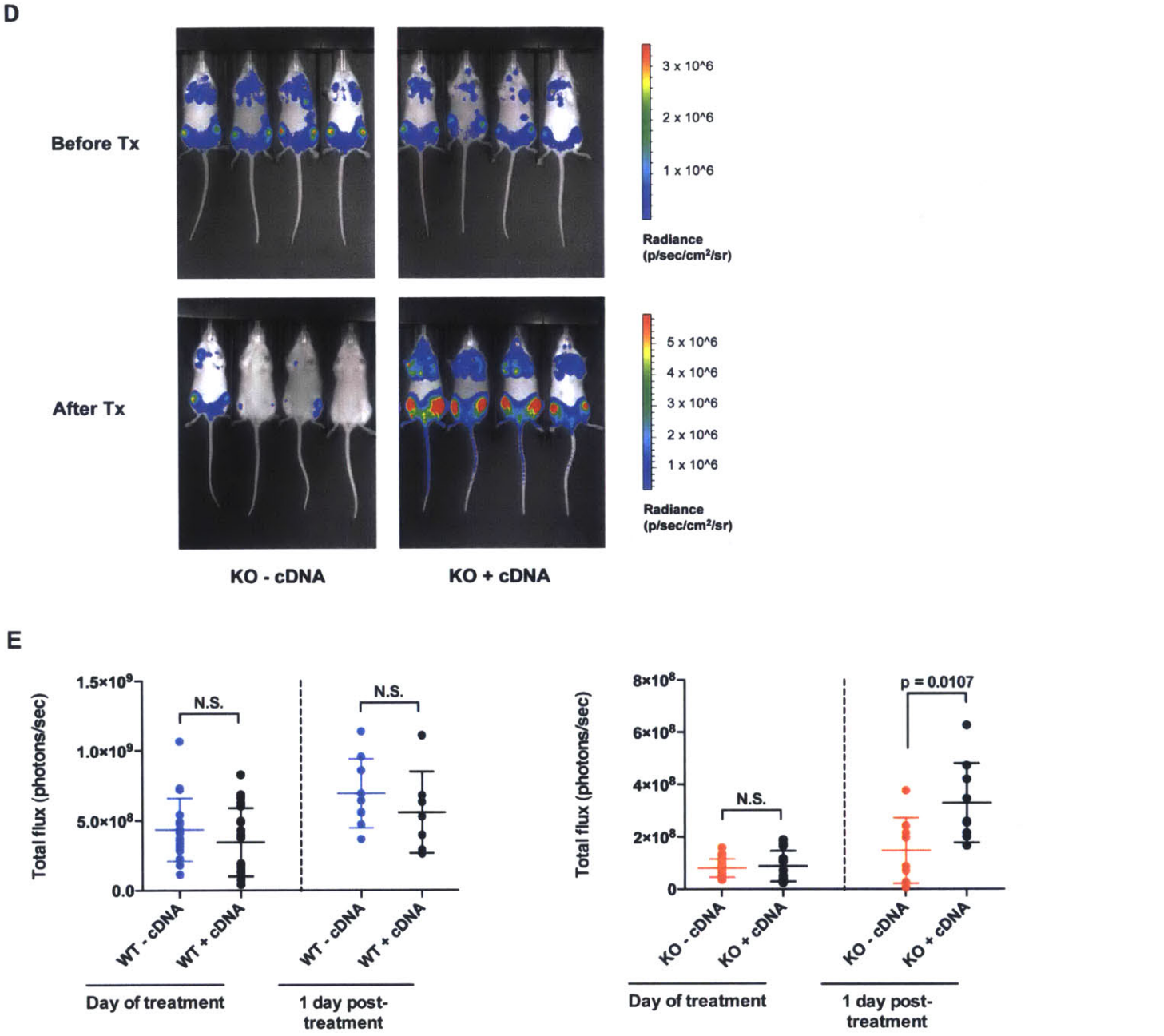


**Figure 2. Crispr/Cas9 mediated knockout of *Pafah1b3* in *BCR-ABL1+* BCP-ALL cells results in increased *in vivo* sensitivity to dasatinib.**
(A) Western blot showing loss of Pafah1b3 expression in single-cell clones (SCCs) generated by using Crispr/Cas9 empty constructs (WT SCC A and WT SCC B) or Crispr/Cas9 constructs targeting the *Pafah1b3* gene (KO SCC A and KO SCC B). Hsp90 is used as a loading control. (B) Survival analysis of mice receiving $10^4$ cells from a Pafah1b3 wild-type (WT) clone with or without Pafah1b3 cDNA expression. Expression of Pafah1b3 cDNA does not affect lifespan in untreated or dasatinib-treated mice. Significance was calculated for survival curves using the Mantel-Cox test; the grey rectangle indicates the time period over which dasatinib was administered. (C) Survival analysis of mice receiving $10^4$ cells from a Pafah1b3 knockout (KO) clone with

or without Pafah1b3 cDNA expression. Dasatinib treated mice that receive Pafah1b3 KO cells lacking the Pafah1b3 cDNA live significantly longer, while Pafah1b3 cDNA expression has no effect on the lifespan of untreated mice. Significance was calculated for survival curves using the Mantel-Cox test; the grey rectangle indicates the time period over which dasatinib was administered. (D) *In vivo* luminescent imaging before and after dasatinib treatment shows significantly less disease burden after dasatinib treatment in mice receiving Pafah1b3 KO cells that lack the Pafah1b3 cDNA. (E) Scatterplots showing that burden in mice receiving transplants of Pafah1b3 KO cells is significantly lower after dasatinib as compared to the Pafah1b3 overexpressing cells from the same clone. Mice receiving transplants of Pafah1b3 WT cells do not have significantly less burden after dasatinib as compared to Pafah1b3 overexpressing cells from the same clone. Values are an average of at least 8 mice per genotype. Error bars indicate standard deviation; p-values were calculated using Student's t-test.

In order to investigate the nature of the sensitization effect of Pafah1b3 loss on dasatinib-treated *BCR-ABL1*+ BCP-ALL cells, we attempted to recapitulate *in vivo* effects by co-culturing leukemia cells with bone marrow- or spleen-derived stromal cells. Interestingly, when we looked at dasatinib-mediated cell killing of wild-type and knockout clones with or without the presence of a Pafah1b3 cDNA, over-expression of the Pafah1b3 resulted in decreased survival of Pafah1b3 knockout cells (Figure 3A). This was true even in the presence of bone marrow- or spleen-derived stromal cells and at multiple dasatinib doses, indicating that sensitization to dasatinib observed upon Pafah1b3 loss *in vivo* cannot be recapitulated simply by exposing leukemia cells to stroma (Figure 3B, C, Supplementary Figure S7). Similarly, hairpins knocking down Pafah1b3 enriched rather than depleted after dasatinib treatment in co-culture with bone marrow stromal cells, and the addition of a Pafah1b3 cDNA did not rescue the enrichment phenotype, indicating that it is not due to *Pafah1b3* loss (Figure 3D). As an orthogonal approach, we also performed a GFP competition assay of the Pafah1b3 cDNA on either wild-type or knockout clones, and found that Pafah1b3 cDNA

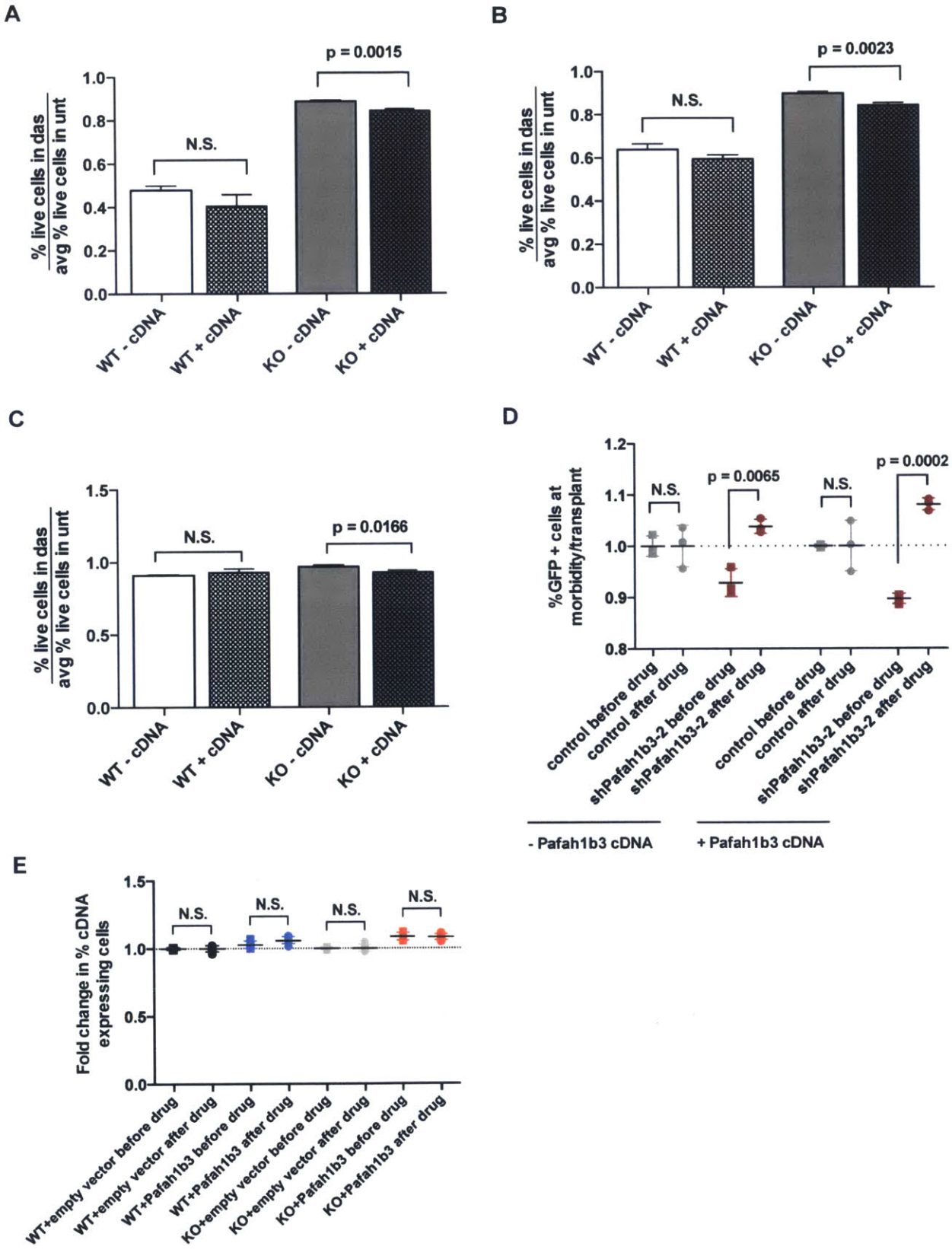
A
p = 0.0015
N.S.
% live cells in das
avg % live cells in unt
1.0
0.8
0.6
0.4
0.2
0.0
WT - cDNA
WT + cDNA
KO - cDNA
KO + cDNA
B
p = 0.0023
N.S.
% live cells in das
avg % live cells in unt
C
p = 0.0166
N.S.
% live cells in das
avg % live cells in unt
1.5
0.5
D
%GFP + cells at
morbidity/transplant
1.2
1.1
p = 0.0065
N.S.
p = 0.0002
control before drug
control after drug
shPafah1b3-2 before drug
shPafah1b3-2 after drug
- Pafah1b3 cDNA
+ Pafah1b3 cDNA
E
Fold change in % cDNA
expressing cells
WT+empty vector before drug
WT+empty vector after drug
WT+Pafah1b3 before drug
WT+Pafah1b3 after drug
KO+empty vector before drug
KO+empty vector after drug
KO+Pafah1b3 before drug
KO+Pafah1b3 after drug

**Figure 3. Loss of *Pafah1b3* does not sensitize *BCR-ABL1*+ BCP-ALL cells to dasatinib *in vitro* (previous page).**
(A), (B) and (C) Bar graphs showing percentage of live cells in 2 nM dasatinib-treated cultures normalized to percentage of live cells in untreated cultures after 4 days of treatment of cells alone (A), with bone marrow-derived stromal cells (B), and with spleen-derived stromal cells. Pafah1b3 loss does not result in increased cell death after dasatinib regardless of the presence of stroma. Error bars for bar graphs indicate standard error of the mean. (D) Scatterplots showing fold change in shRNA-expressing cells in cells that are either wild-type (left) or express a non-targetable Pafah1b3 cDNA (right) in co-culture with bone-marrow derived stromal cells. Fold changes are normalized to a hairpin targeting Renilla luciferase. Pafah1b3 knockdown cells enrich after dasatinib treatment regardless of the presence of a non-targetable Pafah1b3 cDNA. (E) Scatterplots showing fold change in cDNA-expressing cells on Pafah1b3 wild type or KO backgrounds *in vitro* without stromal cells; expression of a Pafah1b3 cDNA is neutral before and after dasatinib treatment. Fold changes are normalized to an empty cDNA expression vector. Percentages are an average of three replicates. Error bars for scatterplots indicate standard deviation; p-values were calculated using Student's t-test.

expressing cells were not enriched after dasatinib therapy *in vitro* regardless of the presence of stromal cells (Figure 3D, Supplementary Figure S7).

In contrast, Pafah1b3 over-expressing cells enriched in the blood, bone marrow, and spleen of mice transplanted with both wild-type and Pafah1b3 knockout *BCR-ABL1*+ BCP-ALL cells after dasatinib therapy in an *in vivo* Pafah1b3 cDNA competition assay (Figure 4A, B, C). In order to determine if Pafah1b3 levels alter the distribution of leukemic cells between different organs, we looked at comparative enrichment of Pafah1b3 over-expressing cells in bone marrow and spleen versus blood. Pafah1b3 over-expressing cells are more enriched in the bone marrow as compared to blood at morbidity, but not before therapy, of dasatinib-treated mice specifically on a Pafah1b3 knockout background (Figure 4D, Supplementary Figure S8). Therefore an increase in Pafah1b3 levels results not only in a general increases in leukemia cell survival after

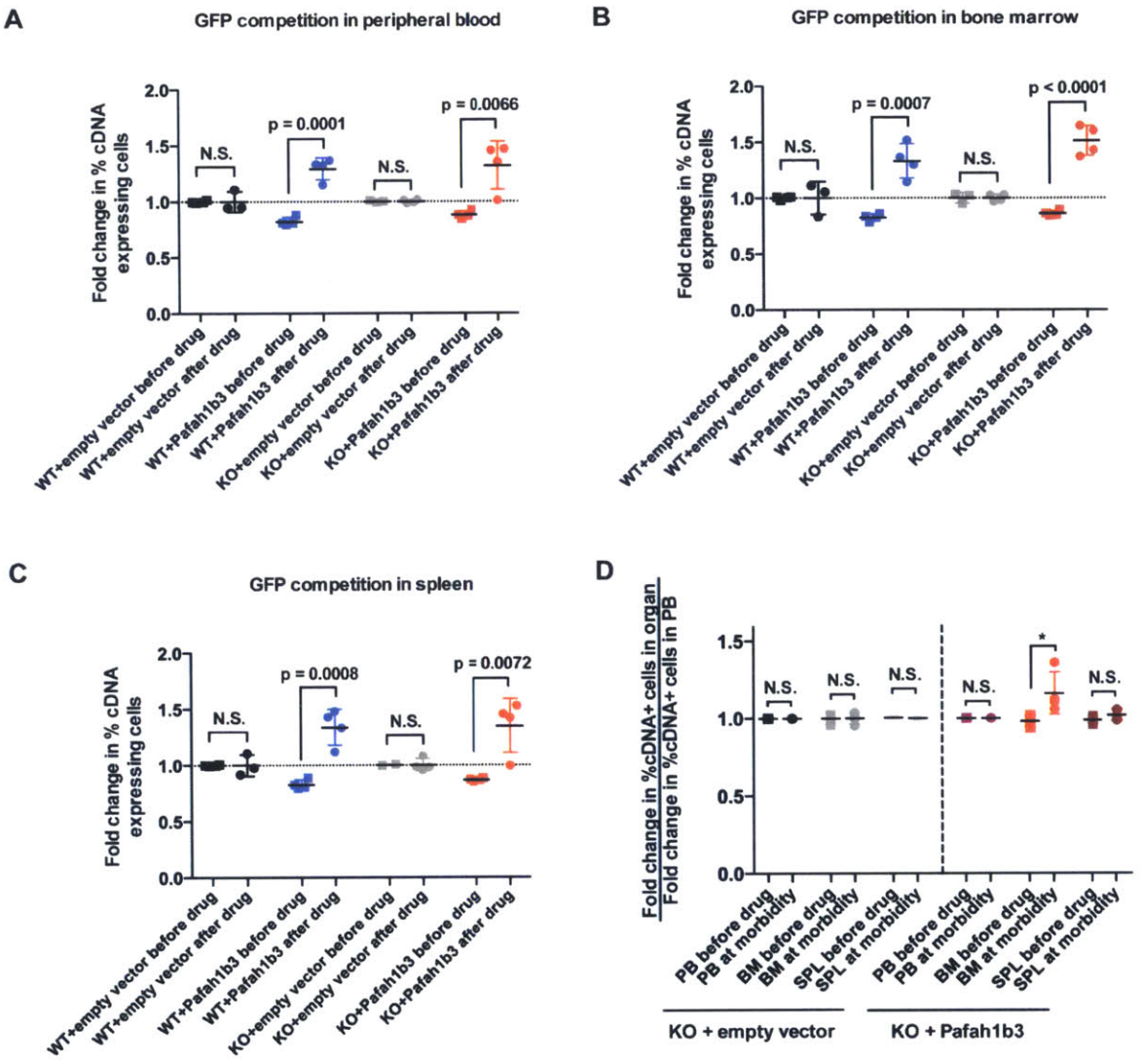


**Figure 4. Pafah1b3 levels in *BCR-ABL1*+ BCP-ALL cells modulate distribution of cells between anatomical sites after dasatinib treatment.** (A), (B), and (C) Scatterplots showing fold change in cDNA-expressing cells on either Pafah1b3 wild type or KO backgrounds before and after dasatinib treatment in mouse (A) peripheral blood, (B) bone marrow, and (C) spleen. Pafah1b3 cDNA+ and thus over-expressing cells significantly enrich after dasatinib treatment in all three organs on both backgrounds. (D) Scatterplots show relative enrichment of cDNA-expressing cells on a Pafah1b3 KO background from transplant to the start of treatment versus relative enrichment from transplant to morbidity. Relative enrichment is defined as the fold change of percent cDNA+ cells in each organ normalized to the fold change of percent cDNA+ cells in the blood of the same mouse. cDNA-expressing cells are significantly enriched in the bone marrow versus the blood of mice transplanted with Pafah1b3 KO cells at morbidity but not before treatment. For all experiments, values are an average of at least 3 mice per genotype. Error bars represent standard deviation; p-values were calculated using Student's t-test.

dasatinib therapy, but also a specific enrichment of leukemia cells after therapy in the bone marrow microenvironment.

To get a better idea of the kinetics of this effect, we looked at distribution of Pafah1b3 over-expressing versus Pafah1b3 wild-type or Pafah1b3 knockout cells in the organs of recipient mice before and at several time-points after dasatinib therapy, and found that Pafah1b3 over-expressing cells are most enriched relative to Pafah1b3 knockout or wild-type cells 5 days after the end of therapy, which is 2-3 days before morbidity (Supplementary Figure S9). At 5 days after the end of therapy, Pafah1b3 over-expressing cells are more enriched in the bone marrow compared to blood on both Pafah1b3 wild type and Pafah1b3 knockout backgrounds, indicating that increased Pafah1b3 levels alter the distribution of leukemic cells between organ compartments *in vivo* after dasatinib therapy regardless of Pafah1b3 wild-type versus knockout background (Supplementary Figure S8).

As before, mice receiving transplants of unrescued Pafah1b3 knockout cells had significantly increased survival after dasatinib therapy as compared to mice receiving transplants containing Pafah1b3 over-expressing cells from the same clone, even though only about half of the cells injected into mice receiving KO + cDNA cells actually expressed the Pafah1b3 cDNA (Supplementary Figure S10). In contrast, Pafah1b3 over-expression has no effect on the survival of untreated mice receiving cells of either background, or of dasatinib-treated mice transplanted with Pafah1b3 wild-type cells (Supplementary Figure S10). Unlike in our previous survival experiment, mice receiving unrescued Pafah1b3 knockout (KO - cDNA) transplants did experience leukemic relapse after dasatinib treatment, likely due to the increase in the number of

transplanted cells from $10^4$ to $10^6$ (Supplementary Figure S10). The higher leukemic burden before treatment in these mice is an aspect of the experimental design that is required for us to be able to study the effect of *Pafah1b3* loss in a competitive environment; complete loss of Pafah1b3 knockout leukemia in this case would not be useful.

**Discussion**

Pafah1b functions to reduce intracellular levels of PAF, which can activate caspase-dependent apoptosis (3, 4). A reduction in *PAFAH1B3* in the presence of active *PAFAH1B2* can promote the activity of Pafah1b enzymes containing the $\alpha_2$ homodimer, which hydrolyze PAF more efficiently and can protect against PAF-mediated apoptosis (3). However, if *PAFAH1B2* levels are insufficient to deal with intracellular PAF levels, loss of *PAFAH1B3* may result in increased PAF signaling; increased PAF signaling is also observed in cells treated with dual Pafah1b2/3 inhibitors (12).

In our experiments, loss of *Pafah1b3* sensitizes *BCR-ABL1*+ BCP-ALL cells to dasatinib specifically *in vivo*, but this is not correlated to increased cell death *in vitro* even if leukemia cells are co-cultured with stromal cells. We did find altered distribution of Pafah1b3 over-expressing as compared to knock-out cells between organ compartments after dasatinib therapy, indicating that loss of *Pafah1b3* may affect the ability of cells to migrate to and colonize distinct microenvironments, rather than directly resulting in apoptosis of treated cells. PAF synthesis and PAF receptor expression are both regulated by various cytokines, and PAF can also stimulate cytokine release.

Cytokine exposure can promote survival or apoptosis in BCP-ALL cells, as well as affect homing and mobilization of leukemic cells to various anatomical sites (20, 21). Additionally, the bone marrow has been demonstrated to be a protective site in both *BCR-ABL1*+ and *BCR-ABL1* negative BCP-ALL, indicating that the relatively decreased ability of *Pafah1b3* knockout cells to localize to and remain in the bone marrow after dasatinib treatment may be the reason for the sensitizing effect of *Pafah1b3* loss (20, 22).

Interestingly, increased expression of PAF receptor has been observed in *BCR-ABL1*+ chronic myelogenous leukemia cells cultured under hypoxic conditions, indicating that hypoxia may induce increased PAF signaling (23). Additionally, PAF signaling is angiogenic, can promote expression of *VEGF* and neoangiogenesis in tumors, and inhibition of Pafah in a mouse tumor model reduced vascularization of solid tumors and inhibited neoangiogenesis *in vitro* (10, 24-26). Leukemic bone marrow is typically hypoxic and angiogenic, and expression of angiogenic factors in BCP-ALL patients is associated with poor prognosis (27-31). Therefore, loss of *Pafah1b3* may also function to alter the ability of *BCR-ABL1*+ BCP-ALL cells to promote angiogenesis and thus alter their microenvironment in order to promote leukemia cell retention and protection from dasatinib-mediated cell killing.

While we have not assayed PAFR levels on the surface of leukemia cells *in vivo*, we did find that dasatinib decreases the percentage of leukemic cells expressing PAFR when cells are co-cultured with stroma. This effect could be due to either a decrease in the surface expression of PAFR or receptor internalization after ligand binding. Assessment of the changes in signaling molecules released by stromal cells after

dasatinib treatment will likely clarify the cause of the decreased in PAFR expressing cells; if PAF or other PAFR ligands are released by stromal cells or by leukemia cells in the presence of stroma after dasatinib treatment, then it is likely that decreased PAFR levels are due to ligand binding and receptor internalization. On the other hand, PAFR expression at the mRNA level is regulated by cytokine exposure, so modulation of the specific cytokines released by stromal cells could also be responsible for the observed changes in PAFR expression after dasatinib treatment (8, 9).

In addition to it role in PAF signaling, Pafah1b can also have PAF-independent effects, some of which are specific to *PAFAH1B3* versus *PAFAH1B2* (5). Both catalytic subunits of Pafah1b localize to Golgi membranes, and knockdown of *PAFAH1B2* and *PAFAH1B3* together results in fragmentation of the Golgi complex and decreased secretion of cargo (4). Knockdown of one catalytic subunit or the other affects distinct aspects of protein trafficking through the Golgi, indicating that PAF-independent effects may be specific to each gene (5). Additionally, a recent study showed that specific knockdown of *PAFAH1B3* but not *PAFAH1B2* had an antitumor effect in a human breast cancer line (32). Metabolic profiling revealed that Pafah1b3 knockdown in these cells results in altered levels of several lipid species, some of which are known to have antitumor effects (32). *Pafah1b3* loss, therefore, may be having a PAF-independent effect on *BCR-ABL1*+ BCP-ALL cells *in vivo* by altering secretory ability or levels of lipid signaling molecules, and this effect may be specific to loss of *Pafah1b3* and not *Pafah1b2*.

PAF signaling and Pafah levels have been shown to play a role in growth and metastasis of Kaposi's sarcoma, colitis associated cancer, breast cancer, ovarian

cancer, lung cancer and prostate cancer (10, 24, 33-37). PAF is particularly well studied in melanoma, in which PAF signaling is thought to promote metastasis and tumor vascularization (10). In acute myeloid leukemia cells and *BCR-ABL1*+ erythroleukemic cells, changes to PAF signaling have been shown to induce apoptosis or terminal differentiation *in vitro* (15, 38). To our knowledge, this is the first identification of *Pafah1b3* or any component of the PAF pathway as a mediator of therapeutic response in *BCR-ABL1*+ BCP-ALL.

Several inhibitors of the Pafah enzymes exist, but most lack specificity and may inhibit other serine hydrolases (12, 39, 40, 41). Recently, a specific Pafah1b2/Pafah1b3 inhibitor was developed and shown to have activity against prostate cancer and neuroblastoma cell lines *in vitro* (41). These inhibitors have not yet been tested *in vivo*, but indicate that specific Pafah inhibition is possible. Our results indicate that combination of a Pafah inhibitor with TKI therapy might be efficacious in *BCR-ABL1*+ BCP-ALL, although we have yet to test the effect of *PAFAH1B3* loss in human leukemic cells. Further identification of the mechanism by which *Pafah1b3* loss alters distribution of leukemic cells after therapy and how this connects to the sensitization effect, the bone marrow niche, and PAF signaling will help clarify whether or not this pathway might be a good target for therapeutic intervention.

**Acknowledgements and Author Contributions**

We'd like to thank Michael Hemann and Yadira Soto-Feliciano for tail vein injections of mice, YSF and Jordan Bartlebaugh for monitoring mice when Eleanor Cameron was out

of town, Luke Gilbert for advice on co-culture experiments, and members of the Hemann lab for advice and technical assistance.

Eleanor Cameron and MH designed the experiments and EC wrote the chapter, which was edited by MH and critically reviewed by Peter Bruno. EC and Emily Lawler performed all experiments.

## References

1. McIntyre, T. M., Prescott, S. M. & Stafforini, D. M. The emerging roles of PAF acetylhydrolase. *J Lipid Res.* **50,** S255–S259 (2008).

2. Prescott, S. M., Zimmerman, G. A., Stafforini, D. M. & McIntyre, T. M. Platelet-activating factor and related lipid mediators. *Annu Rev Biochem.* **69,** 419–445 (2000).

3. Bonin, F. *et al.* Anti-apoptotic actions of the platelet-activating factor acetylhydrolase I α2 catalytic subunit. *J Biol Chem.* **279,** 52425–52436 (2004).

4. Bechler, M. E. *et al.* The phospholipase complex PAFAHIb regulates the functional organization of the Golgi complex. *J Cell Biol.* **190,** 45–53 (2010).

5. Bechler, M. E. & Brown, W. J. PAFAH Ib phospholipase $A_2$ subunits have distinct roles in maintaining Golgi structure and function. *Biochim Biophys Acta.* **1831,** 595–601 (2013).

6. Tjoelker, L. W. & Stafforini, D. M. Platelet-activating factor acetylhydrolases in health and disease. *Biochim Biophys Acta.* **1488,** 102–123 (2000).

7. Arai, H., Koizumi, H., Aoki, J. & Inoue, K. Platelet-activating factor acetylhydrolase (PAF-AH). *J Biochem.* **131,** 635–640 (2002).

8. Denizot, Y., Guglielmi, L., Donnard, M. & Trimoreau, F. Platelet-activating factor and normal or leukaemic haematopoiesis. *Leuk Lymphoma.* **44,** 775–782 (2003).

9. Honda, Z.-I., Ishii, S. & Shimizu, T. Platelet-activating factor receptor. *J Biochem.* **131,** 773–779 (2002).

10. Melnikova, V. & Bar-Eli, M. Inflammation and melanoma growth and metastasis: The role of platelet-activating factor (PAF) and its receptor. *Cancer Metastasis Rev.* **26,** 359–371 (2007).

11. Brown, S. L. *et al.* Activation and regulation of platelet-activating factor receptor: role of $G_i$ and $G_q$ in receptor-mediated chemotactic, cytotoxic, and cross-regulatory signals. *J Immunol.* **177,** 3242–3249 (2006).

12. Chen, J. *et al.* Intracellular PAF catabolism by PAF acetylhydrolase counteracts continual PAF synthesis. *J Lipid Res.* **48,** 2365–2376 (2007).

13. Denizot, Y. *et al.* Detection of functional platelet-activating factor receptors on leukemic B cells of chronic lymphocytic leukemic patients. *Leuk Lymphoma.* **45,** 515–518 (2015).

14. Kuliszkiewicz-Janus, M. *et al.* Platelet-activating factor changes in phospholipid extracts from the plasma, peripheral blood mononuclear cells and bone marrow mononuclear cells of patients with acute leukemia. *Cell Mol Biol Lett.* **13,** 58-66 (2007).

15. Cellai, C. *et al.* Specific PAF antagonist WEB-2086 induces terminal differentiation of murine and human leukemia cells. *FASEB J.* **16,** 733-735. (2002).

16. Shi, J. *et al.* PMS1077 sensitizes TNF-α induced apoptosis in human prostate cancer cells by blocking NF-κB signaling pathway. *PLoS ONE.* **8,** e61132 (2013).

17. Reynaud, S. *et al.* Functional platelet-activating factor receptors in immature forms of leukemic blasts. *Leuk Res.* **31,** 399–402 (2007).

18. Donnard, M. *et al.* Membrane and intracellular platelet-activating factor receptor expression in leukemic blasts of patients with acute myeloid and lymphoid leukemia. *Stem Cells.* **20,** 394–401 (2002).

19. Boulos, N. *et al.* Chemotherapeutic agents circumvent emergence of dasatinib-resistant BCR-ABL kinase mutations in a precise mouse model of Philadelphia chromosome-positive acute lymphoblastic leukemia. *Blood.* **117,** 3585–3595 (2011).

20. Ayala, F., Dewar, R., Kieran, M. & Kalluri, R. Contribution of bone microenvironment to leukemogenesis and leukemia progression. *Leukemia.* **23,** 2233–2241 (2009).

21. Tripodo, C. *et al.* The bone marrow stroma in hematological neoplasms—a guilty bystander. *Nat Rev Clin Oncol.* **8,** 456–466 (2011).

22. Sison, E. A. R. & Brown, P. The bone marrow microenvironment and leukemia: biology and therapeutic targeting. *Expert Rev Hematol.* **4,** 271–283 (2011).

23. Desplat, V. *et al.* Hypoxia modifies proliferation and differentiation of CD34(+) CML cells. *Stem Cells.* **20,** 347–354 (2002).

24. Biancone, L. *et al.* Platelet-activating factor inactivation by local expression of platelet-activating factor acetyl-hydrolase modifies tumor vascularization and growth. *Clin Cancer Res.* **9,** 4214–4220 (2003).

25. Kim, H. A. *et al.* Mechanisms of platelet-activating factor-induced enhancement of VEGF expression. *Cell Physiol Biochem.* **27,** 55–62 (2011).

26. Kim, H. A. *et al.* PTEN/MAPK pathways play a key role in platelet-activating factor-induced experimental pulmonary tumor metastasis. *FEBS Lett.* **586,** 4296–4302 (2012).

27. Konopleva, M., Tabe, Y., Zeng, Z. & Andreeff, M. Therapeutic targeting of microenvironmental interactions in leukemia: Mechanisms and approaches. *Drug Resist Updat.* **12,** 103–113 (2009).

28. Tavor, S. & Petit, I. Can inhibition of the SDF-1/CXCR4 axis eradicate acute leukemia? *Semin Cancer Biol.* **20,** 178–185 (2010).

29. Frolova, O. *et al.* Regulation of HIF-1α signaling and chemoresistance in acute lymphocytic leukemia under hypoxic conditions of the bone marrow microenvironment. *Cancer Biol Ther.* **13,** 858–870 (2012).

30. Wellmann, S. *et al.* Activation of the HIF pathway in childhood ALL, prognostic implications of VEGF. *Leukemia.* **18,** 926–933 (2004).

31. Stachel, D., Albert, M., Meilbeck, R., Paulides, M. & Schmid, I. Expression of angiogenic factors in childhood B-cell precursor acute lymphoblastic leukemia. *Oncol Rep.* **17,** 147–152 (2007).

32. Mulvihill, M. M. *et al.* Metabolic profiling reveals PAFAH1B3 as a critical driver of breast cancer pathogenicity. *Chem Biol.* **21,** 831–840 (2014).

33. Sun, L. *et al.* PAF receptor antagonist Ginkgolide B inhibits tumourigenesis and angiogenesis in colitis-associated cancer. *Int J Clin Exp Pathol.* **8,** 432–440 (2015).

34. Yu, Y. *et al.* Synergistic effects of combined platelet-activating factor receptor and epidermal growth factor receptor targeting in ovarian cancer cells. *J Hematol Oncol.* **7,** 1–11 (2014).

35. Kispert, S. E., Marentette, J. O. & McHowat, J. Enhanced breast cancer cell adherence to the lung endothelium via PAF acetylhydrolase inhibition: a potential mechanism for enhanced metastasis in smokers. *Am J Physiol Cell Physiol.* **307,** C951–C956 (2014).

36. Hackler, P., Reuss, S., Konger, R. & Travers, J. Systemic platelet-activating factor receptor activation augments experimental lung tumor growth and metastasis. *Cancer Growth Metastasis.* **19,** 27–32 (2014).

37. Xu, B. *et al.* Effects of platelet-activating factor and itsdifferential regulation by androgens andsteroid hormones in prostate cancers. *Br J Cancer.* **109,** 1279–1286 (2013).

38. Cellai, C. *et al.* Mechanistic insight into WEB-2170-induced apoptosis in human acute myelogenous leukemia cells: The crucial role of PTEN. *Exp Hematol.* **37,** 1176–1185 (2009).

39. Vlachogianni, I. C. *et al.* Interleukin-1beta stimulates platelet-activating factor production in U-937 cells modulating both its biosynthetic and catabolic enzymes. *Cytokine.* **63,** 97–104 (2013).

40. Quistad, G. *et al.* Platelet-activating factor acetylhydrolase: selective inhibition by potent n-alkyl methylphosphonofluoridates. *Toxicol Appl Pharmacol.* **205,** 149–156 (2005).

41. Chang, J. W. *et al.* Selective inhibitor of platelet-activating factor acetylhydrolases 1b2 and 1b3 that impairs cancer cell survival. *ACS Chem Biol.* **10,** 925–932 (2015).

42. Williams, R. T., Roussel, M. F. & Sherr, C. J. Arf gene loss enhances oncogenicity and limits imatinib response in mouse models of Bcr-Abl-induced acute lymphoblastic leukemia. *Proc Natl Acad Sci U S A.* **103,** 6688–6693 (2006).

43. Dickins, R. A. *et al.* Probing tumor phenotypes using stable and regulated synthetic microRNA precursors. *Nat Genet.* **37**, 1289-1295 (2005).

44. Ran, F. A. *et al.* Genome engineering using the CRISPR-Cas9 system. *Nat Protoc.* **8,** 2281–2308 (2013).

**Materials and Methods**

*Cell culture*

Murine p19$^{Arf-/-}$ *BCR-ABL1*+ BCP-ALL cells (42) and stromal cells isolated from mouse bone marrow or spleen were cultured in RPMI media supplemented with 10% FBS, 4 mM L-glutamine, and 55 μM β-mercaptoethanol. Stromal cells were isolated from non-tumor bearing C57BL/6J mice by culturing bone marrow aspirate or homogenized spleen and removing non-adherent cells every 24 hours for 7-10 days. Stromal cells for co-culture experiments were passaged only once in culture and used within 4 weeks of isolation.

*Vectors*

All shRNAs were expressed in the mir30 context; the vector and shRNA cloning and design are described in the referenced mir30 shRNA study (43). For cDNA expression we excised the puromycin resistance cassette from the pMSCVpuro vector from Clontech, and replaced with either the tdTomato or E2Crimson fluorescent proteins. For Crispr/Cas9 knockout of target genes, we cloned sgRNAs against the gene of interest into the pX458 vector (Addgene plasmid #48138) according to the referenced protocol (44).

*Validation assays*

Hairpin knockdown was assessed via Western blot. Hairpins were validated in GFP competition assays by infecting a pure population of tdTomato or E2Crimson positive leukemia cells at 40 – 50% with single constructs expressing GFP and the shRNA or

cDNA of interest. Spin infections were performed in the presence of 4 ug/mL polybrene, and cells were transplanted into recipient mice 48 - 72 hours after infection. 1 x $10^6$ cells were injected into non-irradiated 6 - 10 week old C57BL6/J female mice, and the GFP percentage at injection was measured using flow cytometry. Pre-treatment blood samples were collected via retro-orbital bleed, and post-treatment blood, bone marrow, and spleen samples were collected immediately after euthanasia of moribund mice; mice were treated with 20 mg/kg dasatinib q.d. via oral gavage for three days. GFP percentage was assessed at pre- and post-treatment by flow cytometric analysis. cDNA competition assays were performed similarly on tdTomato positive clonal populations with Pafah1b3 wild type or Pafah1b3 knockout backgrounds. All flow data was collected on LSR analyzers and was analyzed using FACSDiva software (BD Biosciences). Lifespan analysis and analysis of associated imaging data were performed blinded to genotype of transplanted leukemic cells.

*Western blotting*

*BCR-ABL1*+ BCP-ALL cells were infected with individual shRNAs or cDNA constructs co-expressing a fluorescent marker to a final infection percentage of 40 – 60% and sorted based on marker expression; protein-containing cell lysates were then isolated from the sorted population. In some cases, a selective puromycin cassette in the shRNA expression construct was used to generate pure populations of hairpin-expressing cells rather than cell sorting. The following antibodies were used for protein detection: Pafah1b3 (1:100 or 1:250 in TBS-T with 5% milk; Santa Cruz Biotechnology, SC81950), Hsp90 (1:5000 in TBS-T with 5% milk; BD Transduction Laboratories 610418).

*Preclinical therapeutics*

Dasatinib (LC Laboratories) was dissolved in DMSO and diluted into cell culture media for *in vitro* studies. For *in vivo* use, dasatinib was dissolved in 80 mM citric acid at pH 2.3 and administered via oral gavage at 0.01 mL/g at 20 mg/kg for 3 days.

*Bioluminescent imaging*

Luminescent imaging was performed using albino B6 mice (Jackson Laboratory Strain B6(Cg)-*Tyr*$^{c\text{-}2J}$/J) on a Xenogen IVIS system and analyzed using Living Image version 4.4 software (Caliper Life Sciences). Mice were injected i.p. with 4.5 mg D-Luciferin and anesthetized with 2.5% isofluorane delivered at 1 L/min in $O_2$. Animals were imaged at least 10 minutes after injection to allow for substrate distribution at multiple exposures lasting 5 – 60 seconds with small binning. Total flux measurements (photons/sec) for multiple exposures were averaged for quantification of signal from entire animal. Images were normalized to the same color scale for figure generation.

## Supplementary Figures

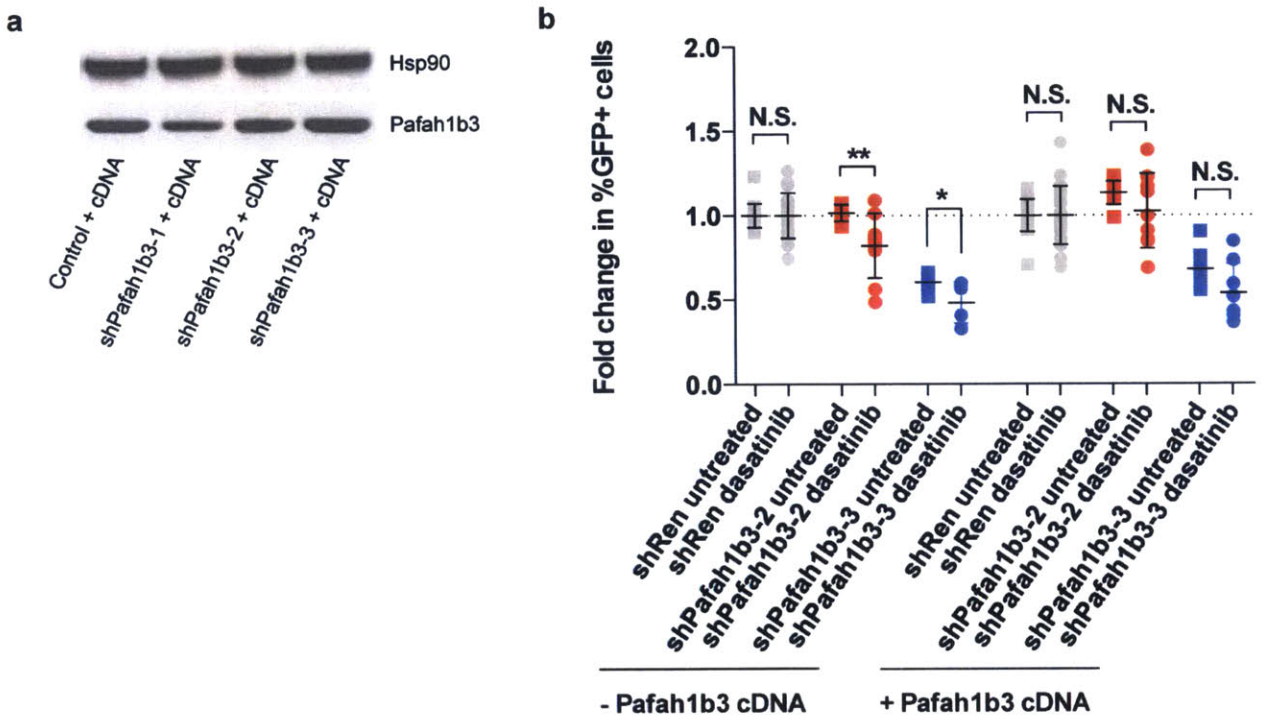


**Supplementary Figure S1. Expression of a Pafah1b3 cDNA can rescue effect of non-targeting shRNAs *in vivo*.** (a) Western blots showing rescue of Pafah1b3 knockdown by expressing a non-targetable Pafah1b3 cDNA in *BCR-ABL1*+ BCP-ALL cells. shPafah1b3-1 targets the coding region of the gene and thus the cDNA, whereas shPafah1b3-2 and shPafah1b3-3 target the 3'UTR of Pafah1b3 and thus cannot knockdown the Pafah1b3 cDNA. (b) Scatterplot showing fold change in percent of shPafah1b3-expressing cells in untreated versus dasatinib treated mice in the presence or absence of Pafah1b3 cDNA. The Pafah1b3 cDNA rescues the effect of both non-targeting shRNAs, indicating that their depletion after dasatinib therapy is in fact due to loss of expression of the Pafah1b3 gene. Values are an average of at least 7 mice from at least two independent experiments. Error bars represent standard deviation; p-values were calculated using Student's t-test.

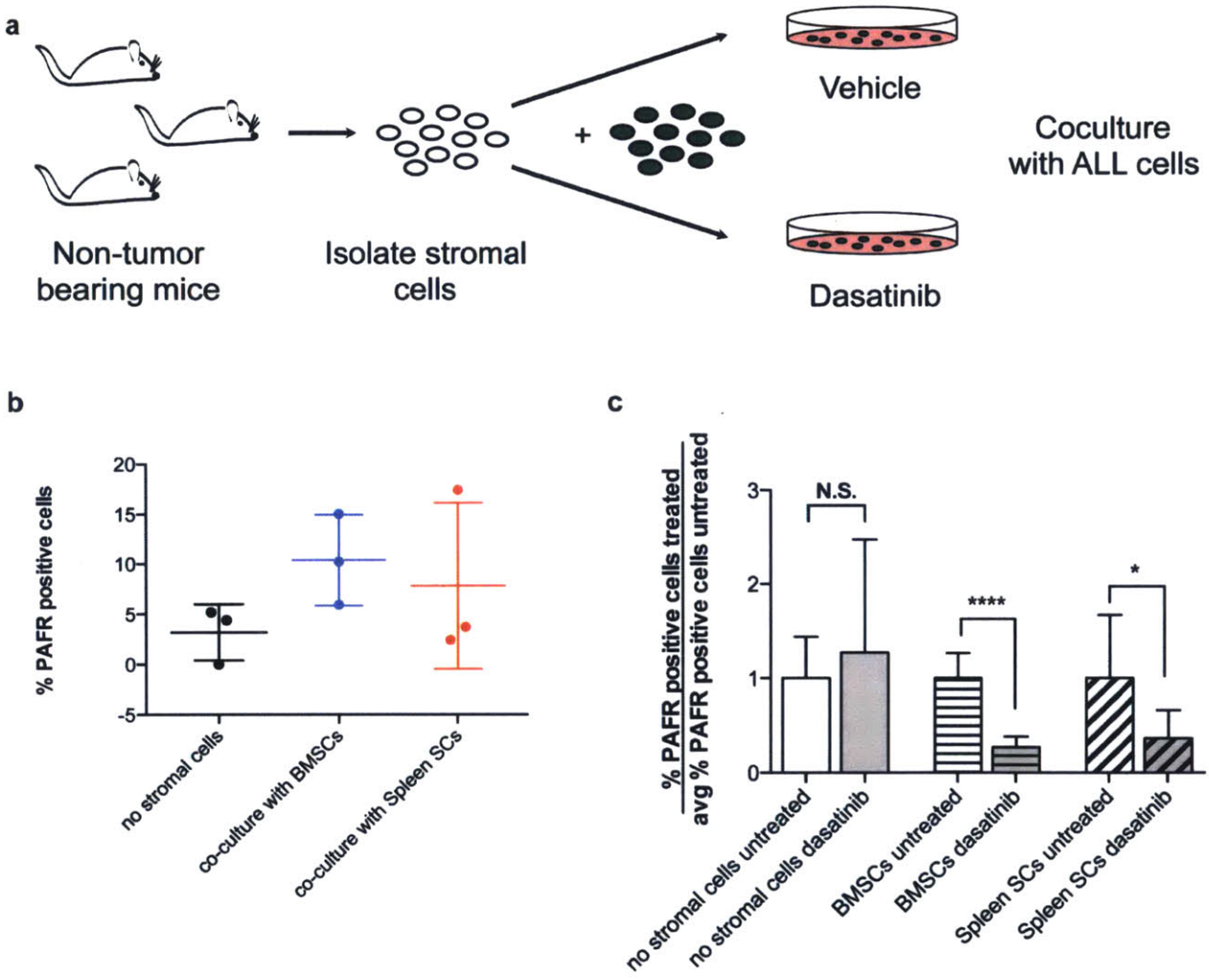


**Supplementary Figure S2. Murine p19$^{Arf-/-}$ *BCR-ABL1*+ BCP-ALL cells express platelet activating factor receptor (PAFR) on the cell surface.** (a) Schematic for co-culture experiments: Adherent cells were isolated from the bone marrow or spleen of non-tumor bearing mice, passaged once, and then co-cultured with leukemic cells in the presence or absence of dasatinib. (b) Scatterplots showing percentage of leukemia cells expressing PAFR on the cell surface when cultured alone or with bone marrow- of spleen-derived stroma cells. There is a nonsignificant increase in membrane expression of PAFR when leukemia cells are co-cultured with stroma. (c) Bar graphs showing percentage of leukemia cells expressing membrane PAFR when cultured in dasatinib normalized to the percentage of untreated cells expressing membrane PAFR. When leukemia cells are co-cultured with bone marrow- or spleen-derived stromal cells, treatment with dasatinib results in a significant decrease of the percentage of cells expressing membrane PAFR. Error bars represent standard deviation; p-values were calculated using Student's t-test.

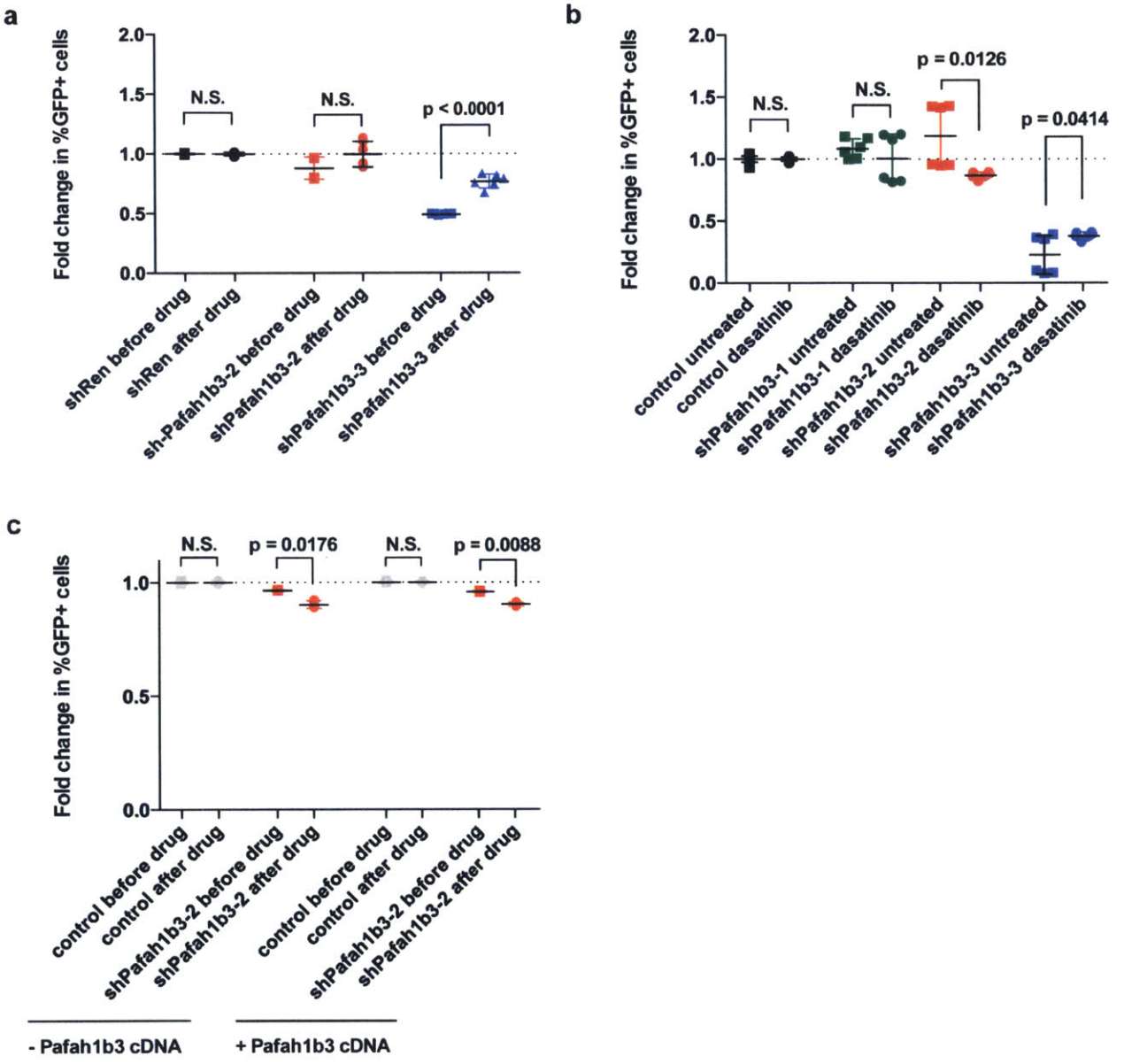


**Supplementary Figure S3. Pafah1b3 loss sensitizes cells to dasatinib *in vivo* but not *in vitro*.** (a) Scatterplot showing fold change in percent shRNA-expressing cells before versus after dasatinib therapy *in vitro* of additional Pafah1b3 hairpins that cannot target the Pafah1b3 cDNA. An shRNA targeting Renilla luciferase, which is not expressed by these cells, is used as a control. (b) Scatterplot showing fold change in percent shRNA-expressing cells of all three Pafah1b3 shRNAs in both untreated and dasatinib-treated cultures. shPafah1b3-1 targets the coding region of the gene and thus the cDNA, whereas shPafah1b3-2 and shPafah1b3-3 target the 3'UTR of Pafah1b3 and cannot knockdown the Pafah1b3 cDNA. (c) Scatterplot showing fold change in shPafah1b3-expressing cells before and after dasatinib treatment *in vitro* in the presence or absence of Pafah1b3 cDNA. The Pafah1b3 cDNA rescues the effect of shPafah1b3-2, indicating that its depletion in dasatinib treated cultures is not due to loss

of the Pafah1b3 gene but rather is the result an off-target effect of the hairpin. Percentages are an average of at least three replicates. Error bars represent standard error of the mean; p-values were calculated using Student's t-test.

**a**

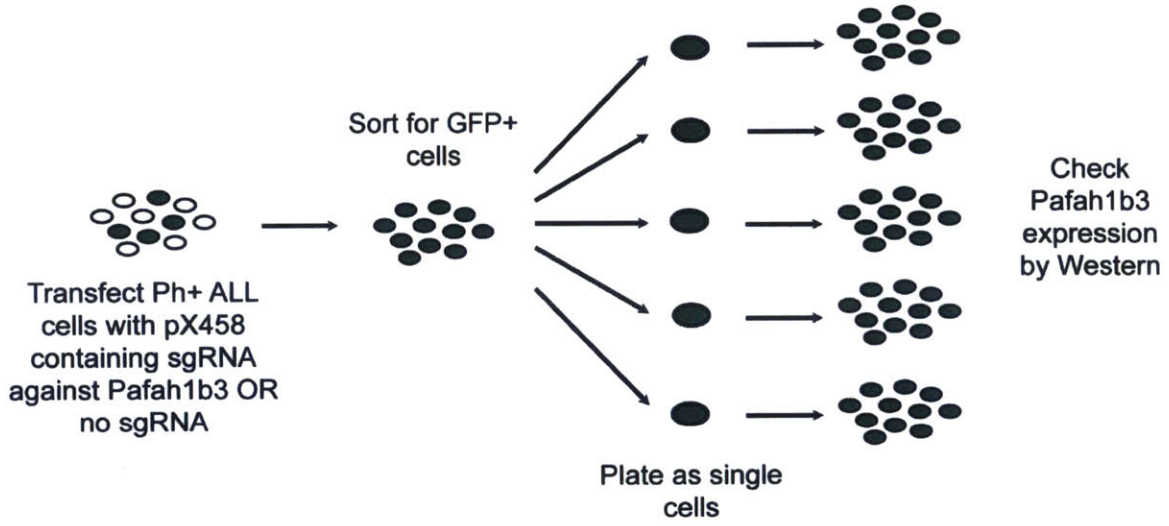


**b**

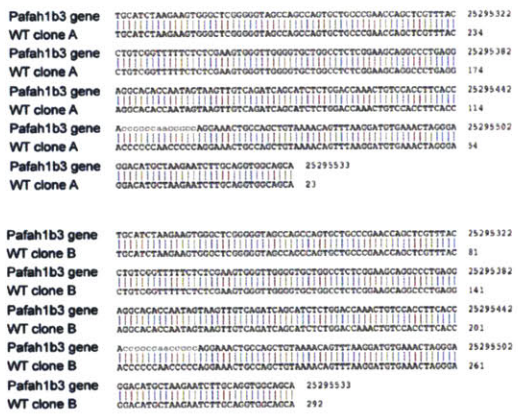


**c**

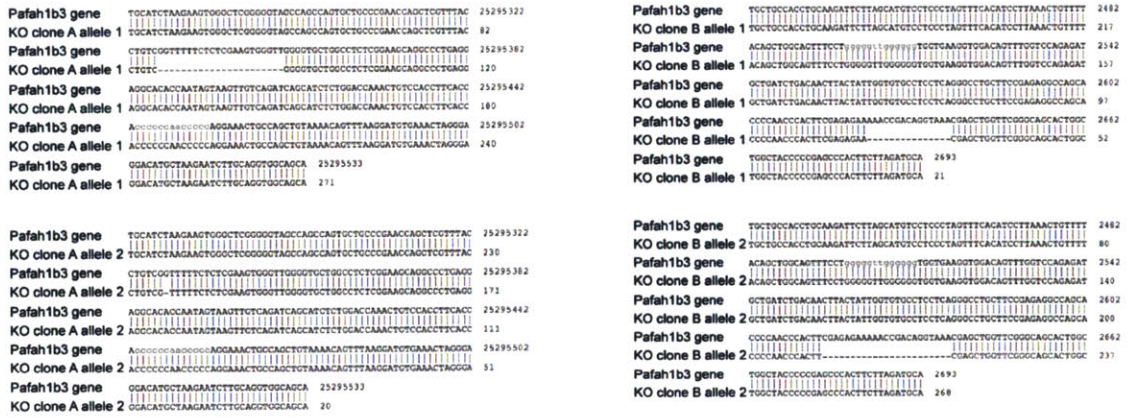

**Supplementary Figure S4. Crispr/Cas9 mediated knockout of *Pafah1b3*.** (a) Schematic of generation of clonal populations of *BCR-ABL1*+ BCP-ALL cells with wild-type Pafah1b3 or Pafah1b3 knockout. Leukemia cells are transfected with either empty pX458 vector or pX458 containing an sgRNA targeting the Pafah1b3 gene, and 24 hours later cells are sorted for the presence of the pX458 construct by using GFP as a marker. pX458 containing cells are then plated out to single cell clones, and once clones have grown out Westerns are performed to check for the presence of the Pafah1b3, and Sanger sequencing of the targeting region is performed on (b) wild-type (pX458) and (c) knockout (pX458 + sgPafah1b3) clones.

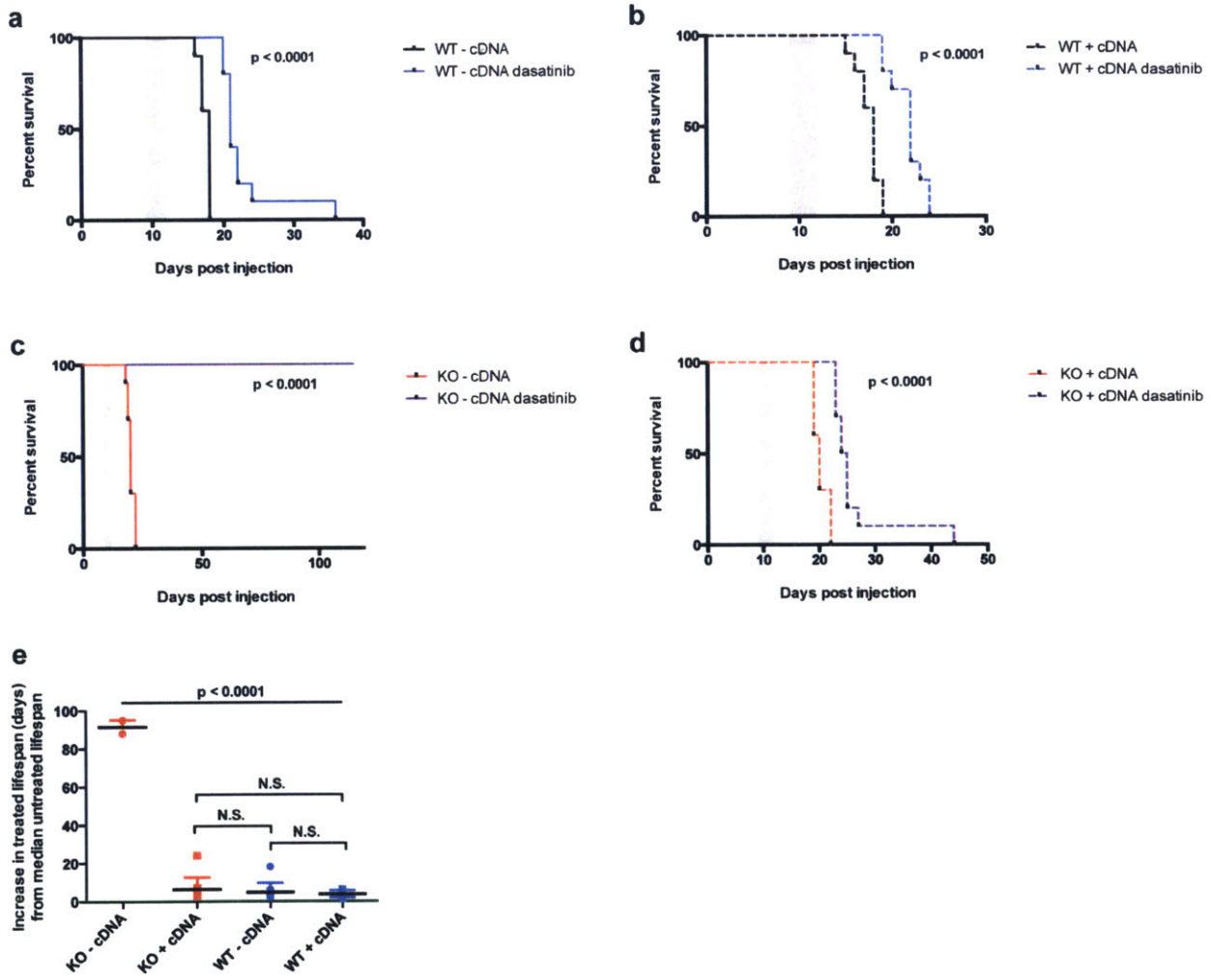


**Supplementary Figure S5. Treatment of mice transplanted with $10^4$ *BCR-ABL1*+ BCP-ALL cells with 3 days of 20 mg/kg dasatinib significantly extends lifespan regardless of genotype.** Survival curves of mice transplanted with (a) Pafah1b3 wild-type cells transduced with a control empty vector, (b) Pafah1b3 wild-type cells transduced with a Pafah1b3 cDNA, (c) Pafah1b3 KO cells transduced with a control empty vector, and (d) Pafah1b3 KO cells transduced with a Pafah13 cDNA and then treated with 20 mg/kg dasatinib or vehicle for 3 days q.d. The grey rectangle indicates the time period in which mice were treated with dasatinib. In all cases, dasatinib

treatment significantly extended the lifespan of recipient mice; p-values were calculated using the Mantel-Cox test. (d) Scatterplot showing the increase in lifespan in dasatinib-treated versus vehicle-treated mice that received transplants of different genotypes; the increase in lifespan was significantly greater for mice receiving transplants of Pafah1b3 KO cells transduced with a control empty vector than for mice transplanted with cells of any other genotype. Values are an average of at least 9 mice per genotype. Error bars represent standard deviation; p-values were calculated using Student's t-test.

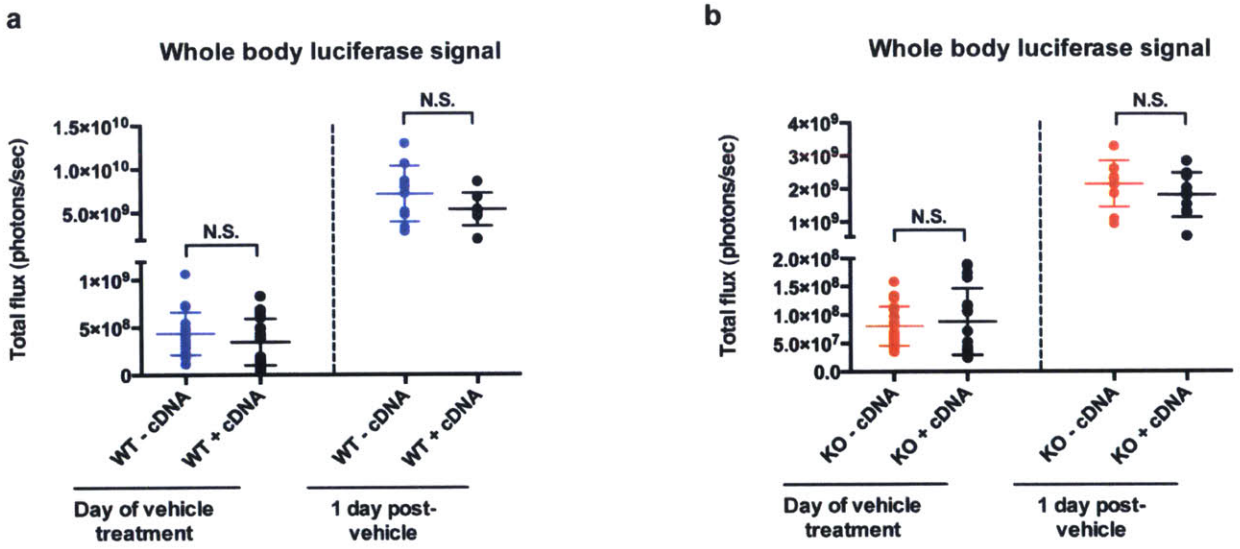


**Supplementary Figure S6. Pafah1b3 levels do not affect leukemic burden of vehicle-treated mice.** Scatterplots showing leukemic burden before and after vehicle treatment as measured by *in vivo* luminescent whole-body imaging of mice that received transplants of (a) Pafah1b3 wild-type cells with or without a Pafah1b3 cDNA and (b) Pafah1b3 KO cells with or without a Pafah1b3 cDNA. Values are an average of at least 8 mice per genotype. Error bars represent standard deviation; p-values were calculated using Student's t-test.

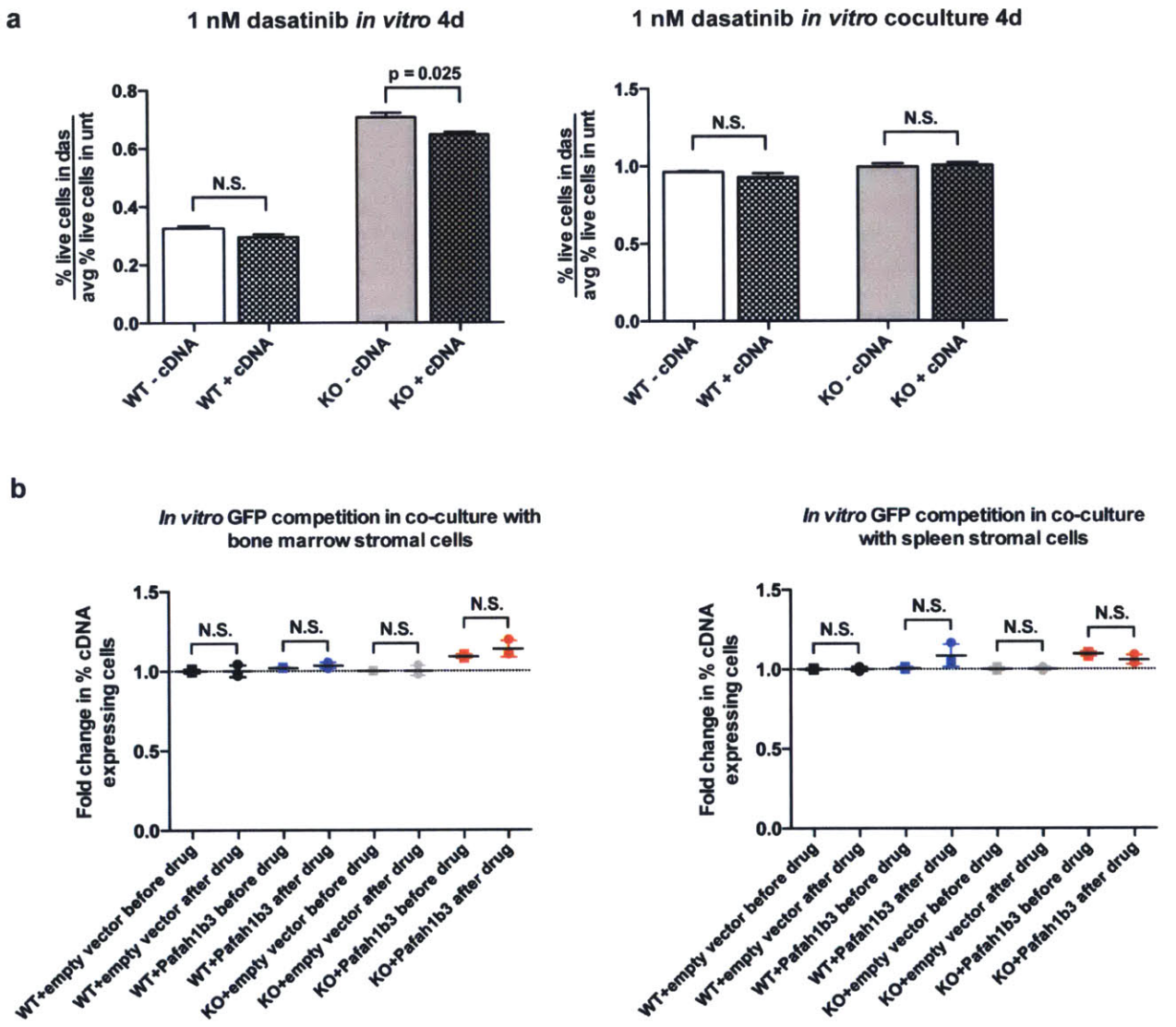


**Supplementary Figure S7. Co-culture of leukemic cells with stroma does not recapitulate *in vivo* phenotype.** (a) Bar graphs showing percentage of live cells in 1 nM dasatinib-treated cultures normalized to percentage of live cells in untreated cultures after 4 days of treatment of cells alone (left) and with bone marrow-derived stromal cells (right). Pafah1b3 loss does not result in increased cell death after dasatinib regardless of the presence of stroma. Error bars for bar graphs indicate standard error of the mean. (b) Scatterplots showing fold change in %GFP+ and thus cDNA-expressing cells on Pafah1b3 wild type or KO backgrounds co-cultured with stromal cells derived from bone marrow (left) and spleen (right); expression of a Pafah1b3 cDNA is neutral before and after dasatinib treatment in the presence of stroma. Fold changes are normalized to an empty cDNA expression vector. Percentages are an average of three replicates. Error bars for scatterplots indicate standard deviation; p-values were calculated using Student's t-test.

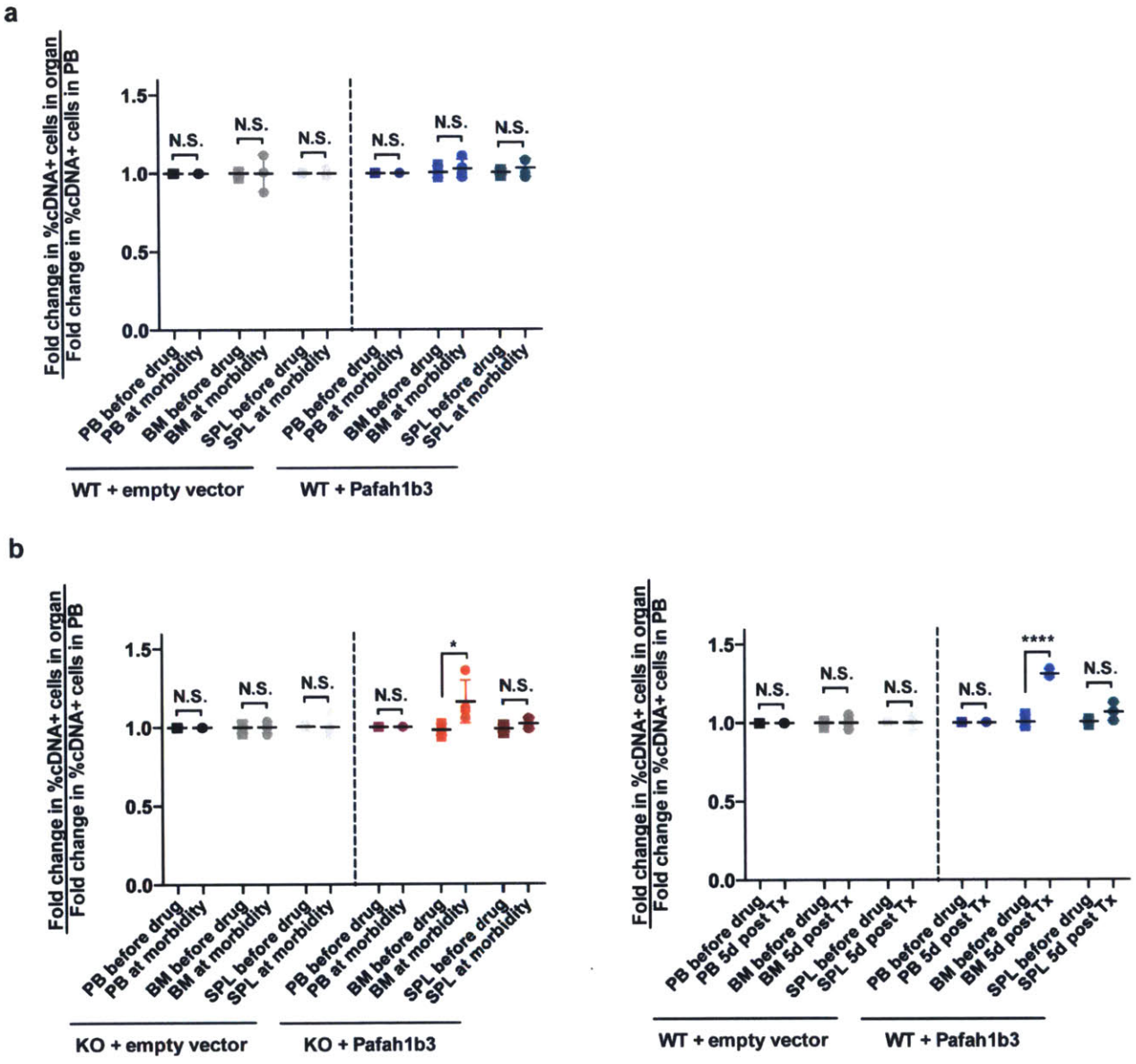


**Supplementary Figure S8. Pafah1b3 over-expressing cells are relatively enriched in the bone marrow after dasatinib treatment.**
(a) Scatterplots show relative enrichment of cDNA-expressing cells on a Pafah1b3 WT background from transplant to the start of treatment versus enrichment from transplant to morbidity. cDNA-expressing cells are not enriched in the bone marrow versus the blood of mice transplanted with Pafah1b3 WT cells at morbidity or before treatment. (b) Scatterplots show relative enrichment of cDNA-expressing cells on a Pafah1b3 KO (left) and WT (right) background from transplant to the start of treatment versus enrichment from transplant to 5 days after start of therapy. Relative enrichment is defined as the fold change of percent cDNA+ cells in each organ normalized to the fold change of percent cDNA+ cells in the blood of the same mouse. cDNA-expressing cells are significantly enriched in the bone marrow versus the blood of mice transplanted with Pafah1b3 KO or WT cells at five days after the start of therapy but not before treatment.

For all experiments, values are an average of at least 3 mice per genotype. Error bars represent standard deviation; p-values were calculated using Student's t-test.

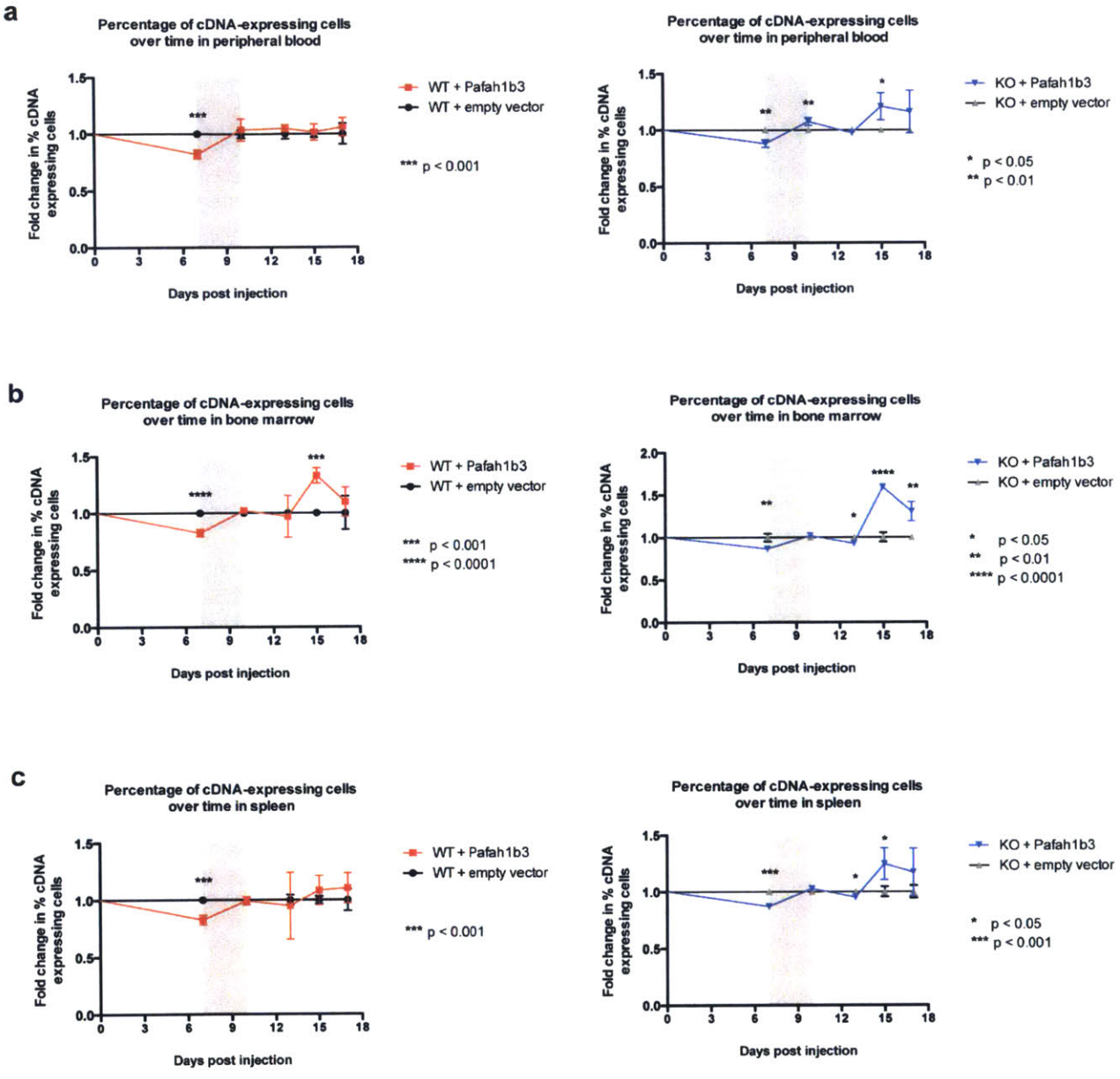


**Supplementary Figure S9. Cells over-expressing Pafah1b3 enrich significantly more in bone marrow at 5 days post cessation of dasatinib therapy than at morbidity.** Plots show the fold change in percent Pafah1b3 cDNA-expressing cells over time in the (a) peripheral blood, (b) bone marrow, and (c) spleen of mice receiving transplants of either Pafah1b3 wild-type or Pafah1b3 KO cells partially transduced with a Pafah1b3 cDNA. In the bone marrow, the most significant enrichment of cDNA-expressing cells on both WT and KO backgrounds is at Day 15, which is 5 days after cessation of therapy, not at morbidity. This is also true for both blood and spleen enrichment of cDNA-expressing cells specifically on a KO background. An empty MSCV

vector is used as a control, and the fold change of cDNA-expressing cells is normalized to control. Each time point is an average of 3 - 4 mice that were sacrificed at that time point; this is not longitudinal data. The grey rectangle indicates the time period in which mice were treated with dasatinib. Error bars represent standard deviation.

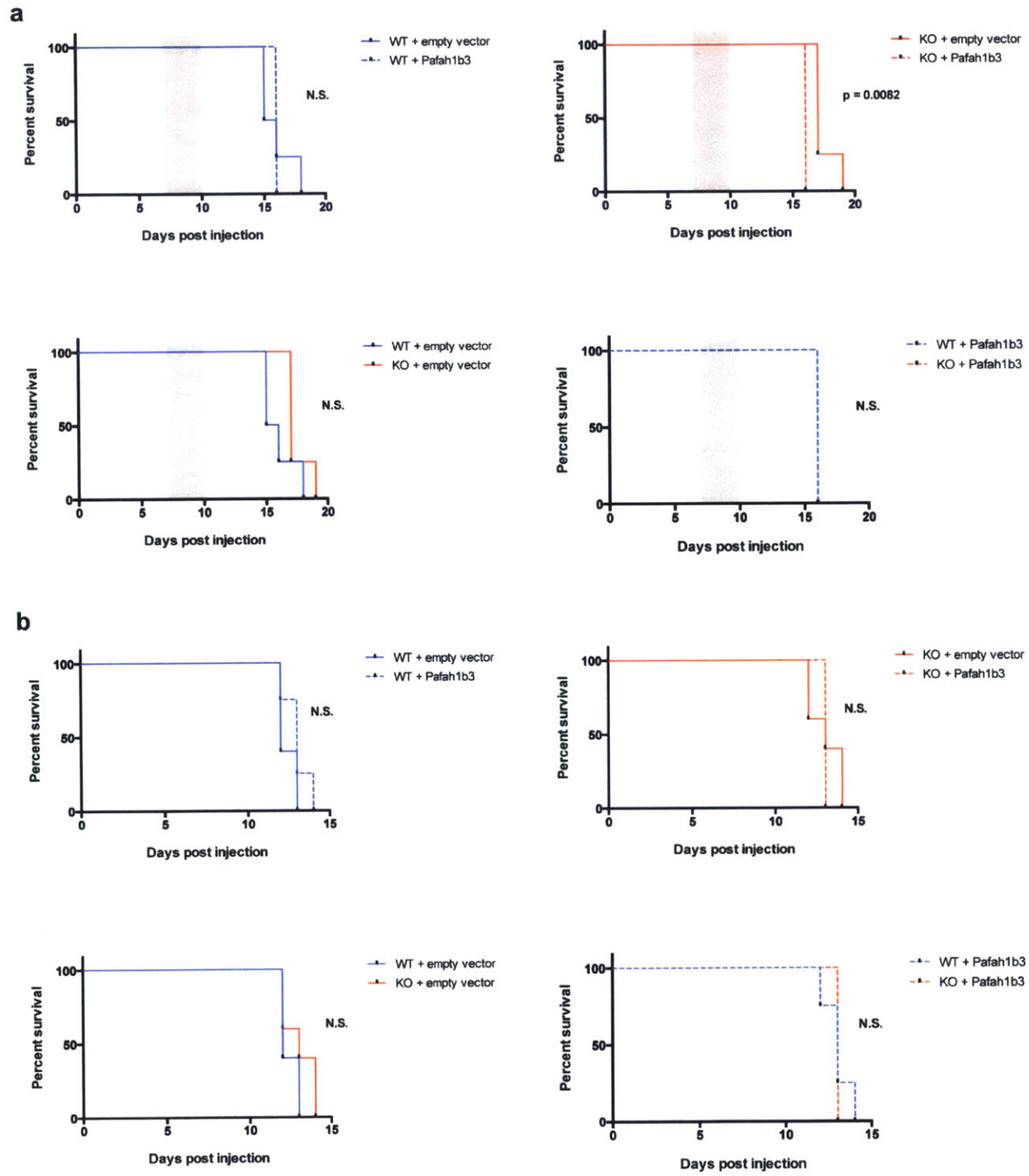

**Supplementary Figure S10. Pafah1b3 loss increases survival of mice transplanted with $10^6$ *BCR-ABL1*+ BCP-ALL cells only after dasatinib treatment.** Pairwise comparisons of survival curves of mice transplanted with $10^6$ Pafah1b3 wild-type or Pafah1b3 KO leukemia cells partially transduced with either a control empty vector (- cDNA) or a Pafah1b3 cDNA (+ cDNA) and then either (a) treated with 20 mg/kg dasatinib for 3 days q.d. or (b) left untreated. The grey rectangle indicates the time period in which mice were treated with dasatinib. After injection of this many cells, there is no significant difference in survival between clones in either untreated or treated mice, although treated Pafah1b3 KO - cDNA mice do generally live longer than treated Pafah1b3 WT - cDNA mice. There is a significant lifespan extension of dasatinib-treated mice receiving Pafah1b3 KO - cDNA transplants as compared to those receiving Pafah1b3 KO + cDNA transplants, even though only about half of the cells given to the Pafah1b3 KO + cDNA mice express the Pafah1b3 cDNA. Four mice were retained until morbidity for each genotype and treatment condition; p-values were calculated using the Mantel-Cox test.

**Chapter IV: Knockdown of *Abi3* promotes resistance to dasatinib in *BCR-ABL1+* BCP-ALL, but expression of the Abi3 protein may be required for leukemia cell survival.**

---

Eleanor R. Cameron, Michael T. Hemann

David H. Koch Institute for Integrative Cancer Research, Massachusetts Institute of Technology. Cambridge, Massachusetts, 02139, United States.

This chapter is not published as of December 2015.

## Introduction

An shRNA targeting the *Abi3* gene was identified in our RNAi screens as promoting resistance to dasatinib therapy both *in vivo* and *in vitro*. Abi3 is one of the Abelson-interacting (Abi) proteins that were originally identified as substrates of the Abelson kinase (c-Abl), which is constitutively activated in *BCR-ABL1*+ precursor B-cell acute lymphoblastic leukemia (BCP-ALL) (1). There is only one Abi protein in flies and worms, but mammals express three Abi family members: Abi1, Abi2, and Abi3, also known as NESH (NEw molecule including SH3) (1, 2). In both flies and worms, the Abi protein interacts physically with the Abl kinase, and these proteins appear to have antagonistic functions in the regulation of cytoskeletal remodeling to promote membrane protrusions and cellular migration (1, 2).

In mammalian cells, the Abi proteins participate in the formation of the WAVE regulatory complex, which promotes Arp2/3 dependent nucleation of F-actin filaments and thus regulates membrane protrusions and cell motility (3, 4). The proteins encoded by *ABI1* and *ABI2* promote the formation of a WAVE complex that also includes the Abl kinase. In this case, Abl phosphorylation of the WAVE complex seems to be required for its activation, and the Abi proteins function as a physical link between Abl and the WAVE complex (5, 6). In contrast, Abi3/NESH associates with a WAVE complex that lacks the Abl kinase, and while Abi1 and Abi2 have been shown to physically interact with Abl in cells, Abi3 does not (4, 6, 7).

Abi proteins also seem to play a role in cellular transformation and cytoskeletal regulation via the Abl kinase; Abi1 and Abi2, though phosphorylated by Abl, can suppress its transforming activity without affecting its kinase activity (7-9). In murine

proB cells transformed with Bcr-Abl, Abi1 was found to be required for Bcr-Abl dependent cytoskeletal remodeling, integrin clustering, and cell adhesion and migration (8, 9). Knockdown of Abi1 or interference with its physical interaction with and/or phosphorylation by Bcr-Abl resulted in a decreased ability of *BCR-ABL1*+ pro-B cells to adhere to or migrate along fibronectin-coated surfaces and decreased the expansion of these cells in an immunocompromised recipient mouse despite having no effect on the cellular growth rate *in vitro* (8, 9). Interestingly, in a mouse model of chronic myelogenous leukemia imatinib-resistant cells that lacked Bcr-Abl mutations were found to have decreased Abi1 with increased expression of α4 integrin and thus increased cell adhesion (10). In this case, forced expression of Abi1 resulted in reduced ability of CML cells to localize to the bone marrow after transplantation into immunocompromised mice, indicating that the effect of altering Abi protein levels is context-dependent and may have different repercussions in myeloid versus lymphoid leukemia (10).

The Abi3/NESH protein is somewhat less well studied than Abi1 and Abi2; it is prominently expressed in the brain and has been shown to play a role in synapse formation and dendritic spine morphogenesis in neurons via its ability to bind F-actin (11, 12). Like Abi1 and Abi2, Abi3 participates in the formation of a WAVE complex, and forced expression of Abi3 in transformed fibroblasts reduces cell motility but not *in vitro* cellular growth, which is similar to the effects of Abi1 loss in transformed proB cells (13). Transformed fibroblasts that ectopically express Abi3 tend to lose Abi3 expression in metastases after transplantation into mice, although the primary tumors continue to express Abi3 (13). However, forced Abi3 expression in carcinomas, which frequently lose Abi3 expression, results in reduced tumor growth *in vitro* and *in vivo* as well as an

increase in cellular senescence. As with other Abi proteins, the effect of alterations of Abi3 levels seems to be dependent on cellular context (14).

Imatinib treatment of Abi3-expressing cells can alter their motility. In mouse tail vein metastasis assays, pre-treatment of Abi3-expressing transformed fibroblasts with imatinib resulted in increased formation of lung nodules without altering Abi3 expression levels (7). In lymphoid cell lines that express low levels of Abi3, imatinib treatment reduces invasive ability in culture, but the opposite effect occurs after imatinib treatment of lymphoid cell lines expressing high levels of Abi3 (7). Knockdown of *ABI3* in lymphoid cells that normally express high Abi3 levels reverts their imatinib response to one of decreased invasive ability (7). Interestingly, cells that express Abi3 often lack PDGF-mediated membrane ruffling, an effect that is thought to be due to Abi3's ability to sequester IRSp53 away from the WAVE complex and thus prevent it from promoting Rac-dependent actin filament assembly and membrane ruffling (15). As imatinib inhibits PDGFR as well as Abl, it is possible that the effect of imatinib on migration of Abi3-expressing cells may be due to modulation of the PDGF response rather than changes in Abl activity, again confirming that Abi3 may affect cell adhesion and motility in an Abl-independent manner (16).

A hairpin targeting *ABI3* was predicted by independent component analysis to enrich after dasatinib treatment, and in our initial validation study we found that this hairpin significantly depleted before treatment *in vivo* and enriched after. Interestingly, this same hairpin was identified in a previous screen in our lab as being deleterious for leukemia progression, and the *ABI3* gene is in a chromosomal region that is sometimes gained in *BCR-ABL1* negative BCP-ALL patients (17, 18). Our screen was designed to

identify *in vivo* specific modulators of Bcr-Abl independent resistance to dasatinib, and as the Abi3 protein is a mediator of cytoskeletal dynamics and cell motility as well as the only member of its family to not interact with the Abl kinase, we decided to further investigate the effect of *Abi3* modulation in *BCR-ABL1*+ BCP-ALL cells. Here we show that Abi3 knockdown does confer resistance to dasatinib *in vivo*, and that its *in vitro* resistance-promoting effect is generally smaller and less consistent, arguing that *Abi3* may have *in vivo* specific roles. We also show that neither lower proliferation rate nor increased survival after dasatinib treatment *in vitro* or in co-culture with stromal cells are responsible for the resistance conferred by Abi3 knockdown. Somewhat surprisingly, we also found that we were unable to knock out *Abi3* in *BCR-ABL1*+ BCP-ALL cells, indicating that *Abi3* may be an essential gene in this mouse model.

**Results**

In our initial screen, a hairpin targeting *Abi3* was found to enrich after dasatinib both *in vivo* and *in vitro*, and we confirmed this effect through several independent GFP competition experiments using the original shRNA (Figure 1A). We then attempted to clone additional hairpins that knockdown *Abi3* and found that it is difficult to generate shRNAs that reliably knockdown Abi3 protein levels. Of the eight hairpins that we cloned, only four deplete Abi3 protein levels at all, and the original shRNA from the screen was the only hairpin to reduce Abi3 levels to less than half those in the parental cell line (Figure 1B).

We tested the four additional shRNAs that do knock down Abi3, and found that in longitudinal GFP competition assays all of the hairpins enrich after dasatinib treatment

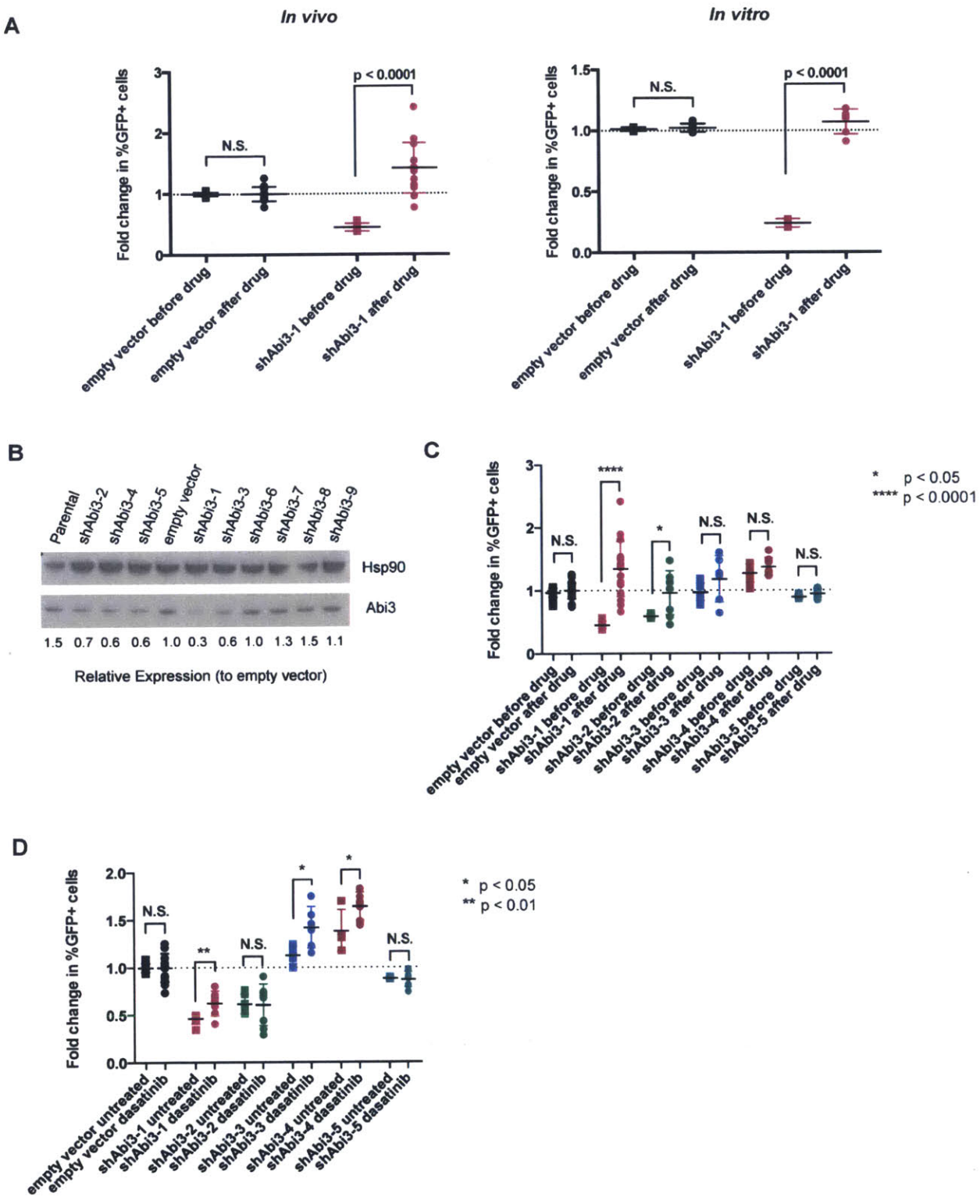


**Figure 1. Partial knockdown of Abi3 can cause enrichment of *BCR-ABL1*+ BCP-ALL cells after dasatinib *in vivo*.**

(A) Scatterplots show that the initial hairpin against *Abi3* from the 20K library screen depletes before dasatinib and then enriches significantly after dasatinib *in vivo* and *in*

*vitro*. Fold changes are normalized to a control empty vector or control hairpin targeting Renilla luciferase, which these cells do not express. Values are derived from thirteen mice from multiple independent experiments and six independent cultures. (B) Western blot showing attempted Abi3 knockdown by shRNAs; shAbi3-1 is the initial shRNA identified in the 20K screen; shAbi3-2, shAbi3-3, shAbi3-4, shAbi3-5 are the only other hairpins that decrease Abi3 protein levels relative to empty vector. Expression is relative to the empty vector and normalized to Hsp90 loading control. (C) Scatterplots show fold change in percent shRNA-expressing cells *in vivo* before versus after dasatinib treatment; some but not all hairpins enrich after dasatinib. Fold changes are normalized to a control empty vector or a hairpin targeting Renilla luciferase. Values are an average of at least six mice from multiple independent experiments. (D) Scatterplots show fold change in percent shRNA-expressing cells at morbidity in untreated versus dasatinib-treated micel some but not all hairpins enrich in dasatinib-treated mice. Fold changes are normalized to a control empty vector or a hairpin targeting Renilla luciferase. Values are an average of at least three mice from multiple independent experiments. Error bars indicate standard deviation; p-values were calculated using Student's t-test.

*in vivo* and *in vitro*, although only shAbi3-2 enriches significantly *in vivo* (Figure 1C, Supplementary Figure S1). Non-significant enrichment of these hairpins is likely due to their poor knockdown of the *Abi3* gene. In a more stringent assay comparing untreated to dasatinib-treated mice, three shRNAs, including the original screening hairpin shAbi3-1, were significantly enriched in dasatinib-treated mice at morbidity as compared to untreated mice (Figure 1D). Interestingly, fewer hairpins were significantly enriched in dasatinib-treated cultures as compared to untreated cultures; one shRNA was even depleted in dasatinib-treated cultures, indicating that *Abi3* loss may have less of an effect *in vitro* as compared to *in vivo* (Supplementary Figure S1).

In order to confirm that enrichment in dasatinib-treated mice is in fact due to *Abi3* loss, we cloned an Abi3 cDNA and expressed it in our *BCR-ABL1*+ BCP-ALL cells. Interestingly, despite proper cloning and good infection rates, expression of an Abi3 cDNA barely increased the level of Abi3 protein in leukemic cells. However, it was capable of rescuing knockdown mediated by shAbi3-3, a hairpin that targets the 3'UTR

of the endogenous *Abi3* (Figure 2A). Expression of the Abi3 cDNA increased but did not fully rescue protein levels in the presence of shAbi3-1, which targets the coding sequence of *Abi3* and therefore can knockdown both endogenous and cDNA-derived Abi3 mRNA transcripts (Figure 2A). Due to the relatively minor change in Abi3 protein levels after cDNA expression, we performed GFP competition experiments using both the rescued hairpin shAbi3-3 and the unrescued protein shAbi3-1 as a control in the presence and absence of the Abi3 cDNA (Figure 2B). As expected, expression of the Abi3 cDNA was able to rescue the enrichment of shAbi3-3 expressing cells in dasatinib-treated versus untreated mice, but was not able to rescue the effect of shAbi3-1, indicating that resistance to dasatinib *in vivo* can in fact be mediated by loss of *Abi3* (Figure 2B).

In parallel *in vitro* GFP competition experiments, hairpins against *Abi3* did not enrich in dasatinib-treated cultures as compared to untreated cultures, regardless of the presence or absence of the Abi3 cDNA (Supplementary Figure S1). To try to recapitulate the *in vivo* effect, we performed repeat rescue experiments *in vitro* both with and without bone-marrow derived stromal cells in co-culture with leukemic cells. However, Abi3 knockdown cells did not enrich after dasatinib treatment *in vitro* regardless of the presence of stromal cells or the expression of an Abi3 cDNA (Figure 2C). Combined with our earlier observation that relatively few Abi3 knockdown cells enrich in dasatinib-treated cultures, this data suggests that the resistance conferred by *Abi3* loss is significantly stronger *in vivo*, and that this effect cannot be mimicked *in vitro* simply by utilizing co-culture systems.

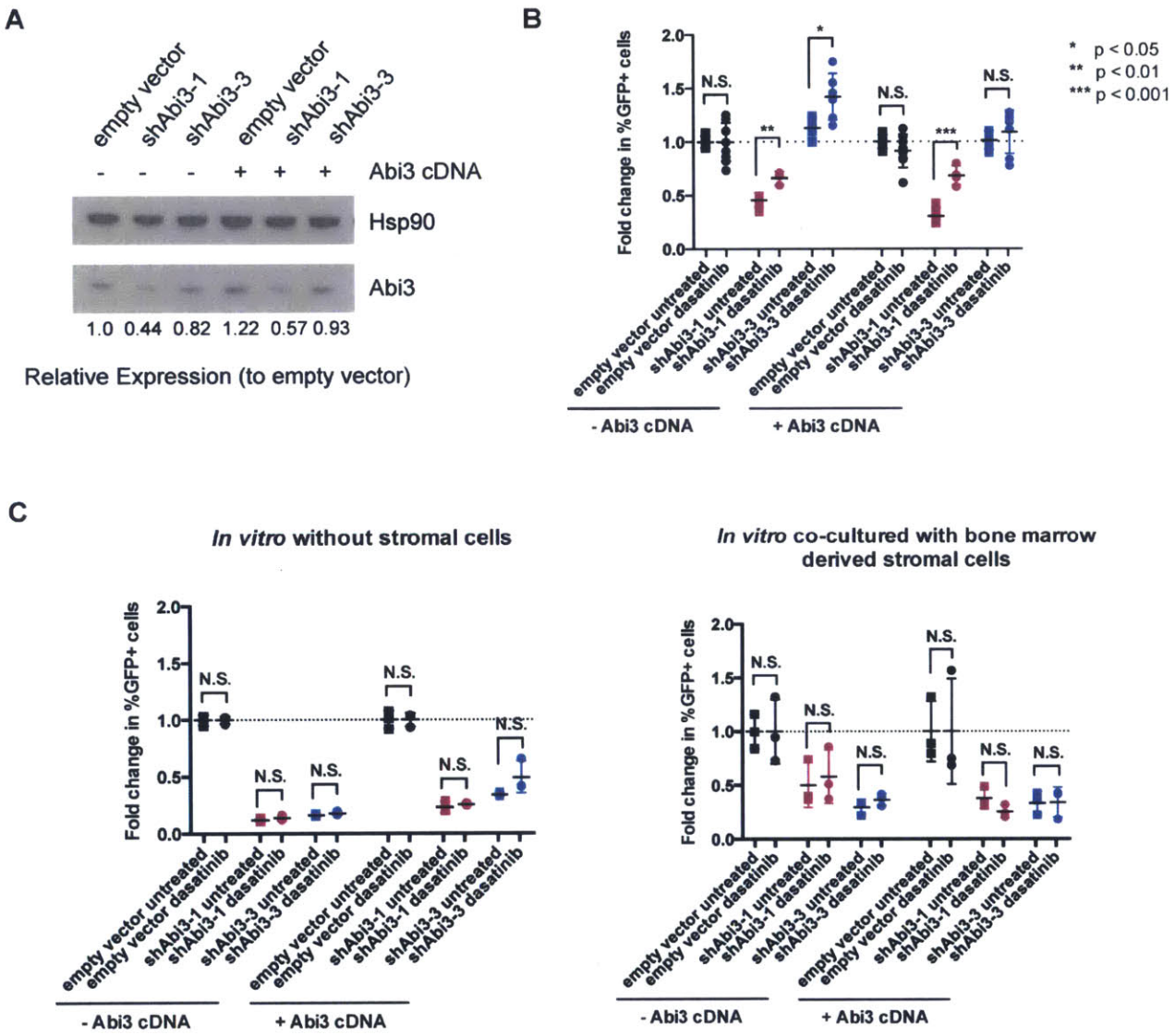


**Figure 2. *In vivo* but not *in vitro* resistance to dasatinib conferred by shAbi3 vectors is due to lower levels of the *Abi3* gene product.**
(A) Western blot showing Abi3 levels of cells expressing a hairpin targeting Renilla luciferase, which these cells do not express (empty vector), a hairpin targeting the coding sequence and thus the endogenous Abi3 mRNA and the Abi3 cDNA (shAbi3-1), and a hairpin targeting the 3'UTR of the *ABI3* gene and thus only the endogenous Abi3 mRNA (shAbi3-3) in the presence or absence of an Abi3 cDNA. Presence of an Abi3 cDNA only minorly increases Abi3 protein levels, but does rescue the non-targeting hairpin. Expression is shown relative to the no cDNA, empty vector condition and is normalized to Hsp90 loading control. (B) Scatterplot showing fold change of shRNA-expressing cells in untreated versus dasatinib treated mice at morbidity in the presence or absence of the Abi3 cDNA. Expression of an Abi3 cDNA rescues the effect of a non-targeting hairpin but not a targeting hairpin. Fold changes are normalized to a hairpin expressing Renilla luciferase with matching cDNA and treatment condition, and values

are an average of at least three mice from multiple independent experiments. (C) Scatterplot showing fold change of shRNA-expressing cells in untreated versus dasatinib treated cultures of either leukemia cells alone (left) or co-cultured with bone marrow-derived stromal cells (right) in the presence or absence of the Abi3 cDNA. Hairpins targeting Abi3 do not significantly enrich regardless of culture conditions or expression of an Abi3 cDNA. Fold changes are normalized to a hairpin expressing Renilla luciferase with matching cDNA and treatment condition, and values are an average of at least six independent cultures. Error bars indicate standard deviation; p-values were calculated using Student's t-test.

A slower proliferation rate would be a possible explanation for both the depletion of Abi3-1 cells before therapy and their enrichment after therapy. Although other hairpins don't deplete before therapy, this could be due to their limited knockdown compared to shAbi3-1. To test this theory, we looked at the proliferation rate of shAbi3-1 cells, which consistently deplete before therapy or in untreated mice or cultures. Interestingly, we saw no significant change in proliferation rate of shAbi3-1 cells as compared with parental leukemic cells or those infected with an empty vector regardless of the presence of bone marrow-derived stromal cells. These data suggest that a slower growth rate is unlikely to be responsible for the phenotypes associated with *Abi3* knockdown (Figure 3A).

Knockdown of *Abi3* might also confer resistance to dasatinib by protecting cells against dasatinib-mediated apoptosis. As shAbi3-1 does confer at least some resistance to dasatinib *in vitro*, we compared dasatinib-mediated killing in pure populations of shAbi3-1 infected cells with cells infected with an empty vector. Surprisingly, Abi3 knockdown cells had significantly poorer survival after dasatinib treatment *in vitro*, and this effect was completely abrogated by the addition of bone marrow-derived stromal cells (Figure 3B). This finding may partially explain the decreased resistance to dasatinib conferred by Abi3 knockdown cells *in vitro* as

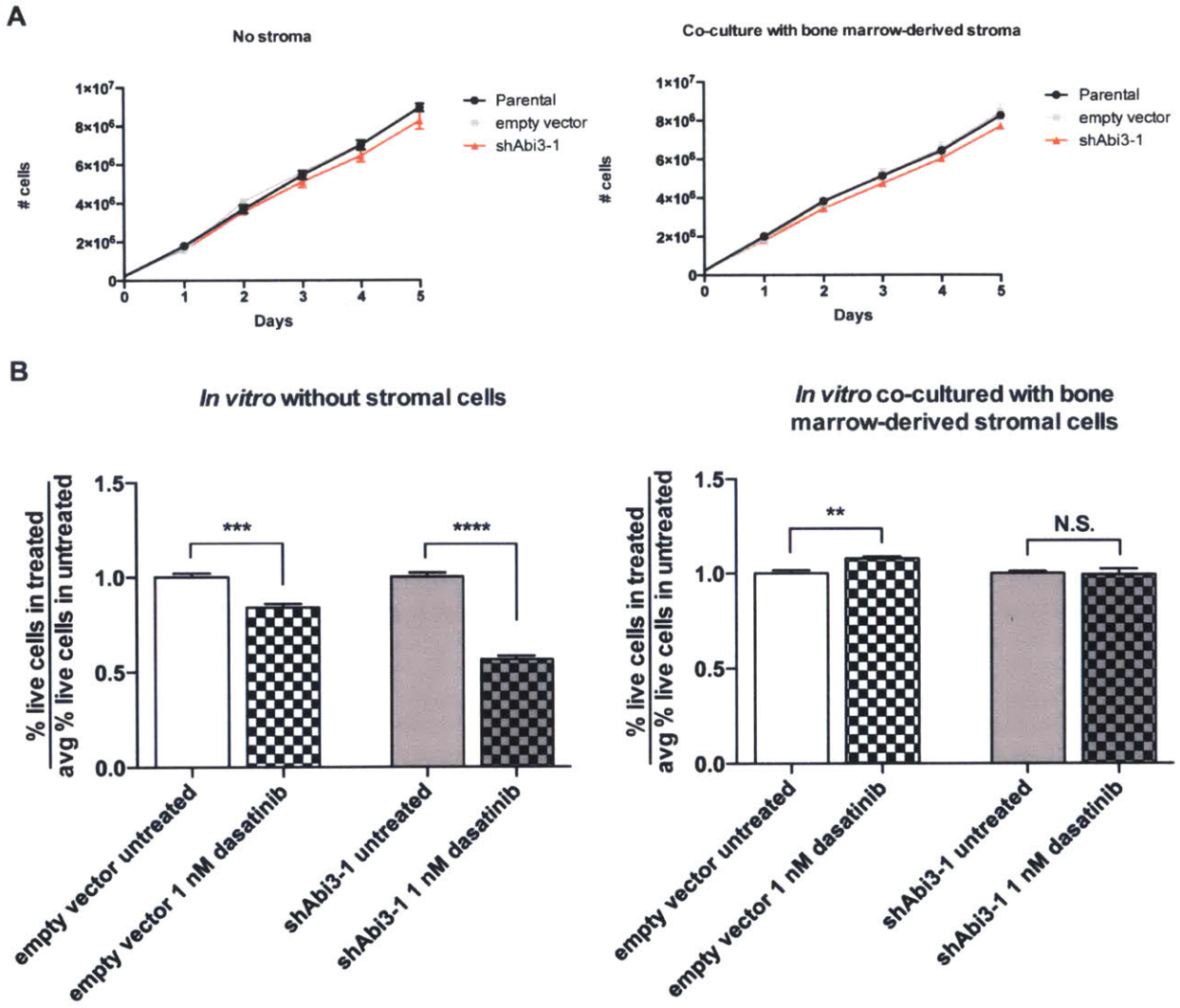


**Figure 3. Abi3 knockdown does not significantly decrease proliferation or protect from dasatinib-mediated cell killing in cultured cells.**
(A) Proliferation assays of leukemic cells cultured alone (left) or in the presence of bone marrow derived stromal cells (right) show no significant decrease in proliferation rate *in vitro* of Abi3 knockdown cells versus the parental cell line or cells infected with an empty vector, based on Student's t-test of proliferation rate at each 24 hour time point calculated from this data. (B) Bar graphs showing percentage of live cells in 1 nM dasatinib treated cultures of leukemia cells alone (left) or with bone marrow-derived stromal cells (right). Values are normalized to percentage of live cells in matching untreated cultures. Abi3 knockdown does not protect against dasatinib-mediated cell death regardless of the presence of stromal cells. Error bars indicate standard error of the mean; p-values were calculated using Student's t-test.

compared to *in vivo*, but it also indicates that a cell-intrinsic resistance to dasatinib-mediated apoptosis is unlikely to be responsible for the drug-resistant phenotype of cells that express lower levels of *Abi3*.

In order to deal with poor knockdown by hairpins targeting the *Abi3* gene, we attempted to utilized Crispr/Cas9 to knockout the *Abi3* gene. We designed four targeting constructs and generated single-cell clones, but were unable to identify a clone that lacked Abi3 expression at the protein level (Figure 4A). Of 130+ clones checked, none were *Abi3* knockout. Either all four sgRNAs fail to target the *Abi3* gene effectively, or expression of *ABI3* is required for the survival of leukemic cells. In order to test the latter theory, we have cloned an inducible Abi3 cDNA that cannot be targeted by any of our sgAbi3 constructs, and will use this cDNA to confirm whether or not *Abi3* is an essential gene in $p19^{Arf-/-}$, *BCR-ABL1*+ BCP-ALL cells (Figure 4B).

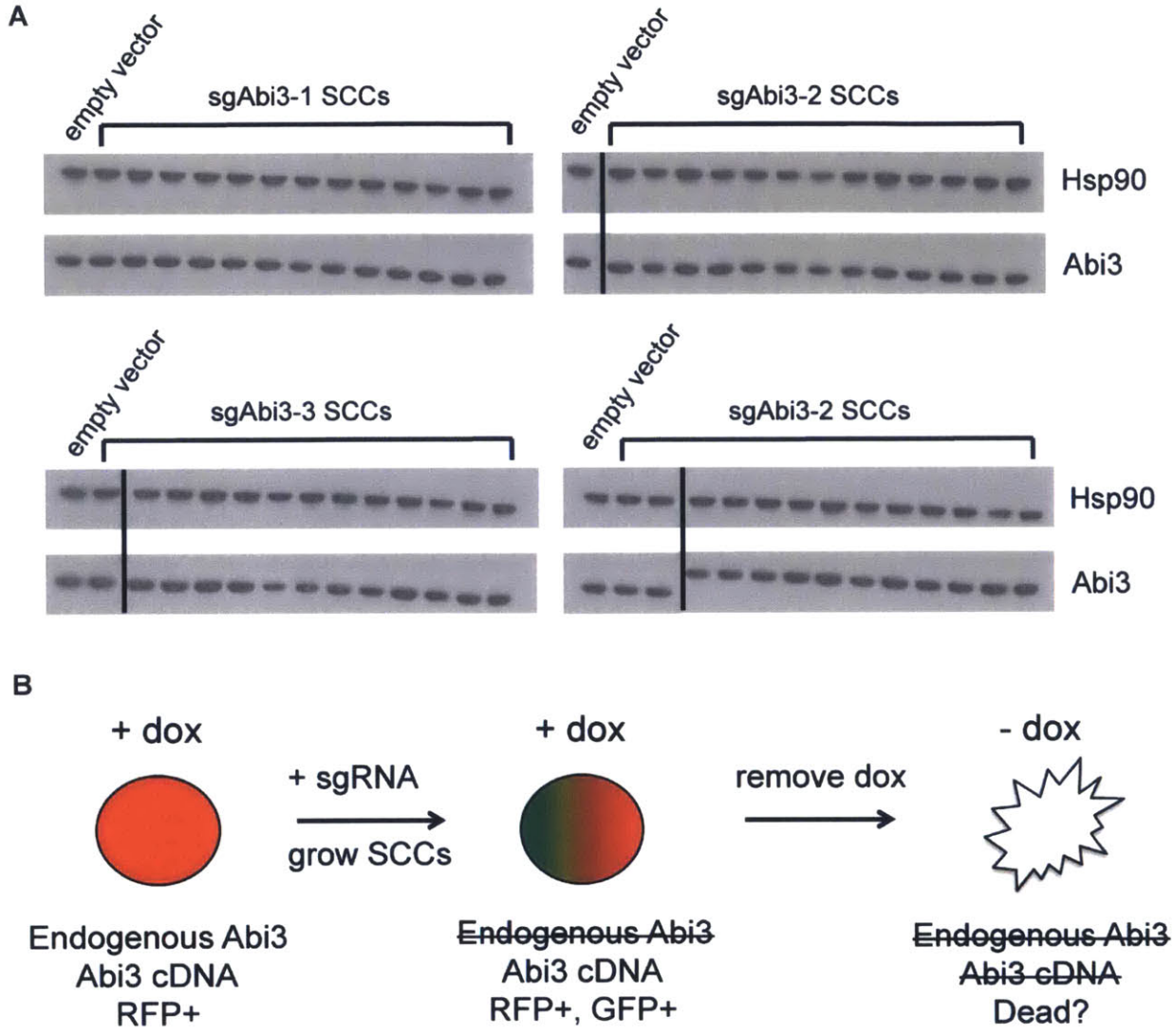


**Figure 4. *Abi3* may be an essential gene in *BCR-ABL1*+ BCP-ALL cells.**
(A) Representative Western blots showing Abi3 levels in multiple single cell-clones (SCCs) from each sgAbi3 targeting construct, as compared to single cell clones made using the empty sgRNA targeting vector (empty vector). Black lines indicate separations in the gels that are edited out in this image. Hsp90 is used as a loading control. (B) Schematic for testing whether or not *Abi3* is an essential gene in *BCR-ABL1*+ BCP-ALL cells. Pure populations of leukemic cells expressing a doxycycline-inducible FLAG-tagged Abi3 cDNA (red) that cannot be targeted by the sgAbi3 constructs will be transfected with sgAbi3 and empty vector sgRNA constructs and single cell clones will be generated. Clones expressing the FLAG-tagged Abi3 cDNA that have taken up sgRNA constructs and lost endogenous Abi3 expression (green) will be isolated, and then upon removal of doxycycline we will monitor cells to see if they die or undergo cellular senescence.

**Discussion**

Our results indicate that levels of *Abi3* expression in *BCR-ABL1*+ BCP-ALL cells affect both leukemia cell survival and response to dasatinib. In wild-type leukemic cells, *Abi3* seems to be highly expressed. Abi3 is difficult to knockdown, is not greatly increased at the protein level by a cDNA vector that results in over-expression of other genes (*Pafah1b3*), and we were unable to get reliable measurements of mRNA level using quantitative reverse-transcriptase polymerase chain reaction due to extremely high amplification of Abi3 mRNA (not shown). We could not generate *Abi3* knockout cells, and Abi3 knockdown cells deplete before treatment *in vivo*, therefore we were unable to utilize pure populations to test whether levels of Abi3 affect invasion after dasatinib *in vivo*. However, the ability of *BCR-ABL1*+ BCP-ALL cells to home to the bone marrow can protect leukemic cells from TKI-mediated cell death, and the CXCR4 receptor, which regulates this process, has increased expression in murine *BCR-ABL1*+ cells after dasatinib treatment (19-21). TKI treatment of Abi3-expressing lymphoid cell lines alters their invasive capacity, perhaps by modulating the interaction between Abi3 and certain TKI target enzymes involved in cell motility, such as PDGFR (7, 15). It is possible that Abi3 knockdown could result in greater ability of leukemia cells to home to or remain in the bone marrow after dasatinib treatment, which would provide Abi3 knockdown cells with a survival advantage after dasatinib treatment specifically *in vivo*.

Despite the increased resistance of Abi3 knockdown cells, we don't see a significant difference in proliferation rate *in vitro*. This result is consistent with previous work showing that changes to Abi3 levels could alter cell motility but not cell growth in some contexts (13). Only some of the hairpins targeting *Abi3* confer a depletion

phenotype on leukemia cells in untreated mice *in vivo*, also arguing that lowering Abi3 levels in these cells does not alter the proliferation rate. Additionally, we don't see increased cell viability after dasatinib treatment upon Abi3 knockdown *in vitro*, although the enrichment phenotype of Abi3 knockdown cells after dasatinib is not as consistent *in vitro* as it is *in vivo*. It is still possible that Abi3 knockdown cells have higher cell viability after dasatinib *in vivo*, particularly in specific microenvironments.

In addition to modulating cell motility and invasiness, there is evidence that alterations to levels of Abi3 or its binding partners may mediate cellular senescence. In some carcinomas, in which increased Abi3 levels result in reduced transformation and less tumor growth, ectopic *ABI3* expression can result in increased cellular senescence (14). In mouse embryonic fibroblasts, knockdown of the target of NESH SH3 domain (*TARSH*) can also inhibit cellular proliferation and results in an increase in p53-dependent cellular senescence (22). It is possible that Abi3 knockdown induces senescence in *BCR-ABL1*+ BCP-ALL, resulting in the decreased leukemic growth before dasatinib *in vivo* and then protection from dasatinib-mediated cell death due to the lack of cell division. However, as not all Abi3 knockdown cells deplete before dasatinib treatment *in vivo* this is somewhat unlikely.

The Abi proteins mediate their effects on the WAVE complex, and thus cytoskeletal dynamics, at least partially through interaction with Ena/VASP family members (23). This family of proteins link cellular pathways downstream of RhoGTPases to actin dynamics and thus can function in WAVE complexes (23). Interaction of the Ena/VASP proteins with Abl and the resulting phosphorylation of Ena/VASP proteins are promoted by Abi1, and Abi1 has been shown to directly interact

with Ena/VASP proteins in cells (4, 23). Phosphorylation of Ena/VASP proteins by Abl regulates their subcellular localization and ability to regulate cell motility and cell-to-cell adhesion (23). The Abi protein in *Drosophilia* and Abi1 in mammalian cells is thought to promote formation of an Ena/VASP-containing WAVE complex and so enhance Arp2/3-dependent actin polymerization (4).

Abi3 has been shown to associate with the Ena/VASP protein Mena in binding experiments done with bacterially-expressed proteins, but has never been shown to interact with Ena/VASP proteins in cells (4). Interestingly, Abi3 can regulate cellular motility via its binding partner IRSp53 by sequestering it away from the WAVE complex, thus preventing IRSp53-induced actin filament assembly (15). If Abi3 does bind to Ena/VASP family members, it may function in a similar manner to sequester Ena/VASP and/or WAVE complex proteins from functional WAVE regulatory complexes that involve Abi1/Abi2 and the Abl kinase, thus altering cell motility. This would fit with our data suggesting that cells with Abi3 knockdown may have increased motility and therefore increased ability to home to protective sites and survive dasatinib treatment *in vivo*. Currently we are attempting to verify whether or not the Abi3 protein does in fact bind to Ena/VASP family members, and if so, whether the ability to bind these proteins affects the motility of leukemia cells or their response to dasatinib *in vivo*.

The effect of alteration of *Abi3* levels in cancer cells is highly context dependent. In some tumor types it seems to function as a tumor suppressor, but other tumors, particularly those with an invasive phenotype, have been found to express functional Abi3 (13, 14). In lymphoid cell lines with high versus low expression levels of Abi3, imatinib induces opposing effects on the invasive capability of cells (7). Our data

suggests that in murine p19$^{ARF-/-}$ *BCR-ABL1*+ BCP-ALL cells, Abi3 is highly expressed, and we have shown that Abi3 knockdown in these cells results in increased resistance to dasatinib *in vivo*. This may be due to altered invasive/motile capability of Abi3 knockdown cells, which would result in increased ability of Abi3 knockdown cells to home to protective sites after dasatinib treatment.

We have also shown that Abi3 levels may predict the response to therapy in a mouse model *BCR-ABL1*+ BCP-ALL. Given that immunotherapies are currently emerging as a potential alternative treatment to TKI therapy for *BCR-ABL1*+ BCP-ALL patients, the ability to predict whether leukemia cells will respond to TKI treatment will be important in stratification of patients into different treatment protocols. We have yet to confirm if lower Abi3 promotes resistance to dasatinib in human leukemia cells, but if that is the case, *ABI3* represents a novel biomarker for response to TKI therapy in *BCR-ABL1*+ BCP-ALL.

Interestingly, we also found that *Abi3* may be an essential gene in p19$^{Arf-/-}$ *BCR-ABL1*+ BCP-ALL. This is consistent with our observation that cells with the most extreme knockdown of Abi3 deplete before dasatinib treatment both *in vivo* and *in vitro*. As in other lymphoid cell lines, the level of Abi3 expression may be extremely important in determining cell survival and response to TKI therapy in the context of *BCR-ABL1*+ BCP-ALL. Further studies will clarify whether Abi3 knockdown modulates invasive capability of leukemic cells *in vivo*, if Abi3 binds to Ena/VASP family members, and whether *Abi3* is in fact an essential gene in this mouse leukemia model.

**Acknowledgments and Author Contributions**

We'd like to thank Michael Hemann and Yadira Soto-Feliciano for tail vein injections of mice, Luke Gilbert for advice on co-culture experiments, and members of the Hemann lab for advice and technical assistance. Thank you also to Frank Gertler for advice on the Abi-Ena/VASP connection, and Frank and Daisy Riquelme for helping us find literature and providing antibodies and experience to try to flush out that interaction. Eleanor Cameron and MH designed the experiments and EC wrote the chpater, which was edited by MH. EC performed all experiments, with the exception of ongoing co-immunoprecipitation experiments, which are being performed by Daisy Riquelme.

**References**

1. Lin, T. Y. *et al.* Abi plays an opposing role to Abl in Drosophila axonogenesis and synaptogenesis. *Development.* **136,** 3099–3107 (2009).

2. Hurwitz, M. E. *et al.* Abl kinase inhibits the engulfment of apopotic cells in Caenorhabditis elegans. *PloS Biol.* **7,** e99 (2009).

3. Goley, E. D. & Welch, M. D. The ARP2/3 complex: an actin nucleator comes of age. *Nat Rev Mol Cell Biol.* **7,** 713–726 (2006).

4. Chen, X. J. *et al.* Ena/VASP Proteins Cooperate with the WAVE Complex to Regulate the Actin Cytoskeleton. *Dev Cell.* **30,** 569–584 (2014).

5. Stuart, J. R., Gonzalez, F. H., Kawai, H. & Yuan, Z. M. c-Abl interacts with the WAVE2 signaling complex to induce membrane ruffling and cell spreading. *J Biol Chem.* **281,** 31290–31297 (2006).

6. Hirao, N. *et al.* NESH (Abi-3) is present in the Abi/WAVE complex but does not promote c-Abl-mediated phosphorylation. *FEBS Lett.* **580,** 6464–6470 (2006).

7. Matsuda, S. *et al.* NESH protein expression switches to the adverse effect of imatinib mesylate. *Mol Oncol.* **2,** 16–19 (2008).

8. Li, Y. *et al.* Bcr-Abl induces abnormal cytoskeleton remodeling, beta1 integrin clustering and increased cell adhesion to fibronectin through the Abl interactor 1 pathway. *J Cell Sci.* **120,** 1436–1446 (2007).

9. Yu, W. *et al.* Abi1 gene silencing by short hairpin RNA impairs Bcr-Abl-induced cell adhesion and migration in vitro and leukemogenesis in vivo. *Carcinogenesis.* **29,** 1717–1724 (2008).

10. Chorzalska, A. *et al.* Low expression of Abelson interactor-1 is linked to acquired drug resistance in Bcr-Abl-induced leukemia. *Leukemia.* **28,** 2165–2177 (2014).

11. Bae, J., Sung, B. H., Cho, I. H., Kim, S.-M. & Song, W. K. NESH regulates dendritic spine morphology and synapse formation. *PLoS ONE.* **7,** e34677 (2012).

12. Bae, J., Sung, B. H., Cho, I. H. & Song, W. K. F-actin-dependent regulation of NESH dynamics in rat hippocampal neurons. *PLoS ONE.* **7,** e34514 (2012).

13. Ichigotani, Y., Yokozaki, S., Fukuda, Y., Hamaguchi, M. & Matsuda, S. Forced expression of NESH suppresses motility and metastatic dissemination of malignant cells. *Cancer Res.* **62,** 2215–2219 (2002).

14. Latini, F. R. *et al.* ABI3 ectopic expression reduces in vitro and in vivo cell growth properties while inducing senescence. *BMC Cancer.* **11,** 11 (2011).

15. Matsuda, S. *et al.* Insulin receptor substrate protein 53 (IRSp53) as a binding partner of antimetastasis molecule NESH, a member of Abelson interactor protein family. *Ann Oncol.* **19,** 1356–1357 (2008).

16. Buchdunger, E. *et al.* Abl protein-tyrosine kinase inhibitor STI571 inhibits in vitro signal transduction mediated by c-kit and platelet-derived growth factor receptors. *J Pharmacol Exp Ther.* **295,** 139–145 (2000).

17. Meacham, C. E. *et al.* A genome-scale in vivo loss-of-function screen identifies Phf6as a lineage-specific regulator of leukemia cell growth. *Genes Dev.* **29,** 483–488 (2015).

18. Kuiper, R. P. *et al.* High-resolution genomic profiling of childhood ALL reveals novel recurrent genetic lesions affecting pathways involved in lymphocyte differentiation and cell cycle progression. *Leukemia.* **21,** 1258–1266 (2007).

19. Konopleva, M., Tabe, Y., Zeng, Z. & Andreeff, M. Therapeutic targeting of microenvironmental interactions in leukemia: Mechanisms and approaches. *Drug Resist Updat.* **12,** 103–113 (2009).

20. Fei, F. *et al.* Development of resistance to dasatinib in Bcr/Abl-positive acute lymphoblastic leukemia. *Leukemia.* **24,** 813–820 (2010).

21. Yu, M. *et al.* AMD3100 sensitizes acute lymphoblastic leukemia cells to chemotherapy in vivo. *Blood Cancer J.* **1,** e14 (2011).

22. Wakoh, T. *et al.* Implication of p53-dependent cellular senescence related gene, TARSH in tumor suppression. *Biochem Biophys Res Commun.* **380,** 807–812 (2009).

23. Döppler, H. & Storz, P. Regulation of VASP by phosphorylation. *Cell Adh Migr.* **7,** 492–496 (2014).

24. Williams, R. T., Roussel, M. F. & Sherr, C. J. Arf gene loss enhances oncogenicity and limits imatinib response in mouse models of Bcr-Abl-induced acute lymphoblastic leukemia. *Proc Natl Acad Sci U S A.* **103,** 6688–6693 (2006).

25. Dickins, R. A. *et al.* Probing tumor phenotypes using stable and regulated synthetic microRNA precursors. *Nat Genet.* **37**, 1289-1295 (2005).

26. Ran, F. A. *et al.* Genome engineering using the CRISPR-Cas9 system. *Nat Protoc.* **8,** 2281–2308 (2013).

**Materials and Methods**

*Cell culture*

Murine p19$^{Arf-/-}$ *BCR-ABL1*+ BCP-ALL cells (24) and stromal cells isolated from mouse bone marrow were cultured in RPMI media supplemented with 10% FBS, 4 mM L-glutamine, and 55 μM β-mercaptoethanol. Stromal cells were isolated from non-tumor bearing C57BL/6J mice by culturing bone marrow aspirate and removing non-adherent cells every 24 hours for 7-10 days. Stromal cells for co-culture experiments were passaged only once in culture and used within 4 weeks of isolation.

*Vectors*

All shRNAs were expressed in the mir30 context; the vector and shRNA cloning and design are described in the referenced mir30 shRNA study (25). For cDNA expression, we excised the puromycin resistance cassette from the pMSCVpuro vector from Clontech, and replaced with either the tdTomato or E2Crimson fluorescent proteins. For Crispr/Cas9 knockout of target genes, we cloned sgRNAs against the gene of interest into the pX458 vector (Addgene plasmid #48138) according to the referenced protocol (26).

*Validation assays*

Hairpin knockdown was assessed via Western blot. Hairpins were validated in GFP competition assays by infecting a pure population of tdTomato or E2Crimson positive leukemia cells at 40 – 50% with single constructs expressing GFP and the shRNA of interest. Spin infections were performed in the presence of 4 ug/mL polybrene, and cells were transplanted into recipient mice 48 - 72 hours after infection. 1 x $10^6$ cells were injected into non-irradiated 6 - 10 week old C57BL6/J female mice, and the GFP percentage at injection was measured using flow cytometry. Pre-treatment blood samples were collected via retro-orbital bleed and post-treatment blood, bone marrow, and spleen samples were collected immediately after euthanasia of moribund mice; mice were treated with 20 mg/kg dasatinib q.d. via oral gavage for three days. GFP percentage was assessed at pre- and post-treatment by flow cytometric analysis. For proliferation studies, fluorescent beads (CountBright™ Absolute Counting Beads, Thermo Fisher) at a defined concentration were added to cells from culture to calculate

the concentration of cells every 24 hours, and then cells were re-plated at a 5 x $10^5$ cells/mL. All flow data was collected on LSR analyzers and was analyzed using FACSDiva software (BD Biosciences).

*Western blotting*

*BCR-ABL1*+ BCP-ALL cells were infected with individual shRNAs or cDNA constructs co-expressing a fluorescent marker to a final infection percentage of 40 – 60% and sorted based on marker expression; protein-containing cell lysates were then isolated from the sorted population. In some cases, a selective puromycin cassette in the shRNA expression construct was used to generate pure populations of hairpin-expressing cells rather than cell sorting. The following antibodies were used for protein detection: Abi3 (1:1000 in TBS-T with 5% milk; Santa Cruz Biotechnology, SC376982), Hsp90 (1:5000 in TBS-T with 5% milk; BD Transduction Laboratories 610418). Relative protein expression is an average of multiple exposures and is normalized to Hsp90 expression. All analysis was done using Image Studio™ Lite (LI-COR Biosciences).

*Preclinical therapeutics*

Dasatinib (LC Laboratories) was dissolved in DMSO and diluted into cell culture media for *in vitro* studies. For *in vivo* use, dasatinib was dissolved in 80 mM citric acid at pH 2.3 and administered via oral gavage at 0.01 mL/g at 20 mg/kg for 3 days.

## Supplementary Figures

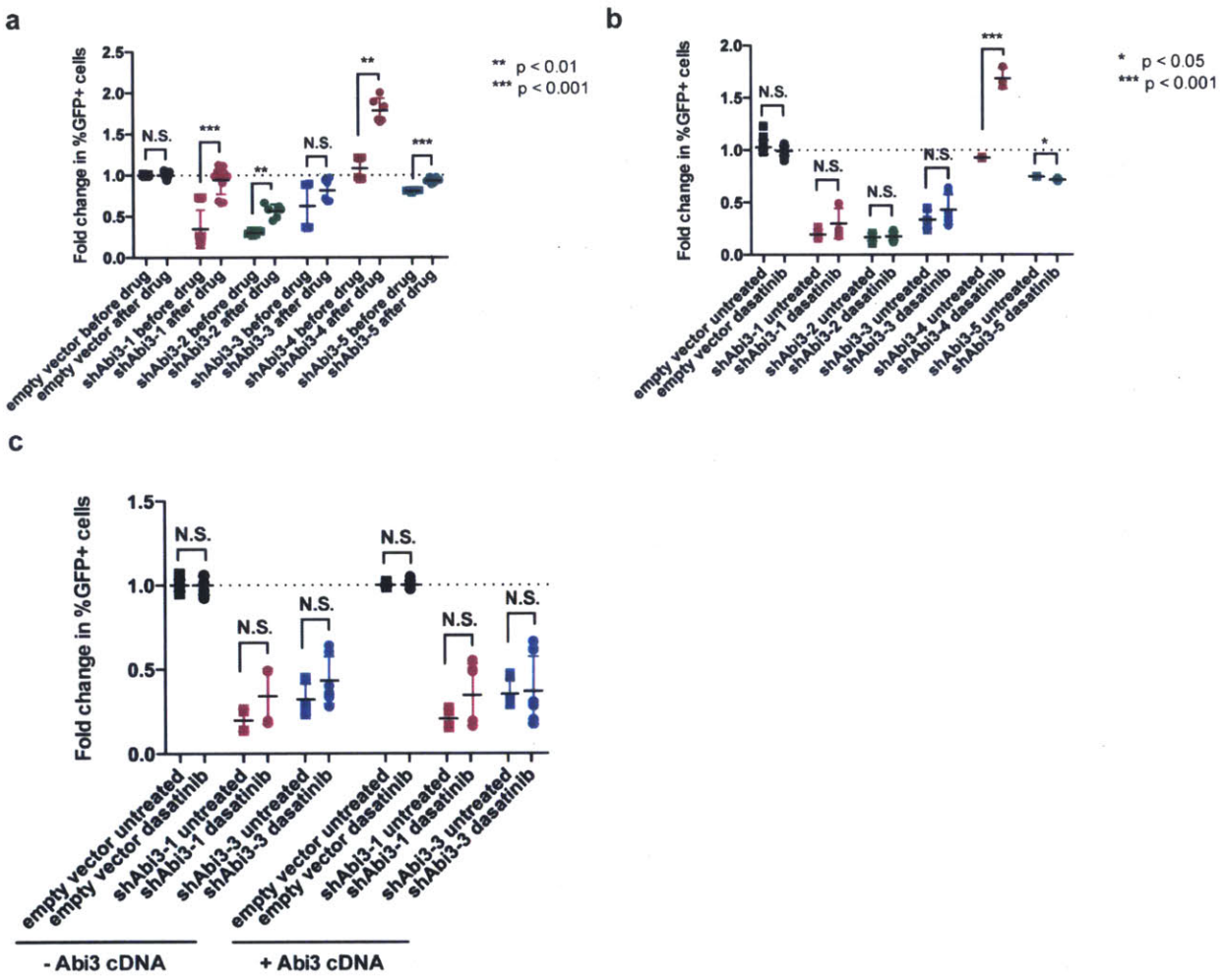


**Supplementary Figure S1. Knockdown of *Abi3* sometimes confers enrichment after dasatinib *in vitro*, but effect is diminished as compared to the *in vivo* effect.** (a) Scatterplots showing fold change in percent shRNA-expressing cells *in vitro* before versus after dasatinib treatment; some but not all hairpins enrich after dasatinib. Fold changes are normalized to a control empty vector or a hairpin targeting Renilla luciferase. Values are an average of at least six independent cultures. (b) Scatterplots showing fold change in percent shRNA-expressing cells at morbidity in untreated versus dasatinib-treated cultures; some but not all hairpins enrich in dasatinib-treated mice. Fold changes are normalized to a control empty vector or a hairpin targeting Renilla luciferase. Values are an average of at least three independent cultures. (c) Scatterplot showing fold change of hairpin-expressing cells in untreated versus dasatinib treated cultures in the presence or absence of the Abi3 cDNA from experiments done in parallel with *in vivo* rescue experiments. Hairpins targeting Abi3 do not significantly enrich regardless of culture conditions or expression of an Abi3 cDNA. Fold changes are normalized to a hairpin expressing Renilla luciferase with matching cDNA and treatment condition, and values are an average of at least six independent cultures. Error bars indicate standard deviation; p-values were calculated using Student's t-test.

This page intentionally left blank.

## Chapter V: Conclusions

Eleanor R. Cameron

David H. Koch Institute for Integrative Cancer Research, Massachusetts Institute of Technology. Cambridge, Massachusetts, 02139, United States.

This chapter is not published as of December 2015.

Precursor B-cell acute lymphoblastic leukemia (BCP-ALL) is a common hematological malignancy for which cure rates are high, particularly in children, but relapse is a consistent problem (1-3). Moreover, relapsed BCP-ALL has an extremely poor outcome in both children and adults, although the recent introduction of immunotherapy into the clinic may improve clinical outcomes for relapsed patients (1, 4-9). The persistence of minimal residual disease (MRD), which is predictive of both relapse and worse clinical outcome, is a result of drug resistance that can arise due to alteration of drug targets in leukemia cells, reduced capacity of cancer cells to arrest or undergo apoptosis, activation of alternative pro-survival signaling pathways, maintenance of a less differentiated cellular state, changes in the intracellular or organismal level of active drug, or cell-extrinsic signaling that promotes survival of leukemia cells despite the continued presence of drug. Here we have utilized a mouse model of *BCR-ABL1*+ BCP-ALL, a subtype of BCP-ALL with particularly poor outcome, to investigate genes or pathways that can modulate leukemic response to drug in the native microenvironment.

In particular, we looked at the response of leukemic cells to the tyrosine kinase inhibitor (TKI) dasatinib, a targeted therapeutic that is used to treat *BCR-ABL1*+ leukemic patients either alone or in combination with chemotherapy (10). Targeted therapeutics, which are so named for their ability to specifically target cancerous cells, are increasingly used to treat a variety of common cancer types (2, 11-13). Resistance to targeted therapeutics via alteration of the target enzyme, as can occur in *BCR-ABL1*+ patients treated with TKIs, has also been described in lung cancer with inhibitors of *EGFR* and *ALK*, gastrointestinal stromal tumors with *KIT* inhibitors (including the TKI

imatinib), chronic lymphocytic leukemia treated with a *BTK* inhibitor, and acute myeloid leukemia treated with *FLT3* inhibitors (12). However, non-mutational resistance can also occur; resistance to targeted therapeutics in lung cancer has also been attributed to activation of alternative oncogenic signaling through both *KRAS* and *KIT* (13). Similarly, resistance to *BRAF* inhibitors in melanoma patients can occur via either mutation of *BRAF* or activation of alternative pro-survival signaling via Erk or the mTOR pathways (11).

As *BCR-ABL1*+ leukemia was the first disease to be treated with targeted therapeutics, this disease provides a model for how resistance to targeted therapeutics can arise. Other malignancies that have been treated with targeted therapies in the years since the development of the first TKI imatinib have developed resistance through mechanisms similar to those that cause TKI resistance in *BCR-ABL1*+ leukemias. Mechanisms of resistance to TKI treatment in *BCR-ABL1*+ BCP-ALL include *BCR-ABL1* alterations, activation of pro-survival signaling via the Jak/Stat or the non-canonical Wnt/$Ca^{2+}$/NFAT pathway, defective apoptosis due to loss of *CDKN2A/B* or upregulation of Bcl6, and interaction with the tumor microenvironment, specifically changes in CXCR4/CXCL12, IL-7, IL-3, and ErbB2 signaling, or β1-integrin mediated adhesion (2, 14-20).

Here we performed unbiased, pool-based RNAi screens both *in vivo* and *in vitro* for novel mediators of genetic response to dasatinib in a mouse model of *BCR-ABL1*+ BCP-ALL. Our lab previously observed that there is significantly greater variation between *in vivo* screening replicates than *in vitro* replicates, and so in this work we utilized a novel longitudinal screen design in which we took multiple samples over time

from the blood of each mouse and each cell culture dish. We found that this approach was sufficient to represent even extremely large hairpin libraries both before and after therapy *in vivo*, indicating that *in vivo* screening methodologies that necessitate extremely high coverage, such as screens utilizing Crispr/Cas9 technology, will be possible in this model of *BCR-ABL1*+ BCP-ALL. A longitudinal screening approach like the one used here reduces noise in the dataset, but necessitates the ability to perform serial sampling; this is easily accomplished in cell culture or in hematopoietic malignancies, but not in solid tumors. The exception might be metastasis screens in which a primary tumor is harvested before the metastatic tumors, or in which the primary tumor is dissociated and then transplanted into secondary recipient mice in order to screen for those cells that have metastatic potential.

Examination of hairpin depletion or enrichment over the course of our longitudinal screens revealed that clonal effects dominate in an *in vivo* setting, while the behavior of hairpins *in vitro* seems to be largely determined by either the presence or absence of therapy. This indicates that clonal effects play a significant role in *in vivo* RNAi screens; unless the phenotype being observed *in vivo* has more of an effect on hairpin behavior than the clonality within each mouse does, analysis of *in vivo* data needs to include some component of either controlling for this clonal effect or separating it from the phenotype of interest. It also reinforces the need for multiple biological replicates when screening *in vivo*, as a higher number of replicates will make it easier to separate out effects due to clonal behavior.

In order to distinugish non-clonal effects, including the effect of dasatinib therapy, from the clonal effects in our *in vivo* RNAi screen, we used independent component

analysis to separate out the signals present in the dataset and quantify to what extent each hairpin contributed to each signal. ICA was able to identify a signature of hairpins that significantly enriched or depleted after therapy as compared to before, and validation analyses of a small set of hairpins from this signature found that 72% of hairpins tested had the general behavior predicted by ICA. We were able to further filter this validation set and found that 28% of the hairpins tested had significantly different behavior after therapy as compared to before, and in half of those cases the behavior was specific to the *in vivo* setting. Gene set enrichment analysis (GSEA) of the hairpins identified by ICA to enrich or deplete after therapy *in vivo*, while not significant, did pull out several expected gene sets, including an enrichment of drug metabolism genes and a depletion of protein tyrosine kinase activity after therapy.

Independent component analysis of longitudinal *in vivo* RNAi screening data is capable of identifying both hairpins that have a general, if not necessarily significant, behavior at different time points as well as those that have significantly different behavior in different therapeutic contexts. The ability of ICA to identify trends in hairpin behavior even if the biological effect of each individual hairpin is small may be useful in future RNAi or Crispr/Cas9 screens that utilize multiple targeting constructs per gene but in which the extent of knockdown or knockout by each individual construct is not known. ICA also represents a method for removing clonality from an RNAi datatset and identifying hairpins that have specific non-clonal behavior that is shared across multiple samples. Here we have used ICA to identify those hairpins whose behavior changes after the introduction of therapy, but this approach could be modified to identify hairpins involved in tumor cell dissemination to or growth in distinct anatomical sites, or those

involved in cancer cell growth or therapeutic response in genetically distinct tumors (e.g. xenografts from multiple patients with the same cancer).

From our data we identified *Abi3* loss as a mechanism of resistance to dasatinib, and this effect was confirmed in independent assays. Additional experiments also suggested that this effect might be specific to the *in vivo* setting, despite the fact that the initial hairpin identified in our screen enriched after dasatinib *in vitro* as well. We were unable to either over-express or knockout *Abi3*, indicating that it may be an essential gene in our model of *BCR-ABL1*+ BCP-ALL and thus may contribute to leukemogenesis as well as therapeutic response. Our data supports the conclusion that *Abi3* levels in leukemia cells may determine response to TKI therapy *in vivo*; if this is the case, the *ABI3* gene represents a potential biomarker. With the introduction of immunotherapy to the clinic, there may now be an alternative option to TKI treatment for *BCR-ABL1*+ BCP-ALL patients if they are predicted to have poor response to targeted therapy. Identification and characterization of genes other than *BCR-ABL1* itself that are predictive of response to TKI therapy will likely be useful for proper patient stratification into treatment groups.

The Abi3 protein is thought to interact with both the WAVE regulatory complex and Ena/VASP family members in an Abl-independent manner, and thus changes in Abi3 levels may alter cell motility and adhesion, functionally changing the invasive and migratory capability of leukemic cells (21-24). This may in turn affect the ability of leukemia cells to respond to microenvironmentally-mediated signaling that normally would cause tumor cells to home to specific microenvironments like the bone marrow, which is known to protect *BCR-ABL1*+ BCP-ALL cells from TKI-mediated cell death (17,

25, 26). Neither the Ena/VASP proteins nor the Abi family genes have been implicated in this process in *BCR-ABL1*+ BCP-ALL patients, and it is unclear exactly what role Abi3 plays in cellular motility in these cells, as the function of the *ABI3* gene is extremely context-dependent. We are currently determining whether Abi3 interacts with Ena/VASP family members in *BCR-ABL1*+ BCP-ALL cells and what effect knockdown of *ABI3* has on the motile and invasive capabilities of these cells in an attempt to answer some of the questions that our work has raised about the role of *ABI3* in therapeutic response.

We also identified loss of *Pafah1b3* via both shRNA-mediated knockdown and Crispr/Cas9-mediated knockout as a mechanism by which *BCR-ABL1*+ BCP-ALL cells can be sensitized to dasatinib therapy specifically in the *in vivo* setting. In competition experiments, we were able to show that leukemia cells that express higher Pafah1b3 were relatively enriched in the bone marrow of recipient mice after dasatinib treatment, indicating that changes in Pafah1b3 level affect the ability of leukemia cells to either migrate to or remain in protective microenvironments after therapy. Rescue of Pafah1b3 knockdown or knockout by a non-targeted Pafah1b3 cDNA reversed the effects of gene loss, indicating that the observed effects are due to changes in Pafah1b3 levels rather than an off-target effect.

The drug sensitizing effect observed upon *Pafah1b3* loss could be due to alterations in PAF signaling, as Pafah1b3 functions to inactivate PAF and thus modulate intracellular PAF levels, or to PAF-independent effects; Pafah1b3 is also important in maintaining effective protein trafficking through the Golgi complex as well as controlling lipid metabolism (27-30). PAF-dependent effects may be due to alterations in cytokine response and secretion in leukemic cells; cytokine signaling is an important mediator of

both BCP-ALL cell homing to or mobilization from protective sites as well as the ability of BCP-ALL cells to remodel microenvironmental niches in order to make them protective against TKI- or chemotherapy-mediated cell death (31-34). Additionally, PAF signaling affects angiogenesis, and the maintenance of an angiogenic and hypoxic bone marrow is thought to be associated with the establishment of minimal residual disease in BCP-ALL (25, 35-38).

Neither *PAFAH1B3* nor any components of the PAF pathway have been previously implicated in TKI response in *BCR-ABL1*+ BCP-ALL, but increased ability of leukemia cells to home to and remain in the bone marrow is an established mechanism by which BCP-ALL cells can evade drug-mediated cell killing (31, 32). *PAFAH1B3* represents a novel gene involved in this process, and one whose protein product is an enzyme that can be directly inhibited to increase the effect of dasatinib therapy. Evidence suggests that interfering with the ability of *BCR-ABL1*+ leukemic cells to interact with the tumor microenvironment may be a potential therapeutic avenue to reduce MRD after TKI treatment; disruption of intergrin-mediated adhesion, IL-7 signaling via the Jak/Stat pathway, or CXCL12/CXCR4-mediated homing the bone marrow sensitizes to TKI therapy in mouse models of *BCR-ABL1*+ BCP-ALL (26, 39, 40). Specific Pafah inhibitors have been developed but never used *in vivo*; we are currently performing preclinical studies in the murine model of *BCR-ABL1*+ BCP-ALL used here to see if we can pharmacologically recapitulate the effects of *Pafah1b3* gene knockdown/knockout (41). Additionally, we are investigating whether the observed sensitization effect of *Pafah1b3* loss is due to alterations in PAF signaling or an alternative PAF-independent mechanism.

The work described here shows that longitudinal, unbiased *in vivo* RNAi screening in combination with independent component analysis can identify groups of hairpins that have a common behavior as well as individual hairpins that have significant non-clonal effects in mice. Specifically, we were able to identify a large signature of hairpins that enrich or deplete after dasatinib treatment as well as individual hairpins that have significantly different behavior before or after therapy *in vivo*. Using the approach described here, we identified hairpins that have behavior that is specific both to therapeutic response as well as to the *in vivo* setting. From this screening data, we identified loss of *Abi3* as a novel mechanism of resistance to dasatinib, and *Pafah1b3* as a novel drug target for combination therapy with dasatinib. *Abi3* levels may also serve as a biomarker for patient response to TKI therapy.

Further investigation both of the general screening data and these specific genes will help elucidate mechanisms of Bcr-Abl-independent resistance to TKIs and may help improve treatment modalities for BCP-ALL. In particular, our findings highlight the role of the microenvironment in the development of minimal residual disease in *BCR-ABL1*+ BCP-ALL and reinforce the need for preclinical studies in this disease to be performed *in vivo* whenever possible. Importantly, the longitudinal screen design used here could be adapted to screen for mediators of metastatic dissemination, a process in solid tumors that also requires interaction with the microenvironment.

*In vivo* RNAi screening combined with independent component analysis as performed here represents a potential experimental methodology for identification of determinants of target-independent resistance to targeted therapies, which are

increasingly utilized in multiple different tumor types, and has identified a novel potential biomarker and a novel drug target for combination treatment of leukemia.

## References


1. Pui, C. H. Genomic and pharmacogenetic studies of childhood acute lymphoblastic leukemia. *Front Med.* **9,** 1–9 (2014).

2. Bernt, K. M. & Hunger, S. P. Current Concepts in Pediatric Philadelphia Chromosome-Positive Acute Lymphoblastic Leukemia. *Front Oncol.* **4,** 1–21 (2014).

3. Litzow, M. R. Evolving paradigms in the therapy of Philadelphia-chromosome-negative acute lymphoblastic leukemia in adults. *Hematology Am Soc Hematol Educ Program.* 362–370 (2009).

4. Nguyen, K. *et al.* Factors influencing survival after relapse from acute lymphoblastic leukemia: a Children's Oncology Group study. *Leukemia.* **22,** 2142–2150 (2008).

5. Mullighan, C. G. New Strategies in Acute Lymphoblastic Leukemia: Translating Advances in Genomics into Clinical Practice. *Clin Cancer Res.* **17,** 396–400 (2011).

6. Forman, S. J. & Rowe, J. M. The myth of the second remission of acute leukemia in the adult. *Blood.* **121,** 1077–1082 (2013).

7. Benjamini, O. *et al.* Phase II trial of hyper CVAD and dasatinib in patients with relapsed Philadelphia chromosome positive acute lymphoblastic leukemia or blast phase chronic myeloid leukemia. *Am J Hematol.* **89,** 282–287 (2014).

8. Jabbour, E., O'Brien, S., Ravandi, F. & Kantarjian, H. Monoclonal antibodies in acute lymphoblastic leukemia. *Blood.* **125,** 4010–4016 (2015).

9. Bouhassira, D. C., Thompson, J. J. & Davila, M. L. Using gene therapy to manipulate the immune system in the fight against B-cell leukemias. *Expert Opin Biol Ther.* **15,** 403–416 (2015).

10. Fielding, A. K. *et al.* UKALLXII/ECOG2993: addition of imatinib to a standard treatment regimen enhances long-term outcomes in Philadelphia positive acute lymphoblastic leukemia. *Blood.* **123,** 843–850 (2014).

11. Niezgoda, A., Niezgoda, P. & Czajkowski, R. Novel approaches to treatment of advanced melanoma: A review on targeted therapy and immunotherapy. *Biomed Res Int.* **2015,** 851387 (2015).

12. Woyach, J. A. & Johnson, A. J. Targeted therapies in CLL: mechanisms of resistance and strategies for management. *Blood.* **126,** 471–477 (2015).

13. Rolfo, C. *et al.* ALK and crizotinib: after the honeymoon...what else? Resistance mechanisms and new therapies to overcome it. *Transl Lung Cancer Res.* **3,** 250–261 (2014).

14. Duy, C. *et al.* BCL6 enables Ph+ acute lymphoblastic leukemia cells to survive BCR-ABL1 kinase inhibition. *Nature.* **473,** 384–388 (2012).

15. Gregory, M. A. *et al.* Wnt/Ca2+/NFAT Signaling Maintains Survival of Ph+ Leukemia Cells upon Inhibition of Bcr-Abl. *Cancer Cell.* **18,** 74–87 (2010).

16. Mullighan, C. G., Williams, R. T., Downing, J. R. & Sherr, C. J. Failure of CDKN2A/B (INK4A/B-ARF)-mediated tumor suppression and resistance to targeted therapy in acute lymphoblastic leukemia induced by BCR-ABL. *Genes Dev.* **22,** 1411–1415 (2008).

17. Fei, F. *et al.* Development of resistance to dasatinib in Bcr/Abl-positive acute lymphoblastic leukemia. *Leukemia.* **24,** 813–820 (2010).

18. Hazlehurst, L. A., Argilagos, R. F. & Dalton, W. S. β1 integrin mediated adhesion increases Bim protein degradation and contributes to drug resistance in leukaemia cells. *Br J Haematol.* **136,** 269–275 (2007).

19. Koss, B. *et al.* Requirement for antiapoptotic MCL-1 in the survival of BCR-ABL B-lineage acute lymphoblastic leukemia. *Blood.* **122,** 1587–1598 (2013).

20. Liu, J. *et al.* BCR-ABL mutants spread resistance to non-mutated cells through a paracrine mechanism. *Leukemia.* **22,** 791–799 (2008).

21. Matsuda, S. *et al.* Insulin receptor substrate protein 53 (IRSp53) as a binding partner of antimetastasis molecule NESH, a member of Abelson interactor protein family. *Ann Oncol.* **19,** 1356–1357 (2008).

22. Chen, X. J. *et al.* Ena/VASP proteins cooperate with the WAVE complex to regulate the actin cytoskeleton. *Dev Cell.* **30,** 569–584 (2014).

23. Döppler, H. & Storz, P. Regulation of VASP by phosphorylation. *Cell Adh Mig.* **7,** 492–496 (2014).

24. Hirao, N. *et al.* NESH (Abi-3) is present in the Abi/WAVE complex but does not promote c-Abl-mediated phosphorylation. *FEBS Lett.* **580,** 6464–6470 (2006).

25. Konopleva, M., Tabe, Y., Zeng, Z. & Andreeff, M. Therapeutic targeting of microenvironmental interactions in leukemia: Mechanisms and approaches. *Drug Resist Updat.* **12,** 103–113 (2009).

26. Yu, M. *et al.* AMD3100 sensitizes acute lymphoblastic leukemia cells to chemotherapy in vivo. *Blood Cancer J.* **1,** e14 (2011).

27. Bechler, M. E. *et al.* The phospholipase complex PAFAH Ib regulates the functional organization of the Golgi complex. *J Cell Biol.* **190,** 45–53 (2010).

28. Bechler, M. E. & Brown, W. J. PAFAH Ib phospholipase $A_2$ subunits have distinct roles in maintaining Golgi structure and function. *Biochim Biophys Acta.* **1831,** 595–601 (2013).

29. Bonin, F. *et al.* Anti-apoptotic actions of the platelet-activating factor acetylhydrolase I α2 catalytic subunit. *J Biol Chem.* **279,** 52425–52436 (2004).

30. Mulvihill, M. M. *et al.* Metabolic profiling reveals PAFAH1B3 as a critical driver of breast cancer pathogenicity. *Chem Biol.* **21,** 831–840 (2014).

31. Ayala, F., Dewar, R., Kieran, M. & Kalluri, R. Contribution of bone microenvironment to leukemogenesis and leukemia progression. *Leukemia.* **23,** 2233–2241 (2009).

32. Tripodo, C. *et al.* The bone marrow stroma in hematological neoplasms—a guilty bystander. *Nat Rev Clin Oncol.* **8,** 456–466 (2011).

33. Duan, C. W. *et al.* Leukemia propagating cells rebuild an evolving niche in response to therapy. *Cancer Cell.* **25,** 778–793 (2014).

34. Mallampati, S. *et al.* Tyrosine kinase inhibitors induce mesenchymal stem cell-mediated resistance in BCR-ABL+ acute lymphoblastic leukemia. *Blood.* **125,** 2968–2973 (2015).

35. Tavor, S. & Petit, I. Can inhibition of the SDF-1/CXCR4 axis eradicate acute leukemia? *Semin Cancer Biol.* **20,** 178–185 (2010).

36. Frolova, O. *et al.* Regulation of HIF-1α signaling and chemoresistance in acute lymphocytic leukemia under hypoxic conditions of the bone marrow microenvironment. *Cancer Biol Ther.* **13,** 858–870 (2012).

37. Wellmann, S. *et al.* Activation of the HIF pathway in childhood ALL, prognostic implications of VEGF. *Leukemia.* **18,** 926–933 (2004).

38. Stachel, D., Albert, M., Meilbeck, R., Paulides, M. & Schmid, I. Expression of angiogenic factors in childhood B-cell precursor acute lymphoblastic leukemia. *Oncol Rep.* **17,** 147–152 (2007).

39. Appelmann, I. *et al.* Janus kinase inhibition by ruxolitinib extends dasatinib- and dexamethasone-induced remissions in a mouse model of Ph+ ALL. *Blood.* **125,** 1444–1451 (2015).

40. Hu, Z. & Slayton, W. B. Integrin VLA-5 and FAK are good targets to improve treatment response in the Philadelphia chromosome positive acute lymphoblastic leukemia. *Front Oncol.* **4,** 112. (2014).

41. Chang, B. H. *et al.* YM155 potently kills acute lymphoblastic leukemia cells through activation of the DNA damage pathway. *J Hematol Oncol.* **8,** 39 (2015).

This page intentionally left blank.

**Appendix: Response to tyrosine kinase inhibitors in a transplantable mouse model of *BCR-ABL1*+ BCP-ALL**

---

Eleanor R. Cameron, Michael T. Hemann

David H. Koch Institute for Integrative Cancer Research, Massachusetts Institute of Technology. Cambridge, Massachusetts, 02139, United States.

This chapter is not published as of December 2015.

## Introduction

The work described here makes use of a transduction/transplantation $p19^{ARF-/-}$ *BCR-ABL1*+ BCP-ALL mouse model that produces a multiclonal leukemia after transplantation into syngeneic immunocompetent recipient mice (1, 2). We have previously shown that after transplantation, these *BCR-ABL1*+ BCP-ALL cells seed to the bone marrow and spleen and then expand out (3). Treatment of this model with continuous dasatinib therapy results in prolonged survival of recipient mice followed by inevitable relapse, often with mutations in the Bcr-Abl kinase that prevent drug binding (4). Combination of dasatinib with additional chemotherapeutic agents traditionally used to treat *BCR-ABL1*+ BCP-ALL, Jak kinase inhibitors, or cyclosporine A further prolongs the survival of recipient mice (4-6). *In vivo*-specific resistance to dasatinib in this model has previously been ascribed to signaling via the common γ chain associated with the receptors for IL-7 and related cytokines (2, 5).

Here we describe additional characterization of the response to dasatinib in the transduction/transplantation $p19^{ARF-/-}$ *BCR-ABL1*+ BCP-ALL mouse model. We found that even brief dasatinib treatment *in vivo* is sufficient to extend the lifespan of recipient mice and to induce apoptosis in multiple organ compartments. However, we did see less cell death after dasatinib therapy in particular microenvironments, and found that co-culture of leukemic cells with bone marrow- or spleen-derived stromal cells can protect from dasatinib-mediated cell death via a combination of secreted factors and direct cell-cell contact. We also found that dasatinib-treated leukemia cells had greater adherence to stroma as well as increased migration towards stromal cells or other chemoattractants *in vitro*. Additionally, after long-term dasatinib treatment *in vivo*, re-

transplantation of leukemia cells into secondary recipient mice reveals that cells from all organ compartments have leukemia-initiating potential, and that those taken from previously dasatinib-treated mice result in more aggressive secondary leukemia with decreased latency. Follow up experiments showed that we were not able to replicate this effect by re-transplanting either Bcr-Abl wild-type or T315I-mutated cells treated for a shorter period of time *in vivo*.

**Results**

In order to perform *in vivo* RNAi screens for dasatinib response, we needed a brief dosing schedule that would result in a leukemia cell response to drug without significantly depleting leukemic burden and thus library representation. We found that if we waited until overt leukemia presentation and then treated mice with 10 mg/kg dasatinib once a day for three days, we could significantly extend the lifespan of mice transplanted with wild-type *BCR-ABL1*+ BCP-ALL cells but not mice transplanted with dasatinib-resistant T315I-mutated *BCR-ABL1*+ BCP-ALL (Figure 1A). Examination of the percentage of leukemia cells in multiple lymphoid organs before and after therapy showed a significant decrease of leukemic burden in blood immediately after 10 mg/kg dasatinib, and a delayed decrease of burden in the lymph nodes and spleen; there was no significant decrease of burden in the bone marrow or brain (Figure 1B). We also stained cells isolated from leukemic organs before and after 10 mg/kg dasatinib with Annexin V, which recognizes phosphatidylserine on the exterior surface of cell membranes and thus is a marker of early apoptosis. The percentage of Annexin V positive leukemia cells was significantly increased in all leukemic organs one day after

A

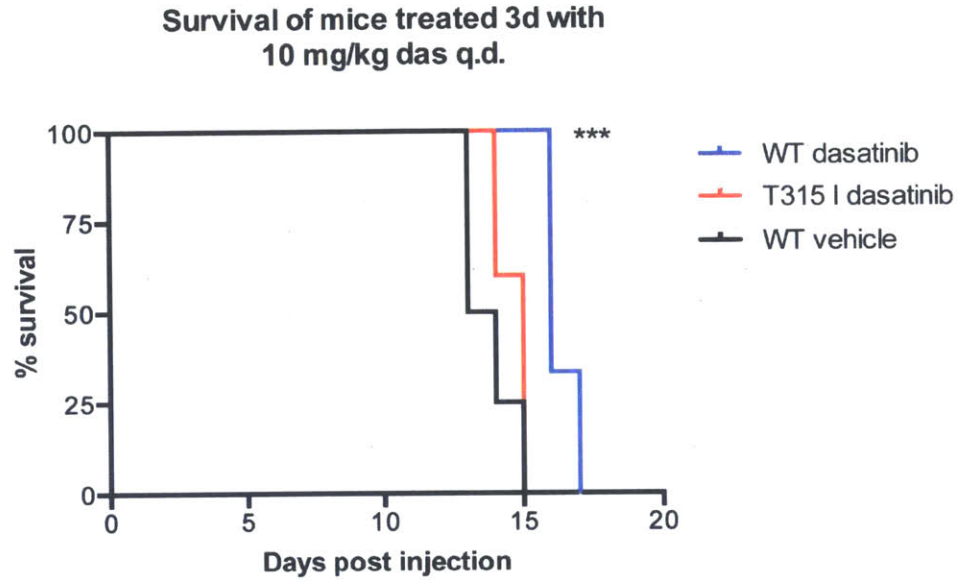
Survival of mice treated 3d with
10 mg/kg das q.d.
100
75
50
25
0
% survival
0
5
10
15
20
Days post injection
***
WT dasatinib
T315 I dasatinib
WT vehicle

B

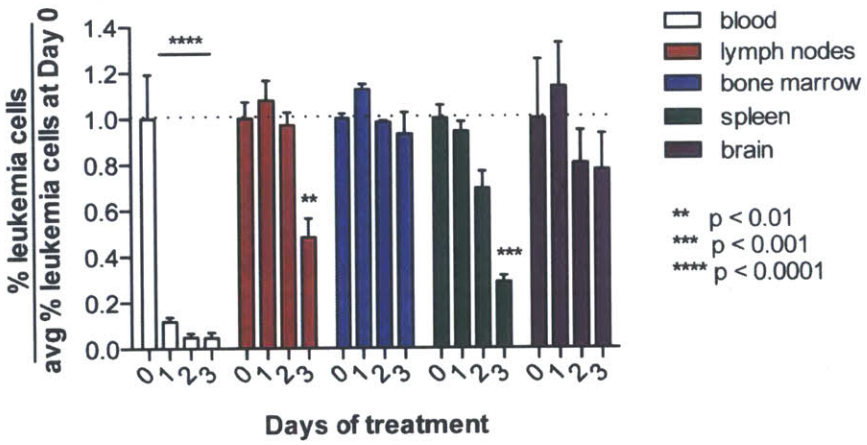
% leukemia cells
avg % leukemia cells at Day 0
1.4
1.2
1.0
0.8
0.6
0.4
0.2
0.0
****
**
***
0 1 2 3 0 1 2 3 0 1 2 3 0 1 2 3 0 1 2 3
Days of treatment
blood
lymph nodes
bone marrow
spleen
brain
** p < 0.01
*** p < 0.001
**** p < 0.0001

C

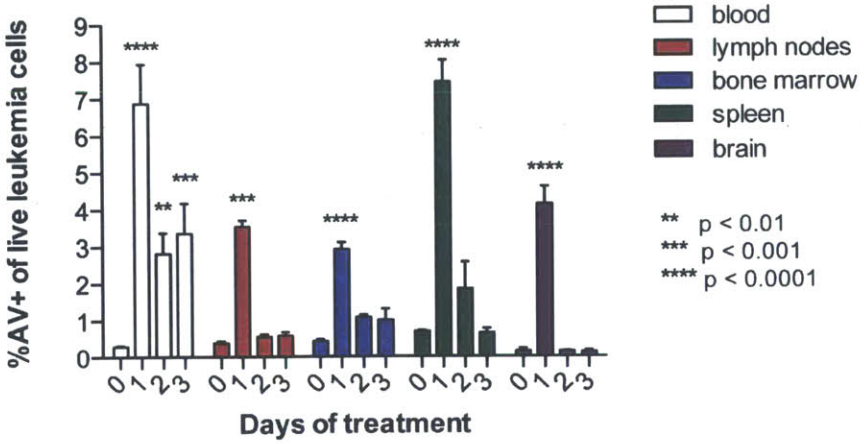
%AV+ of live leukemia cells
9
8
7
6
5
4
3
2
1
0
****
**
***
***
****
****
****
0 1 2 3 0 1 2 3 0 1 2 3 0 1 2 3 0 1 2 3
Days of treatment
blood
lymph nodes
bone marrow
spleen
brain
** p < 0.01
*** p < 0.001
**** p < 0.0001

**Figure 1. Brief dasatinib treatment extends lifespan of mice transplanted with *BCR-ABL1*+ BCP-ALL by inducing apoptosis in all organs.**
(A) $10^6$ *BCR-ABL1*+ wild-type or T315I-mutated BCP-ALL cells were transplanted into syngeneic recipient mice, and mice were treated starting at overt leukemia presentation (Day 11 after transplant) for three days with 10 mg/kg dasatinib q.d. or vehicle. Dasatinib therapy significantly extended lifespan in mice bearing wild-type Bcr-Abl1 tumors but not those bearing T315I-mutated Bcr-Abl1 tumors. Significance was calculated using the Mantel-Cox test. (B) Bar graph showing the percentage of leukemia cells in mouse blood, lymph nodes, bone marrow, spleen, and brain after 0,1, 2, or 3 days of dasatinib 10 mg/kg q.d. normalized to percentage of leukemia cells at Day 0 (start of treatment = Day 11 after transplantation of $10^6$ *BCR-ABL1*+ wild-type BCP-ALL cells). Significant depletion occurs in the blood, lymph nodes, and spleen after dasatinib treatment, but not in the bone marrow or brain. (C) Bar graph showing percentage Annexin V positive cells of live leukemia cells isolated from mouse blood, lymph nodes, bone marrow, spleen, and brain after 0,1, 2, or 3 days of dasatinib 10 mg/kg q.d. normalized to percentage Annexin V positive cells of leukemia cells at Day 0 (start of treatment = Day 11 after transplantation of $10^6$ *BCR-ABL1*+ wild-type BCP-ALL cells). After dasatinib treatment there is a significant increase in Annexin V positive cells in every organ tested. Error bars represent standard error of the mean; p-values were calculated using Student's t-test.

the start of treatment, and in the blood high levels of apoptotic cells persisted for all three days of dasatinib therapy (Figure 1C). These data indicate that brief dasatinib treatment at 10 mg/kg for 3 days resulted in an extension of survival and induced apoptosis in all leukemic organs, but the bulk of leukemic burden was maintained with the bone marrow and brain emerging as sites of residual disease. Similarly, we found that if we increased the dose of dasatinib to 20 mg/kg but still treated for three days starting at overt leukemia presentation, the burden in the blood and spleen were significantly reduced during treatment but burden in the bone marrow was not significantly reduced until after the end of therapy (Supplementary Figure S1).

We also looked at the effect of continuous dasatinib therapy on mice transplanted with *BCR-ABL1*+ BCP-ALL. Leukemic burden in peripheral blood was decreased by dasatinib therapy throughout treatment, whereas burden in other organs

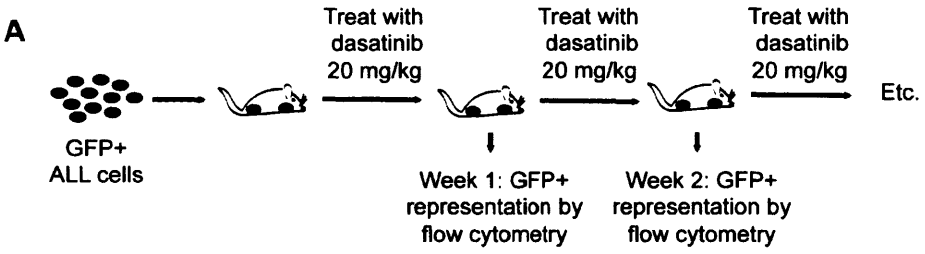
A
Treat with dasatinib 20 mg/kg
Treat with dasatinib 20 mg/kg
Treat with dasatinib 20 mg/kg
Etc.
GFP+ ALL cells
Week 1: GFP+ representation by flow cytometry
Week 2: GFP+ representation by flow cytometry

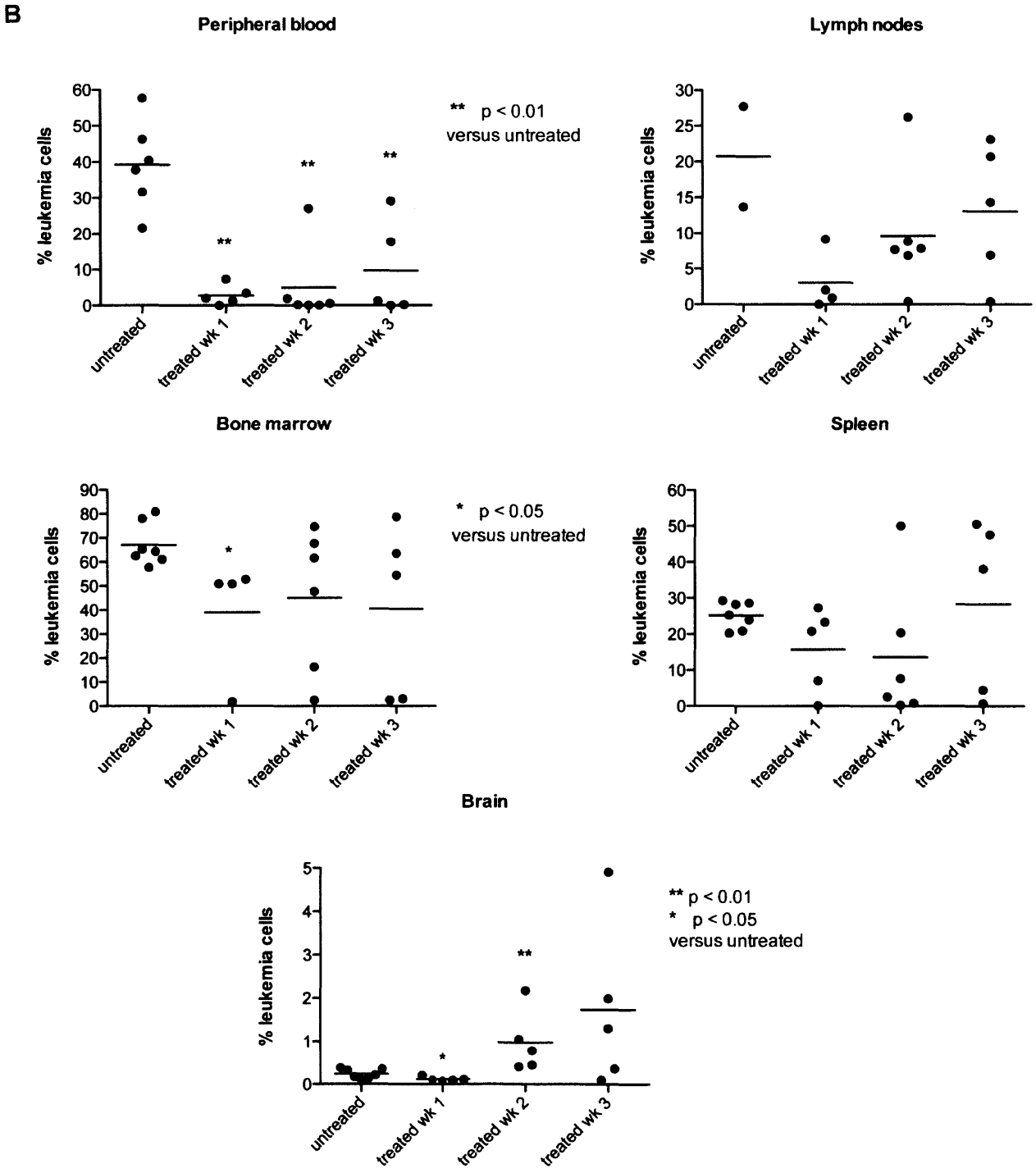
B
Peripheral blood
Lymph nodes
% leukemia cells
** p < 0.01
versus untreated
untreated
treated wk 1
treated wk 2
treated wk 3
Bone marrow
Spleen
* p < 0.05
versus untreated
Brain
** p < 0.01
* p < 0.05
versus untreated

**Figure 2. Continuous dasatinib therapy results in initial response followed by relapse.**
(A) Schematic for analyzing leukemic burden via flow cytometry. Mice were transplanted with $10^6$ *BCR-ABL1*+ BCP-ALL cells, and after infiltration into the central nervous system (at Day 8), mice were continuously treated with 20 mg/kd dasatinib q.d. At the start of treatment and each week after treatment, several mice were sacrificed and leukemic burden was assessed via flow cytometry, which is shown in scatterplots in (B). Leukemic burden is significantly reduced at all time points after treatment in the blood, at one week after treatment in the bone marrow and brain, and then significantly enriched in the brain after two weeks of treatment.

decreased initially after the start of treatment and then increased back to pre-therapeutic levels in several mice (Figure 2). Interestingly, we found that leukemic burden in the brain significantly increased after extended dasatinib treatment. This parallels what other groups have seen using this model (Figure 2, ref. 4). After a week or more of dasatinib therapy, we also noticed significant variation in burden between mice in all leukemic organs, which may signify the emergence of cell-intrinsic resistance to therapy. Re-isolation and dasatinib treatment *in vitro* of *BCR-ABL1*+ BCP-ALL cells from several mice after a week or more of dasatinib therapy revealed that with prolonged treatment *in vivo* there is an increase in leukemia cells that are resistant to dasatinib therapy *in vitro,* regardless of whether the mice had experienced leukemic relapse or not (Supplementary Figure S2).

In order to determine if *BCR-ABL1*+ BCP-ALL cells retain leukemia-initiating potential after extended dasatinib treatment *in vivo*, we re-isolated cells from all leukemic organs of either untreated or dasatinib treated mice and transplanted them into secondary recipient mice (Figure 3A). We found that leukemia cells retain leukemia-initiating potential regardless of the organ from which they were isolated, and in all cases leukemia cells isolated from dasatinib-treated mice resulted in significantly

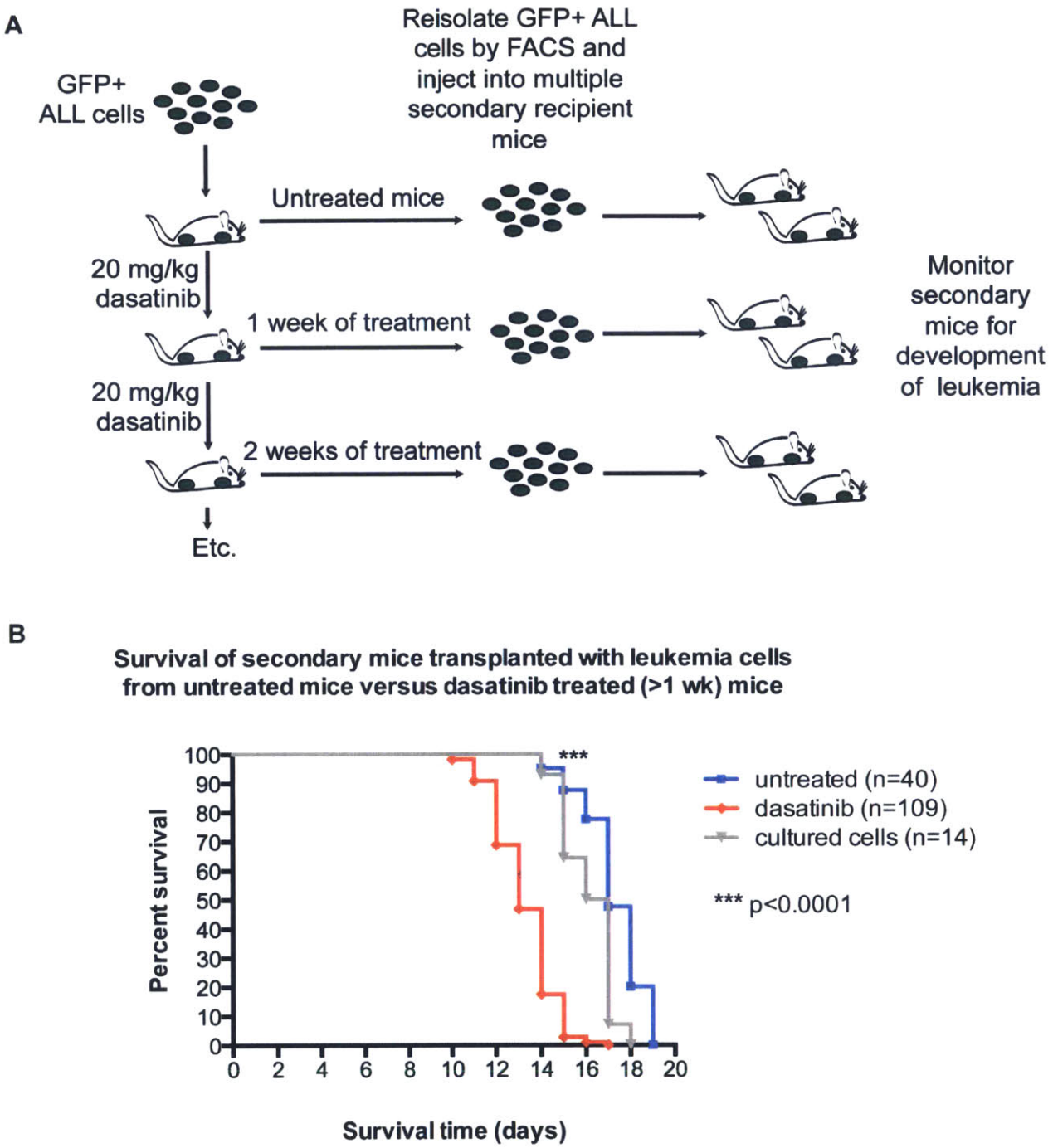


**Figure 3. Secondary transplant of *BCR-ABL1*+ BCP-ALL cells after dasatinib treatment *in vivo* results in more aggressive disease.**
(A) Schematic for re-transplantation experiments: Primary mice were transplanted with $10^6$ *BCR-ABL1*+ BCP-ALL cells, and after infiltration into the central nervous system (at Day 8), mice were continuously treated with 20 mg/kd dasatinib q.d. Leukemia cells were re-isolated from all leukemic organs of untreated mice and dasatinib-treated mice after a week or more of continuous dasatinib therapy, and cells from each leukemic organ from each mouse were transplanted into multiple (at least three) secondary

recipient mice at 2 x $10^4$ cells per mouse. Cultured cells were also transplanted into secondary recipient mice at 2 x $10^4$ cells per mouse as a control. (B) Survival curve showing that secondary mice receiving transplants of cells isolated from previously dasatinib-treated primary mice have significantly shorter lifespan than mice receiving transplants of cells isolated from untreated primary mice or of cultured cells. Significance was calculated using the Mantel-Cox test.

decreased disease latency as compared to cells isolated from untreated mice or cells from culture (Figure 3B, Supplementary Figure 3). Additionally, we found that secondary mice receiving transplants from dasatinib-treated mice had significantly larger spleens than mice receiving transplants from untreated mice or of cultured cells (Figure 4A). Histological examination of the spleens of secondary mice showed that spleens of mice receiving secondary transplants from previously dasatinib-treated mice have less clear delineation between red and white pulp and fewer red blood cells in general (Figure 4B). This may also be an indicator of the more aggressive disease characteristic of cells isolated from primary mice treated with continuous dasatinib therapy for a week or more.

A

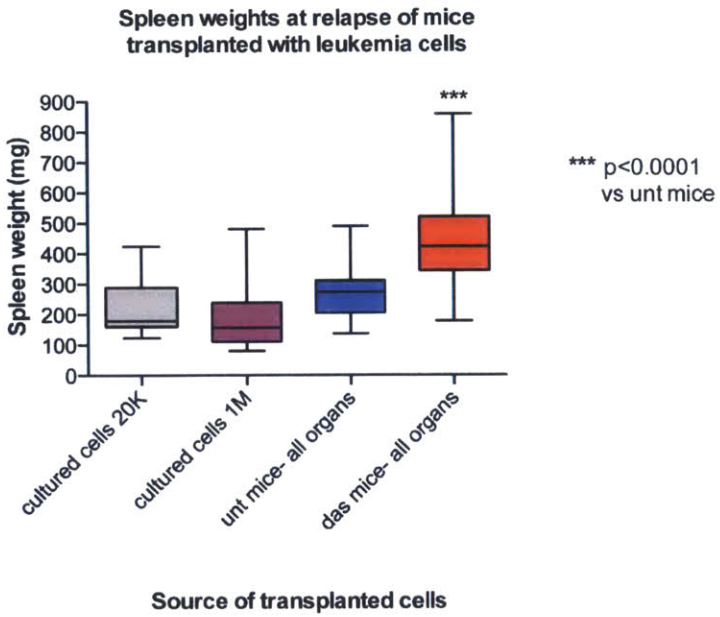


B

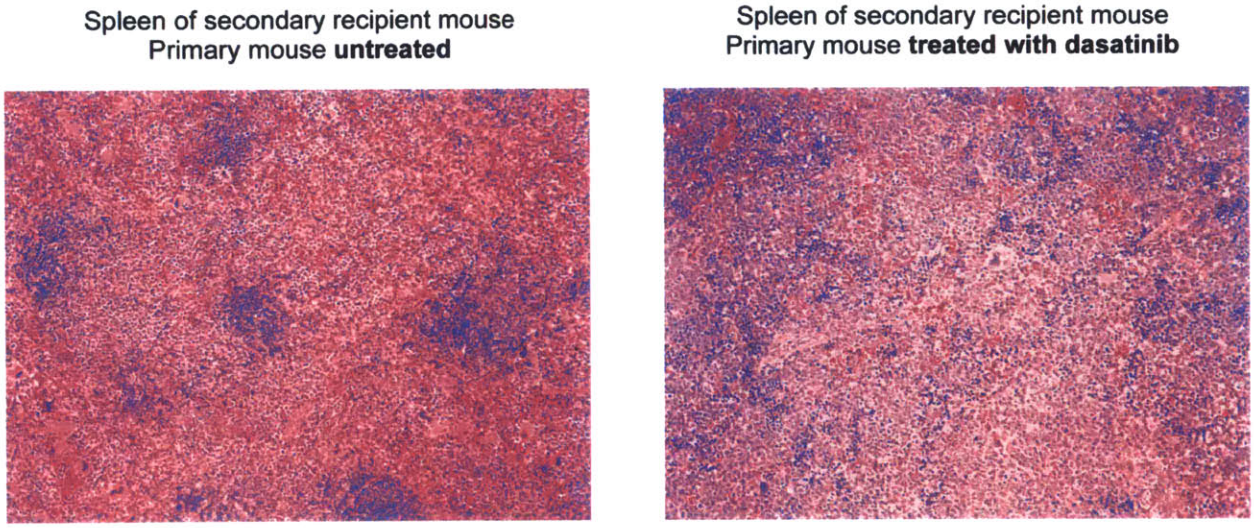


**Figure 4. Mice receiving transplants of leukemia cells isolated from dasatinib-treated mice have larger spleens than mice receiving transplants from untreated mice.**

(A) Box and whisper plots showing spleen weights of mice receiving transplants of cultured cells or cells isolated from either untreated or dasatinib treated mice. Comparison of mice receiving transplants of $10^6$ or $2 \times 10^4$ have no difference in spleen weight, indicating that the significantly larger spleens found in mice receiving transplants from dasatinib-treated mice are not due to a difference in the number of transplanted cells. P-values were calculated by Student's t-test. (B) Representative H&E staining of fixed spleens from secondary mice. Spleens of secondary mice receiving transplants from previously dasatinib-treated mice have a less organized structure and fewer red blood cells than spleens of secondary mice receiving transplants from untreated mice.

The more aggressive disease that we observed after dasatinib treatment *in vivo* could be due to the emergence of Bcr-Abl1 mutations after prolonged dasatinib therapy. To test this theory, we re-isolated cells from primary mice transplanted with cells expressing either wild-type or T315I mutated Bcr-Abl1 that were either mock treated or treated with dasatinib for three days. We found that regardless of *BCR-ABL1* genotype, three days of dasatinib treatment in the primary mice did not result in decreased disease latency in secondary mice (Figure 5A, 5B). Additionally, there was no significant difference in the spleen weights of the secondary mice, regardless of whether they express wild-type or T315I-mutated Bcr-Abl1 or whether the primary mice were treated with dasatinib or not (Figure 5C). Thus, the more aggressive disease observed after a week or more of dasatinib treatment *in vivo* cannot be explained by either the presence of the T315I-mutated Bcr-Abl1 or by brief (3 day) dasatinib treatment *in vivo*.

A

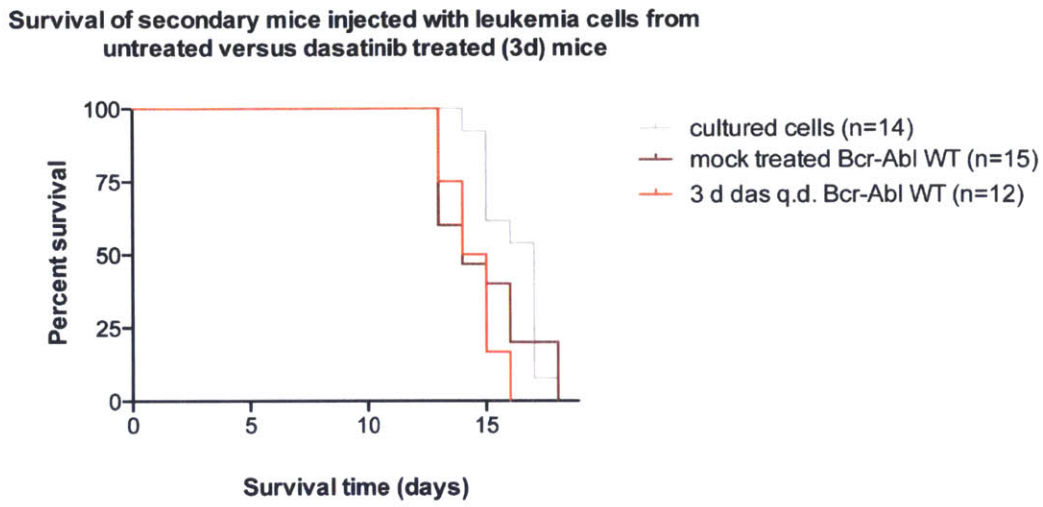
Survival of secondary mice injected with leukemia cells from untreated versus dasatinib treated (3d) mice
Percent survival
100
75
50
25
0
0
5
10
15
Survival time (days)
cultured cells (n=14)
mock treated Bcr-Abl WT (n=15)
3 d das q.d. Bcr-Abl WT (n=12)

B

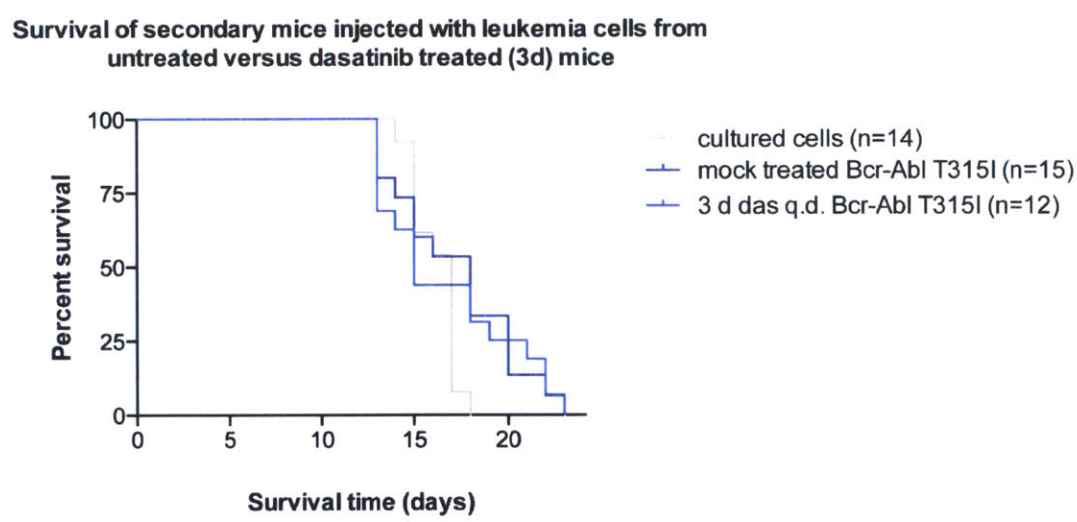
Survival of secondary mice injected with leukemia cells from untreated versus dasatinib treated (3d) mice
Percent survival
100
75
50
25
0
0
5
10
15
20
Survival time (days)
cultured cells (n=14)
mock treated Bcr-Abl T315I (n=15)
3 d das q.d. Bcr-Abl T315I (n=12)

C

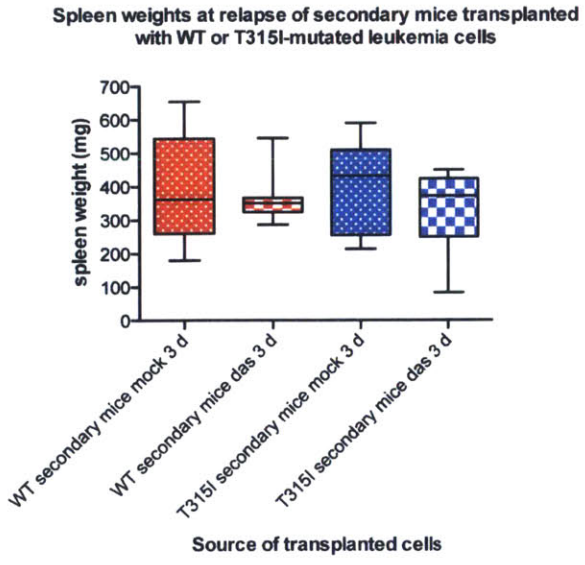
Spleen weights at relapse of secondary mice transplanted with WT or T315I-mutated leukemia cells
spleen weight (mg)
700
600
500
400
300
200
100
0
WT secondary mice mock 3 d
WT secondary mice das 3 d
T315I secondary mice mock 3 d
T315I secondary mice das 3 d
Source of transplanted cells

**Figure 5. More aggressive disease after > 1 week of dasatinib treatment *in vivo* cannot be explained by either the presence of the T315I mutation or by short (3 d) dasatinib treatment *in vivo*.**
(A) and (B) Survival curves showing that secondary mice receiving transplants of (A) wild-type or (B) T315I mutated Bcr-Abl1 expressing cells isolated from primary mice treated with dasatinib for 3 days have no significant difference in lifespan as compared to mice receiving transplants of cells isolated from untreated primary mice or of cultured cells. Significance was calculated using the Mantel-Cox test. (C) Box and whisper plots showing spleen weights of mice receiving transplants of cultured cells or cells isolated from either wild-type or T315I mutated Bcr-Abl1 expressing untreated mice or mice treated with dasatinib for 3 days or > 1 week. There is no significant increase in spleen weight in mice receiving transplants from primary mice treated with dasatinib for 3 days, regardless of *BCR-ABL1* genotype. P-values were calculated using Student's t-test.

Given that the bone marrow appears to be a protective site after dasatinib treatment *in vivo*, we tested whether or not co-culture of leukemia cells with spleen- or bone marrow-derived stromal cells is protective against dasatinib-mediated killing. At multiple time points after culturing cells in 2 nM dasatinib, both spleen- and bone marrow-derived stromal cells protect *BCR-ABL1*+ BCP-ALL cells from dasatinib-mediated killing (Figure 6A). Insertion of a micropore filter to physically separate leukemia cells from stromal cells significantly decreased their protective effect but did not abrogate it, indicating that the protective effect of co-culture is mediated by both secreted factors and direct cell-to-cell contact (Figure 6B). Additionally, we found that over a 3 hour period, treatment of leukemia cells with 1 nM dasatinib resulted in a significant increase in leukemic cell migration towards both CXCL12 and bone marrow-derived stromal cells (Figures 6C, 6D). Adhesion of leukemia cells to bone marrow-derived stromal cells after overnight incubation is also significantly increased after treatment with 1 nM dasatinib, but adhesion to fibronectin is not (Figures 6E, 6F).

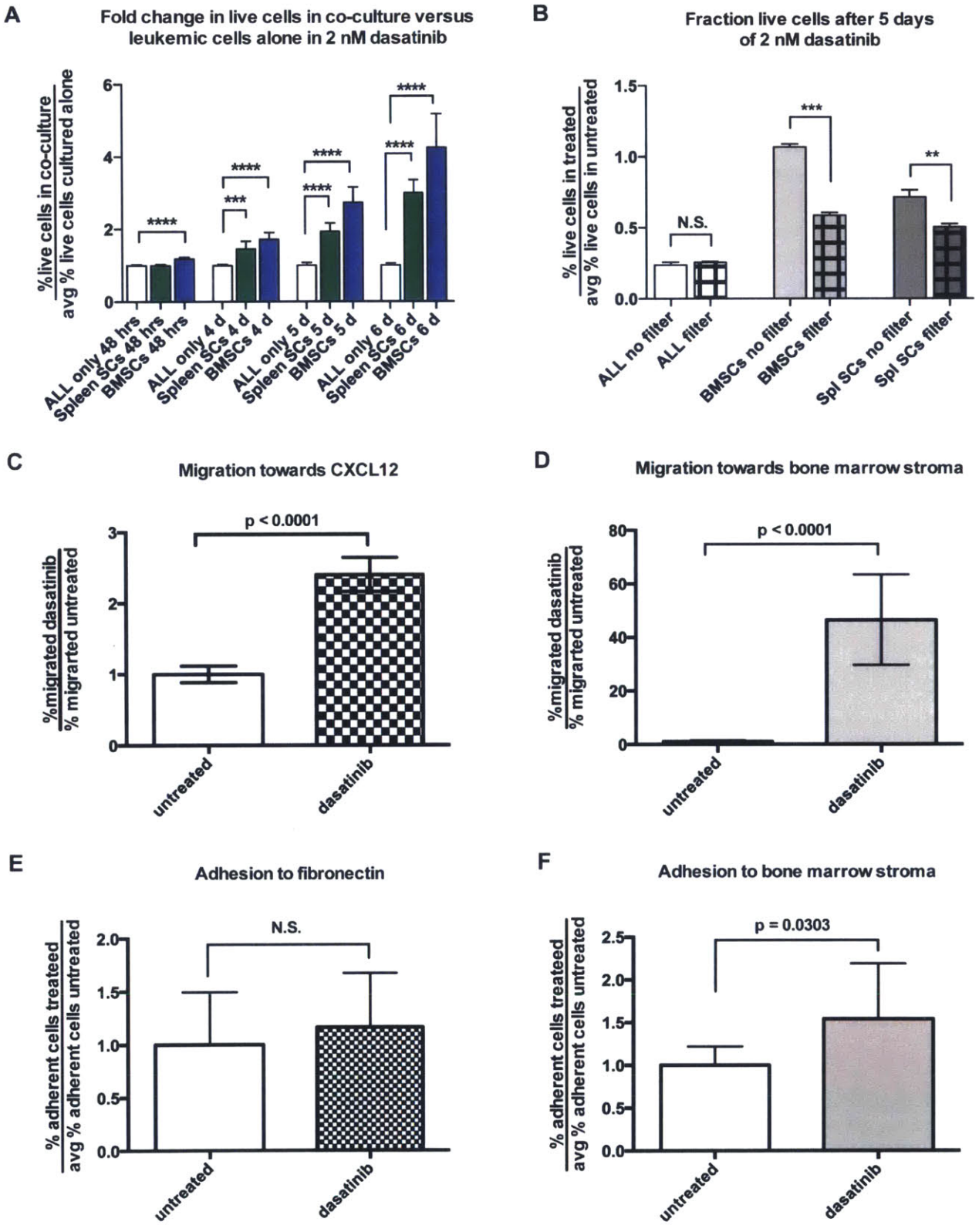
A
Fold change in live cells in co-culture versus leukemic cells alone in 2 nM dasatinib
%live cells in co-culture / avg % live cells cultured alone
ALL only 48 hrs
Spleen SCs 48 hrs
BMSCs 48 hrs
ALL only 4 d
Spleen SCs 4 d
BMSCs 4 d
ALL only 5 d
Spleen SCs 5 d
BMSCs 5 d
ALL only 6 d
Spleen SCs 6 d
BMSCs 6 d
B
Fraction live cells after 5 days of 2 nM dasatinib
% live cells in treated / avg % live cells in untreated
N.S.
ALL no filter
ALL filter
BMSCs no filter
BMSCs filter
Spl SCs no filter
Spl SCs filter
C
Migration towards CXCL12
p < 0.0001
%migrated dasatinib / % migrarted untreated
untreated
dasatinib
D
Migration towards bone marrow stroma
p < 0.0001
%migrated dasatinib / % migrarted untreated
untreated
dasatinib
E
Adhesion to fibronectin
N.S.
% adherent cells treateed / avg % adherent cells untreated
untreated
dasatinib
F
Adhesion to bone marrow stroma
p = 0.0303
% adherent cells treateed / avg % adherent cells untreated
untreated
dasatinib

**Figure 6. Stromal cells isolated from bone marrow or spleen are protective against dasatinib-mediated leukemia cell killing *in vitro*.**
(A) Bar graph showing fold change in percentage of live cells in co-culture with bone marrow- or spleen-derived stromal cells compared to leukemia cells alone in 2 nM dasatinib. All values are normalized to untreated cells in the same culture conditions. At 48 hours, 4, 5, and 6 days, co-culture with both spleen- and bone marrow-derived stromal cells resulted in more live cells than leukemia cells cultured alone. (B) Bar graph showing percentage of live cells in 2 nM dasatinib-treated cultures normalized to untreated cultures of leukemia cells alone or co-cultured with bone marrow- or spleen-derived stromal cells either with or without the insertion of a micropore filter to physically separate leukemia cells from stroma. Physical separation of leukemia cells from stroma in dasatinib-treated cultures significantly decreases the protective effect of stromal cells but does not abrogate it. (C) and (D) Bar graphs showing percent of cells migrated towards (C) SDF1alpha or (D) bone marrow-derived stromal cells (BMSCs) in 1 nM dasatinib-treated cultures normalized to untreated cultures; in both cases there is a significant increase in leukemia cell migration towards the attractant over a 3 hour time period after dasatinib treatment. (E) and (F) Bar graphs showing percentage of leukemia cells adherent to (E) fibronectin or (F) BMSCs overnight in 1 nM dasatinib-treated cultures normalized to untreated cultures. There is a significant increase in adhesion to BMSCs but not fibronectin overnight in dasatinib-treated cultures.

## Discussion

Here we have utilized a novel short-term 10 mg/kg dasatinib treatment of only three days to induce apoptosis in all leukemic organs and extend the survival of recipient mice transplanted with p19$^{ARF-/-}$ *BCR-ABL1*+ BCP-ALL cells without significantly reducing disease burden in all organs. Additionally, we showed that after short-term treatment with either 10 mg/kg or 20 mg/kg dasatinib leukemia cells appear to persist in the bone marrow of recipient mice by flow cytometric analysis. Importantly, the processing necessary to perform flow cytometry on tumors always results in some loss of sample; while this isn't a problem for competitive analyses, it makes the analysis of total leukemic burden by flow cytometry less than accurate. Histological analysis of the bone marrow of untreated and dasatinib treated mice is currently underway in order

to confirm if the bone marrow is indeed a protective site after dasatinib treatment in this model.

After continuous dasatinib therapy for a week or more *in vivo*, we saw an increase in variation of the leukemic burden in all organs along with an increased proportion of cells that were resistant to drug *in vitro*, indicating the emergence of cell-intrinsic resistance; this is consistent with previous studies that have found mutations in Bcr-Abl after a week or more of dasatinib therapy in this model (4). We also confirmed the finding that in this model of *BCR-ABl1*+ BCP-ALL, leukemic burden in the central nervous system can actually be increased by dasatinib treatment (4). Dasatinib, unlike imatinib, is capable of crossing the blood-brain barrier and inducing leukemia cell death, and so it is unclear whether the observed effect is an artifact of the mouse model or something that actually occurs in patients (7). Importantly, *BCR-ABl1*+ BCP-ALL patients are often also treated with the glucocorticoid dexamethasone, which is capable of reducing leukemic burden in the central nervous system, and so the observed increase of leukemic burden in the brain of mice after dasatinib treatment is unlikely to be relevant to the clinical setting (8).

We also found that the leukemia-initiating potential of *BCR-ABL1*+ BCP-ALL cells is retained after dasatinib treatment *in vivo* in all leukemic organs, indicating that minimal residual disease could hypothetically arise from the blood, bone marrow, lymph nodes, spleen, or brain of mice treated with dasatinib. Interestingly, exposure to a week or more of dasatinib treatment *in vivo* resulted in a more aggressive disease upon secondary transplant, and this effect could not be explained by either the presence of the dasatinib-resistant T315I mutated version of Bcr-Abl or by a shorter three day

treatment with dasatinib. Persistent dasatinib exposure *in vivo* seems to select for more aggressive cells, although those cells are not necessarily resistant to dasatinib in culture. This increase in aggressiveness may therefore be a representation of both Bcr-Abl dependent and Bcr-Abl-independent resistance to dasatinib in *BCR-ABL1*+ BCP-ALL cells, and may arise via one of the mechanisms by which MRD typically arises: alteration of drug target (Bcr-Abl), decreased ability to undergo apoptosis or cell cycle arrest, increased pro-survival signaling, maintenance of a less differentiated state, decreased intracellular drug concentrations, or increased ability to home to and remain in protective microenvironments (2, 9-19). Importantly, this increased aggressiveness correlates with an increase in *in vitro* drug resistance but cannot be explained by a model of *in vitro* drug resistance (T315I mutated Bcr-Abl), and therefore may be at least partially due to cell-extrinsic effects from the leukemic microenvironment *in vivo*.

Co-culture with bone marrow stroma has been shown to be protective against chemotherapy-induced cell death in BCP-ALL (20-22). Here we show that co-culture of murine *BCR-ABL1*+ BCP-ALL cells with either bone marrow- or spleen-derived stromal cells can protect from dasatinib-induced cell death, and that this effect is mediated by a combination of secreted factors and direct cell-to-cell adhesion. Cytokines, particularly IL-7, are known to be protective against TKI-mediated cell death in this leukemia model and thus may be responsible for the protective effect of factors secreted by the stroma (2, 5). Direct adhesion to stroma has been shown to be protective against leukemic cell killing by TKIs in *BCR-ABL1*+ BCP-ALL cells previously, but this is the first description of this effect in the $p19^{ARF-/-}$ *BCR-ABL1*+ BCP-ALL mouse model (18, 19, 23, 24).

Interestingly, we also observed increased adhesion to bone marrow-derived stromal cells but not to fibronectin in dasatinib-treated *BCR-ABL1*+ BCP-ALL cells. Fibronectin can be a counter receptor for integrins, which have been shown to play a role in cell adhesion-mediated resistance to therapy in BCP-ALL, but it is likely that stromal cells express an increased amount of integrin counter receptors (20-25). Expression of these counter receptors may also be altered by the presence of drug, thus resulting in a significant increase in adherent leukemia cells after dasatinib treatment.

In general, our results agree with previous studies showing that the transduction/transplantation $p19^{ARF-/-}$ *BCR-ABL1*+ BCP-ALL mouse model responds to therapy in a manner similar to the human disease in that recipient mice initially respond to therapy but eventually relapse, often with cell-intrinsic resistance to drug (4). Similarly, we see that the bone marrow may be a protective site against TKI-mediated leukemia cell killing, and that both secreted factors from and direct cell-to-cell contact to stroma can protect leukemia cells from dasatinib-mediated cell death *in vitro*. Importantly, we also find that dasatinib treatment increases the propensity of leukemia cells to both migrate towards and adhere to bone marrow stroma, as well as the tendency to migrate towards the known BCP-ALL chemoattractant CXCL12. The CXCR4/CXCL12 axis is thought to be important in establishment of MRD in patients with BCP-ALL, and our results show that this model may recapitulate that phenotype (20, 26-28). Importantly, our studies also show that prolonged *in vivo* dasatinib treatment results in a more aggressive disease that cannot be explained simply by the presence of Bcr-Abl mutations. This increase in leukemia aggressiveness may be

indicative of the changes that are thought to occur in leukemia cells during the establishment of MRD, arguing that the transduction/transplantation $p19^{ARF-/-}$ *BCR-ABL1*+ BCP-ALL mouse model is an ideal model in which to study the mechanisms of drug response and the emergence of minimal residual disease.

**Acknowledgements and Author Contributions**

We'd like to thank Michael Hemann and Christian Pallasch for tail vein injections of mice, Luke Gilbert for advice on co-culture experiments, Eric Bent for advice and literature for migration experiments, Christian Pallasch and Corbin Meacham for advice on secondary transplantation experiments, and members of the Hemann lab for advice and technical assistance.

Eleanor Cameron and MH designed the experiments and EC wrote the chapter, which was edited by MH. EC and Emily Lawler performed all experiments.

**References**

1. Williams, R. T., Roussel, M. F. & Sherr, C. J. Arf gene loss enhances oncogenicity and limits imatinib response in mouse models of Bcr-Abl-induced acute lymphoblastic leukemia. *Proc Natl Acad Sci U S A.* **103,** 6688–6693 (2006).

2. Williams, R. T., Besten, den, W. & Sherr, C. J. Cytokine-dependent imatinib resistance in mouse BCR-ABL+, Arf-null lymphoblastic leukemia. *Genes Dev.* **21,** 2283–2287 (2007).

3. Meacham, C. E. *et al.* A genome-scale in vivo loss-of-function screen identifies Phf6 as a lineage-specific regulator of leukemia cell growth. *Genes Dev.* **29,** 483–488 (2015).

4. Boulos, N. *et al.* Chemotherapeutic agents circumvent emergence of dasatinib-resistant BCR-ABL kinase mutations in a precise mouse model of Philadelphia chromosome-positive acute lymphoblastic leukemia. *Blood.* **117,** 3585–3595 (2011).

5. Appelmann, I. *et al.* Janus kinase inhibition by ruxolitinib extends dasatinib- and dexamethasone-induced remissions in a mouse model of Ph+ ALL. *Blood.* **125,** 1444–1451 (2015).

6. Gregory, M. A. *et al.* Wnt/Ca2+/NFAT signaling maintains survival of Ph+ leukemia cells upon inhibition of Bcr-Abl. *Cancer Cell.* **18,** 74–87 (2010).

7. Porkka, K. *et al.* Dasatinib crosses the blood-brain barrier and is an efficient therapy for central nervous system Philadelphia chromosome-positive leukemia. *Blood.* **112,** 1005–1012 (2008).

8. Inaba, H., Greaves, M. & Mullighan, C. G. Acute lymphoblastic leukaemia. *Lancet.* **381,** 1943–1955 (2013).

9. Swerts, K. *et al.* Prognostic significance of multidrug resistance-related proteins in childhood acute lymphoblastic leukaemia. *Eur J Cancer.* **42,** 295–309 (2006).

10. Bhatla, T. *et al.* The biology of relapsed acute lymphoblastic leukemia. *J Pediatr Hematol Oncol.* **36,** 413–418 (2014).

11. Cario, G. *et al.* Distinct gene expression profiles determine molecular treatment response in childhood acute lymphoblastic leukemia. *Blood.* **105,** 821–826 (2005).

12. Bhojwani, D. & Pui, . C. H. Relapsed childhood acute lymphoblastic leukaemia. *Lancet Oncol.* **14,** e205–e217 (2013).

13. Lønning, P. E. & Knappskog, S. Mapping genetic alterations causing chemoresistance in cancer: identifying the roads by tracking the drivers. *Oncogene.* **32,** 5315–5330 (2013).

14. Sitthi-amorn, J. *et al.* Transcriptome analysis of minimal residual disease in subtypes of pediatric B cell acute lymphoblastic leukemia. *Clin Med Instights Oncol.* **9,** 51–60 (2015).

15. Uckun, F. M. & Qazi, S. SYK as a new therapeutic target in B-cell precursor acute lymphoblastic leukemia. *J Cancer Ther.* **5,** 124–131 (2014).

16. Mullighan, C. G. Genomic profiling of B-progenitor acute lymphoblastic leukemia. *Best Pract Res Clin Haematol.* **24,** 489–503 (2011).

17. Georgopoulos, K. Acute lymphoblastic leukemia--on the wings of IKAROS. *N Engl J Med.* **360,** 524–526 (2009).

18. Hsieh, Y. T. *et al.* Integrin α4 blockade sensitizes drug resistant pre-B acute lymphoblastic leukemia to chemotherapy. *Blood.* **121,** 1814–1818 (2013).

19. Hsieh, Y. T. *et al.* Effects of the small-molecule inhibitor of integrin α4, TBC3486, on pre-B-ALL cells. *Leukemia.* **28,** 2101–2104 (2014).

20. Sison, E. A. R. & Brown, P. The bone marrow microenvironment and leukemia: biology and therapeutic targeting. *Exp Rev Hematol.* **4,** 271–283 (2011).

21. Zhang, Y. *et al.* Bone marrow mesenchymal stromal cells affect the cell cycle arrest effect of genotoxic agents on acute lymphocytic leukemia cells via p21 down-regulation. *Ann Hematol.* **93,** 1499–1508 (2014).

22. Mudry, R. E. *et al.* Stromal cells regulate survival of B-lineage leukemic cells during chemotherapy. *Blood.* **96,** 1926–1932 (2000).

23. Shishido, S. *et al.* Role of integrin alpha4 in drug resistance of leukemia. *Front Oncol.* **4,** 99. (2014).

24. Hu, Z. & Slayton, W. B. Integrin VLA-5 and FAK are good targets to improve treatment response in the Philadelphia chromosome positive acute lymphoblastic leukemia. *Front Oncol.* **4,** 112 (2014).

25. Konopleva, M., Tabe, Y., Zeng, Z. & Andreeff, M. Therapeutic targeting of microenvironmental interactions in leukemia: Mechanisms and approaches. *Drug Resist Updat.* **12,** 103–113 (2009).

26. de Lourdes Perim, A. *et al.* CXCL12/CXCR4 axis in the pathogenesis of acute lymphoblastic leukemia (ALL): a possible therapeutic target. *Cell Mol Life Sci.* **72,** 1715–1723 (2015).

27. van den Berk, L. C. J. *et al.* Disturbed CXCR4/CXCL12 axis in paediatric precursor B-cell acute lymphoblastic leukaemia. *Br J Haematol.* **166**, 240–249 (2014).

28. Konoplev, S. *et al.* Phosphorylated CXCR4 is associated with poor survival in adults with B-acute lymphoblastic leukemia. *Cancer.* **117,** 4689–4695 (2011).

29. Dickins, R. A. *et al.* Probing tumor phenotypes using stable and regulated synthetic microRNA precursors. *Nat Genet.* **37**, 1289-1295 (2005).

## Materials and Methods

*Cell culture*

Murine p19$^{ARF-/-}$ *BCR-ABL1*+ BCP-ALL cells (1) and stromal cells isolated from mouse bone marrow or spleen were cultured in RPMI media supplemented with 10% FBS, 4 mM L-glutamine, and 55 μM β-mercaptoethanol. Stromal cells were isolated from gender-matched non-tumor bearing C57BL/6J mice by culturing bone marrow aspirate or homogenized spleen and removing non-adherent cells for 7 or more days. Stromal cells for co-culture experiments were passaged only once in culture and used within 4 weeks of isolation.

*Co-culture experiments*

Stromal cells were plated at a density of 5.3 x $10^4$ cells/cm$^2$ and allowed to adhere overnight before any co-culture, migration or adhesion assays were performed. FIbronection-coated plates were generated by incubating with 20 μg/mL fibronection (Roche) for 1 hour at room temperature, washing three times with filtered phosphobuffered saline (PBS), incubating with 1% bovine serum albumin (New England BioLabs) in filtered PBS for 30 minutes at room temperature and then washing a final time with filtered PBS before use. For adhesion assays, leukemia cells were plated at a density of 0.5 x $10^6$ cells/mL on stromal layers or plates coated with fibronectin with or without 1 nM dasatinib and incubated for approximately 15 hours. Adherent and non-adherent cells were then counted using flow cytometry by adding fluorescent beads (CountBright™ Absolute Counting Beads, Thermo Fisher) at a defined concentration to cells from culture, allowing for direct calculation of leukemia cell concentration. For

migration assays, a 5 μm polycarbonate micropore filter (Corning, catalog #3421) was placed with stromal cells or recombinant murine CXCL12 at 200 ng/mL (Peprotech) in media basolateral to the filter; leukemia cells were placed on the apical side of the filter at 2.5 x $10^6$ cells/mL. Cells were allowed to migrate for four hours, and then migrated cells were counted as previously described. For the physical separation of leukemia cells from stromal layers, a 0.4 μm polyethylene terephthalate micropore filter (Millipore, catalog #PIHT12R48) was placed with stromal cells on the basolateral side; leukemia cells were cultured as usual on the apical side of the filter.

*Vectors*

Leukemic cells were labeled with tdTomato or GFP in the context of a miR30 or cDNA expression vector with no shRNA or cDNA cloned in. The miR30 vector is described in the referenced mir30 shRNA study (29). The cDNA vector is the expression pMSCVpuro vector from Clontech with the puromycin resistance cassette excised and replaced with tdTomato.

*Flow cytometry and staining*

All flow cytometric analysis was performed on an LSR analyzer; sorting to re-isolate leukemic cells was performed on an Aria cell sorter (BD Biosciences). Analysis was performed using FACSDiva software (BD Biosciences). Cells were stained with Annexin V conjugated to phycoerythrin (BD Biosciences catalog # 560930) according to the BD protocol and 4',6-diamidino-2-phenylindole

(DAPI, Invitrogen) was used as a vitality stain to gate out dead cells.

*Preclinical therapeutics*

Dasatinib (LC Laboratories) was dissolved in DMSO and diluted into cell culture media for *in vitro* studies. For *in vivo* use, dasatinib was dissolved in 80 mM citric acid at pH 2.3 and administered via oral gavage at 0.01 mL/g.

*Histopathologic examination*

Dissected spleen was fixed in 10% neutral buffered formalin for 48 hours and then embedded in paraffin for sectioning. Pathologic review of hematoxylin and eosin-stained sections (4 μm) was performed blinded to sample identity.

## Supplementary Figures

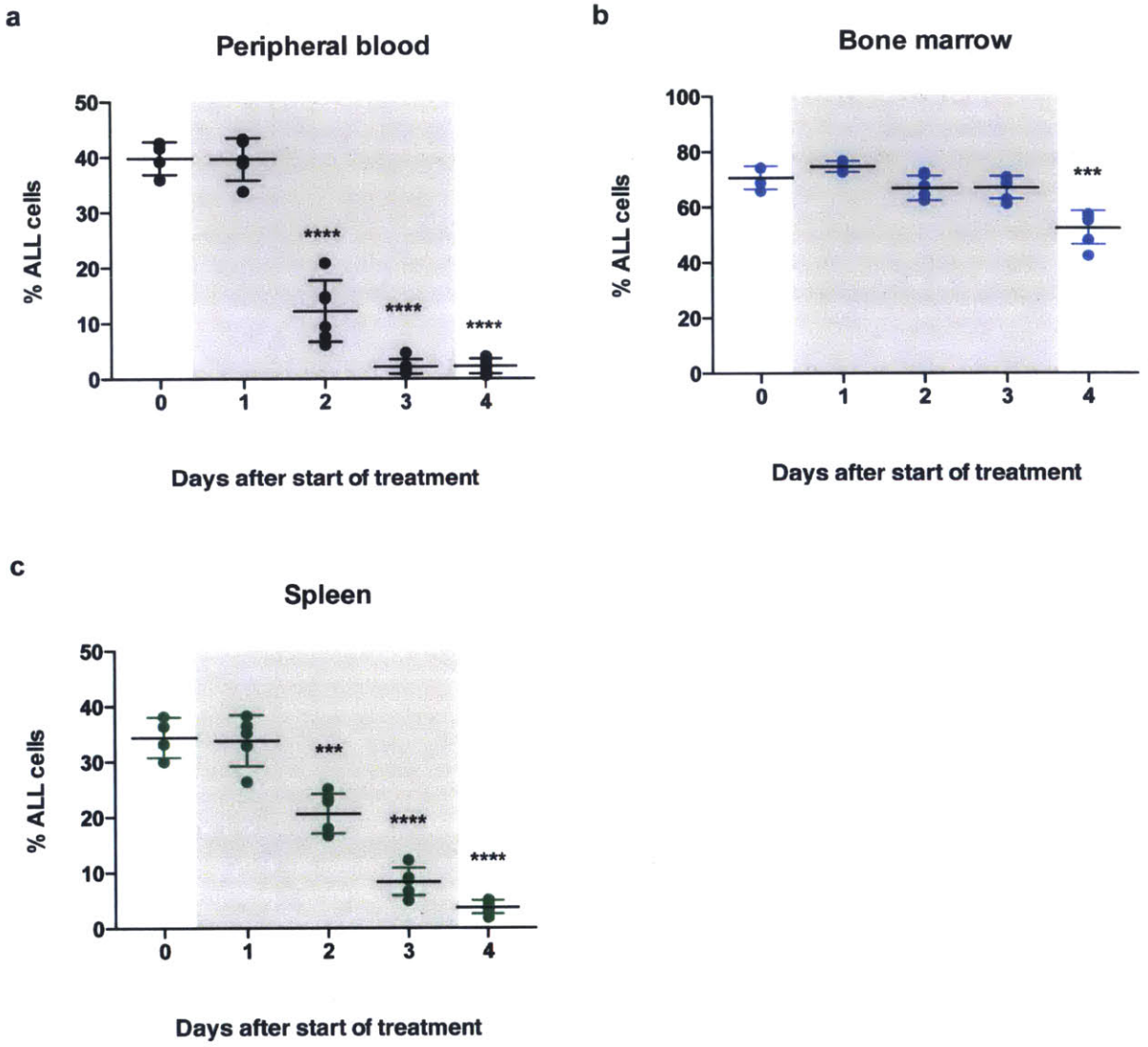


**Supplementary Figure S1. 20 mg/kg dasatinib for three days reveals bone marrow as potential protective site.** Scatterplots showing percentage of leukemia cells in (a) blood, (b) bone marrow, and (c) spleen before, during, and after three days of 20 mg/kg dasatinib q.d. Grey rectangle indicates the time when mice are treated. From Day 2 after start of treatment, blood and spleen have significantly reduced leukemic burden, but burden in bone marrow is not significantly reduced until the end of treatment. Error bars indicate standard deviation; p-values were calculated using Student's t-test.

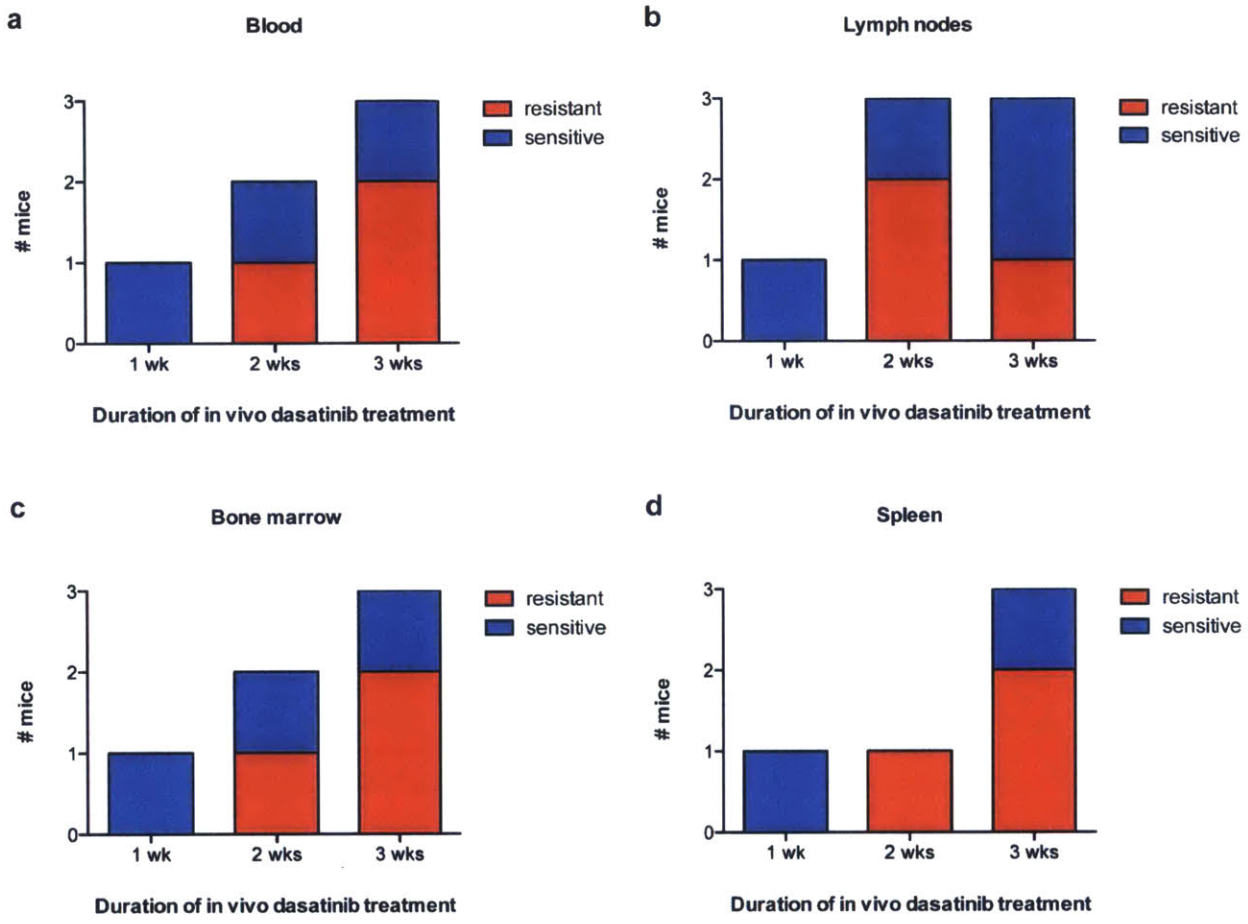


**Supplementary Figure S2. *In vitro* resistance to dasatinib increases with longer continuous treatment *in vivo*.** Bar graphs show the proportion of mice that produced leukemia cells that were resistant to dasatinib *in vitro* after isolation from (a) peripheral blood, (b) lymph nodes, (c) bone marrow, and (d) spleen. Resistant cells were isolated from all organs, and the proportion of mice with resistant cells increased with longer dasatinib treatment.

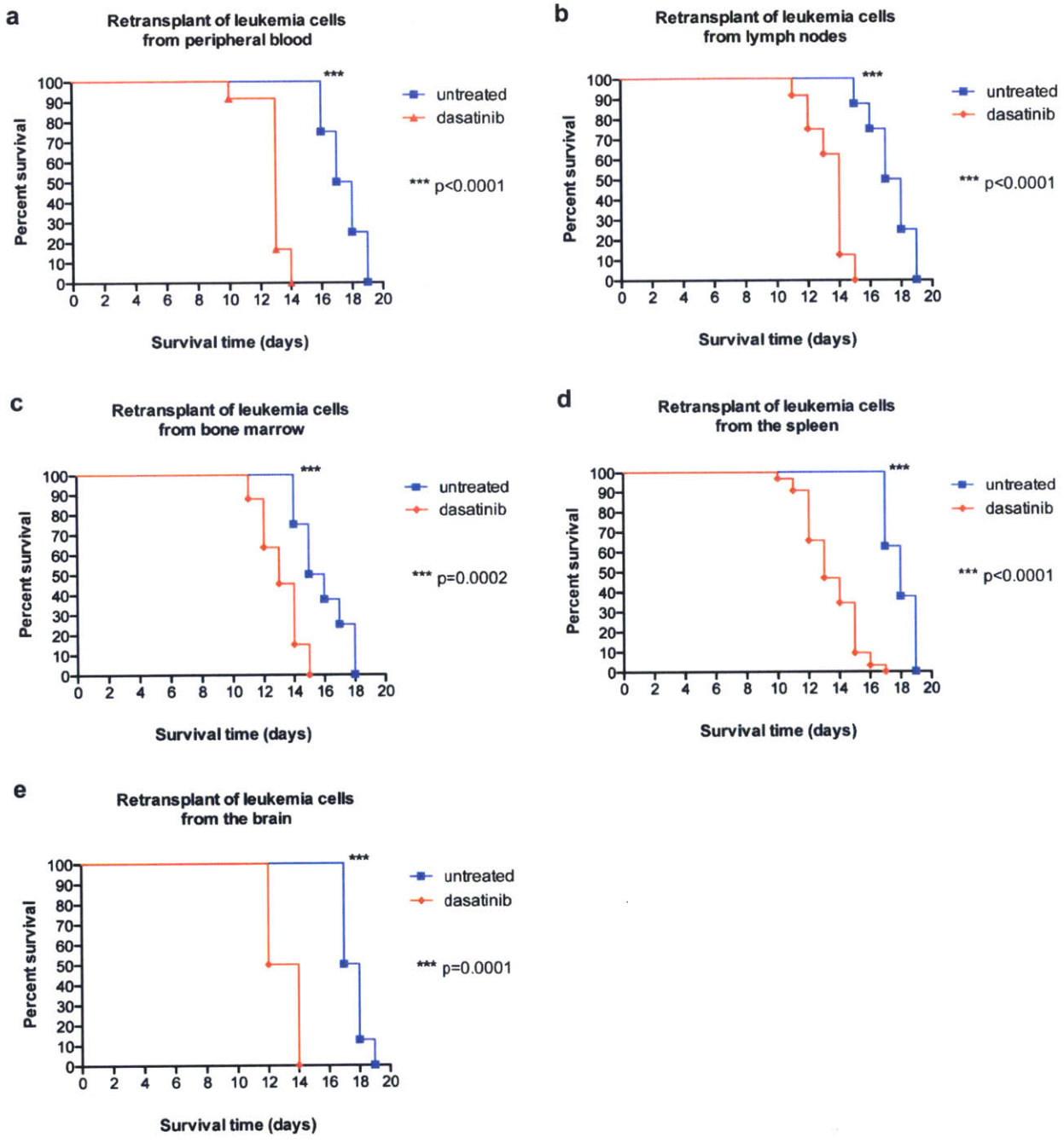


**Supplementary Figure S3. *BCR-ABL1*+ BCP-ALL cells in all organs of untreated and dasatinib treated mice retain leukemia-initiating potential.** Survival curves of secondary mice transplanted with 2 x $10^4$ cells isolated from (a) blood, (b) lymph nodes (c) bone marrow, (d) spleen, and (e) brain of untreated and dasatinib-treated mice. Cells from all mice retain leukemia-initiating potential, and dasatinib-treated mice result in a more aggressive disease regardless of the organ from which cells were isolated.